The University of Melbourne

Sleep/wake Disruptions in a Neurodegenerative Tauopathy Mouse Model: Role of Tau and Therapeutic Potential of Orexin Receptor Antagonists

Ryan John Keenan

ORCID identifier: 0000-0003-0768-0582

A thesis submitted in total fulfilment of the requirements of the degree Doctor of Philosophy – Medicine, Dentistry and Health Sciences

March 2020

Faculty of Medicine, Dentistry and Health Sciences
Department of Pharmacology and Therapeutics

The Florey Institute of Neuroscience and Mental Health

Abstract

Sleep disturbances and neurodegenerative diseases are prevalent in an aging population and represent a major health concern. Mounting evidence highlights a bidirectional relationship between neurodegenerative disease and sleep disturbances, whereby initial pathology disrupts sleep/wake regulation which subsequently exacerbates pathology, leading to a detrimental cycle that accelerates disease progression and cognitive decline. Hence, targeting sleep is a promising therapeutic option to slow disease progression and functional decline.

The exact mechanisms underlying this bidirectional relationship, however, are incompletely understood, especially with respect to the processes that initiate sleep/wake disturbances. Initial research focused on sleep and amyloid beta (Aβ) in animal models of Alzheimer's disease (AD). More recently, attention has turned to pathological tau variants, yet there are few studies investigating the impact of sleep in models of tauopathies, or vice versa.

The aim of this thesis was to investigate the role that mutant tau expression plays in mediating sleep/wake disruptions and cognitive deficits, primarily using the inducible/conditional rTg4510 tau transgenic mouse model, which overexpresses mutant human tau, containing the P301L *MAPT* mutation, in the forebrain.

Given the key role of the orexin neuropeptide system in sleep/wakefulness, initial experiments characterised orexin receptor mRNA expression in rTg4510 and tau knockout (KO) mouse brains using *in situ* hybridisation. Both strains exhibited a specific and comparable decrease in orexin receptor 1 (OX_1R) mRNA expression in the sleep/wake regulating locus coeruleus (LC). These data indicate that orexinergic input to the LC is modulated under conditions of altered/lost tau function, linking tau to molecular changes in the ascending arousal system.

Functional and behavioural studies were then carried out to assess the cognitive, neurodegenerative and sleep/wake phenotype of rTg4510 mice. Tau transgene expression was suppressed in rTg4510 mice by administering doxycycline (Dox) in the diet from 4.5-6.5 months of age. Control rTg4510 mice displayed a markedly disrupted sleep/wake phenotype manifesting primarily as a hyperarousal phenotype during the active phase, and was exacerbated in female rTg4510 mice. rTg4510 mice exhibited elevated tau and phosphorylated tau levels in the hippocampus and cortex, accelerated brain atrophy, white matter deficits, substantial spatial recall deficits and locomotor hyperactivity. Suppression of the tau transgene with Dox prevented or attenuated all measured outcomes, with the noted exception of the sleep/wake phenotype. Thus, tau pathology may preferentially target the arousal-regulating

nuclei in the brain, which may be less responsive to reducing hyperphosphorylated tau accumulation.

The bidirectional relationship between sleep and tau pathology was further probed in rTg4510 mice, by enhancing sleep with orexin receptor antagonist hypnotics. Correcting REM sleep deficits with the dual orexin receptor antagonist, suvorexant, did not ameliorate the rTg4510 phenotype. In contrast, the selective orexin receptor 2 (OX_2R) antagonist, MK-1064, effectively promoted sleep and attenuated the hyperarousal phenotype of rTg4510 mice and partially improved spatial memory recall, but only in male and not female rTg4510 mice. These data revealed striking sex differences in the sleep/wake phenotype of rTg4510 mice, which pointed to a tau- and sex-dependent enhanced hyperarousal drive, and potential modulation in OX_2R signalling, in female rTg4510 mice.

Together these studies have enabled the identification of key, converging factors underlying cognitive restoration in this mouse model. These included reducing hyperphosphorylated tau accumulation, the rescue of long white matter tracts and/or promoting sleep, in particular slow delta wave sleep. Accessing these features by enhancing sleep may thus provide potentially viable, effective therapeutic strategies for tauopathies. Noted sex differences may have implications for the application of OX_2R selective antagonists in a sex-hormone dependent manner.

Declaration

This is to certify that:

(i) this thesis comprises only my original work towards the PhD except where indicated in the preface;
(ii) due acknowledgement has been made in the text to all other material used; and
(iii) this thesis is less than 100,000 words in length, exclusive of tables, maps, bibliographies and appendices.

Ryan John Keenan

Sleep and Cognition Laboratory
The Florey Institute of Neuroscience and Mental Health

Translational Neuropharmacology Laboratory
Department of Pharmacology and Therapeutics
The University of Melbourne
Parkville, Victoria 3010
Australia

Signature: _____

Preface

I acknowledge that specific contributions to the experiments carried out in this thesis were performed by others:

- cDNA templates used to generate the RNA probes in Chapter 2 were provided by Dr. Romke Bron.
- The customised script used for image analysis in Chapter 2 was written by Cameron Nowell.
- *Ex vivo* MRI scans in Chapter 3 were performed by Dr. David Wright.
- EEG/EMG surgeries were completed by Heather Daykin or Linda Cornthwaite-Duncan.
- Daily administration of compounds in Chapter 4 was completed with the assistance of Heather Daykin, Linda Cornthwaite-Duncan, Sara Oberrauch, Maddison Brian and Jeremy Metha.
- Barnes maze behavioural testing for one cohort (n = 8 mice) in Chapter 4 was performed by Heather Daykin.
- Acute administration of compounds and polysomnography recording setup in Chapter 5 were performed with the assistance of Heather Daykin and Linda Cornthwaite-Duncan.
- Polysomnographic scoring in Chapter 5 was completed with the assistance of Jiahui Chu.

Publication status of chapters presented in article format

Chapter 2: Submitted for publication to Journal of Alzheimer's Disease on May 23, 2019.

Chapter 3: Unpublished material not yet submitted for publication.

Chapter 4: Unpublished material not yet submitted for publication.

Chapter 5: Unpublished material not yet submitted for publication.

This thesis was supported by the Alzheimer's Association grant NIRG-396905 and the Australian Postgraduate Award (APA)/Australian Government Research Training Program Scholarship.

Acknowledgements

A PhD without a doubt requires a substantial concerted effort. The successful completion of this thesis warrants due acknowledgment and gratitude to those who have offered me their assistance, support and time over the past four years.

First and foremost, I would like to thank my supervisor and head of the Sleep and Cognition Laboratory, A/Prof. Laura Jacobson. Thank you for giving me the opportunity to complete my PhD in your lab and for putting your faith in me to conduct these experiments. I have learned and achieved so much over these past four years and have developed as both a scientific researcher and a person. Your support and guidance have been invaluable to helping me complete these experiments and this thesis – for that I am truly grateful.

Thank you to my PhD advisory committee member and head of the Translational Neuropharmacology Laboratory, Prof. Daniel Hoyer. It has been incredible to have someone as experienced and knowledgeable in the area of scientific research as you, to offer their advice, support and feedback. It has been extremely helpful – thank you.

I would like to thank my PhD advisory committee – my supervisors A/Prof. Laura Jacobson and Prof. Steve Petrou, my committee chair A/Prof. James Ziogas and committee members Prof. Daniel Hoyer and Dr. Peregrine Osborne. Thank you all for your support and advice throughout my candidature and for helping me overcome the challenges that have arisen.

I am incredibly grateful to Heather Daykin for all her hard work and support. Heather, your contributions to this research have been invaluable to helping me complete this thesis. Thank you also to Linda Cornthwaite-Duncan and Sara Oberrauch for your helpful input to the planning and conduction of these experiments. To all other members of the Sleep and Cognition and Translational Neuropharmacology laboratories, both past and present – Aileen, Angus, Iris, Jake, Jeremy, Jiahui, Kat, Maddi, Mathilde, Sanjida and Zhilin – thank you all for your support and assistance and for being wonderful colleagues and friends.

Thank you to Dr. Giancarlo Allocca for providing the software platform used for polysomnography analysis and for your ongoing technical support.

I am very grateful for the wonderful colleagues I have worked alongside at both the University of Melbourne and the Florey Institute of Neuroscience and Mental Health, as well as my collaborators from other institutes/universities. I am especially grateful to the Core Animal Services team at the Florey Institute for their support with my experiments and training.

To all my fellow peers, from both the Students of Pharmacology (SToP) and Students of the Florey Institute (SOFI) – it has been incredible to have the support of so many other students who are all going through similar experiences. I have made countless friends over these past four years and friendships which will no doubt extend well into the future.

Finally, I am sincerely grateful for all my family and friends. A special thanks to my mum, Iolanda – thank you for supporting me over the past four years and allowing me to focus on my PhD.

Table of Contents

List of Figures

List of Tables

Chapter 1

General Introduction

1.1 Preface

The bidirectional relationship between sleep and neurodegenerative disease is emerging as a potentially crucial, yet until relatively recently, under-appreciated aspect of these disorders. Mounting evidence from both animal and clinical studies suggests that initial disease pathology disrupts sleep/wake regulation, leading to a variety of sleep/wake disturbances commonly experienced by patients, occurring prior to any substantial cognitive impairment. Animal models indicate that these sleep/wake disturbances exacerbate pathology, proposing a detrimental cycle that accelerates disease progression and cognitive decline. The exact mechanisms underlying this bidirectional relationship are incompletely understood, especially the pathological processes that promote sleep/wake disturbances in the first place. Nevertheless, targeting sleep/wakefulness appears to be a promising therapeutic option for slowing disease progression. However, many of the current hypnotic drug therapies, especially benzodiazepines and non-benzodiazepine "Z-drugs", have detrimental effects on memory and cognition. Such treatments are hence contraindicated in neurodegenerative disorders in which cognitive deficits are prevalent. The need for efficacious sleep-promoting therapeutics without negative influences on cognition is imperative, as is the restoration of balanced/physiological sleep. The recently discovered orexin neuropeptide system has emerged as the newest central nervous system (CNS) target for sleep/wake modulation. Activation of orexin receptors stimulates arousal and wakefulness, whereas orexin receptor antagonists (selectively targeting orexin receptor 2, or both orexin receptor 1 and 2) present as a promising class of therapeutics which effectively promote sleep with minimal side-effects. The potential therapeutic utility of using orexin receptor antagonists to manage sleep/wake disruptions in neurodegenerative disorders has yet to be exploited.

1.2 What is sleep?

Sleep is a naturally recurring altered state of consciousness in which an organisms' ability to react to external stimuli is diminished. Prolonged periods of severe sleep deprivation in humans can lead to hallucinations, delirium (Waters et al., 2018) and eventually death (Cortelli et al., 1999), which underpins the critical importance of this physiological process. Sleep is divided into two distinct modes: non-rapid eye movement (NREM) sleep and rapid eye movement (REM) sleep; the latter is also termed paradoxical sleep due to complete paralysis of all muscles with the exception of the ocular muscles, which cause the eyes to dart around rapidly underneath the eyelids. Humans suffer from a variety of sleep disorders including insomnia, narcolepsy (see section 1.8.2), sleep apnea and REM sleep behaviour disorder (Schenck and Mahowald, 2002; Panossian and Avidan, 2009). Sleep architecture changes naturally as people age but is also negatively affected particularly in various neurological diseases such as Alzheimer's disease and Frontotemporal dementia.

1.2.1 Measuring sleep: Electroencephalography and electromyography

Sleep is objectively measured by polysomnography (PSG) which combines the use of electroencephalography (EEG) and electromyography (EMG). EEG is an electrophysiological method which measures the electrical activity of the brain and can be used to infer the vigilance state of various species, including humans and rodents (Campbell, 2009; Mang and Franken, 2012). EEG involves placing recording electrodes over the scalp/skull in humans, or embedding the electrodes through the skull to record from the cortical surface in animals, which measure voltage fluctuations resulting from electrical activity of neurons within the brain. The EEG oscillations that occur during sleep and wakefulness are generated in the thalamus and cerebral cortex, mediated primarily by reciprocal thalamocortical loops (Steriade et al., 1993; McCormick and Bal, 1997). Thalamocortical neurons project to cortical pyramidal cells and are active in two distinct electrophysiological states: a synchronised or bursting (oscillatory) state such as that during sleep; or a tonically active state such as that during wakefulness (McCormick and Bal, 1997). Thalamocortical neurons receive projections from wake-promoting nuclei in the ascending reticular activating system (ARAS) which depolarise thalamocortical neurons, inducing the tonically active state. When tonically active, thalamocortical neurons transmit information to the cortex, promoting a state that is conducive to sensory processing and is associated with a high level of alertness and wakefulness (Steriade et al., 1993; McCormick and Bal, 1997). Gamma aminobutyric acid (GABA)ergic neurons in the thalamic reticular nucleus receive ascending projections from the brainstem and descending

projections from the cortex. Stimulation from reticular cells causes thalamocortical neurons to hyperpolarise which generates the rhythmic bursting activity which is responsible for the low frequency and high amplitude EEG signal observed during sleep (McCormick and Bal, 1997). In summary, brainstem regulation of the thalamus and cortex is responsible for the modulation of the thalamocortical loop which generates the EEG signal of the brain, across varying vigilance states (Steriade et al., 1993; McCormick and Bal, 1997).

EEG signals are categorised into five main patterns (also termed bands or waves), based on their frequency and amplitude characteristics (precise definitions of the frequency ranges may vary slightly) termed alpha, beta, delta, theta, and gamma (Zielinski et al., 2016). The key frequency bands primarily associated with sleep are delta and theta waves. Delta waves (typically < 4 Hz) are particularly prominent during NREM or slow-wave sleep and are characterised by low frequency, high amplitude EEG waves, generated as a result of the hyperpolarisation of cortical pyramidal and thalamic relay neurons (Zielinski et al., 2016). Theta waves (approx. 4-9 Hz) are prominent during REM sleep, particularly in rodents, and are characterised by faster, highly synchronised EEG activity with a low amplitude (Zielinski et al., 2016). Theta is also present in the wake state and is associated with spatial navigation and cognitive processes in the hippocampus (Drieu and Zugaro, 2019). Alpha and beta waves are characteristic of the wake state. Historically, alpha waves have been defined as being prominent during relaxed wakefulness when the eyes are closed, whereas beta waves dominate when the eyes are open. The high frequency gamma band in wakefulness is associated with cognitive and perceptive processes (Karakas and Barry, 2017).

EMG measures the electrical activity of skeletal muscles and is typically utilised alongside EEG to help infer vigilance states, particularly during theta-dominant activity that may represent wakefulness and cognitive processes or REM sleep. In rodents, EMG electrodes are generally inserted into the neck musculature and the electrical activity of the muscle is measured alongside the EEG signal (Mang and Franken, 2012). A high EMG signal is indicative that the rodent is freely moving and hence awake, whereas a lower or flat EMG signal suggests the rodent is likely in NREM or REM sleep, respectively. EMG is particularly relevant for distinguishing REM sleep, where the brain activity is high and rather reminiscent of wakefulness and thus difficult to identify in the absence of EMG.

1.2.2 Key functions of sleep

The precise functions of sleep are incompletely defined, with both NREM and REM sleep each purported to play differing roles (Plihal and Born, 1997; Hobson and Pace-Schott, 2002; Siegel,

2005; McCarley, 2007). Sleep has been implicated in a variety of processes including physical and immune system restoration/recovery, maintenance of homeostatic functions, growth, clearance of brain metabolites, consolidation of memory and the preservation of cognitive faculties (Stickgold, 2005; Walker and Stickgold, 2006; Diekelmann and Born, 2010; Krueger et al., 2016). Some of the key functions of sleep particularly relevant to the present work are briefly outlined below.

Learning and memory

One of the earliest identified functions of sleep is its proposed role in the consolidation of learning and memory (Stickgold, 2005; Walker and Stickgold, 2006; Diekelmann and Born, 2010). Sleep has been implicated in memory encoding and consolidation (Walker and Stickgold, 2006). The role of NREM (or slow-wave) sleep has been particularly associated with the consolidation of hippocampus-dependent memory consolidation, involving the re-activation and redistribution of memories to neocortical sites (Marshall and Born, 2007; Diekelmann and Born, 2010). It is this critical function of sleep that emphasises its importance in neurodegenerative disorders – where memory decline is a prominent symptom.

Glymphatic clearance

The glymphatic clearance function of sleep is supported by recent evidence that sleep enhances the clearance of metabolites from the brain (Xie et al., 2013; Tarasoff-Conway et al., 2015; Krueger et al., 2016). This function is dependent on the enhanced convective cerebral blood flow from the brain to the circulation during sleep, which in turn removes toxins and other brain metabolites. Xie and colleagues (2013) demonstrated that sleep enhances the exchange between interstitial fluid (ISF) and cerebrospinal fluid (CSF) resulting in the increased clearance of brain products, including amyloid beta (Aβ). The glymphatic function of sleep may play a particularly important protective role in neurodegenerative disorders (Tarasoff-Conway et al., 2015), which are often characterised by the build-up of toxic metabolites such as Aβ and/or tau (see section 1.6.2 for more detail).

Synaptic homeostasis

The synaptic homeostasis function of sleep proposes that sleep is the price we pay for neuronal plasticity (Tononi and Cirelli, 2003, 2006, 2014). During wakefulness plastic processes occur, resulting in a net increase in synaptic strength. The proposed role of sleep is to downscale or normalise synaptic strength to a level that is energetically sustainable and that restores cellular

homeostasis (Tononi and Cirelli, 2003, 2006, 2014). The activity-dependent down-selection of synapses is also thought to prioritise specific synaptic connections, providing the benefits of sleep on memory acquisition, consolidation, and integration, as well as the process of "forgetting" non-prioritised memories (Tononi and Cirelli, 2003, 2006, 2014; Poe, 2017; Sara, 2017).

1.3 A brief introduction to the orexin neuropeptide system

The orexin system (also termed hypocretin) is a recently discovered neuropeptide system which plays a key role in regulating sleep and wakefulness (de Lecea et al., 1998; Sakurai et al., 1998). The two neuropeptides orexin-A (hypocretin-1) and orexin-B (hypocretin-2) act on two identified G-protein coupled receptors (GPCRs): orexin receptor 1 (OX_1R; hypocretin receptor 1, *HCRTR1*, *hcrtr 1*) and orexin receptor 2 (OX_2R; hypocretin receptor 2, *HCRTR2*, *hcrtr 2*). The activation of these receptors stimulates arousal and wakefulness, whereas antagonism of the receptors can effectively promote sleep. Some debate exists regarding the nomenclature to employ when referring to these peptides and their receptors. Official nomenclature references use the term hypocretin to denote the genes of the peptides and receptors according to HUGO (The Human Genome Organisation), whereas orexin is used to denote the precursor and processed protein products of the peptide and the receptors according to IUPHAR (The International Union of Pharmacology; Gotter et al., 2012). Orexin is the most widely accepted designation as it refers to the gene products (Gotter et al., 2012), hence for consistency, the terms orexin and orexin receptor will be used throughout this thesis. For a more detailed overview of the orexin system, see section 1.8.

1.4 Key substrates implicated in sleep/wake disturbances: amyloid beta and tau

Amyloid beta (Aβ) peptide and tau proteins are involved in the pathogenesis of neurodegenerative disorders, most notably of Alzheimer's disease (AD; Blennow et al., 2006; Goedert and Spillantini, 2006). These two species have been implicated in the bidirectional relationship between sleep and neurodegenerative disease pathology, particularly Aβ, although attention is also now deservedly turning to the role of tau.

Aβ is generated following specific enzymatic cleavage of the amyloid precursor protein (APP; Kamenetz et al., 2003) and is the major component of the characteristic extracellular senile or neuritic plaques present in AD brains. Aβ is thought to be a toxic root-cause of AD (see section 1.5.1). The exact functions of Aβ and APP, however, are incompletely understood, although, APP and its homologs appear to play a role in cell adhesion, cell migration and

synaptogenesis (Guo et al., 2012; Ludewig and Korte, 2016). At physiological levels, endogenous Aβ has been proposed to be necessary for long-term potentiation (LTP) and synaptic plasticity (Puzzo et al., 2011). Furthermore, as will be discussed further below, Aβ dynamics have been demonstrated to influence and be regulated by the sleep-wake cycle.

Tau is encoded by the microtubule-associated protein tau (*MAPT*) gene and alternative splicing gives rise to six different isoforms in the human brain (Goedert et al., 1989; Spillantini and Goedert, 2013). Intracellular neurofibrillary tangles (NFTs) are another major hallmark of AD brains and are composed of filaments of hyperphosphorylated tau protein (Blennow et al., 2006; Goedert and Spillantini, 2006). Similar to Aβ, the exact functions of tau are incompletely understood, although it is purported to play a key role in stabilising microtubules, amongst many other functions (Avila et al., 2004; Ittner and Ittner, 2018). Post-translational modifications of tau, especially phosphorylation, alter tau's properties and are strongly implicated in neurodegenerative disorders (Buee et al., 2000; Gotz et al., 2010; Martin et al., 2011). Phosphorylation of tau commonly results in dissociation from microtubules (Lindwall and Cole, 1984; Biernat et al., 1993; Yoshida and Ihara, 1993; Trinczek et al., 1995) and/or the increased propensity for tau to aggregate into pathological inclusions such as NFTs (Despres et al., 2017). Tau plays a key role in the neurodegeneration observed in AD and other tauopathy-related disorders (Iqbal et al., 2005; Spillantini and Goedert, 2013), however, the impact of tau on sleep/wake disruptions has not been thoroughly investigated thus far.

1.5 Neurodegenerative disorders with prevalent sleep/wake disturbances

Sleep/wake disturbances are prevalent in several neurodegenerative disorders including Alzheimer's disease (AD), Frontotemporal dementia (FTD), Parkinson's disease (PD), Huntington's disease (HD), narcolepsy and stroke, in addition to numerous neuropsychiatric disorders such as depression, anxiety, post-traumatic stress disorder (PTSD) and schizophrenia. Here, the focus will be on two common neurodegenerative disorders with defined proteinopathies (AD and FTD).

1.5.1 Alzheimer's disease

AD is a debilitating and progressive neurodegenerative disorder and is the most common cause of dementia, accounting for 50-70% of all cases (Blennow et al., 2006; Gotz and Ittner, 2008; Prince et al., 2013). Despite the prevalence and distress caused by this disease over numerous decades, the underlying pathogenesis and mechanisms are still incompletely understood. AD pathology encompasses extensive degeneration and loss of neurons and synapses, including

dramatic atrophy, in affected brain regions (Dickson, 1997; Selkoe, 2002; Stokin et al., 2005; Blennow et al., 2006; Holtzman et al., 2011). The characteristic lesions of AD are extracellular senile or neuritic plaques, composed of aggregated Aβ peptides, and intracellular NFTs composed of hyperphosphorylated tau protein (Braak and Braak, 1991b; Dickson, 1997; Selkoe, 1997, 2001; Blennow et al., 2006; Ballatore et al., 2007; Querfurth and LaFerla, 2010; Ballard et al., 2011; Holtzman et al., 2011).

AD is a complex and heterogeneous disorder, presented in both familial and sporadic forms. Sporadic AD accounts for greater than 99% of cases and typically begins after 65 years of age, hence often termed late onset AD (LOAD; Blennow et al., 2006; Hardy et al., 2014; Carmona et al., 2018). AD also clusters within families as a genetic disorder, inherited in an autosomal dominant fashion with 100% penetrance. Familial Alzheimer's disease (FAD) accounts for less than 1% of all cases, with a generally earlier age of onset of between 30-60 years (Blennow et al., 2006). The first genetic cause of AD was attributed to mutations in the gene encoding APP (Goate et al., 1991), which generates the Aβ peptide following specific enzymatic cleavage (Kamenetz et al., 2003). In 1984, the Aβ peptide was isolated as the predominant species in cerebral amyloid angiopathy (CAA; Glenner and Wong, 1984). The following year the same peptide was isolated from amyloid plaques of patients with AD and Down syndrome (Masters et al., 1985). It was already known that Down syndrome, caused by complete trisomy of chromosome 21, leads to the development of extensive Aβ deposition in the brain. Speculation that the gene encoding Aβ would be located on chromosome 21 proved to be correct when the complementary cDNA encoding Aβ was eventually cloned (Goldgaber et al., 1987; Kang et al., 1987; Tanzi et al., 1987). More common forms of FAD have also been identified from specific mutations in the genes encoding the presenilin-1 (PSEN1) and presenilin-2 (PSEN2) proteins (Holtzman et al., 2011). These proteins constitute the catalytic subunits of the γ-secretase complex, which is involved in the enzymatic pathway that generates Aβ from APP (Vassar et al., 1999; Kamenetz et al., 2003). Although FAD is relatively rare, the resulting phenotypes all exhibit overproduction of Aβ peptides in the brain (Selkoe, 2001; Hardy et al., 2014), which has proved instrumental in aiding the understanding of the underlying pathology of AD.

Despite the substantial advances made over the past 2-3 decades, significant controversy regarding the exact cause and progression of AD pathogenesis still exists. Built largely on the foundations of the evidence outlined above, the 'amyloid hypothesis' (Selkoe, 1991; Hardy and Higgins, 1992) is one of the oldest and most prominent theories regarding the pathological origin and progression of AD. This hypothesis proposes that a dysregulation

between the production and clearance of Aβ is the root cause of the subsequent neurodegenerative cascade seen in AD (Hardy and Higgins, 1992; Hardy and Selkoe, 2002). The amyloid cascade implicates the eventual impairment of tau kinase/phosphatase activity, therefore resulting in hyperphosphorylation of tau and the development of NFTs (Hardy and Selkoe, 2002). Like any theory, the amyloid hypothesis has its various strengths and weaknesses (Hardy and Selkoe, 2002; Hardy, 2009; De Strooper and Karran, 2016; Ricciarelli and Fedele, 2017); however, one of its key premises is that Aβ is initiatory, imperative and independent of tau with regards to the development of AD pathogenesis. Several findings have suggested this may not necessarily be the case and other hypotheses have emerged (Terry, 1996; Mesulam, 1999) which propose that Aβ toxicity is dependent on, and directly mediated by tau (Rapoport et al., 2002; Roberson et al., 2007; Ittner et al., 2010); or that Aβ and tau target specific cellular processes symbiotically and hence intensify each other's toxic effects (Mesulam, 1999; Small and Duff, 2008; Rhein et al., 2009; Ittner and Gotz, 2011; Spires-Jones and Hyman, 2014; Nisbet et al., 2015; He et al., 2018; Busche et al., 2019). Somewhat controversially, it has also been proposed that tau pathology may actually precede Aβ deposition by a considerable period (Braak and Del Tredici, 2004; Braak et al., 2006; Braak and Del Tredici, 2011; Braak et al., 2011; Braak and Del Tredici, 2015). In fact, the severity of cognitive impairment in AD correlates best with NFT burden as opposed to Aβ plaque burden (see Nelson et al., 2012 for review). Furthermore, multiple phase III clinical trials directed specifically at reducing Aβ levels either by acting on enzymes (beta-secretase (BACE) and gamma-secretase (GACE)) or by immunotherapy (monoclonal antibodies/vaccination) have failed (Cummings et al., 2014; Panza et al., 2018; Imbimbo and Watling, 2019), although Aβ-targeted trials continue.

1.5.2 Frontotemporal dementia

Behind AD, Frontotemporal dementia (FTD) is the second most common cause of dementia and accounts for approximately 5-15% of all cases (Rademakers et al., 2012). FTD is a heterogeneous disorder which arises in several forms. Variants of FTD are characterised by differing degrees of deterioration in behaviour, personality, language and occasionally memory (Bathgate et al., 2001; Liu et al., 2004; Rademakers et al., 2012). Certain genetic variants are caused by mutations in the tau (*MAPT*) gene located on chromosome 17 (Hutton et al., 1998; Spillantini et al., 1998; Forrest et al., 2018). Mutations in the *MAPT* gene account for up to 20% of all FTD cases, with over 40 mutations identified (Goedert et al., 2012; Rademakers et al., 2012; Spillantini and Goedert, 2013). Tau-variant frontotemporal dementia (FTD-tau) is

the variant predominantly discussed and referred to throughout this thesis. Mutations in the *MAPT* gene result in a variety of tauopathies (Spillantini and Goedert, 2013; Rossi and Tagliavini, 2015) typically mediated through the hyperphosphorylation of tau (Buee et al., 2000; Alonso Adel et al., 2004; Gotz et al., 2010), which increases the propensity for tau to aggregate into pathological inclusions (Despres et al., 2017).

1.6 The bidirectional relationship between sleep and disease pathology

The bidirectional relationship between sleep and disease pathology in neurodegenerative disorders is being recognised, particularly regarding Aβ and tau pathologies (Fig. 1.1; Ju et al., 2014; Lim et al., 2014; Vanderheyden et al., 2018; Wang and Holtzman, 2020). Below, current evidence supporting this relationship will be discussed, along with the potential mechanisms involved.

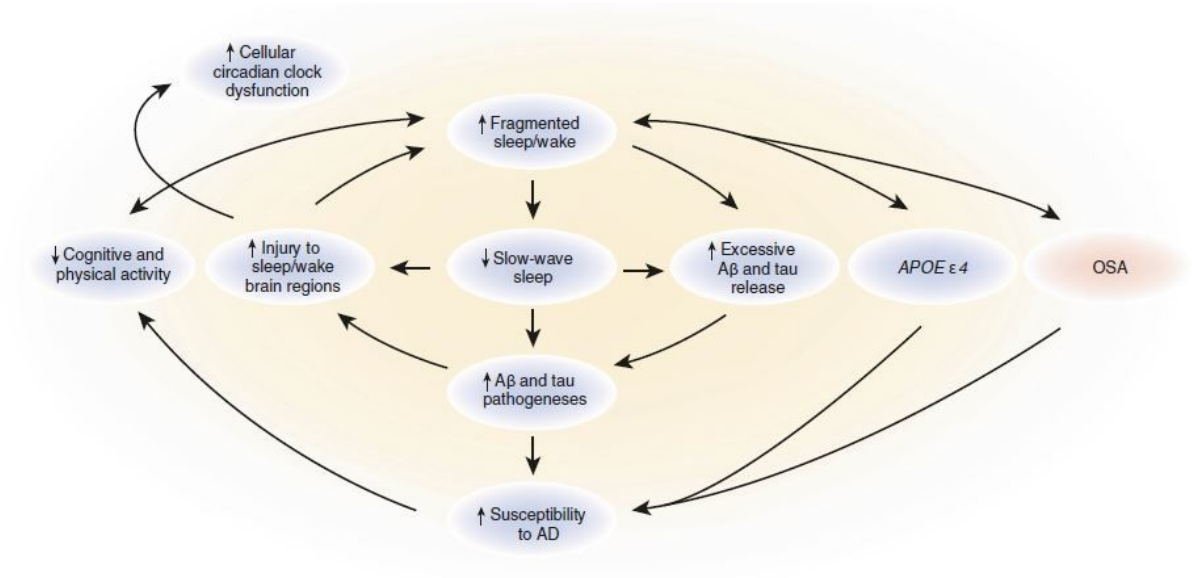

Figure 1.1. Proposed model of the interaction between sleep/wake dysfunction and Alzheimer's disease. Sleep/wake disruptions are prevalent in Alzheimer's disease (AD), which encompasses both amyloid beta (Aβ) and tau pathologies. In this proposed model, decreased sleep exacerbates existing disease pathology, mediated primarily via the increased extracellular release of both Aβ and tau. Subsequent pathological insult to sleep/wake regulating brain circuitry further impairs and fragments sleep/wake function, initiating a detrimental cascade leading to cognitive and functional decline. *OSA* Obstructive sleep apnea. *From Wang and Holtzman (2020) Neuropsychopharmacology 45:104-120.*

1.6.1 Current evidence

AD is typically characterised by global cognitive and functional decline, leading to complete dependence on carers and eventual death within less than ten years from diagnosis. AD is also commonly accompanied by sleep disturbances, reported in up to 60% of patients and which often present early in disease development, preceding any cognitive impairment (Prinz et al., 1982; Moran et al., 2005; Westerberg et al., 2012; Ju et al., 2014; Lim et al., 2014). Common sleep/wake disturbances include insomnia, severe sleep fragmentation, excessive daytime sleepiness, decreased NREM/REM sleep and considerable shifts in circadian rhythms (Bonanni et al., 2005; Crowley, 2011; Slats et al., 2013; Lim et al., 2014; Musiek et al., 2015; Peter-Derex et al., 2015; Urrestarazu and Iriarte, 2016; Cagnin et al., 2017). These early sleep/wake disturbances may contribute to the exacerbation of disease progression and evidence suggests that a bidirectional relationship exists between sleep/wake disturbances and AD pathology. In this model, a positive feedback loop is instigated in which the initial AD pathology disrupts the sleep-wake cycle, which subsequently negatively influences disease development to exacerbate and accelerate AD pathology. Sleep-promoting regions of the brain are further affected to worsen sleep quality, continue the cycle, and severely influence disease progression (Ju et al., 2014; Lim et al., 2014; Vanderheyden et al., 2018). Given the prevalence of AD and distinct involvement of Aβ in AD pathology, much of the preclinical literature has focused on the relationship between sleep and Aβ. Nevertheless, patients with FTD, which lack considerable (or any) Aβ pathology, often experience even more severe sleep and circadian disturbances than AD patients (Bonakis et al., 2014). Additionally, given that hyperphosphorylation of tau and the development of NFTs is a major hallmark of AD pathology, taken together, these observations promote the potentially vital role that tau plays in mediating sleep/wake disturbances in neurodegenerative disorders such as AD and FTD-tau.

Numerous transgenic mouse models of amyloid pathology, expressing human APP containing various mutations identified in the human population, have been utilised to examine the effects of Aβ on sleep. Age-dependent alterations in sleep states, disrupted circadian patterns and highly fragmented sleep are common sleep characteristics observed in these mice, likely as a result of Aβ overexpression and/or deposition (Huitron-Resendiz et al., 2002; Wisor et al., 2005; Zhang et al., 2005; Platt et al., 2011; Duncan et al., 2012; Schneider et al., 2014; Colby-Milley et al., 2015; Sethi et al., 2015). Tg2576 transgenic mice (which overexpress human APP containing the Swedish mutation) (Hsiao et al., 1996) exhibit disrupted circadian rhythms, age-dependent reductions in delta power during NREM sleep and age-dependent decreases in REM sleep (Wisor et al., 2005; Zhang et al., 2005). Importantly, the reduction in

the proportion of REM sleep described by Wisor et al. (2005) was reversed by anti-Aβ immunisation. Furthermore, Zhang et al. (2005) reported that Tg2576 mice exhibit remarkably fragmented sleep including frequent transitions between sleep and wake states. 5xFAD transgenic mice, an amyloidogenesis model harbouring three APP and two PSEN1 FAD mutations (Oakley et al., 2006) also exhibit similarly highly fragmented sleep (Schneider et al., 2014; Colby-Milley et al., 2015; Sethi et al., 2015), in addition to age-dependent increases in wake, decreases in NREM and REM sleep as well as altered brain wave activity, particularly increased beta (β) and gamma (γ) activity during wakefulness (Colby-Milley et al., 2015). Abnormal circadian rhythms and fragmented sleep patterns have also been reported in APP/PS1 (Duncan et al., 2012) and PLB1 (Platt et al., 2011) transgenic mice.

Levels of Aβ in the ISF and CSF exhibit a diurnal fluctuation in mice and humans (Bateman et al., 2006; Kang et al., 2009; Huang et al., 2012b; Huang et al., 2012a; Roh et al., 2012; Lucey et al., 2017; Boespflug and Iliff, 2018). This fluctuation parallels the sleep-wake cycle, peaking during wakefulness and decreasing during sleep. Roh et al. (2012) emphasised the influence that Aβ plaques have on the sleep-wake cycle using the APP/PS1 mouse model of amyloid pathology (Savonenko et al., 2005), which develop plaques from 6-9 months. Prior to plaque formation, normal sleep patterns and diurnal fluctuations of ISF Aβ were present, however, from 6-9 months of age, significant increases in wakefulness and decreases in NREM and REM sleep were observed. The diurnal fluctuation of ISF Aβ was also attenuated after the mentioned time period in these mice (Roh et al., 2012). Importantly, active immunisation with $A\beta_{1\text{-}42}$ in these transgenic mice normalised both the diurnal fluctuation of Aβ and the sleep-wake cycle, further implicating a direct influence for Aβ accumulation at disrupting sleep (Roh et al., 2012). Injection of Aβ oligomers disrupted sleep and impaired memory when combined with further chronic sleep restriction in mice (Kincheski et al., 2017). An association between amyloid levels/deposition and poor sleep quality/efficiency has also been identified in humans (Ju et al., 2013; Spira et al., 2013; Sprecher et al., 2015; Sprecher et al., 2017), which suggests that initial Aβ accumulation has a direct negative impact on normal sleep/wake function.

A detrimental consequence of an initial disruption in a function as important as sleep is that sleep disturbances also appear to be a key mediator in the exacerbation and acceleration of disease pathology. Sleep deprivation can induce cellular damage (with subsequent repair following sleep recovery) (Everson et al., 2014) which is counter-productive for neurodegenerative disorders. Chronic sleep deprivation in 3xTg mice, expressing APP_{swe}, $MAPT_{P301L}$ and PSEN1 mutations (see Oddo et al., 2003) resulted in irregular sleeping patterns, impaired memory/cognition and altered tau phosphorylation (Di Meco et al., 2014). Using a

similar sleep restriction paradigm, Rothman et al. (2013) also demonstrated impaired memory in 3xTg mice as assessed in the Morris water maze. Increases in Aβ and phosphorylated tau (p-tau) levels were also observed in the cortex of sleep restricted mice, but interestingly, no changes were observed in the hippocampus (Rothman et al., 2013). Given the vital role the hippocampus plays in the consolidation of long-term memory, these results highlight the potential importance of sleep, not just pathology, in impairing cognitive function. Further emphasising this point, Mander et al. (2015) demonstrated in humans that levels of Aβ deposition in the medial prefrontal cortex (mPFC) correlated with fewer 0.6-1 Hz slow waves generated in the mPFC, a frequency associated with the consolidation of memory (Marshall et al., 2006; Diekelmann and Born, 2010; Chauvette et al., 2012). These studies demonstrated that slow-wave activity predicted subsequent memory performance with greater reliability than Aβ deposition, and concluded that it is the influence Aβ exerts on sleep, rather than Aβ itself, that is responsible for diminished memory consolidation (Lucey and Holtzman, 2015; Mander et al., 2015). Hence, not only does poor sleep quality directly exacerbate the pathology of AD, but it also further negatively influences the ability to consolidate declarative memories (Stickgold, 2005; Backhaus et al., 2007; Mander et al., 2013) – which is one of the primary cognitive processes affected in AD.

A landmark paper by Kang et al. (2009) further demonstrated that increased ISF Aβ levels correlated with wakefulness and that either intracerebroventricular infusion of orexin-A or acute sleep deprivation significantly increased ISF Aβ. Furthermore, chronic sleep deprivation in AD mouse models resulted in considerably increased plaque burden (Kang et al., 2009; Minakawa et al., 2017). Consistent with the proposed bidirectional relationship, chronic treatment with the dual orexin receptor antagonist (DORA) almorexant, to promote sleep, significantly attenuated plaque burden compared to vehicle treated mice (Kang et al., 2009). Another noteworthy study implicating sleep and orexin with AD pathology demonstrated that APP/PS1/OXR$^{-/-}$ mice exhibited a marked reduction in wakefulness and consequently reduced Aβ pathology (Roh et al., 2014). Importantly, local expression of orexin in the hippocampus had no effect on Aβ pathology, whereas restoration of orexin signalling in the hypothalamus, or sleep deprivation in orexin knockout (KO) mice, increased Aβ burden. Together, these findings suggest that increased wakefulness is associated with augmented Aβ deposition and importantly, that it is the effect orexin has on the sleep network and not necessarily orexin signalling itself, that influences Aβ burden (Roh et al., 2014). In humans, insomnia, poor or fragmented sleep and altered circadian rhythms have all been associated with a higher incidence of developing AD and accelerated cognitive decline (Moe et al., 1995;

Blackwell et al., 2006; Osorio et al., 2011; Tranah et al., 2011; Lim et al., 2012; Potvin et al., 2012; Lim et al., 2013; Hahn et al., 2014; Yaffe et al., 2014; Benedict et al., 2015; Shi et al., 2018; Burke et al., 2019), as well as increased Aβ deposition (Branger et al., 2016; Brown et al., 2016). Additionally, sleep deprivation and/or insomnia increases CSF Aβ levels (Ooms et al., 2014; Ju et al., 2017; Chen et al., 2018; Lucey et al., 2018); further implicating poor sleep as a substantial risk factor for developing AD.

Current evidence in pure tauopathy mouse models is relatively limited in comparison with amyloid models, although more recent efforts have shifted to investigate the link between sleep and tau. Similar to Aβ dynamics, it was recently demonstrated that the sleep-wake cycle also regulates ISF tau levels in mice and CSF tau levels in humans, with tau levels increasing during wakefulness and following sleep deprivation (Holth et al., 2019). Such findings support the concept that neuronal activity regulates the release of tau as well as Aβ (see section 1.6.2). It has further been demonstrated that tau can affect sleep/wake behaviour independently of Aβ. Holth et al. (2017b) showed that tau transgenic mice exhibited age-dependent sleep/wake disturbances including prominent increases in wake and decreases in NREM and REM sleep time, indicative of a hyperarousal phenotype. The authors concluded that tau pathology alone is sufficient to drive sleep/wake changes (Holth et al., 2017b). In $PLB2_{Tau}$ mice, similar increases in wake and decreases in NREM sleep have also been observed (Koss et al., 2016). Consistent with the view that poor sleep exacerbates AD-related pathology (as discussed above regarding Aβ), chronic sleep disruption accelerated the established temporal progression of tauopathy in tau transgenic mice (Zhu et al., 2018). In that study, sleep restriction resulted in elevated p-tau levels and advanced tau pathology, in addition to increasing neuronal loss in the locus coeruleus (LC; Zhu et al., 2018). In humans, decreased NREM sleep has been associated with increased tau pathology, assessed via positron emission tomography (PET) imaging and CSF biomarkers (Lucey et al., 2019). Taken together, these studies demonstrate that tau alone is capable of negatively influencing, and is regulated by, the sleep-wake cycle. The role that tau plays in mediating both sleep/wake and cognitive impairments is thus critical to understating sleep/wake disturbances in neurodegenerative disorders. Investigations elucidating exactly how tau and Aβ pathologies may interact to influence sleep in a complex disease like AD are thus warranted.

1.6.2 Potential mechanisms perpetuating sleep/wake disturbances and exacerbated disease pathology

As outlined above, growing evidence supports the notion that Aβ and/or tau pathology disrupts sleep and poor sleep quality subsequently exacerbates disease progression, however, the exact mechanisms driving these relationships are incompletely understood (Cedernaes et al., 2017). One plausible mechanism relates to the release and clearance of potentially toxic species such as Aβ and/or tau. Heightened neuronal activity – e.g. during extended periods of wakefulness or sleep deprivation – increases the release of both Aβ (Kamenetz et al., 2003; Cirrito et al., 2005; Cirrito et al., 2008; Wei et al., 2010; Bero et al., 2011; Tabuchi et al., 2015) and tau (Yamada et al., 2011; Pooler et al., 2013; Wu et al., 2016; Wang et al., 2017a). Supporting this, Brody et al. (2008) found that ISF Aβ levels correlated with neurological status following traumatic brain injury. Aβ concentrations decreased as neurological status declined and increased as it improved (Brody et al., 2008). Sleep decreases neuronal activity and potentially protects against rising Aβ/tau levels (Lim et al., 2014).

The notion that increased brain activity regulates the release of Aβ is further supported by findings that the brain's default mode network (DMN; Raichle et al., 2001; Buckner et al., 2008) is particularly vulnerable to AD pathology and Aβ deposition (Greicius et al., 2004; Lucey and Bateman, 2014). The DMN is a large-scale brain network with numerous functions that is particularly active during wakeful rest (Buckner et al., 2008). Sleep has been associated with decreased functioning of the DMN and hence may be protective against neuronal activity-induced Aβ vulnerability (Horovitz et al., 2009). Default mode activity, amyloid deposition and memory correlate in humans and the proposed role that the DMN serves for memory may explain why this is one of the first cognitive functions affected in AD (Buckner et al., 2005; Sperling et al., 2009). Transgenic mouse models have also yielded similar findings (Bero et al., 2011; Bero et al., 2012). In Tg2576 transgenic mice, amyloid deposition was most prominent in brain regions comprising the DMN, which importantly includes the mPFC and hippocampus (Bero et al., 2011). Since neuronal activity regulates Aβ release, ISF Aβ levels are a reliable predictor of region-specific amyloid plaque deposition (Bero et al., 2011).

Further supporting the protective role of sleep, recent evidence demonstrates that sleep actually enhances the clearance of metabolites from the brain (Iliff et al., 2012; Iliff et al., 2013; Xie et al., 2013; Tarasoff-Conway et al., 2015). Xie and colleagues (2013) demonstrated in mice that sleep is associated with a 60% increase in the interstitial space and an augmented exchange between ISF and CSF – thereby increasing the clearance of Aβ via a 'glymphatic' pathway, a term conjoining the proposed role that glial ("g-") cells play in a lymphatic ("-

lymphatic") drainage system of the brain. Additionally, the glymphatic efflux was reduced by 60% following traumatic brain injury in mice, which consequently resulted in enhanced tauopathy (Iliff et al., 2014); thus, supporting that extracellular tau is also potentially cleared from the brain via this mechanism (De Strooper and Karran, 2016). In clinical trials, treating sleep disturbances has also been demonstrated to improve cognitive function (Ancoli-Israel et al., 2008). Such evidence suggests that promoting sleep may help to slow neurodegenerative disease progression and further understanding of the mechanisms that drive sleep/wake disturbances are imperative.

As a final adjunct to the plausible role of neuronal network activity, recent findings demonstrated positive effects of the antiepileptic drug levetiracetam in an AD mouse model expressing human APP (hAPPJ20; Sanchez et al., 2012). Levetiracetam reduced abnormal spike activity, reversed behavioural abnormalities, improved memory and learning and reversed synaptic deficits in the hippocampus of hAPPJ20 mice however; interestingly, it had no effect on the levels of hAPP, Aβ or Aβ deposition (Sanchez et al., 2012). The authors concluded that levetiracetam's influence on network activity restored normal hippocampal functioning leading to the recovery of cognitive functions (Sanchez et al., 2012). Supporting this conclusion, reducing hippocampal hyperactivity with levetiracetam was able to improve cognition in patients with amnestic mild cognitive impairment (aMCI; Bakker et al., 2012). Furthermore, Aβ-overexpressing *drosophila melanogaster* treated with levetiracetam exhibited suppressed neuronal firing and prolonged lifespan compared to untreated controls, however, no significant influence on sleep deprivation-induced Aβ burden was found (Tabuchi et al., 2015). Such studies demonstrate that improving AD symptoms and pathology by reducing aberrant neuronal network activity has additional positive effects other than simply decreasing the release of Aβ.

1.6.3 Tau pathology in the ascending arousal regions as the initiation point?

An outstanding question regarding the bidirectional relationship between sleep/wakefulness and neurodegenerative pathology, is exactly how and where disease pathology causes emergence of the initial sleep disturbances. One possible explanation, which requires validation, is that disease pathology – in particular tau – may affect sleep/wakefulness by influencing the normal functioning of the orexin system and ARAS early on in the disease process.

It has been well established that orexin drives wakefulness (see section 1.8). It is therefore interesting to note that clinical studies have identified significant increases in CSF

orexin levels in AD patients, which are particularly evident in the moderate to severe stage of the disease (Dauvilliers et al., 2014b; Liguori et al., 2014b; Liguori et al., 2016; Gabelle et al., 2017; Heywood et al., 2018). Positive correlations between orexin and total tau or p-tau levels have also been found (Deuschle et al., 2014; Liguori et al., 2014b; Liguori et al., 2016; Osorio et al., 2016). Higher CSF p-tau levels are thought to reflect the presence of pathological NFTs composed of hyperphosphorylated tau (Liguori et al., 2014b). Furthermore, increased CSF tau levels have been proposed as a marker of rapid cognitive decline and faster neuronal degeneration in AD (Blennow and Hampel, 2003; Kester et al., 2009). In fact, increased CSF levels of tau and p-tau (and Aβ) are considered a reliable biomarker for AD (Galasko et al., 1998; Andreasen et al., 2001; Blennow et al., 2001; Blennow and Hampel, 2003; Fagan et al., 2006; Craig-Schapiro et al., 2009; Tapiola et al., 2009; Blennow et al., 2010; Fagan and Holtzman, 2010; Tarawneh and Holtzman, 2010; Jack and Holtzman, 2013; Liguori et al., 2017). Additionally, CSF orexin levels negatively correlate with sleep efficiency (SE) and percentage of REM sleep in these patients, whilst positively correlating with increased wake after sleep onset (WASO) and sleep onset latency (Liguori et al., 2014b; Liguori et al., 2016). Finally, in FTD, CSF orexin levels negatively correlate with daytime somnolence (Liguori et al., 2014a).

Despite substantial evidence that AD is associated with increased CSF orexin levels, there are also studies that have found the opposite. Fronczek et al. (2012) observed decreased orexin levels in the CSF, in addition to an approximate 40% decrease in orexin neuronal counts in the hypothalamus of AD patients compared with controls. Even more substantial decreases in orexin neuronal counts in the lateral hypothalamic area (LHA) have also been observed (Oh et al., 2019). Interestingly, increased wake fragmentation has been associated with lower CSF orexin levels in AD patients (Friedman et al., 2007). It is evident that the precise impact of AD on the orexin system remains unclear and often contradictory. Future work is required to elucidate the detailed changes in the orexin system (including CSF, neuronal and receptor changes) over the progression of the disease. Reconciliation against disease stage, which has not been well addressed to date, is particularly important given the known widespread neurodegeneration (including in the hypothalamus) that occurs late in the disease. Nevertheless, the association between orexin and tau levels suggests tau-mediated neurodegeneration in AD and FTD-tau could be driving dysregulation of the orexin system (Liguori et al., 2014b). Therefore, tau loss, dysfunction or toxicity may be directly affecting orexin system function to disrupt sleep/wakefulness. Substantial work undertaken by Heiko Braak and colleagues regarding the pathology of AD (Braak and Braak, 1991b, a, 1995; Braak

et al., 1996; Braak and Braak, 1997; Braak and Del Tredici, 2004; Braak et al., 2006; Braak and Del Tredici, 2011; Braak et al., 2011; Braak and Del Tredici, 2015) may help to substantiate how sleep disturbances originate in the early stages of neurodegenerative disorders.

Following their detailed studies, Braak and colleagues developed a categorical neuropathology staging procedure based on neurofibrillary changes in the brain over the course of the disease (see Braak and Braak, 1991b, 1995; Braak et al., 2006). These studies are especially relevant to sleep in that neurofibrillary changes do not appear in a random fashion, but rather are initially confined to specific subcortical nuclei, particularly those comprising the ARAS, such as the LC (Braak and Del Tredici, 2015; Theofilas et al., 2015; Stratmann et al., 2016). The tuberomammillary nucleus (TMN; Nakamura et al., 1993; Shan et al., 2012) and lateral hypothalamus (LH) are also affected in the early stages of AD, whereas the pedunculopontine tegmental nucleus (PPT) and laterodorsal tegmental nucleus (LDT) develop tau pathology later in the disease course (Stern and Naidoo, 2015; Stratmann et al., 2016; Holth et al., 2017a). Many of these brainstem nuclei appear to have a specific and consistent 'selective vulnerability' to developing AD pathologies (Parvizi et al., 2001). German et al. (1987) identified particularly high densities of NFTs in the LH, dorsal raphe nucleus (DRN), LC and the nucleus basalis of the basal forebrain, in patients with AD. Increased tau pathology was also identified in the LC of patients with mild cognitive impairment (MCI) compared to healthy controls, and correlated with cognitive status (Grudzien et al., 2007). Not only do the above-mentioned regions innervate widespread parts of the cerebral cortex, but they are also anatomically connected with the orexin system and are major drivers in the regulation of sleep and wakefulness. Interestingly, Braak and colleagues identified that pathological changes in the LC potentially begin at a very early age, possibly even before the age of 30 in some cases (Braak and Del Tredici, 2011; Braak et al., 2011). The LC is crucial for the regulation of sleep and arousal (Valentino and Van Bockstaele, 2008; de Lecea et al., 2012). Insult to the LC at an early age may thus help to explain the development of disrupted sleep/wakefulness experienced by patients before the onset of any substantial cognitive impairment.

AD pathology has long been associated with substantial loss of LC neurons (Bondareff et al., 1982; Bondareff et al., 1987; German et al., 1987; German et al., 1992; Manaye et al., 1995) and preferentially, the loss of LC neurons that project diffusely to the cerebral cortex (German et al., 1987; German et al., 1992). Similar observations have been reproduced in mouse models of amyloid and tau pathology (O'Neil et al., 2007; Liu et al., 2008b; Manaye et al., 2013). Additionally, it has been demonstrated that LC neuronal degeneration may actually exacerbate the pathology of AD (Heneka et al., 2006; Heneka et al., 2010; Jardanhazi-Kurutz

et al., 2010), since lesioning the LC increased amyloid plaque load in regions depleted of noradrenaline such as the frontal cortex and hippocampus in Aβ overexpression mouse models (Heneka et al., 2006). Further emphasising the bidirectional relationship between sleep and AD, extended wakefulness or disrupted sleep has also been shown to exacerbate LC cell loss in tau transgenic mice (Zhang et al., 2014; Zhu et al., 2016). Finally, in addition to its critical role in sleep/wakefulness, the LC is also important for cognitive processes such as attention and memory (see Sara, 2009 for review) – clearly damage to this brain region is likely to have adverse consequences in AD (Daulatzai, 2016). Cholinergic neurons of the basal forebrain (Lee et al., 2005b) and serotonergic neurons of the dorsal raphe (McGinty and Harper, 1976; Hornung, 2003) – also key regulators of sleep and arousal – are also particularly susceptible to developing early AD pathology (Davies and Maloney, 1976; Bartus et al., 1982; Whitehouse et al., 1982; Coyle et al., 1983; Mufson et al., 1988; Busser et al., 1998; Chen et al., 2000; Rub et al., 2000; Auld et al., 2002; Mesulam et al., 2004; Geula et al., 2008; Grinberg et al., 2009; Simic et al., 2009; Rodriguez et al., 2012; Kerbler et al., 2015) and likely contribute to the sleep disturbances observed in AD.

Furthermore, work from Braak and Del Tredici (2015) proposes that phylogenetically late occurring brain structures, such as the transentorhinal and entorhinal cortex, are more susceptible to developing AD pathology. These brain regions tend to serve higher CNS functions, whereas more primitive regions are generally conserved. Aggregated tau, for example, tends to develop in neuronal cells that are not absolutely essential for basic human survival (Braak and Del Tredici, 2015). However, it appears that the secondary influence that damage to these regions has on sleep severely accelerates disease progression – making a better understanding of these processes crucial to efforts to slow or reverse AD-related changes. Recently, it was demonstrated with the rTg4510 transgenic mouse model of tau pathology (Ramsden et al., 2005; Santacruz et al., 2005; Spires et al., 2006) that hyperphosphorylated tau accumulation disrupts global neocortical network activity (Menkes-Caspi et al., 2015). These neuronal activity changes may help to explain aspects of cognitive decline as a result of tau pathology that occurs prior to any substantial neurodegeneration or NFT development (Menkes-Caspi et al., 2015). Local field potential recordings revealed spectral differences such as a decreased spindle-delta ratio and a decreased principal frequency during slow-wave sleep in rTg4510 compared with control mice, further linking hyperphosphorylated tau with disrupted sleep (Menkes-Caspi et al., 2015). Importantly, the structural and functional changes observed in neurons affected by hyperphosphorylated tau likely precede the presence of any NFTs (Gomez-Isla et al., 1997; Trojanowski and Lee, 2005; Oddo et al., 2006; Hoover et al.,

2010; Rocher et al., 2010; Crimins et al., 2012; Perez-Nievas et al., 2013), which could explain why marked disruptions in sleep appear so early in the disease process, prior to neurodegeneration and cognitive impairment. Similar correlations between Aβ and dysfunctional neural network activity have also been identified (Palop and Mucke, 2010). Nevertheless, research demonstrating the nature of the interaction between amyloid, tau, the orexin system and the ARAS in mediating sleep/wake disturbances is still in an early phase and many questions remain to be answered. Investigating the role that tau plays in these processes is a key focus of this thesis.

1.7 Sleep as a therapeutic target – the potential of orexin receptor antagonists

In light of the substantial evidence linking impaired sleep with neurodegenerative disease, it appears that sleep itself presents as a potential therapeutic target and may even be utilised as an adjunct biomarker or diagnostic tool for classifying certain disorders. The majority of clinical studies conducted to date have measured sleep using wrist actigraphy (due mainly to practicality and suitability) rather than EEG/PSG recordings, although the ability to detect basic sleep/wake states between the two techniques is quite consistent (Ancoli-Israel et al., 1997). However, two potential issues with these studies is that they are unable to discern the exact effect that disease pathology has on sleep architecture, nor are they able to confidently conclude that any observed sleep disturbances are due to actual pathology rather than other confounding factors. As previously discussed, amyloid deposition is associated with a marked reduction in slow-wave sleep, especially in the < 1 Hz range (Lucey and Holtzman, 2015; Mander et al., 2015). EEG studies detecting these specific changes in sleep architecture may thus prove extremely valuable for predicting the risk of subsequent dementia development or memory decline, and importantly, at identifying the people likely to respond positively to sleep-targeted therapeutic strategies. Studies have long been conducted trying to identify differential EEG characteristics of AD (Brenner et al., 1986; Soininen et al., 1989; Vitiello et al., 1990; for a comprehensive review see Jeong, 2004; Hassainia et al., 1997; Petit et al., 2004). EEG characterisation of REM sleep was recently utilised to successfully discriminate aMCI patients, non-amnestic MCI patients and controls (Brayet et al., 2016).

At present, various approaches to treating sleep disturbances in neurodegenerative disorders have been examined – both pharmacological and non-pharmacological – but with limited or varying success. Non-pharmacological approaches include cognitive behavioural therapy and sleep hygiene measures (Boland et al., 2019) such as regular exercise, keeping to a strict sleep schedule, restricting nap duration or reserving the bedroom for sleep only.

Limiting the intake of stimulants such as coffee and tea is also advised (Peter-Derex et al., 2015). Bright light therapy (BLT) which involves the exposure of patients to periods of intense light, usually in the morning, helps synchronise circadian rhythms and reduce sleep fragmentation. This treatment strategy has been shown to be reasonably efficacious with minimal adverse side effects (Lyketsos et al., 1999; Ancoli-Israel et al., 2003; Fetveit et al., 2003; Dowling et al., 2005; Fetveit and Bjorvatn, 2005). Current pharmacological treatments include melatonin, non-benzodiazepine hypnotics (Z-drugs), antidepressants, antipsychotics, acetylcholinesterase inhibitors and antihistaminic drugs. Melatonin is a hormone involved in primarily regulating circadian rhythms and is therefore an intriguing therapeutic option for treating sleep disturbances. However, the results from clinical trials are mixed, with a number of studies failing to demonstrate adequate effectiveness (Serfaty et al., 2002; Asayama et al., 2003; Singer et al., 2003; Mahlberg and Walther, 2007; Dowling et al., 2008; Gehrman et al., 2009; Wang et al., 2017b). In mouse studies, results for the efficacy of melatonin at ameliorating AD pathology are inconclusive (Quinn et al., 2005; Feng et al., 2006; Olcese et al., 2009; Garcia-Mesa et al., 2012).

A core issue with many of the other pharmacotherapies (particularly $GABA_A$ receptor modulators such as Z-drugs or benzodiazepines) is the risk of adverse side effects which often negate or even outweigh their potential benefit as a sleep-promoting therapeutic. In particular, their adverse effects on cognition and memory are a prominent characteristic and concern for the application of these drugs in AD or FTD (Balkin et al., 1992; Mattila et al., 1998; Mintzer and Griffiths, 1999; Verster et al., 2002; Wesensten et al., 2005; Otmani et al., 2008; Huang et al., 2010; Makaron et al., 2013; Soto et al., 2013; Uslaner et al., 2013; Zanin et al., 2013; Defrancesco et al., 2015). Indeed, drugs that promote sleep but have adverse effects on memory are undesirable for all diseases in which a prominent symptom is memory decline. Several studies have demonstrated the ineffectiveness of varying hypnotics for promoting memory consolidation (Vienne et al., 2012; Feld et al., 2013; Hall-Porter et al., 2014). Possible explanations include off-target influences on memory related pathways or the induction of non-physiological sleep (Vienne et al., 2012). A possible reason for this is the induced variations between the coupling of sleep spindles and NREM slow waves as described by Mander et al. (2016). This coupling mechanism has been demonstrated to be essential to hippocampal memory consolidation (Diekelmann and Born, 2010; Mednick et al., 2013; Ngo et al., 2013; Staresina et al., 2015) and therefore even drugs that enhance slow-wave sleep may impair memory by negatively affecting this process (Feld et al., 2013). The need for more efficacious and tolerable sleep-promoting therapeutics is evident and pressing.

Orexin receptor antagonists present as an alternative and favourable class of drugs for treating sleep disturbances in neurodegenerative disorders (Wang et al., 2018). These drugs (especially OX_2R selective antagonists; see section 1.8.4 and 1.8.5) have the potential to promote sleep which appears more physiological/natural than classic hypnotics and are reasonably well tolerated, with no reported adverse effects on memory or cognition. In rodents, administration of almorexant preserved spatial memory and learning in the Morris water maze whereas zolpidem (Morairty et al., 2014) or scopolamine (Dietrich and Jenck, 2010) significantly impaired it. Even more promising is the ability of these drugs, as a result of varying receptor subtype antagonism (see section 1.8.5), to selectively and specifically alter sleep architecture. As understanding of these processes improves and the development of new orexin receptor antagonists continues, a time may be realised where patients are prescribed specific types of antagonists based on their identified (by EEG recording) sleep deficits. For example, AD patients bereft of adequate REM sleep (a common occurrence in AD) may be prescribed orexin receptor antagonists that preferentially enhance REM sleep. Increases in REM sleep has already been established in clinical studies as the dominant effect for several DORAs including suvorexant and almorexant (see section 1.8.5). Conversely, if deficits in both NREM and REM sleep are evident, an OX_2R selective antagonist may be indicated. In either case, orexin receptor antagonists may therefore prove to be the most appropriate first line of treatment for neurodegenerative related sleep/wake disturbances. Recently completed clinical studies with suvorexant and lemborexant support this premise (Herring et al., 2019; Thein et al., 2019).

1.8 The orexin neuropeptide system

The following section will give a more detailed overview of the orexin system. Here, how the advancement of the understanding of this recently discovered neuropeptide system has led to the development of tolerable and effective sleep-promoting therapeutics will be discussed.

1.8.1 Overview of the orexin system

In 1998, two research groups independently published papers outlining their discovery – via distinct molecular biology and biochemical approaches – of the neuropeptides orexin-A (hypocretin-1) and orexin-B (hypocretin-2). de Lecea et al. (1998) identified rat mRNAs selectively expressed within the hypothalamus. One of the mRNAs encoded the precursor protein of two peptides structurally related to each other and to secretin. The term hypocretin was coined – indicating a hypothalamic member of the incretin family (de Lecea et al., 1998). Expression of the hypocretin peptides were specifically restricted to a few thousand neuronal cell bodies in the dorsal and lateral hypothalamus, with fibers projecting widely to regions throughout the brain (de Lecea et al., 1998). Independently, Sakurai et al. (1998), using 'reverse pharmacology' identified two peptides derived from the same precursor protein that activated two previously discovered orphan GPCRs. The precursor mRNA and the translated peptides were found to be located within the lateral and posterior hypothalamus – a region of the brain implicated in the regulation of feeding behaviour (Bernardis and Bellinger, 1993). Furthermore, administration of these peptides in rats stimulated feeding behaviour and the mRNA precursor was up-regulated in response to fasting (Sakurai et al., 1998). It was suggested that these peptides played a critical role in the regulation of feeding behaviour and were thus termed orexins, from the Greek word 'orexis', meaning appetite. The precursor mRNA was named prepro-orexin and the two structurally similar GPCRs activated by orexin were termed orexin receptor 1 (OX_1R) and orexin receptor 2 (OX_2R) (Sakurai et al., 1998). Ultimately hypocretins and orexins were confirmed to be the same peptides.

Studies performed in rats and mice (and later in human tissue) further elucidated the distribution of orexin neurons and their fiber projections throughout the brain. Orexin neuronal cell bodies were identified predominantly in the perifornical and dorsomedial hypothalamic nuclei, as well as the dorsal, lateral and posterior hypothalamus (Peyron et al., 1998; van den Pol et al., 1998; Nambu et al., 1999). Although orexins are synthesised by only a relatively small number of neurons within the hypothalamus (approximately 3000, 7000 and 50000-80000 in mice, rats and humans respectively (Modirrousta et al., 2005; de Lecea, 2015)), their fibers innervate widespread regions of the brain (Peyron et al., 1998; Nambu et al., 1999).

Furthermore, orexin receptors are expressed throughout the CNS (including the spinal cord), and also in the peripheral nervous system (Leonard and Kukkonen, 2014). A distinct and often complementary expression profile of the two receptors is observed throughout the brain (Marcus et al., 2001). OX_1R is densely expressed in brain regions such as the prefrontal and infralimbic cortex, bed nucleus of the stria terminalis, hippocampus, paraventricular nucleus of the thalamus (PVT), anterior hypothalamic nucleus and rather specifically in the LC (Marcus et al., 2001). OX_2R is heavily expressed throughout the cerebral cortex, hippocampus, septal nuclei, rhomboid nucleus of the thalamus, arcuate nucleus/paraventricular nucleus of the hypothalamus (PVH), LHA and specifically in the TMN (Marcus et al., 2001). Dense orexinergic innervation and high orexin receptor expression levels are present in several brain regions involved in the promotion of arousal. These include the noradrenergic cells of the LC, serotonergic cells of the DRN, histaminergic cells of the TMN, dopaminergic cells of the ventral tegmental area (VTA) and the cholinergic cells of the basal forebrain and PPT (Marcus et al., 2001). The DRN and PPT express moderate levels of both receptors whereas; the LC and TMN express almost exclusively OX_1R and OX_2R, respectively (Marcus et al., 2001). The importance of this expression profile and the relative contributions of these brain regions to certain aspects of sleep regulation will be discussed below.

The regulation of sleep/wake states, via the innervation of arousal promoting brain regions, has been identified as a primary function of the orexin system (Sutcliffe and de Lecea, 2002). This has been substantiated by convincing evidence showing that deficits in orexin functioning leads to a narcoleptic/cataplectic phenotype in rodents, canines and humans. The discovery that narcolepsy that occurs in some dog breeds was caused by a mutation in the orexin receptor 2 gene (Lin et al., 1999) emphasised the prominent role that OX_2R plays in sleep regulation. This was particularly important given the discovery that human narcolepsy with cataplexy is caused by the loss of orexin producing cells in the LH (see section 1.8.2), although, there is no evidence for a receptor defect in human narcoleptics. Due to its extensive projections throughout the brain it became rapidly apparent that the orexin system would be involved in the regulation of more than just feeding behaviour and sleep/wake control (Peyron et al., 1998; van den Pol et al., 1998; Marcus et al., 2001). In the ensuing years, various findings have also implicated the orexin system with reward and addiction (Harris et al., 2005), emotion and emotional memory (Sakurai, 2014), autonomic function (Samson et al., 2005), cognition (Li et al., 2014), locomotion (Nakamura et al., 2000; Hu et al., 2015), nociception (Bingham et al., 2001), stress (Kuru et al., 2000; Winsky-Sommerer et al., 2004), several psychiatric disorders including anxiety, depression, post-traumatic stress disorder (PTSD) and

schizophrenia (Wulff et al., 2010; Gotter et al., 2012; Chen et al., 2015; Li et al., 2016) as well as neurodegenerative diseases including AD and FTD (Kang et al., 2009; Fronczek et al., 2012; Slats et al., 2013; Liguori et al., 2014b; Roh et al., 2014; Liguori et al., 2016).

1.8.2 Consequences of orexin system dysfunction: narcolepsy with cataplexy

Narcolepsy is a neurological disorder characterised by excessive daytime sleepiness, fragmented sleep (including frequent transitions between sleep and wakefulness), abnormal REM sleep (including sleep onset REM periods), hypnagogic hallucinations, vivid dreaming and sleep paralysis (Mignot, 1998; Siegel and Boehmer, 2006; Sakurai, 2007; Scammell, 2015; Kornum et al., 2017). Narcolepsy is also commonly accompanied by cataplexy (termed type 1 narcolepsy) – a sudden and transient weakening or complete loss of muscle tone typically resulting in paralysis and collapse, whilst maintaining conscious awareness, or direct transitions into REM sleep. Cataplexy is frequently triggered by strong positive (laughter or excitement) or negative (fear, anger or surprise) emotions in both humans and canines (Siegel and Boehmer, 2006; Sakurai, 2007; Dauvilliers et al., 2014a; Scammell, 2015; Liu et al., 2016). Canine and rodent genetic studies demonstrated that dysfunction in the orexin system produced phenotypes strikingly similar to that of human narcolepsy with cataplexy, proposing a role for the orexin system in the regulation and maintenance of sleep and wakefulness (Kilduff and Peyron, 2000).

Before the discovery of orexin, it was known that a form of canine narcolepsy was caused by an unidentified autosomal recessive gene with full penetrance (Foutz et al., 1979; Baker et al., 1982). Lin et al. (1999) subsequently identified this phenotype was caused by a mutation in the gene encoding the orexin receptor 2 – promoting the link between the orexin system and normal sleep regulation. Further rodent studies demonstrated that certain dysfunctions in the orexin system induced a narcoleptic/cataplectic phenotype. Mice lacking the prepro-orexin gene (Chemelli et al., 1999; Diniz Behn et al., 2010), both orexin receptor genes (Kalogiannis et al., 2011) or the orexin receptor 2 gene to a limited extent (Willie et al., 2003) (but not the orexin receptor 1 gene alone), and mice or rats with ablated orexin producing neurons (Hara et al., 2001; Beuckmann et al., 2004; Tabuchi et al., 2014; Bernard-Valnet et al., 2016; Branch et al., 2016) all exhibited characteristic signs of human narcolepsy with cataplexy. Despite the different methods used, these animal models all displayed remarkably similar phenotypes including the presence of behavioural arrests typical of human cataplexy, frequent direct wake-to-REM sleep transitions, severely fragmented sleep and included emotional triggering of cataplectic events (Morawska et al., 2011; Mang et al., 2012; Leibiger

and Fendt, 2014). Notably, altered sleep/wakefulness patterns were particularly evident during the dark phase (when mice are normally awake). Significant decreases in time spent awake and increases in time spent in REM and NREM sleep were apparent, including significantly shorter latencies and intervals between REM sleep periods (Chemelli et al., 1999), indicative of highly fragmented sleep. Recent findings suggest that orexin neurons are critical for the maintenance of long bouts of wakefulness; the loss of these neurons consequently leads to an increased number of fragmented transitions between sleep and wake (Branch et al., 2016), possibly mediated by subsequent enhanced firing of noradrenergic LC neurons (Tsujino et al., 2013). Importantly, orexin peptide administration in orexin neuron ablated mice (Mieda et al., 2004) or gene transfer in orexin KO mice were able to diminish narcoleptic/cataplectic behaviour (Liu et al., 2008a). Overall, these models have highlighted a potential increased pressure for sleep during the normally waking phase – characteristic of the excessive daytime sleepiness experienced by narcolepsy patients.

The association between orexin system dysfunction and narcolepsy has been thoroughly substantiated in humans. The majority of patients with type 1 narcolepsy have very low (Nishino et al., 2001; Kanbayashi et al., 2002; Mignot et al., 2002), or virtually undetectable (Nishino et al., 2000; Ripley et al., 2001) levels of orexin-A in the CSF. Furthermore, post-mortem studies have identified extensive or complete loss of orexin containing neurons in the hypothalamus (Thannickal et al., 2000), in addition to undetectable levels of orexin in the cortex and pons of narcolepsy with cataplexy patients (Peyron et al., 2000). Importantly, melanin-concentrating hormone (MCH) containing neurons, which are co-located in the hypothalamus, are not affected in human narcolepsy (Peyron et al., 2000; Thannickal et al., 2000). Other peptides co-localised with orexin, such as dynorphin or neuronal activity-regulated pentraxin (NARP) are also reduced in narcolepsy (Crocker et al., 2005). This supports the hypothesis that human narcolepsy is caused by a specific loss of orexin containing neurons, potentially mediated by an autoimmune disease, although the exact cause is not known (Longstreth et al., 2007; Scammell, 2015; Kornum et al., 2017). It should also be noted that in humans with narcolepsy without cataplexy (type 2 narcolepsy), CSF orexin levels are typically within the normal range (Kanbayashi et al., 2002; Mignot et al., 2002). Therefore, the cataplectic component relates centrally to the absence of orexin producing neurons and/or the depletion of orexin levels in the CSF. Overall, the narcoleptic/cataplectic phenotypes resulting from orexin dysfunction across multiple species, including humans, has confirmed the important role this system plays in sleep/wake control.

1.8.3 Orexinergic control of sleep and wakefulness

Studies such as those described above clearly demonstrated that the orexin system plays a crucial role in sleep/wake regulation. However, exactly how orexins mediate this vital behaviour and why a deficit in this system results in narcolepsy remains to be fully elucidated. Intracerebroventricular injection of orexin-A dose-dependently increased wakefulness and suppressed NREM and REM sleep in rodents (Hagan et al., 1999; Piper et al., 2000; Xi et al., 2001), furthermore, fos immunoreactivity in orexin neurons was positively correlated with wakefulness and negatively correlated with the amount of NREM and REM sleep in rats (Estabrooke et al., 2001). The level of orexin in the CSF correlates with the sleep-wake cycle, peaking during the active phase in rodents and decreasing during the inactive phase (Fujiki et al., 2001; Yoshida et al., 2001). Interestingly, orexin levels and/or orexin neuronal activity is highest just before the beginning of the transition from wake to sleep (Yoshida et al., 2001; Kiyashchenko et al., 2002; Lee et al., 2005a). Additionally, optogenetic stimulation of orexin neurons in the LH or LC promotes increased probability of transitions from sleep to wakefulness (Adamantidis et al., 2007; de Lecea et al., 2012). Such evidence suggests that orexins are wake-active neurons (Kiyashchenko et al., 2002; Takahashi et al., 2008) which initiate and maintain wakefulness.

Brain regions containing monoaminergic neurons such as the TMN, LC and DRN, in addition to the cholinergic basal forebrain, receive dense orexinergic input and promote arousal and wakefulness (Fig. 1.2; Saper et al., 2005; Scammell et al., 2017). These neurons fire actively during wakefulness, are slower during NREM sleep and fall virtually silent during REM sleep (Sakurai, 2007). The firing of orexin neurons themselves also follows this pattern (Lee et al., 2005a; Mileykovskiy et al., 2005). Furthermore, monoaminergic neurons including noradrenergic cells of the LC (Hagan et al., 1999; Horvath et al., 1999), serotonergic cells of the DRN (Brown et al., 2001), histaminergic cells of the TMN (Eriksson et al., 2001; Yamanaka et al., 2002) and dopaminergic cells of the VTA (Nakamura et al., 2000) are all activated by orexins *in vitro*. Such observations suggest that the arousal promoting effects of orexins stem, at least in part, from their excitatory input to wake-active monoaminergic neurons. Sleep promoting brain regions such as the ventrolateral preoptic nucleus (VLPO) and the median preoptic nucleus (MnPO) send inhibitory projections to arousal promoting areas such as the TMN, LC, DRN and PPT, including orexin neurons in the LH (Fig. 1.3; Saper et al., 2005; Saper et al., 2010). The activity of wake promoting neurons is therefore largely dependent on the balance of inhibitory signals from sleep promoting regions and excitatory signals from orexin neurons (Gotter et al., 2012). Saper and colleagues put forward a simplified

model of sleep state switching (Saper et al., 2005; Saper et al., 2010) incorporating the activity of orexin neurons on sleep/wake promoting neuronal populations. Orexin neurons excite 'REM-off' and 'wake-on' neuronal populations (which subsequently inhibit 'sleep-on' and 'REM-on' populations) making it nearly impossible for individuals with normal orexin functioning to transition directly from wakefulness to REM sleep. When normal orexin functioning is lost, these mechanisms become destabilised, disrupting the homeostatic switching between arousal states, leading to increased sleep/wake fragmentation (Saper et al., 2010). The substantial loss of orexin producing neurons in narcolepsy therefore results in diminished activation of wake promoting neurons leading to excessive sleepiness (Saper et al., 2010; Scammell, 2015). Reduced orexin signalling also causes a disinhibition of REM sleep promoting ('REM-on') brain regions, facilitating the abnormal REM sleep and sleep onset REM periods characteristic of human narcolepsy (Saper et al., 2010; Scammell, 2015).

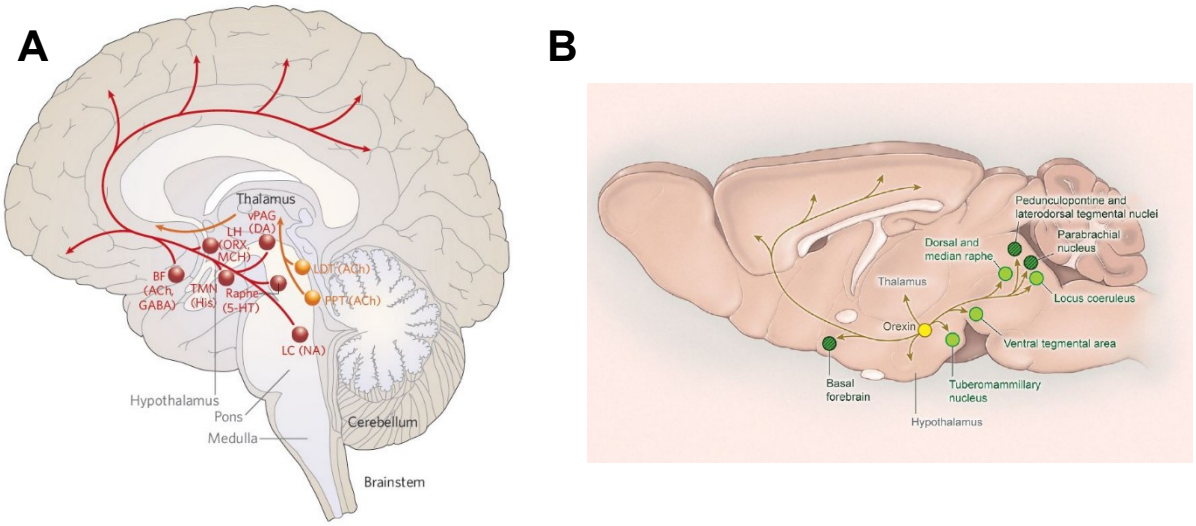

Figure 1.2. Promotion of wakefulness by orexin and the ascending reticular activating system.
A-B, Schematic of the ascending reticular activating system (ARAS) in humans (***A***) and rodents (***B***). Wake-promoting nuclei in the ARAS receive dense orexinergic input and project vastly throughout the cortex to promote wakefulness. *5-HT* serotonin; *ACh* acetylcholine; *BF* basal forebrain; *DA* dopamine; *His* histamine; *GABA* gamma-aminobutyric acid; *LC* locus coeruleus; *LDT* laterodorsal tegmental nuclei; *LH* lateral hypothalamus; *MCH* melanin-concentrating hormone; *NA* noradrenaline; *ORX* orexin; *PPT* pedunculopontine nucleus; *TMN* tuberomammillary nucleus; *vPA*G ventral periaqueductal gray. *From Saper, Scammell and Lu (2005) Nature 437:1257-1263* and *Scammell, Arrigoni and Lipton (2017) Neuron 93:747-765.*

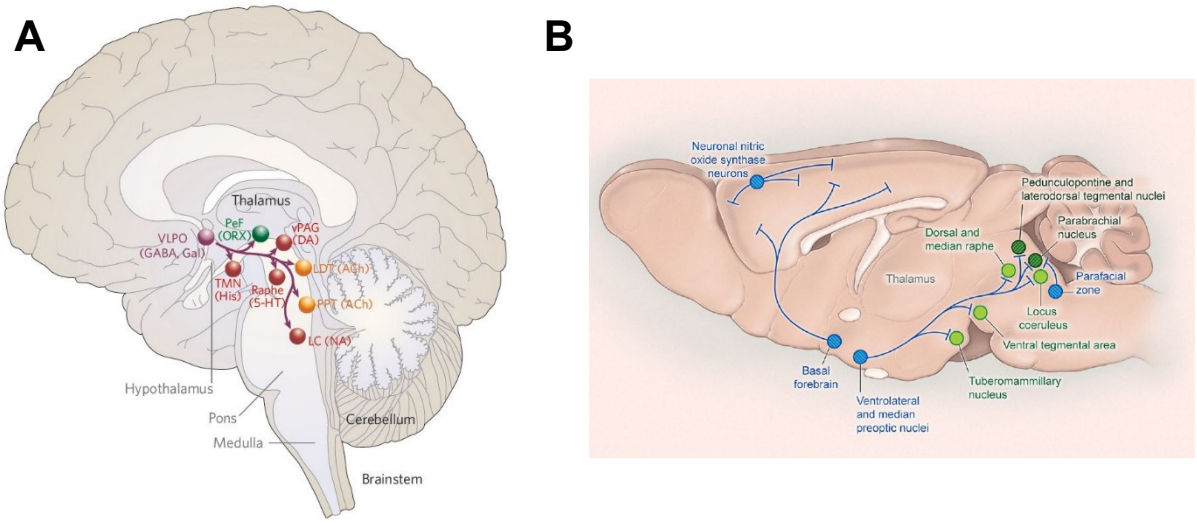

Figure 1.3. Inhibition of the ascending reticular activating system to promote sleep.

A-B, Schematic of sleep-promoting pathways in humans (***A***) and rodents (***B***). The ventrolateral (and median) preoptic nuclei (VLPO) inhibit orexinergic and wake-promoting nuclei to promote sleep. *5-HT* serotonin; *ACh* acetylcholine; *DA* dopamine; *His* histamine; *GABA* gamma-aminobutyric acid; *Gal* galanin; *LC* locus coeruleus; *LDT* laterodorsal tegmental nuclei; *NA* noradrenaline; *ORX* orexin; *PeF* perifornical; *PPT* pedunculopontine nucleus; *TMN* tuberomammillary nucleus; *VLPO* ventrolateral preoptic nucleus; *vPA*G ventral periaqueductal gray. *From Saper, Scammell and Lu (2005) Nature 437:1257-1263* and *Scammell, Arrigoni and Lipton (2017) Neuron 93:747-765.*

The expression profiles for the orexin receptors highlight potentially diverse roles for the various sleep/wake functions. Evidence suggests that the wake promoting influence of orexins is mediated predominantly via OX_2R activation, particularly through activation of histaminergic neurons in the TMN (Huang et al., 2001; Yamanaka et al., 2002). In support of this, OX_2R KO mice exhibit a moderate narcoleptic phenotype whereas OX_1R KO mice show only mild sleep fragmentation with no behavioural abnormalities (Willie et al., 2001). Interestingly, dual orexin receptor KO mice display a more severe narcoleptic phenotype than either receptor KO alone, and this is similar to the phenotype observed for orexin KO mice (Willie et al., 2003). In comparison to the dual receptor KO mice, OX_2R KO mice display a lesser degree of disrupted wakefulness and are rarely affected by attacks of cataplexy. In addition, they show very few direct wake-to-REM sleep transitions (Chemelli et al., 1999; Willie et al., 2003; Mochizuki et al., 2004). Such observations indicate that both receptors contribute to the regulation of sleep and wakefulness, although OX_2R perhaps to a greater extent for sleep induction. Nevertheless, OX_1R is certainly implicated in the regulation of transitions between behavioural states (Mieda et al., 2011).

1.8.4 Orexin receptor antagonists

Since the discovery that orexin activity mediates wakefulness, and that orexin system dysfunction leads to a narcoleptic phenotype, it became apparent that pharmacological blockade of orexin receptors may be effective for the promotion of sleep. This led to a number of drug discovery programs towards the development of orexin receptor antagonists. Orexin receptor antagonists have promising potential for the beneficial treatment of sleep disorders such as insomnia, which is characterised predominantly by difficulties initiating or maintaining sleep, premature morning awakenings, dissatisfaction with sleep quality, and negatively affects normal daytime functioning (Ohayon, 2002; Buysse, 2013). Orexin receptor antagonists also have the advantage of producing a more 'targeted' induction of sleep with a more natural architecture (Fox et al., 2013) as opposed to common treatments such as benzodiazepines or Z-drugs. Z-drugs induce sleep via a global inhibition of CNS activity – mediated predominantly via the positive allosteric modulation of $GABA_A$ receptors (Buysse, 2013), which are expressed vastly throughout the brain. Given that $GABA_A$ receptors are also targets of alcohol and certain anaesthetics there is potential for undesirable additive drug-drug interactions. Furthermore, due to their widespread activity, in addition to the long pharmacokinetic half-life of many of these agents, these drugs have the potential for adverse effects such as next day cognitive impairment, in addition to tolerance and dependence (Winrow and Renger, 2014). Such adverse effects were not anticipated and are typically not observed with orexin receptor antagonists (Dietrich and Jenck, 2010; Morairty et al., 2014; Tannenbaum et al., 2016).

High-throughput screening techniques have identified numerous chemical leads which after optimisation have resulted in a number of potent and specific orexin receptor antagonists which can selectively target only one (single orexin receptor antagonists; SORAs) or both (dual orexin receptor antagonists; DORAs) receptors. Selectively inhibiting the activity of only one receptor subtype has allowed its relative influence to sleep architecture to be thoroughly investigated. In agreement with findings from KO models, studies using these compounds revealed that the promotion of arousal is indeed primarily mediated via OX_2R signalling (Dugovic et al., 2009; Gozzi et al., 2011; Mang et al., 2012; Betschart et al., 2013); hence its antagonism could effectively induce sleep, a hypothesis which has now been demonstrated with a number of compounds.

Initial medicinal chemistry programs identified several potent SORAs including the OX_1R selective antagonists SB-408124 (Langmead et al., 2004; Dugovic et al., 2009), SB-334867 (Duxon et al., 2001; Smart et al., 2001; Smith et al., 2003) and ACT-335827 (Steiner et al., 2013), as well as the OX_2R selective antagonists JNJ-10397049 (McAtee et al., 2004;

Dugovic et al., 2009), JNJ-42847922/MIN-202 (Bonaventure et al., 2015; Letavic et al., 2015), EMPA (Malherbe et al., 2009b; Malherbe et al., 2009a), MK-3697 (Roecker et al., 2014b), MK-8133 (Kuduk et al., 2015), MK-1064 (Roecker et al., 2014a; Gotter et al., 2016) and IPSU (Betschart et al., 2013; Callander et al., 2013; Hoyer et al., 2013). Preclinical studies utilising these compounds has helped to discern the relative functions of each receptor subtype and indeed confirmed that OX_2R antagonism alone is sufficient to promote sleep. However, due in part to the fact that dual orexin receptor KO mice exhibit a more severe sleep phenotype than either receptor KO alone, the clinical focus for hypnotics development focused initially in DORAs, with OX_2R selective SORAs (2-SORAs) MIN202, MK-3697 and MK-1064 only very recently entering clinical trials, thus currently available data on their clinical efficacy is limited (Jacobson et al., 2017; Hoyer et al., 2019).

The first DORA to enter clinical development, almorexant, was effective at promoting sleep in rats, canines and humans (Brisbare-Roch et al., 2007). Almorexant dose-dependently decreased wakefulness and locomotion, whilst increasing NREM and REM sleep time (Brisbare-Roch et al., 2007; Dugovic et al., 2009; Mang et al., 2012). Almorexant was as effective at inducing sleep in rats as the $GABA_A$ modulator zolpidem (a Z-drug, albeit administered at supranormal doses in this study); however, although NREM was enhanced, REM sleep was over-proportionally increased. In contrast, zolpidem promoted only NREM sleep whilst substantially suppressing REM sleep in rodents (Brisbare-Roch et al., 2007), as do all $GABA_A$ positive allosteric modulators. Initial studies indicated that almorexant was well tolerated in humans, and in rats even at doses up to 1,000 mg/kg (Brisbare-Roch et al., 2007). Furthermore, almorexant was ineffective in dual orexin receptor or OX_2R KO mice, providing a proof of concept for its mechanism of action (Mang et al., 2012). Interestingly, almorexant was still able to effectively induce sleep in OX_1R KO mice, confirming the essential requirement of the OX_2R for the hypnotic actions of DORAs (Mang et al., 2012). It is interesting to note, also, that almorexant disproportionally enhanced REM sleep in the OX_1R KO mice (Mang et al., 2012). In clinical trials performed in volunteers and insomniac patients, almorexant was shown to be effective and well tolerated (Hoever et al., 2010; Hoever et al., 2012a; Hoever et al., 2012b). Increases in SE and total sleep time (TST) as well as decreases in latency to persistent sleep (LPS), latency to REM and WASO were observed (Hoever et al., 2012b). However, there was no conclusive evidence that almorexant was increasing NREM sleep in humans. The development of almorexant ceased during phase III trials for undisclosed reasons. Other notable and efficacious DORAs to have entered clinical studies include SB-649868 (Bettica et al., 2012c; Bettica et al., 2012a; Bettica et al., 2012b), filorexant (MK-6096,

Coleman et al., 2012; Winrow et al., 2012) and suvorexant (MK-4305, Cox et al., 2010; Coleman et al., 2011; Winrow et al., 2011; Connor et al., 2012; Herring et al., 2012a; Herring et al., 2012b; Ivgy-May et al., 2012; Hoyer et al., 2013; Radl, 2013; Sun et al., 2013; Michelson et al., 2014; for a comprehensive review see Jacobson et al. 2014).

Numerous studies have clearly demonstrated the effectiveness of DORAs in inducing sleep in various species including humans, however, to date, only suvorexant is currently marketed – approved in Japan in 2013, by the FDA in 2014 and in Australia in 2016, whereas lemborexant has just been approved by the FDA (Hoyer et al., 2019). Initial studies using suvorexant in rats indicated favourable pharmacokinetic properties and demonstrated significant increases in REM and delta sleep time with decreases in active wake (Cox et al., 2010). Further studies established adequate safety, tolerability and efficacy of suvorexant in pre-clinical (Winrow et al., 2011) and clinical settings (Connor et al., 2012; Herring et al., 2012a; Herring et al., 2012b; Ivgy-May et al., 2012; Sun et al., 2013; Michelson et al., 2014). Although again, there is inconclusive evidence that suvorexant increases NREM sleep in insomniac patients. Nevertheless, the lack of drug-drug interactions, no negative effects on memory and high tolerability suggests orexin receptor antagonists may present as a favourable class of drugs for promoting sleep and treating sleep/wake disorders. The relative contribution of each receptor subtype to sleep architecture, however, remains to be fully established.

1.8.5 Contributions of orexin receptor subtypes to sleep architecture

The availability of orexin receptor KO rodents to model various aspects of narcolepsy and the combined use of SORAs or DORAs in these (and normal) animals has aided in elucidating the differing roles that each orexin receptor plays in various physiological functions such as sleep. Yet the question remains as to whether blockade of only one or both receptors is more beneficial for the treatment of disorders such as insomnia. The influence of SORAs or DORAs on sleep architecture is critically important to answering this question, and to selecting the appropriate treatment to induce a balanced sleep that is physiologically similar to naturally occurring sleep.

Clearly OX_2R plays a vital role in sleep induction/maintenance and various studies have shown that OX_2R antagonism alone is sufficient for the induction of sleep (Dugovic et al., 2009; Gozzi et al., 2011; Mang et al., 2012; Betschart et al., 2013; Gotter et al., 2016). Recently, Gotter et al. (2016) published the first study demonstrating the efficacy of an OX_2R antagonist in rodent, canine and human trials. The 2-SORA MK-1064 (Roecker et al., 2014a) decreased arousal and promoted both NREM and REM sleep in human subjects and was well tolerated in

two separate studies (Gotter et al., 2016). However, rodent studies found that MK-1064 requires higher OX_2R occupancy to promote sleep in comparison to DORA-12, suggesting that OX_1R antagonism may also be contributing to the sleep-promoting efficacy of DORAs (Gotter et al., 2016). Conversely, certain findings have suggested that the additional blockade of OX_1R is detrimental to the sleep promoting effects of OX_2R antagonism. Coadministration of an OX_1R and OX_2R antagonist increased the latency to NREM and decreased the duration of NREM sleep compared to the OX_2R antagonist alone, indicating attenuation of its sleep promoting effects (Dugovic et al., 2009). Interestingly, the latency to REM sleep decreased and the REM duration exhibited a non-significant increase (Dugovic et al., 2009). Similar results were observed in a separate study, suggesting that the additional OX_1R antagonism may be unfavourably contributing to sleep architecture by enhancing REM sleep at the expense of NREM sleep (Dugovic et al., 2014). Furthermore, the DORA suvorexant was shown to alter sleep architecture in mice by selectively and disproportionately increasing REM sleep during the inactive phase, whereas the OX_2R specific antagonist IPSU did not exhibit this effect (Hoyer et al., 2013).

In contrast, other studies have suggested that dual orexin receptor antagonism is more favourable than selective OX_2R antagonism. Mieda et al. (2011) emphasised the importance of OX_1R for the regulation of sleep (especially REM) but did not specifically investigate the respective contributions of OX_1R or OX_2R antagonism. Additionally, the DORA almorexant was shown to be more effective at inducing sleep in rats than either an OX_1R selective SORA (1-SORA) or 2-SORA alone (Morairty et al., 2012). However, although almorexant increased the total amount of sleep it was more fragmented, including more bouts of wake and REM sleep, with the number of REM bouts particularly prominent. This further supports the hypothesis that the effect of OX_1R antagonism facilitates REM sleep (Morairty et al., 2012). It should, however, be noted that almorexant exhibits interesting kinetic properties, including a very slow dissociation constant from OX_2R. Therefore, for short durations it behaves much like a DORA but for longer durations (at equilibrium) it appears to act more like a selective OX_2R antagonist (Callander et al., 2013). Further studies are required to elucidate the effects on sleep architecture of different hypnotics. However, the current results suggest that hypnotic drugs like zolpidem promote only NREM sleep and substantially suppress or delay the onset of REM sleep; DORAs promote sleep but primarily by increasing REM sleep at the expense of NREM sleep and 2-SORAs promote a more balanced increase of NREM and REM sleep (at least in rodent and canine models). Therefore, assuming the high translatability of preclinical studies for DORAs remains true for 2-SORAs, 2-SORAs may prove to be the hypnotics that

produce the most physiological-like sleep in a clinical setting (Hoyer and Jacobson, 2013; Jacobson et al., 2017; Hoyer et al., 2019).

Research into the orexin system and orexin receptor antagonists implicate the LC as potentially playing a crucial role in the regulation of REM sleep. The LC receives abundant projections from orexin neurons and expresses the densest levels of OX_1R of any brain region. The LC sends inhibitory inputs to 'REM-On' brain regions including the PPT, laterodorsal tegmental nucleus (LDT) and sublaterodorsal nucleus (SLD) and sends excitatory inputs to 'REM-off' regions in the ventral periaqueductal gray (vPAG) and lateral pontine tegmentum (LPT; Saper et al., 2010). LC neuronal activity is also correlated with the sleep-wake cycle (Aston-Jones and Bloom, 1981). Furthermore, optogenetic stimulation of the LC promotes arousal and sleep-to-wake transitions (Carter et al., 2010; Carter et al., 2012), whilst orexin-A also activates LC neurons to promote arousal (Hagan et al., 1999; Gompf and Aston-Jones, 2008) and importantly, suppress REM sleep (Bourgin et al., 2000; Smith et al., 2003). This suppression effect was reversed by a selective OX_1R antagonist (Smith et al., 2003). Ablation of LC neurons in rats attenuated the relative increases in REM sleep typically observed following almorexant treatment (Schwartz et al., 2016). LC-ablated rats exhibited a decreased time spent in REM and a decreased REM:NREM ratio as compared to non-ablated rats following almorexant. The effect of LC ablation was not observed with zolpidem, indicating specificity for orexin system involvement and the requirement of an intact LC (Schwartz et al., 2016). These findings indicate that alterations in sleep architecture by increasing REM sleep are likely mediated by blockade of OX_1R in the LC. Antagonism of OX_1R is therefore likely to enhance REM sleep in the presence of OX_2R antagonism, whereas 1-SORAs alone do not promote sleep of any sort (Dugovic et al., 2009; Dugovic et al., 2014). Further research into the role the LC and OX_1R plays in the regulation of REM sleep is warranted.

1.9 Summary

Disrupted sleep has been associated with a number of neuropsychiatric and neurodegenerative disorders including AD and FTD. The bidirectional relationship between sleep and disease pathology has developed from numerous lines of evidence, particularly involving Aβ and tau pathologies. Various approaches for treating sleep/wake disturbances are currently available, however, in general, their adverse drug-drug interactions, potential for dependence and/or tolerance, impairment of memory/cognition and inability to produce physiological-like sleep architecture renders them undesirable for treating sleep/wake disturbances, especially in neurodegenerative disorders such as AD and FTD.

The orexin system is the newest target for sleep promoting therapeutics and the development of orexin receptor antagonists has enabled the specific and selective modulation of this system to promote sleep. Orexin receptor antagonists have numerous potential advantages including lack of drug-drug interactions with alcohol or other narcoleptics, no cognitive impairment and there is no evidence at present for a risk of tolerance/dependence. DORAs and 2-SORAs have differing effects on sleep architecture – DORAs promote sleep primarily by increasing REM sleep at the expense of NREM sleep as evidenced from both preclinical and clinical studies, whereas 2-SORAs tend to induce a more balanced and physiologically natural sleep (at least in preclinical species). As the understanding of these mechanisms evolves and the development of more selective compounds continues, the indications for orexin receptor antagonists are likely to extend beyond the treatment of insomnia. Improving sleep with orexin receptor antagonists therefore presents as a potentially viable and efficacious therapeutic option in neurodegenerative disorders. The concept that early sleep disturbances derive from tau pathologies in the ascending arousal regions of the brain, which receive dense orexinergic inputs, further supports the idea of using orexin receptor antagonists to manage sleep in the preclinical stages of neurodegenerative disorders, before the onset of any substantial physiological insult or cognitive impairment.

Despite the emerging evidence outlined above, there is still substantial research required to further elucidate the interactions between the pathogenesis of neurodegenerative disorders and sleep/wake disruptions. In particular, there is a considerable gap in the preclinical literature regarding the relationship between tau and sleep/wake behaviour and studies reporting the sleep/wake phenotype in pure tauopathy mouse models are currently limited.

1.10 Thesis objectives

The primary research focus of this thesis was to investigate the role that hyperphosphorylated tau plays in mediating sleep/wake disturbances and cognitive impairments in a transgenic mouse model of tauopathy. The therapeutic potential of restoring physiological sleep using orexin receptor antagonists was also assessed. The rTg4510 transgenic mouse model of tauopathy (Ramsden et al., 2005; Santacruz et al., 2005) was primarily used throughout these studies. rTg4510 mice overexpress human tau containing the P301L *MAPT* mutation (genetically associated with FTD-tau) and are a model of FTD-tau and also of the neuronal tau hyperphosphorylation observed in AD. Transgene expression is specifically restricted to forebrain structures (due to a Ca^{2+}-calmodulin-dependent protein kinase II (CaMKII) promoter) and inactivated by administration of the tetracycline analogue doxycycline (Dox). The repressible transgene expression was ideal for investigating the specific hypotheses of this thesis and was a key reason rTg4510 mice were selected. Although recently, more extensive characterisation of the rTg4510 model has revealed non-targeted gene KO (Gamache et al., 2019), which may influence the breadth of conclusions that can be drawn from this model (see Chapter 6 for more detail).

The first experiment in this series of studies (Chapter 2) aimed to characterise orexin receptor mRNA expression in the brains of both rTg4510 and tau KO mice using *in situ* hybridisation (ISH). The hypotheses tested, generated from the observed hyperarousal phenotype of both tau KO and transgenic mice, was that tau alterations would modify the expression of these receptors in components of the ARAS. This experiment thus provided information as to whether tau affects the orexin system at the molecular level, hence potentially contributing to sleep/wake disturbances in tauopathy.

Next, the functional and behavioural consequences of hyperphosphorylated tau were investigated (Chapter 3). Here, the aim was to characterise the sleep/wake phenotype of rTg4510 mice and to investigate the effects of suppressing tau transgene expression with Dox treatment on sleep/wake behaviour, in conjunction with its effects on the more thoroughly established cognitive and neurodegenerative phenotype of rTg4510 mice. This experiment provided information as to the role of tau at mediating sleep/wake and cognitive impairments and aimed to determine if these deficits can be attenuated or reversed by reducing tau levels.

The bidirectional relationship between sleep and tau pathology was then further investigated (Chapter 4). In this experiment, the hypothesis was that restoring sleep in a model of tauopathy would improve the cognitive and other tau-associated phenotypes. The aim was to determine if pharmacologically promoting sleep, with two different orexin receptor

antagonists and treatment approaches, improved cognition and/or slowed tauopathy progression in rTg4510 mice. These experiments provided information as to the potential therapeutic benefit of sleep in neurodegenerative mouse models, further implicating their bidirectional link.

Finally, the sleep/wake profile of rTg4510 mice in response to acute administration of hypnotic drugs was assessed (Chapter 5). These experiments provide the first investigation of the effects of different hypnotic principles in a model of tauopathy. Furthermore, they facilitated comparisons between the acute (Chapter 5) and chronic (Chapter 4) responses of rTg4510 mice to orexin receptor antagonists.

Information generated in this thesis thus provides new insights into a rather neglected, but vitally important, component of AD and FTD research, by further defining the role of tau in the bidirectional relationship between sleep and disease. Furthermore, this research highlights implications for the use of sleep-promoting hypnotics as potential therapeutic tools in tauopathy-related disorders.

Chapter 2

Decreased Orexin Receptor 1 mRNA Expression in the Locus Coeruleus in both Tau Transgenic rTg4510 and Tau Knockout Mice

Ryan J. Keenan[a], Romke Bron[b], Cameron J. Nowell[b], Daniel Hoyer[a,c,d] and Laura H. Jacobson[*a,c]

[a] Department of Pharmacology and Therapeutics, School of Biomedical Sciences, Faculty of Medicine, Dentistry and Health Sciences, The University of Melbourne, Parkville, Victoria, 3010, Australia.

[b] Drug Discovery Biology, Monash Institute of Pharmaceutical Sciences, Parkville, Victoria, 3010, Australia.

[c] Florey Institute of Neuroscience and Mental Health, Parkville, Victoria, 3010, Australia.

[d] Department of Molecular Medicine, The Scripps Research Institute, La Jolla, California, 92037, USA.

Submitted to:
Journal of Alzheimer's Disease (May, 2019)

This chapter represents the prepared manuscript submitted for publication to Journal of Alzheimer's Disease, with slight revisions and modifications to comply with thesis formatting requirements as per University of Melbourne policy.

2.1 Abstract

Sleep/wakefulness disturbances are a hallmark of the neurodegenerative disorders Alzheimer's disease (AD) and Frontotemporal dementia (FTD). A bidirectional relationship between sleep and disease pathology has been proposed, leading to a detrimental cycle that accelerates disease progression and cognitive decline. Typical sleep problems in dementia include insomnia and sleep fragmentation, which are, to some extent, reminiscent of the neurological disorder narcolepsy with cataplexy, which is caused by the loss of orexin-producing neurons. This similarity in symptoms may suggest a dysregulation in the orexin system in AD/FTD, and clinical evidence exists to support this notion. AD and FTD-tau also share the accumulation of central nervous system (CNS) tau fibrils as a core, diagnostic pathology. It was therefore aimed to characterise orexin receptor mRNA expression in the brains of tau transgenic rTg4510 and $tau^{-/-}$ knockout (KO) mice using *in situ* hybridisation (ISH), focusing on regions involved in sleep/wakefulness regulation. These data show that both rTg4510 and $tau^{-/-}$ KO mice exhibit a similarly decreased orexin receptor 1 (OX_1R) mRNA expression in the locus coeruleus (LC) compared with wildtype (WT) controls. Orexin receptor 2 (OX_2R) mRNA levels were not altered in the brains of either model. The LC is strongly implicated in the regulation of sleep/wakefulness and expresses abundant levels of OX_1R. These findings thus raise interesting questions regarding the effects of altered tau on the orexin system, specifically OX_1R, and emphasise a potential mechanism which could help to explain sleep/wakefulness disturbances reported in AD and FTD.

2.2 Introduction

Sleep/wakefulness disturbances are common in Alzheimer's disease (AD) and Frontotemporal dementia (FTD), in which they often present very early in the course of disease progression, typically preceding cognitive impairment (Prinz et al., 1982; Bathgate et al., 2001; Liu et al., 2004; Moran et al., 2005; Anderson et al., 2009; Westerberg et al., 2012; Bonakis et al., 2014; Ju et al., 2014; Lim et al., 2014). Common sleep disturbances include insomnia, sleep fragmentation, excessive daytime sleepiness, decreased NREM/REM sleep, considerable shifts in circadian rhythms and an abnormally elevated level of arousal around bedtime (sundowning syndrome) (Bonanni et al., 2005; Crowley, 2011; Slats et al., 2013; Lim et al., 2014; Musiek et al., 2015; Peter-Derex et al., 2015; Urrestarazu and Iriarte, 2016; Cagnin et al., 2017). There are numerous lines of evidence suggesting that a bidirectional relationship exists between sleep disturbances and AD pathology. A positive feedback loop has been proposed in which the initial AD pathology disrupts the sleep-wake cycle, which subsequently negatively influences disease development to exacerbate and accelerate AD pathology (Ju et al., 2014; Lim et al., 2014). Animal models are currently being used to delve deeper into the potential mechanisms mediating these processes, however, the root causes of these sleep/wakefulness disturbances remain to be determined.

Although not as severe, sleep/wakefulness disruptions in AD parallel some of the distinguishing features of the neurological disorder narcolepsy with cataplexy (type 1 narcolepsy). In humans, narcolepsy with cataplexy (Mignot, 1998; Siegel and Boehmer, 2006; Sakurai, 2007; Scammell, 2015; Kornum et al., 2017) is caused by the loss of orexin-producing neurons and is characterised, amongst other features, by highly fragmented sleep including fast transitions from wakefulness to sleep, with a sudden loss of muscle tone. Furthermore, mice with disruptive modifications of the orexin system (at the gene, neuronal, peptide or receptors level) all exhibit remarkably similar phenotypes (Chemelli et al., 1999; Hara et al., 2001; Willie et al., 2003; Beuckmann et al., 2004; Kalogiannis et al., 2011; Tabuchi et al., 2014; Bernard-Valnet et al., 2016; Branch et al., 2016), which echo the characteristic symptoms of human narcolepsy with cataplexy, cementing orexin neuron loss as the primary mechanism underlying this disorder.

The orexin system (de Lecea et al., 1998; Sakurai et al., 1998) plays a crucial role in the regulation of sleep and wakefulness (Sutcliffe and de Lecea, 2002; Hoyer and Jacobson, 2013). The two neuropeptides orexin A and orexin B are synthesised by neuronal cell bodies restricted primarily to the lateral hypothalamus (LH; Peyron et al., 1998; van den Pol et al., 1998; Nambu et al., 1999). Orexin fibres broadly innervate the central nervous system (CNS;

Peyron et al., 1998; Nambu et al., 1999) and the neuropeptides act on two G-protein coupled receptors (GPCRs) – orexin receptor 1 (OX_1R) and orexin receptor 2 (OX_2R). A widespread, but distinct expression profile of the two receptors is observed throughout the brain (Marcus et al., 2001). Dense orexinergic innervation and high orexin receptor expression levels are found especially in brain regions involved in the regulation of arousal and accordingly, activation of orexin receptors promotes wakefulness (Marcus et al., 2001), whereas antagonism of OX_2R, or OX_2R and OX_1R together, promotes sleep (Hoyer and Jacobson, 2013; Jacobson et al., 2017). The arousal promoting effects of orexin originate from their excitatory inputs to wake-active neuronal populations, including the noradrenergic locus coeruleus (LC), histaminergic tuberomammillary nucleus (TMN), serotonergic dorsal raphe nucleus (DRN), dopaminergic ventral tegmental area (VTA) and the cholinergic basal forebrain (Saper et al., 2010). In particular, the LC and TMN play key roles in the regulation of arousal and express almost exclusively OX_1R and OX_2R, respectively (Marcus et al., 2001). Dysfunctions in the orexin system therefore have the potential to cause sleep/wakefulness disturbances. The similarities in sleep/wakefulness symptoms of AD and narcolepsy with cataplexy may be suggestive of a dysregulation of the orexin system in the early stages of AD. Indeed, there is clinical evidence to support the concept that orexin signalling is altered in AD, given that cerebrospinal fluid (CSF) orexin levels are elevated (Liguori et al., 2014b; Liguori et al., 2016; Gabelle et al., 2017) and negatively correlate with daytime somnolence (Liguori et al., 2014b). Additionally, there is a reduced expression of OX_1R mRNA in the hippocampus of AD patients (Davies et al., 2015).

The characteristic lesions of AD are extracellular senile or neuritic plaques composed of aggregated amyloid beta (Aβ) peptides and intracellular neurofibrillary tangles (NFTs) comprised of hyperphosphorylated tau protein (Braak and Braak, 1991b; Dickson, 1997; Selkoe, 1997, 2001; Blennow et al., 2006; Querfurth and LaFerla, 2010; Ballard et al., 2011; Holtzman et al., 2011). Many of the preclinical studies conducted so far have focused on the Aβ aspect of the bidirectional relationship between sleep and AD pathology (Cirrito et al., 2005; Kang et al., 2009; Bero et al., 2011; Roh et al., 2012), however, it is plausible that tau could also play a key role in this process. Patients with frontotemporal dementia (FTD) exhibit substantial sleep and circadian disturbances (Bathgate et al., 2001; Liu et al., 2004; Anderson et al., 2009), which are similar to, and possibly even more severe than those experienced by AD patients (Bonakis et al., 2014). Although FTD is genetically heterogeneous, one genetic variant (FTD-tau; Forrest et al., 2018) is caused by a mutation in the tau gene (*MAPT*) located on chromosome 17 (Hutton et al., 1998; Goedert and Spillantini, 2006) and sporadic tauopathy

in FTD also exists. Furthermore, both tau transgenic mice and tau$^{-/-}$ knockout (KO) mice show disrupted sleep/wakefulness phenotypes (Cantero et al., 2010; Holth et al., 2017b). Together these data may point to a role of altered tau function and/or its negative neurobiological consequences in mediating sleep/wake disturbances in AD and FTD.

In light of these findings, the present study resolved to test the hypothesis that tau influences the orexin system and that this influence may be implicated in the underlying mechanisms of sleep/wakefulness disturbances in both AD and FTD-tau. This study therefore aimed to characterise and quantify orexin receptor mRNA expression in the brains of rTg4510 mice which overexpress human tau harbouring the FTD-associated P301L mutation, and tau$^{-/-}$ KO mice, using *in situ* hybridisation (ISH), focusing in particular on brain regions associated with the regulation of sleep and wakefulness.

2.3 Materials and methods

Animals

Mice used in this study were the rTg4510 transgenic mouse model of tauopathy (Ramsden et al., 2005; Santacruz et al., 2005) and tau$^{-/-}$ KO mice on a C57BL/6 background (Dawson et al., 2001; Lei et al., 2014).

rTg4510 mice were bred in house, as previously described (Ramsden et al., 2005; Santacruz et al., 2005). In brief, FBV/N mice expressing human tau containing the *MAPT* P301L mutation (associated with FTD-tau in humans) downstream of a tetracycline operon-responsive element (TRE) were crossed with 129SVeV mice expressing a tetracycline-controlled transactivator (tTA) under control of the Ca^{2+}-calmodulin-dependent protein kinase II (CaMKII) promotor. In this mouse, constitutive expression of the tau transgene (in the absence of doxycycline) is specifically restricted to forebrain structures due to the CaMKII promotor.

Tau KO (tau$^{-/-}$) or WT (tau$^{+/+}$) mice as initially described in Dawson et al. (2001) were bred in house as previously reported (Lei et al., 2014). Mice bred on the C57BL/6 background were used for the present experiments. All mice were genotyped using a standardised polymerase chain reaction (PCR) assay for tail DNA (Transnetyx Inc., Cordova, TN, USA).

5.2-month-old male rTg4510 (n = 6) and WT (n = 6) mice were used. This age was selected as modified variants of tau and tangle-like inclusions have already begun to develop

however, neurodegeneration and extensive neuronal or synaptic loss has yet to occur (Ramsden et al., 2005).

6-month-old tau$^{-/-}$ (n = 5 males; n = 4 females) and tau$^{+/+}$ (n = 5 males; n = 3 females) mice were also used in this study. This age was selected given the fragmented sleep (Cantero et al., 2010) and olfactory deficit (Beauchamp et al., 2018) phenotype manifested in these mice around this age.

All mice were group-housed in standard transparent individually ventilated cages (IVC; 29.5 x 16 x 13 cm) with sawdust and tissue paper nesting material. The holding room was under a 12 h light/dark cycle (lights on at 0700h). Standard rodent food and water were available *ad libitum.* All experimentation was performed in accordance with the Prevention of Cruelty to Animals Act (2004), under the guidelines of the National Health and Medical Research Council Code of Practice for the Care and Use of Animals for Experimental Purposes in Australia (2013) and approved by The Florey Animal Ethics Committee (AEC number: 16-022). All efforts were made to minimise animal suffering.

Perfusion and brain collection

Mice were culled during the inactive phase (between 1000-1600h). All sample collection was performed under RNase-free conditions (all instruments and surfaces were pre-treated with RNase Zap®, Sigma-Aldrich). Mice were terminally anaesthetised with a lethal dose of sodium pentobarbitone (80 mg/kg) and perfused with approximately 3 times their blood volume (estimated as 7% of body weight) of 0.01M phosphate-buffered saline (PBS) containing heparin (55.6 mg/L) immediately followed by the same volume of 4% paraformaldehyde (PFA). Brains were extracted and post-fixed in 4% PFA for 24 h at 4°C, washed (2 x 30 mins) in ice-cold 0.1% diethylpyrocarbonate (DEPC)-treated PBS and then equilibrated in 30% (w/v) molecular grade sucrose in DEPC-treated PBS until the brain had sunk (2-3 days). Brains were snap-frozen in isopentane cooled on dry ice and stored at -80°C until sectioning.

Cryosectioning

All brains were placed in a -20°C freezer the day before sectioning. 30 µm-thick coronal sections of a 1 in 5 series (A→E) were cut through the brain (minus the olfactory bulbs) on a cryostat (Leica, Leica Microsystems, Wetzlar, Germany). Sections were mounted 12 sections per slide on positively charged Superfrost Ultra Plus glass slides (Thermo Scientific) and air-dried for at least 1-2 h at room temperature to ensure adequate adherence. Slides were then

stored at -80°C, with desiccant, until ISH procedures. All cryosectioning was performed under RNase-free conditions.

In situ hybridisation (ISH)

Generation of digoxigenin (DIG) labelled cRNA probes

The forward and reverse primers used to amplify the mouse orexin receptor probe sequences were designed using Vector NTI® software (ThermoFisher Scientific) as previously described (Bron et al., 2013; Bron et al., 2014). Briefly, the Ensembl database was used to identify target sequences for the genes of interest (*mHcrtr1* and *mHcrtr2*) and to design the forward and reverse primers. The primer sequences were as follows:

mHcrtr1 forward primer: TGAACTCTACCCCAAGATCTATCACA

mHcrtr1 reverse primer:

GAATTCTAATACGACTCACTATAGGGAGAGTGAATATGTCTGTGGGGACCTTT

mHcrtr2 forward primer: ATTCCCGGAACTTCTTCTGTGGTT

*mHcrtr*2 reverse primer:

GAATTCTAATACGACTCACTATAGGGAGATGACATCTCACATCGAAGGCTTGA

Underlined sequences represent the T7 recognition sites located in the reverse primers. All primers were initially made up to a 40 µM stock solution in endotoxin free TE buffer (Invitrogen) and then diluted with molecular grade ultrapure water (Invitrogen) to a working solution of 2 µM.

cDNA containing both the *mHcrtr1* and *mHcrtr2* sequences for the cRNA probes were generated from RNA extracted from the trigeminal ganglion of a C57BL/6 mouse using a Qiagen RNAEasy® kit (Chatsworth, CA, USA). RNA concentration and purity were determined using a Nanodrop 1000 Spectrophotometer. Reverse-transcription (RT) of RNA was performed using SuperScript® III (Invitrogen) according to the manufacturer's instructions.

PCR was performed on a mixture containing PCR mastermix (5 Prime), the relevant forward primer, the relevant reverse primer, molecular grade ultrapure water and cDNA. Thermal cycler settings were as follows: 1 hold at 94°C (3 min) followed by 12 touchdown cycles of 94°C (40 s), 68-57°C (40 s, 1°C decrease per cycle), 72°C (90 s), then 35 cycles of 94°C (40 s), 56°C (40 s), 72°C (90 s) and finally holds of 72°C (10 min) and 12°C (∞). The PCR product (containing the specific T7 polymerase promotor sequence) was used to generate the cRNA probes by *in vitro* transcription. Briefly, a master mix containing 1x transcription buffer (Roche), 10 mM Dithiothreitol (DTT; Sigma-Aldrich), DIG-RNA labelling mix

(Roche), molecular grade ultrapure water, RNAse out (Invitrogen), the generated PCR templates and T7 RNA polymerase (Roche) was incubated at 37°C for 90 min. DNase (Roche) was then added to destroy the DNA template and the solution was incubated at 37°C for a further 7 min. The reaction was stopped with molecular grade 0.5 M ethylenediaminetetraacetic acid (EDTA; Sigma-Aldrich) and the nucleic acid precipitated with 8 M lithium chloride solution (Sigma-Aldrich). 70 µL of 100% ethanol was then added and the solution stored at -20°C overnight. The following day probe mixtures were centrifuged at 21,000 x g for 10 min at room temperature, the supernatant was discarded and the pellet was re-suspended in 70% ethanol in ultrapure water. Following re-centrifugation at 21,000 x g for 5 min at room temperature the supernatant was discarded and the pellet allowed to air dry for 45 min. The pellet was suspended in ultrapure water and 100 mM DTT was added to a final concentration of 10 mM. To confirm generation of the cRNA probes, 5 µL of solution was run in a 0.6% agarose gel for 12 mins at 70V and imaged on a Bio-Rad Chemi Doc™ MP imager (Hercules, CA, USA) coupled with Bio-Rad Image Lab™ software version-4.1. OX_1R and OX_2R cRNA probes were stored at -80°C until required.

ISH protocol

One slide from series B, C and D and two from series E (due the small size of the LC brain structure located in this series) were allocated to hybridisation with the OX_1R receptor probe from each mouse. One slide from series B, C, D and E were allocated to hybridisation with the OX_2R receptor probe. During workup of the ISH protocol and validation of the cRNA probes, several ‘no probe’ controls were also run. No detectable staining was observed (Fig. 2.1A-C).

All steps performed prior to hybridisation of the cRNA probes were conducted under RNase-free conditions. Required slides were removed from -80°C storage and allowed to dry at room temperature for 1-2 h. Slides were placed in Hellendahl jars and washed (2 x 10 min) in DEPC-PBS then placed flat in slide boxes (Kartell Labware) filled with 50 ml of humidifying buffer containing 50% formamide (Sigma-Aldrich) and 1x salts solution. The OX_1R and OX_2R RNA probes were diluted (1:100) separately in hybridisation buffer containing 50% formamide, 10% dextran sulphate (ThermoFisher Scientific), 1x salts solution, 1 mg/ml RNA from yeast (Sigma-Aldrich) and 1x Denhardt’s solution (Invitrogen), then heated in a water bath at 70°C for 20 min. 300 µL of the relevant probe mixture was added to each slide, a coverslip was added and the lid of the slide box closed and sealed with masking tape. Slides were incubated overnight in an oven at 60°C to allow hybridisation of the cRNA probe to the complimentary mRNA sequence of the orexin receptors. The following day the coverslips were

detached via gravity and the slides washed (2 x 30 min) at 60°C in Hellendahl jars containing pre-heated (~20 min) washing solution consisting of 1x saline sodium citrate (SSC), 50% formamide and 0.1% Tween-20 (Sigma-Aldrich). The slides were then washed (5 x 10 min) at room temperature on a rocker with 1x MABT solution (100 mM maleic acid (Sigma-Aldrich), 150 mM sodium chloride (Sigma-Aldrich), 0.1% Tween-20 (Sigma-Aldrich), pH 7.5). Slides were then incubated for 90 min at room temperature with blocking solution consisting of 2% Roche blocking reagent (Roche), 1x MABT and 20% inactivated sheep serum (Sigma-Aldrich). After blocking, the slides were incubated with Sheep anti-DIG-AP Fab fragments (Roche, Cat. No. 11093274910) in blocking solution (1:2000), overnight at 4°C in slide boxes containing water. The antibody binds to the DIG-labelled cRNA probe. The following day excess antibody solution was removed and the slides washed (5 x 10 min) in 1x MABT solution at room temperature on a rocker. This was followed by (2 x 10 min) washes with alkaline phosphatase (AP) buffer consisting of 100 mM sodium chloride, 50 mM magnesium chloride, 100 mM Tris pH 9.5 and 0.1% Tween-20. Staining solution was prepared by dissolving 5% (w/v) Mowiol (polyvinylalcohol 4-88; Sigma-Aldrich) in AP buffer with heating and stirring and then adding 20 µL/ml of nitro-blue tetrazolium/5-bromo-4-chloro-3'-indolyphosphate (NBT/BCIP; Roche). Slides were dried and positioned in slide boxes then 400 µL of staining solution was added. The NBT/BCIP reagent generates an intense purple/black precipitate when reacted with the AP-conjugated antibody. The reaction was allowed to proceed at room temperature and monitored using a dissection microscope every 30-60 min until sufficient staining had developed, typically 6-8 h. Once sufficient staining had developed excess solution was removed and slides were washed (3 x 10 min) with PBS at room temperature on a rocker. Slides were air-dried and then mounted with Fluorescence Mounting Medium (DAKO), a coverslip added and then stored at 4°C in the dark to dry, until imaging.

Image acquisition and analysis

ISH-stained slides were scanned using a Pannoramic Scan II (3DHISTECH) digital slide scanner. Images were captured using Pannoramic Scanner version 1.22 SP software (3DHISTECH) and manually viewed using CaseViewer version 2.2 software (3DHISTECH) to determine appropriate sections for analysis. Once sections were assigned for quantitative analysis the relevant images were exported as TIFF files using Pannoramic Viewer version 1.15.4 (3DHISTECH).

The brain regions analysed included the cerebral cortex, DRN, hippocampus, LH, LC, paraventricular nucleus of the thalamus, TMN and the VTA (Fig. 2.1). 2-3 sections per brain

region were selected for analysis using Fiji/ImageJ software (Schindelin et al., 2012) and mRNA receptor expression was quantified using custom written analysis scripts.

An investigator blinded to animal genotype and sex manually outlined the individual brain regions of interest (ROI) using the freehand region tool (see Lazic, 2009) and the area and outline of the region was measured and saved. A Gaussian blur (sigma = 2) was applied to the image and the background staining subtracted using a rolling ball subtraction (radius = 50). After background subtraction, positive staining was extracted from the image using the colour deconvolution plugin built into Fiji/ImageJ and the extent of positive staining was thresholded using the IJ_IsoData auto threshold algorithm. The automatically set threshold value was then manually adjusted to closely match the intensity of staining on the section. The original image was positioned side by side with the thresholded image when setting the threshold value, for accuracy and consistency. Once the threshold was set, the ROIs were reloaded onto the image and the area of positive staining within the ROI was calculated. Therefore, the percentage of stain-positive pixels in a target region was determined and was considered a reliable estimate of the relative expression of OX_1R or OX_2R receptor mRNA. Typically, 2-4+ ROI replicates per brain region were used, taken from up to 3 different brain sections, and averaged together for the overall value specified for that brain region.

Statistical analysis

Statistical analyses were performed using the software package GraphPad Prism (Version 8.0.0 for Windows). Effects of sex or brain region hemisphere on expression of OX_1R or OX_2R were first analysed by Student's t-test to determine if any sex or hemisphere differences were evident. Percentage OX_1R or OX_2R mRNA expression were analysed using Student's t-test between genotype (rTg4510 vs. WT; or $tau^{-/-}$ vs. $tau^{+/+}$) for both receptors (OX_1R and OX_2R) and within each brain region. For all analyses, $P < 0.05$ was considered to be statistically significant.

2.4 Results

rTg4510 and tau$^{-/-}$ KO mice do not exhibit brain hemisphere or sex differences in orexin receptor mRNA expression

There was no effect of brain hemisphere or sex in either the rTg4510 or tau$^{-/-}$ KO strain (Appendix II), therefore averages across hemispheres were used and the data from the two sexes pooled for subsequent analyses. Representative images of ISH staining are shown in Fig. 2.1.

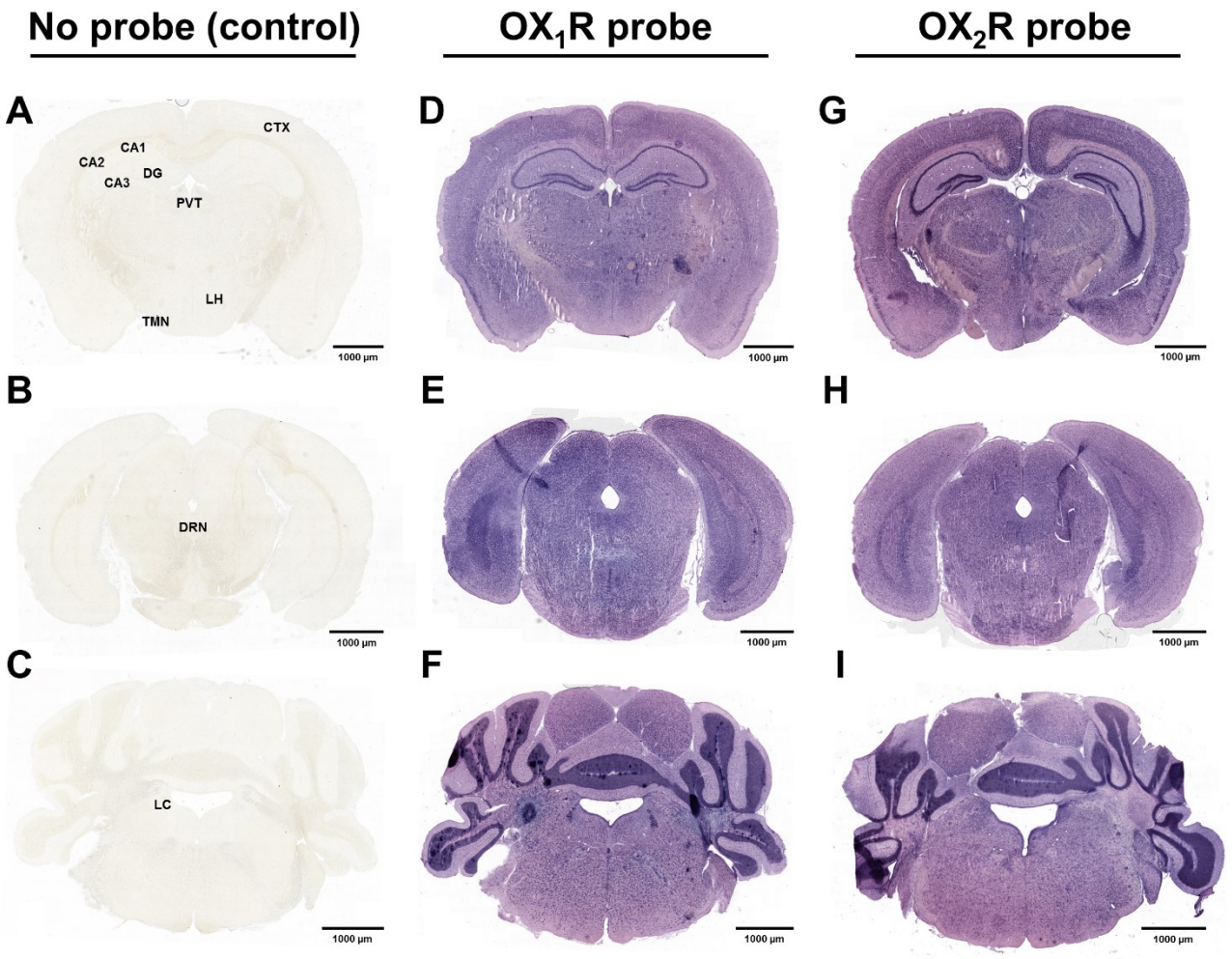

Figure 2.1. Representative sections hybridised with orexin receptor RNA probes.
A-I, Coronal brain sections following *in situ* hybridisation (ISH) procedures hybridised with no probe (***A-C***), OX_1R RNA probe (***D-F***) and OX_2R RNA probe (***G-I***). The locus coeruleus (LC) expresses abundant OX_1R and is distinctly visible in F. *CA1* CA1 subfield of hippocampus; *CA2* CA2 subfield of hippocampus; *CA3* CA3 subfield of hippocampus; *CTX* cerebral cortex; *DG* dentate gyrus; *DRN* dorsal raphe nucleus; *LC* locus coeruleus; *LH* lateral hypothalamus; *PVT* paraventricular nucleus of the thalamus; *TMN* tuberomammillary nucleus.

rTg4510 mice exhibit decreased orexin receptor 1 mRNA expression in the locus coeruleus

rTg4510 mice exhibited a decreased OX_1R mRNA expression in the LC compared with their WT controls ($M_{WT} - M_{rTg4510} = 11.47$, $t = 3.216$, $df = 9$, $P = 0.0105$; Fig. 2.2A). rTg4510 mice also exhibited an increased OX_1R mRNA expression in the CA1 subfield of the hippocampus ($M_{WT} - M_{rTg4510} = -15.55$, $t = 3.260$, $df = 9$, $P = 0.0098$; Fig. 2.2A). No statistically significant differences were observed in OX_1R mRNA expression between genotype for all other brain regions measured. No differences were observed in OX_2R mRNA expression between genotype for all brain regions (Fig. 2.2B).

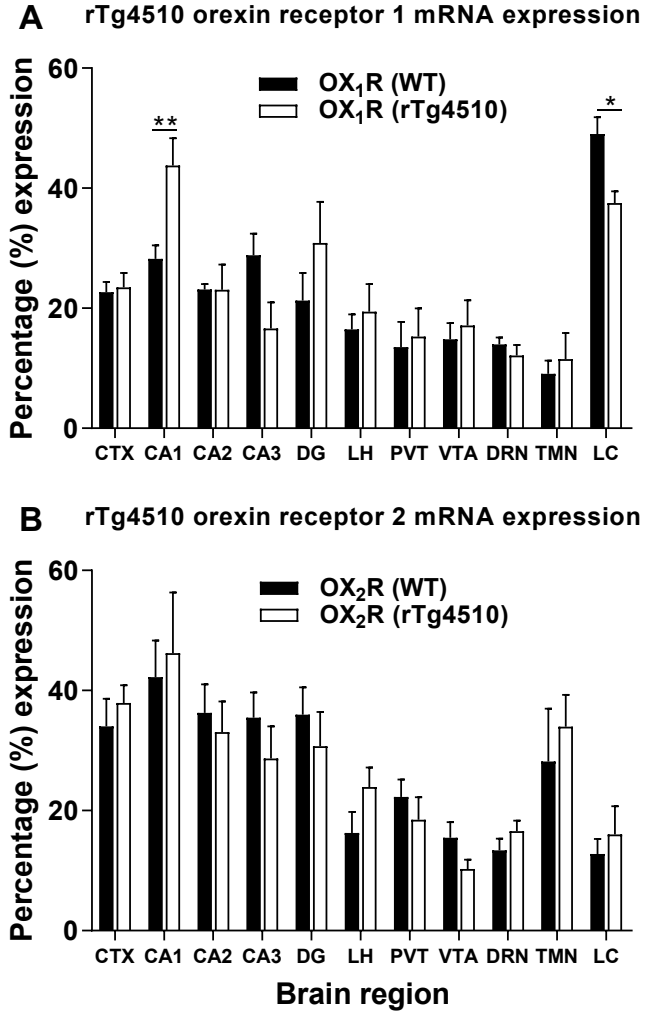

Figure 2.2. Orexin receptor mRNA expression in the brains of rTg4510 mice.

A-B, Percentage expression of OX_1R mRNA (***A***) and OX_2R mRNA (***B***) per brain region. Data are means ± SEM. n = 4-6 per brain region. $^{*}P < 0.05$, $^{**}P < 0.01$ vs. WT within brain region, by Student's t-test. *CA1* CA1 subfield of hippocampus; *CA2* CA2 subfield of hippocampus; *CA3* CA3 subfield of hippocampus; *CTX* cerebral cortex; *DG* dentate gyrus; *DRN* dorsal raphe nucleus; *LC* locus coeruleus; *LH* lateral hypothalamus; *PVT* paraventricular nucleus of the thalamus; *TMN* tuberomammillary nucleus; *VTA* ventral tegmental area.

Tau$^{-/-}$ KO mice exhibit decreased orexin receptor 1 mRNA expression in the locus coeruleus

Tau$^{-/-}$ KO mice also exhibited decreased OX_1R mRNA expression in the LC compared with their respective tau$^{+/+}$ (WT) controls ($M_{WT} - M_{tau\ KO} = 10.76$, $t = 2.939$, $df = 14$, $P = 0.0108$; Fig. 2.3A). No differences were observed in OX_1R mRNA expression between genotype for all other brain regions measured. Analogous to rTg4510 mice, no differences were observed in OX_2R mRNA expression between genotype for all brain regions (Fig. 2.3B).

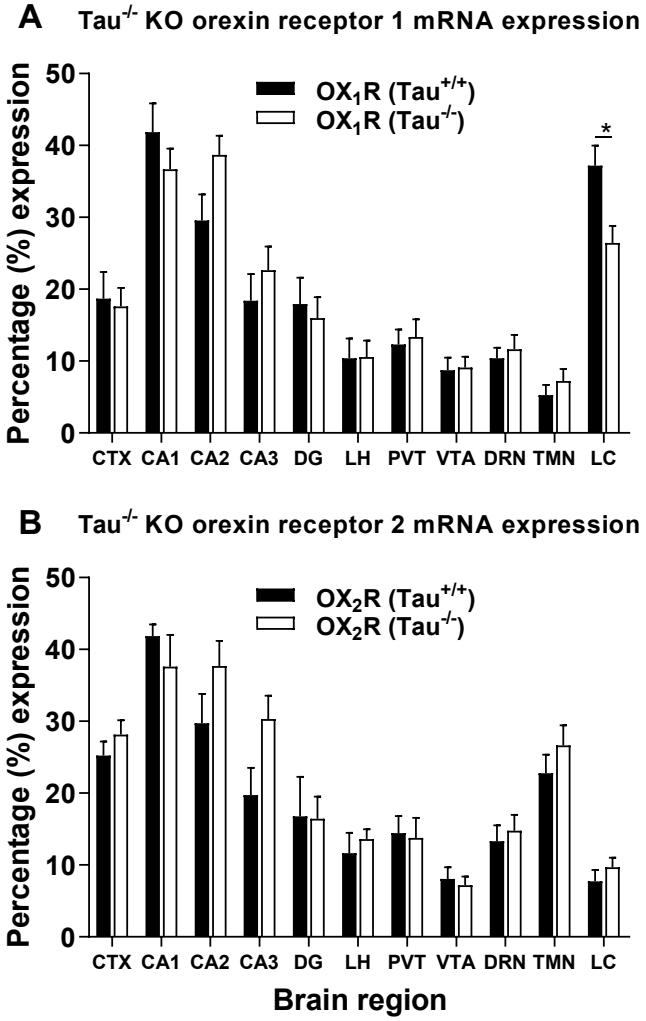

Figure 2.3. Orexin receptor mRNA expression in the brains of tau$^{-/-}$ KO mice.

A-B, Percentage expression of OX_1R mRNA (***A***) and OX_2R mRNA (***B***) per brain region. Data are means ± SEM. n = 7-9 per brain region. $^{*}P < 0.05$ vs. WT within brain region, by Student's t-test. *CA1* CA1 subfield of hippocampus; *CA2* CA2 subfield of hippocampus; *CA3* CA3 subfield of hippocampus; *CTX* cerebral cortex; *DG* dentate gyrus; *DRN* dorsal raphe nucleus; *LC* locus coeruleus; *LH* lateral hypothalamus; *PVT* paraventricular nucleus of the thalamus; *TMN* tuberomammillary nucleus; *VTA* ventral tegmental area.

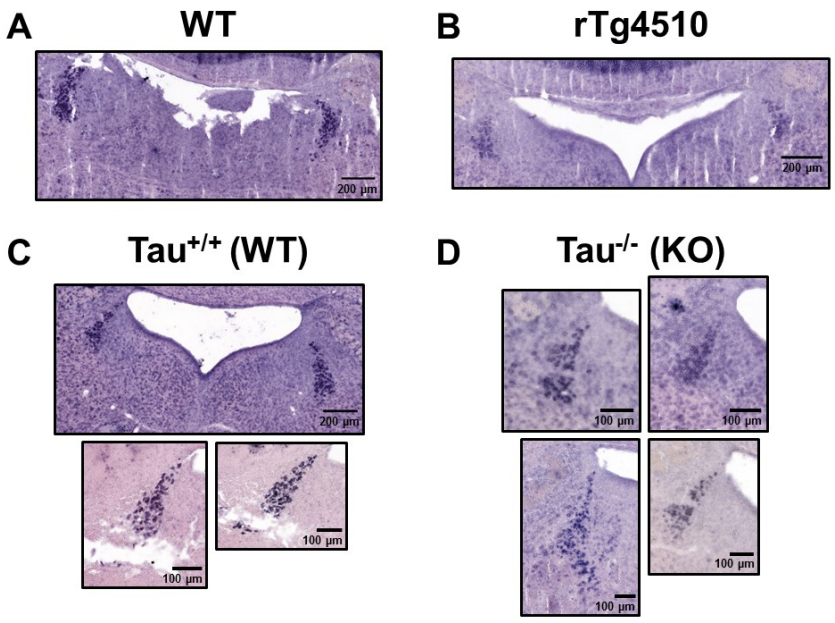

Figure 2.4. Representative orexin receptor 1 mRNA expression in the locus coeruleus.
A-D, Zoomed images of the locus coeruleus (LC) hybridised with the OX_1R RNA probe in WT (***A***), rTg4510 (***B***), $tau^{+/+}$ WT (***C***) and $tau^{-/-}$ KO (***D***) mice.

2.5 Discussion

The aim of this study was to quantify orexin receptor mRNA levels in the brains of rTg4510 and $tau^{-/-}$ KO mice compared to their WT controls, with a particular focus on brain regions involved in the regulation of sleep and wakefulness. The principle finding was a similarly decreased OX_1R mRNA expression in the LC of both mouse strains investigated. An increased OX_1R mRNA expression was also observed in the CA1 hippocampal subfield in rTg4510 mice. Similar findings across both strains raises interesting questions regarding the potential mechanisms by which altered tau function may be influencing the orexin system. Furthermore, given the critical role the LC plays in the regulation of sleep and wakefulness, these results are suggestive of a process which could help to explain the sleep disturbances reported in AD and FTD.

In the present study, OX_1R mRNA expression in the LC was reduced in both rTg4510 and $tau^{-/-}$ KO mice. The LC is a central node in the arousal pathway, a highly conserved network that promotes and maintains wakefulness (Saper et al., 2005) in humans and rodents. Wakefulness is promoted via the release of noradrenaline (NA), and over half of the brain NA and all neocortex NA comes from the LC (Valentino and Van Bockstaele, 2008; de Lecea et

al., 2012). The LC is a critical effector of sleep-to-wake transitions (Carter et al., 2010; Carter et al., 2012; Yamaguchi et al., 2018) and it receives particularly dense projections from orexinergic neurons of the LH (Peyron et al., 1998). A number of studies have illustrated the functional integration of orexin and LC neurons in gating sleep/wake arousal states (Hagan et al., 1999; Horvath et al., 1999; Gompf and Aston-Jones, 2008; Carter et al., 2012). The present data therefore suggest that alterations in tau influences the relationship between the orexinergic and LC/noradrenergic components of the ascending arousal system at a molecular level.

This alteration may be associated with previously described sleep/wakefulness phenotypes in both tau transgenic and tau$^{-/-}$ KO mice. The PS19 tau transgenic mouse, which harbour a similar tau mutation (P301S) to the rTg4510 mice used here (P301L), was recently demonstrated to exhibit a progressive hyperarousal phenotype (Holth et al., 2017b). Similarly, Cantero et al. (2010) observed that tau$^{-/-}$ KO mice also exhibit a hyperarousal phenotype, in addition to severe sleep fragmentation. In this regard, it is interesting to consider that OX_1R KO mice also exhibit mildly fragmented sleep/wakefulness (Willie et al., 2001), whereas dual receptor KO mice exhibit a more severe narcoleptic/cataplectic phenotype (Willie et al., 2003). This aligns with the alteration of OX_1R in the LC observed in the present study and with the sleep/wakefulness disturbances reported in tau mutant strains. Proportional decreases in OX_1R mRNA expression of 25-30% of WT levels were observed in the LC in this experiment. Several studies utilising siRNA have demonstrated that even subtle alterations (10-20%) in mRNA expression can result in profound behavioural and functional changes (Thakker et al., 2005; Hoyer et al., 2006; O'Connor et al., 2013) and supports the concept that these receptor changes may be contributing to the sleep/wakefulness phenotypes observed in tau mutant mice. Furthermore, given the influence of orexin on arousal and the reported elevation in orexin CSF levels in AD (Dauvilliers et al., 2014b; Liguori et al., 2014b; Liguori et al., 2016; Gabelle et al., 2017), in addition to the positive correlation between CSF orexin levels and total tau and phosphorylated tau levels in AD (Deuschle et al., 2014; Liguori et al., 2014b; Liguori et al., 2016; Osorio et al., 2016), it will therefore be of interest to assess other aspects of the orexin system in tau transgenic and tau$^{-/-}$ KO mice in the future.

The focal effect of OX_1R reduction in the LC is of particular interest since it has been amply demonstrated that the LC is selectively vulnerable in AD. Braak and colleagues recently suggested that the development of tau pathology specifically affects brain regions involved in the regulation of sleep/wakefulness first, particularly the LC (Braak and Del Tredici, 2015; Stratmann et al., 2016), and postulated this preceded amyloid pathology by a considerable period in AD (Braak and Braak, 1991b, 1995; Braak et al., 2006; Braak et al., 2011).

Pathological tau variants affecting these regions may thus contribute to sleep/wakefulness disruptions in AD and FTD-tau patients. Selective vulnerability of the LC to tau pathology has also been demonstrated in preclinical models. Iba et al. (2013) injected synthetic fibrils of recombinant tau into the hippocampus or cortex/striatum of tau transgenic (P301S) mice. Immunohistochemical analysis showed time- and region-specific development of tau pathology throughout the brain – with the LC exhibiting rapid and advanced pathology despite being physically distant from the injection site (Iba et al., 2013). In fact, tau pathology developed faster and was more advanced in the LC than at the injection site itself, demonstrating that the LC is particularly vulnerable to the development of tau pathology. These data further suggest that excitatory input to the LC, in the form of orexin, is modulated under conditions of altered tau.

The mechanism responsible for altering OX_1R in the LC in tau mutant mice in the present study has yet to be defined. It is currently unclear if the LC expressed less OX_1R mRNA per neuron or if there was a loss of LC cells. If the latter was the case it may also have been expected to observe a decrease in OX_2R mRNA expression in the LC of tau mutant mice, which was not the case. However, the LC expresses minimal OX_2R and therefore ISH may not have been sensitive/specific enough to detect subtle difference at this level of expression. Alternatively, the loss of LC neurons has been associated with AD pathology in both humans (Bondareff et al., 1982; Bondareff et al., 1987; German et al., 1987; German et al., 1992; Manaye et al., 1995) and rodent models (O'Neil et al., 2007; Liu et al., 2008b; Manaye et al., 2013). Pertinently for this study, extended wakefulness/disrupted sleep has also been demonstrated to cause LC cell loss in WT mice (Zhang et al., 2014; Zhu et al., 2016).

Almost identical results were observed in this study in the LC, across the two strains investigated. This is interesting given that tau pathology in the form of a toxic gain of function may be proposed to have contributed to the observed alterations in rTg4510 mice, however, the same mechanism cannot be proposed in the $tau^{-/-}$ KO mice given the absence of tau. Tau hyperphosphorylation has also been suggested to induce tau loss of function (Iqbal et al., 2005) – an explanation that is compatible with the phenocopy of tau transgenic and KO mice in the present study, and indeed with the similar hyperarousal and fragmented sleep/wakefulness phenotype between $tau^{-/-}$ KO (Cantero et al., 2010) and P301S mice (Holth et al., 2017b). Given the two distinct mouse models used in the current study it appears that irrespective of the specific mechanism by which tau function is lost the resulting phenotype is similar at both a functional (hyperarousal and sleep/wakefulness fragmentation) and molecular (OX_1R expression) level.

An increase in OX_1R mRNA expression in the CA1 subfield of the hippocampus was also observed in rTg4510 mice but not in $tau^{-/-}$ KO mice. Changes in hippocampal OX_1R have been reported in AD post-mortem tissue using PCR methods (Davies et al., 2015), although specific subfields were not analysed in that study. It is difficult to interpret these findings based solely on the present data and in the context of scarce literature regarding specific orexin receptor/system changes in the hippocampus in AD. Although no changes in the hippocampus were observed in $tau^{-/-}$ KO mice, given that the two models are genetically diverse and on different background strains, identical results across all measured parameters were not expected. As discussed above, the LC appears to be susceptible in both models and is potentially due to the loss of function of tau. Furthermore, rTg4510 mice have been shown to develop hippocampal-dependent cognitive deficits (Ramsden et al., 2005; Santacruz et al., 2005; Blackmore et al., 2017) whereas $tau^{-/-}$ KO mice have no reported cognitive impairment at the age investigated in this study (Morris et al., 2013; Lei et al., 2014). Akbari et al. (2006) found that antagonism of OX_1R in the CA1 subfield impaired spatial memory in rats, implicating its involvement in hippocampal-dependent learning. The differences observed in the CA1 subfield could thus be compensatory upregulation of OX_1R mRNA in response to hippocampal insult from hyperphosphorylated tau and the resulting cognitive decline – a phenotype not present in $tau^{-/-}$ KO mice at 6 months of age. Further investigations are warranted.

In conclusion, the aim of this study was to characterise and quantify orexin receptor mRNA expression in the brains of rTg4510 and $tau^{-/-}$ KO mice using ISH, focusing in particular on brain regions associated with the regulation of sleep and wakefulness. It was observed that rTg4510 and $tau^{-/-}$ KO mice exhibited decreased OX_1R mRNA expression in the LC compared to WT controls. The similar findings across the two models highlights a comparable molecular consequence – which may relate to the loss of function of tau in both the KO and the rTg4510 model. The differences observed in the LC aligns with the current literature regarding the vulnerability of the LC and spread of tau pathology in AD. Furthermore, given the LC's crucial role in arousal regulation, these data offer an insight into how sleep/wakefulness disturbances may manifest over the course of AD progression.

Conflicts of interest

The authors have no conflict of interest to report.

Acknowledgements

The authors thank Sanjida Mir, Tina Carter and Leah Beauchamp for expert technical assistance and advice. This work was funded by the Alzheimer's Association Grant 2016-NIRG-396905 to LHJ and DH. The Florey Institute of Neuroscience and Mental Health acknowledge the support of the Victorian Government and in particular the funding from the Operational Infrastructure Support Grant.

Chapter 3

Tau Transgene Suppression Rescues Cognitive and Neurodegenerative Phenotypes but not Hyperarousal in the rTg4510 Mouse Model of Tauopathy

3.1 Abstract

Alzheimer's disease (AD) and tau-variant frontotemporal dementia (FTD-tau) are neurodegenerative disorders which share the development of tau pathologies and sleep/wakefulness disturbances. A bidirectional relationship between sleep and disease pathology has been proposed and current evidence suggests tau may play a key role in mediating sleep/wake disturbances. The present work aimed to characterise the sleep/wake profile of tau transgenic rTg4510 mice and to explore whether reducing hyperphosphorylated tau accumulation by suppressing transgene expression (with chronic doxycycline (Dox) treatment) affected this phenotype, in conjunction with its effects on the known cognitive and neurodegenerative phenotype of the rTg4510 mouse. Four and a half-month-old male and female rTg4510 mice were administered 200 ppm Dox for a period of nine weeks during which polysomnographic and behavioural assessments were carried out, followed by *ex vivo* magnetic resonance imaging (MRI) and biochemical measures. Dox treatment reduced hippocampal and cortical tau levels, attenuated brain atrophy, prevented cognitive deficits and mitigated locomotor hyperactivity. rTg4510 mice exhibited a hyperarousal sleep/wake phenotype particularly prominent during the active phase, in addition to altered sleep/wake architecture and electroencephalography (EEG) power spectral deficits; however, this phenotype was largely unaffected by Dox. These data indicate the hyperarousal phenotype is due to the invasion of tau pathology into the arousal circuitry and the blunted effect of Dox suggests pathology in these regions may be more severe and less reversible than in other brain regions. Collectively, these findings highlight a role of hyperphosphorylated tau in mediating sleep/wake disturbances in neurodegenerative disorders and provides incentive for further research into mechanisms underlying non-plastic alterations induced by tau variants in the ascending arousal circuitry.

3.2 Introduction

Alzheimer's disease (AD) and tau-variant frontotemporal dementia (FTD-tau) are debilitating and progressive neurodegenerative disorders which share the accumulation of CNS hyperphosphorylated tau fibrils as a core, diagnostic pathology (Hutton et al., 1998; Blennow et al., 2006; Ballatore et al., 2007; Gotz and Ittner, 2008; Forrest et al., 2018). AD and FTD-tau also share several common symptomologies, including prominent sleep/wake disturbances, which often present well in advance of cognitive impairment (Moran et al., 2005; Anderson et al., 2009; Westerberg et al., 2012; Musiek et al., 2015). A bidirectional relationship between sleep and disease pathology has been proposed (Ju et al., 2014; Lim et al., 2014), particularly for AD; although much of the research so far has focused on the effects of amyloid-β (Aβ; Cirrito et al., 2005; Kang et al., 2009; Bero et al., 2011; Roh et al., 2012), whereas tau has not yet been as extensively studied. Nevertheless, tau pathology is a major hallmark of AD, and neurofibrillary tangle (NFT) burden correlates more strongly with cognitive impairment in AD than does Aβ plaque burden (Nelson et al., 2012). Furthermore, patients with FTD exhibit substantial sleep and circadian disturbances, which are similar to, and possibly even more severe than those experienced by AD patients (Bonakis et al., 2014). This may point to a role of tau pathology and/or its negative neurobiological consequences in mediating sleep disturbances in AD and FTD-tau.

Current preclinical findings regarding the relationship between tauopathy and sleep are limited. Holth et al. (2017b) showed that tau transgenic mice with the human P301S *MAPT* mutation (PS19 mice) exhibited age-dependent sleep/wake disturbances including prominent increases in wake and decreases in NREM and REM sleep time. PS19 mice also exhibited a reduced number of wake bouts, although with longer bout durations, indicative of a hyperarousal phenotype. Reduction in electroencephalography (EEG) power during sleep were also observed. It was concluded that tau pathology alone is sufficient to drive sleep/wake changes (Holth et al., 2017b). In $PLB2_{Tau}$ mice, similar increases in wake and decreases in NREM sleep were also observed, however this only occurred during the light phase (Koss et al., 2016). One key concept of the bidirectional relationship between sleep and disease pathology is that heightened neuronal activity such as during extended wakefulness, or sleep deprivation, regulates the extracellular release of both Aβ (Cirrito et al., 2005; Cirrito et al., 2008; Bero et al., 2011; Tabuchi et al., 2015) and tau (Pooler et al., 2013; Yamada et al., 2014; Wu et al., 2016; Wang et al., 2017a). In accordance with this, chronic sleep disruption was shown to advance the established temporal progression of tauopathy in PS19 (P301S) mice

(Zhu et al., 2018), supporting the notion that hyperarousal and/or poor sleep can exacerbate tau pathology, potentially via the increased cellular release of tau.

Currently, no study has yet reported the effect of reducing hyperphosphorylated tau accumulation on sleep/wakefulness and EEG architecture in tau transgenic mice. In the present study, the conditional/inducible rTg4510 transgenic mouse model of tauopathy (Ramsden et al., 2005; Santacruz et al., 2005), which overexpresses human tau containing the P301L *MAPT* mutation (associated with FTD-tau in humans), was used to investigate this concept. In this model, tau transgene expression is specifically restricted to forebrain structures and is inactivated by administration of the tetracycline analogue doxycycline (Dox). rTg4510 mice are therefore an ideal strain to model the effects of tau reduction on sleep/wakefulness. Given the similarity in mutations between PS19 (P301S) and rTg4510 (P301L) mice, a similarly disrupted sleep/wake phenotype in rTg4510 mice was anticipated.

The present study aimed to characterise the sleep/wake phenotype of rTg4510 mice using polysomnography (EEG/EMG recordings) and to investigate the effects of repressing tau transgene expression with Dox treatment on sleep/wake behaviour, and its relationship with the effects on the more thoroughly established cognitive and neurodegenerative phenotype of rTg4510 mice (Ramsden et al., 2005; Santacruz et al., 2005; Spires et al., 2006; Yue et al., 2011; Blackmore et al., 2017).

3.3 Materials and methods

Animals

Male and female rTg4510 transgenic mice and wildtype (WT) littermate controls were used (Ramsden et al., 2005; Santacruz et al., 2005). rTg4510 mice were bred in house as previously described (Ramsden et al., 2005; Santacruz et al., 2005). In brief, FBV/N mice expressing human tau containing the P301L *MAPT* mutation (associated with FTD-tau in humans) downstream of a tetracycline operon-responsive element (TRE) were crossed with 129SVeV mice expressing a tetracycline-controlled transactivator (tTA) under control of the Ca^{2+}-calmodulin-dependent protein kinase II (CaMKII) promotor. In this mouse, constitutive expression of the tau transgene (in the absence of Dox) is specifically restricted to forebrain structures due to the CaMKII promotor. All mice were genotyped using a standardised polymerase chain reaction (PCR) assay for tail DNA (Transnetyx Inc., Cordova, TN, USA). rTg4510 mice and WT controls were used in this study from 4.5 months of age. The objective

was to define the effects of reducing hyperphosphorylated tau after its initial accumulation, but before substantial neurodegeneration had begun. Hence, this age was selected as modified variants of tau and tangle-like inclusions have already begun to develop, whereas actual neurodegeneration and extensive neuronal or synaptic loss have yet to occur (Ramsden et al., 2005). All mice were group-housed in standard, transparent open-top cages (29.5 x 16 x 13 cm), unless intra-cage aggression necessitated single housing, on sawdust with tissue paper nesting materials. Standard rodent food and water were available *ad libitum.* All experimentation was performed in accordance with the Prevention of Cruelty to Animals Act (2004), under the guidelines of the National Health and Medical Research Council Code of Practice for the Care and Use of Animals for Experimental Purposes in Australia (2013) and approved by The Florey Animal Ethics Committee (AEC number: 16-022). All efforts were made to minimise animal suffering.

Procedure and study design

rTg4510 mice and WT littermates were allocated to one of four groups: WT Control; WT Dox; rTg4510 Control or rTg4510 Dox. The experimental study timeline is presented in Fig. 3.1. Briefly, at 4.5 months of age mice were provided a diet containing 200 ppm Dox (SF11-059, Specialty Feeds) or control diet for nine weeks. Four weeks after treatment initiation mice were surgically implanted with EEG/EMG recording head mounts. Mice were initially housed under a 12 h light/dark cycle (lights on at 0700h) until five months of age, they were then transitioned to an experimental housing area with a new light cycle (lights on at 0200h), ten days before EEG/EMG surgery. Following surgery recovery and a one-week acclimatisation to recording chambers, three 23 h polysomnographic recordings were conducted over three consecutive days. Cognition was assessed in a six-day Barnes maze behavioural test followed by locomotor activity determination in an open field. At 6.5 months of age mice were culled and samples collected. Mice entered the protocol in staggered cohorts of up to eight mice at a time with treatments pseudorandomly allocated within each cohort. A satellite cohort of mice did not receive EEG/EMG surgery but went through all other procedures until the brains were extracted for *ex vivo* magnetic resonance imaging (MRI) scanning at the end of the behavioural protocol.

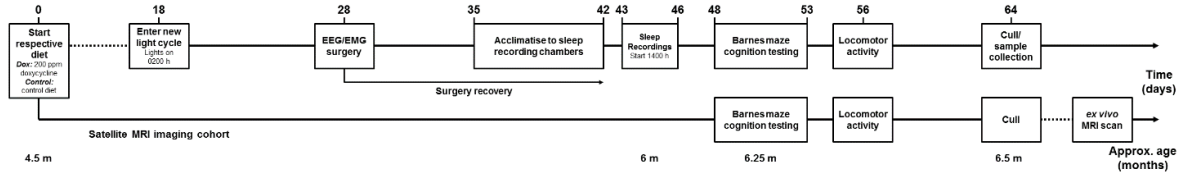

Figure 3.1. Experimental timeline schematic.

Four and a half-month-old rTg4510 mice and WT littermates were given a chow diet containing 200 ppm doxycycline (Dox) or a control diet. Four weeks after treatment initiation, mice were surgically implanted with EEG/EMG recording devices. Polysomnographic recordings were conducted at 6 months of age, followed by cognition testing in the Barnes maze and then locomotor activity assessment. Mice were culled at 6.5 months of age and samples collected. Mice entered this protocol in staggered cohorts of up to eight mice at a time. A satellite cohort of mice did not receive EEG/EMG surgery but went through all other procedures until brains were extracted for an *ex vivo* MRI scan at the cessation of treatment.

Brain tissue collection

All culls and tissue collection occurred between 0930-1400h. Mice were deeply anaesthetised with a lethal dose of sodium pentobarbitone (80 mg/kg) and perfused with approximately three times their blood volume (estimated as 7% of body weight) of 0.01M phosphate-buffered saline (PBS) containing heparin (55.6 mg/L). Brains were extracted and dissected down the midline, the right hemisphere was used to micro dissect regions containing the hippocampus and cerebral cortex, which were then immediately frozen on dry ice and stored at -80°C.

Western blotting

Tissue preparation: Dissected brain samples were homogenised on ice using a probe sonicator (~10 s; 0.5 s on, 0.5 s off) in sodium dodecyl sulfate (SDS) lysis buffer (1:3; tissue weight (mg): buffer volume (µL)) containing 2% SDS (BioRad) and 10 mM Tris (pH 6.8), plus protease and phosphatase inhibitors (Roche). Homogenates were centrifuged at 13000 rpm for 30 min at 4°C. The supernatant was collected and total protein concentration was determined using the bicinchoninic acid (BCA) assay (Pierce).

Immunoblotting: Samples were diluted in SDS lysis buffer and 4X sample buffer (250 mM Tris (pH 6.8), 8% SDS, 20% Glycerol. 0.2% Bromo Blue, 10 mM Dithiothreitol (DTT)) was added to yield a final protein concentration of 1.67 µg/µL. Samples were heated at 95°C for 5-10 min, thoroughly mixed, then briefly spun down. 15 µL of sample (25 µg of protein) were added to the relevant well. Proteins were electrophoresed at 200V for 35 min on 4-20% polyacrylamide gels (BioRad) and transferred on to 0.45 µm (pore-size) nitrocellulose membranes (BioRad). Membranes were blocked in tris-buffered saline with 0.05% Tween20

(TBS-T) containing 5% skim milk powder for 1 h at room temperature. Membranes were first incubated with mouse anti-β-actin (1:10000, catalogue number: A5441; Sigma-Aldrich) for 1 h at 4°C, then with anti-mouse secondary (1:10000, catalogue number: #7076; Cell Signaling Technology) for 1 h at room temperature. Proteins were detected using enhanced chemiluminescence (ECL; BioRad) and visualised using the ChemiDoc (BioRad). Membranes were then incubated with rabbit primary antibodies (Total tau, 1:10000, catalogue number: A0024; DAKO or phospho-tau S404, 1:4000, catalogue number: ab92676; Abcam) overnight at 4°C followed by anti-rabbit secondary (same dilution as primary, catalogue number: #7074; Cell Signaling Technology) for 2 h at room temperature. All antibodies were diluted in 5% skim milk in TBS-T. All membranes were washed with TBS-T (3 x 5-10 min) before and after incubation with secondary antibodies. Proteins were detected as described above and analysed via densitometry (ImageLab version 6.0.1, BioRad). A reference sample homogenate taken from the same WT mouse, rTg4510 mouse and tau knockout ($tau^{-/-}$) mouse were loaded onto every gel. Protein levels were first normalised to β-actin and then to the reference samples. All values are expressed as a percentage of the WT Control group.

Ex vivo MRI scan

Cull and sample preparation: Mice were deeply anaesthetised with a lethal dose of sodium pentobarbitone (80 mg/kg) and perfused with approximately three times their blood volume (estimated as 7% of body weight) of PBS containing heparin (55.6 mg/L), immediately followed by the same volume of 4% paraformaldehyde (PFA). Brains were extracted and post-fixed in 4% PFA for 24 h at 4°C, then washed (3 x 10 min) in ice-cold phosphate buffer (PB). Brains were then embedded in a 1% agarose solution (containing 0.05% ProClin antimicrobial, Sigma-Aldrich) in clear plastic vials and stored at 4°C until scanning.

MRI scan: Brains were scanned with a Bruker 9.4T MRI operated via ParaVision version 6.1 software (Bruker). Imaging was performed using actively decoupled volume transmit and surface receive coils and consisted of T2-weighted and diffusion-weighted images (DWI) for assessing structural and microstructural changes, respectively. Three dimensional T2-weighted images were acquired with a multi-echo sequence and the following imaging parameters: repetition time (TR) = 1,000 ms; number of echoes = 12; echo times = 10, 20, 30, …, 120 ms; number of excitations (NEX) = 1; field of view (FOV) = 20.48 × 12.32 × 7.2 mm^3; and resolution = 80 × 80 × 80 μm^3. Diffusion imaging was performed over 60 directions with a 4-shot echo planar imaging sequence and the following imaging parameters: TR/TE = 750/31

ms; NEX = 2; FOV = 16 × 12.8 × 7.4 mm^3; resolution = 100 × 100 × 100 μm^3; and b-value = 4,000 s/mm^2. Two b_0 images were also acquired.

MRI image analysis: The mean echo image was calculated for each T2-weighted image and the left and right hippocampus, left and right cortex, and corpus callosum were segmented using ITK-SNAP version 3.8.0 (www.itksnap.org; Yushkevich et al., 2006). Volumes were calculated for each of the five regions of interest (ROIs) using FMRIB Software Library (FSL). Diffusion tensor images (DTI) were reconstructed using MRtrix3 software (Tournier et al., 2019). The mean b_0 image was registered to the mean T2-weighted image using Advanced Normalization Tools (ANTs, http://stnava.github.io/ANTs/) and the resulting inverse diffeomorphism used to register each segmentation to its corresponding DTI. The mean fractional anisotropy (FA), apparent diffusion coefficient (ADC), radial diffusivity (RD) and axial diffusivity (ADi) were calculated for each ROI using FSL. All measurements were averaged across the left and right hippocampus and cortex.

Behaviour

Barnes maze

The Barnes maze (Barnes, 1979) was used to interrogate hippocampal-dependent spatial learning and memory in rTg4510 and WT mice. The Barnes maze comprised a circular platform (120 cm diameter) with 36 evenly spaced holes (5 cm diameter) around its perimeter, raised 56 cm off the ground. Two floodlights and two additional 3D visual cues (tall lamp and yellow biohazard bin affixed to a steel pole) were positioned around the maze. Laminated, patterned A2 sheets (stripes or dots) were attached to the floodlight stands as further visual cues. A cylindrical container (13 cm diameter x 10 cm height) was used to hold mice in the centre of the maze at the start of each trial and was raised to the ceiling via a pulley system. A small black container (14 x 9.5 x 5 cm) with a wire mesh ramp was used as an escape box and positioned under one hole in the maze. A camera mounted to the ceiling was positioned directly above the maze. TopScan Lite version 2.00 (CleverSys Inc.) was used for tracking analysis.

Day 0 – Habituation trials: Each mouse performed one habituation trial on day 0. All visual cues were removed for the habituation trial. The mouse was placed under the start-container, the floodlights switched on and the container raised using the pulley. After 15-30 s, the mouse was gently guided into the escape box and allowed to remain inside for 2 min, then returned to its home cage.

Days 1-4 – Acquisition trials: Each mouse performed 4 acquisition trials per day for 4 consecutive days, with an inter-trial interval of 25-27 min. Acquisition trials were performed

during the active phase, typically between 1500-1900h each day. Mice were randomly assigned a target escape box location (hole 1, 9, 18 or 27). The escape box was positioned under this hole for every trial for that mouse. Acquisition trials lasted 4 min or until the mouse entered the escape box; if it had not entered after 4 min had elapsed, the mouse was guided inside by hand. Once the mouse was inside the escape box, the floodlights were immediately switched off. Mice remained inside the box for 30-60 s and were then returned to their home cage. The maze surface was wiped down with 80% ethanol between each trial.

The acquisition trial parameters measured included: *Total errors:* the number of nose pokes into a hole that was not the target hole, with consecutive dips into the same hole considered a single error. *Hole deviation:* the difference in the number of holes between the first hole the mouse visited and the target hole (range 0-18). *Latency to investigate any hole:* the time it took the mouse to move from the centre starting point and poke its nose into any hole on the maze. *Primary latency to escape hole:* the time it took the mouse to first poke its nose into the target hole. *Latency to enter escape box:* the time it took the mouse to enter the escape box. *Search strategy:* the search strategy mice used to locate the escape box. A spatial search strategy occurred when the mouse moved directly to within three holes either side of the target and then quickly located the escape box thereafter. The serial search strategy occurred when the mouse moved around the edge of the maze making errors at sequential holes before locating the escape box. The random search strategy occurred when the mouse investigated the maze in an unsystematic fashion, often moving through the centre of the maze and returning to holes previously visited. *Proportion of mice requiring guidance:* the proportion of mice that had not entered the escape box after the 4 min trial limit had elapsed and hence needed to be guided inside. *Proportion of mice failing to explore the maze:* the proportion of mice that remained in the centre of the maze for the entire 4 min trial limit (see Appendix III).

Day 5 – Probe trial: Each mouse performed one 3 min probe trial in which the escape box had been removed. The maze surface was wiped down with 80% ethanol between each probe trial. Probe trial parameters measured included: *Hole deviation:* see above. *Nose pokes into each hole:* the number of times the mouse poked its nose into each hole on the maze. In this case, consecutive dips into the same hole were considered as multiple nose pokes. Only the first 90 s (or second 90 s if the mouse took longer to move from the centre) of the trial were analysed. A higher number of nose pokes into the target and adjacent holes was indicative of heightened spatial recall and cognitive ability.

Locomotor activity

Locomotor activity in an open field was assessed by placing mice individually into the locomotor cell (27.3 x 27.3 x 20 cm) and activity monitored for 1 h by a grid of infrared beams. Locomotor activity was assessed during the active (dark) phase. All locomotor cells were cleaned with 80% ethanol and dried between each trial. The data (ambulatory distance travelled and time spent ambulatory) were analysed using Activity Monitor version 7.0.5.10 (MED Associates, Inc).

Polysomnographic recordings and analysis

Surgery: Mice were anaesthetised with isoflurane in air (5% for induction, 2-3% for maintenance) and placed in a stereotaxic frame. Meloxicam (1-3 mg/kg, Ilium) and 500 µL of warm saline were administered subcutaneously. 50 µL of 1% lignocaine HCl (Pfizer) was administered near the incision site, then the skull was exposed and EEG/EMG preformed head mounts (Catalogue number: #8201-SS, Pinnacle Technology Inc.) were surgically implanted. EEG1 and EEG2 electrodes (screws inserted into the head mount) were positioned over the parietal and frontal lobe, respectively. Reference and ground electrodes were positioned at equivalent regions, with reference embedded in the parietal region and ground in the frontal, in addition to a non-penetrating anchor screw embedded into the skull over the motor cortex. Two EMG wires attached to the head mount were inserted into the neck musculature and sutured (7-0 Prolene, Ethicon) into place. Sutures were used to close the scalp around the head mount. Dental cement was positioned under and around the head mount using an 18G drawing-up needle and allowed to set. The mouse was removed from the stereotaxic frame and placed into a warmed recovery box (30°C) until it was moving freely, then returned to its original cage.

Recordings: Mice were individually housed in transparent, cylindrical sleep recording chambers (29 cm diameter, x 30 cm height) for a further week of recovery and acclimatisation. Head mounts were plugged into pre-amplifiers 24 h before recordings began. Three individual 23 h recordings were then acquired over three consecutive days using Sirenia Acquisition version 1.8.0 software (Pinnacle Technology Inc.). Three channels were recorded: EEG1, EEG2 and EMG. The sampling rate was 200 Hz. 100 Hz EEG and EMG filters were applied. Recordings began at 1400h (Circadian time (CT)12) and finished at 1300h (CT11). Following EEG/EMG recordings all mice were returned to their original cages.

Analysis: Sirenia recording files (.pvfs) were exported as European Data Format (.edf) and imported into Somnivore™ (Allocca et al., 2019) in 4 s epochs for vigilance state and power

spectral analysis. The final 23 h recording from each mouse was used for analysis, unless faulty or otherwise unavailable, in which case the recording from day two or one was used. Each recording was scored by first training the Somnivore machine learning algorithm with 101 epochs of wake, NREM and REM. The entire hypnogram was then populated using Somnivore's auto-score function. Contextual scoring rules included a minimum bout length setting of 8 s (two contiguous epochs) for both wake and NREM and 12 s (three contiguous epochs) for REM. A further 50 epochs of each state were then trained, and the auto-score function was run again. The entire recording was then manually checked and corrected. All sleep scoring was performed blinded to genotype and treatment. Vigilance state-specific (wake, NREM or REM) normalised power spectral data were obtained using Somnivore's built in power spectral analysis capabilities (Allocca et al., 2019). For power spectral analysis, all transition epochs were excluded and signals from EEG1 and EEG2 electrodes were averaged. Frequencies in the 0-20 Hz range were selected for statistical analysis.

Statistical analysis

Statistical analyses were performed using GraphPad Prism (version 8.0.0) or R (version 3.6.1)/RStudio (version 1.2.5001). Relative tau levels (western blots), brain volumes and white matter parameters (MRI), hole deviation during the probe trial (Barnes maze) and ambulatory distance and time (locomotor activity) were all analysed by two-way ANOVA with Tukey's multiple comparisons test. Due to overly hyperactive mice, one statistical outlier from WT Control (Distance travelled: 10560.91 cm vs. group average of 4096.13 cm), WT Dox (40329.22 vs. 4013.29) and rTg4510 Dox (24330.30 vs. 5634.03) groups, and two outliers from the rTg4510 Control group (74653.96 and 82782.51 vs. 8152.07) were removed from locomotor activity analysis. Search strategy during acquisition trials were analysed by a repeated measures linear mixed effects model in R, using the *lmer* function, incorporating the factors of genotype, treatment and day (repeated factor). Nose poke distributions during the Barnes maze probe trial were analysed using one-way repeated measures ANOVA followed by Fisher's LSD multiple comparisons test, versus the target hole. One mouse from the WT Control, eleven mice from the rTg4510 Control and six mice from the rTg4510 Dox groups were excluded from probe trial analyses due to lack of movement. Time spent in each vigilance state (sleep/wake data) across the 23 h recording were analysed using the R *lme*r function, incorporating the factors of genotype, treatment, sex and time (repeated factor). Bout numbers, bout durations, EEG power per specified frequency range and time spent in each vigilance state per phase were analysed by a linear mixed effects model in R, using the *lm* function,

incorporating the factors of genotype, treatment and sex. Vigilance state-specific normalised EEG power were analysed using the *lme*r function, incorporating the factors of genotype, treatment and frequency (repeated factor). Correlation between ambulatory time and average wake time during the active phase were analysed by Pearson's correlation. Akaike information criterion (AIC) was used to determine the model of best fit for all R related analyses. For vigilance state time, average EEG power, bout numbers and bout durations, sex was a significant contributing factor and hence data from both male and female mice are presented separately. All R related post hoc analyses were performed using the *emmeans* function, with Tukey's multiple comparisons test. For all analyses, $P < 0.05$ was considered to be statistically significant.

3.4 Results

Dox treatment reduced tau and phosphorylated tau in the hippocampus and cortex

Tau expression in the hippocampus and cortex was assessed by western blot (Fig. 3.2A). Phosphorylated tau (p-tau) S404 levels were 7.67-fold higher in the hippocampus and 6.20-fold higher in the cortex of rTg4510 Control mice compared with WT Control mice (Fig. 3.2B, D). Dox treatment significantly reduced p-tau S404 levels in rTg4510 mice without affecting p-tau S404 levels in WT mice, in the hippocampus (Genotype: $F_{(1, 42)} = 795.9$, $P < 0.0001$; treatment: $F_{(1, 42)} = 104.6$, $P < 0.0001$; interaction: $F_{(1, 42)} = 90.11$, $P < 0.0001$, Fig. 3.2B) and cortex (Genotype: $F_{(1, 42)} = 488.2$, $P < 0.0001$; treatment: $F_{(1, 42)} = 62.08$, $P < 0.0001$; interaction: $F_{(1, 42)} = 51.74$, $P < 0.0001$, Fig. 3.2D). Total tau levels were 2.70-fold higher in the hippocampus and 2.89-fold higher in the cortex of rTg4510 Control mice compared with WT Control mice (Fig. 3.2C, E). Dox treatment significantly reduced total tau levels in rTg4510 mice without affecting total tau levels in WT mice, in the hippocampus (Genotype: $F_{(1, 42)} = 112.8$, $P < 0.0001$; treatment: $F_{(1, 42)} = 20.8$, $P < 0.0001$; interaction: $F_{(1, 42)} = 26.43$, $P < 0.0001$, Fig. 3.2C) and cortex (Genotype: $F_{(1, 42)} = 142.2$, $P < 0.0001$; treatment: $F_{(1, 42)} = 54.75$, $P < 0.0001$; interaction: $F_{(1, 42)} = 23.92$, $P < 0.0001$, Fig. 3.2E).

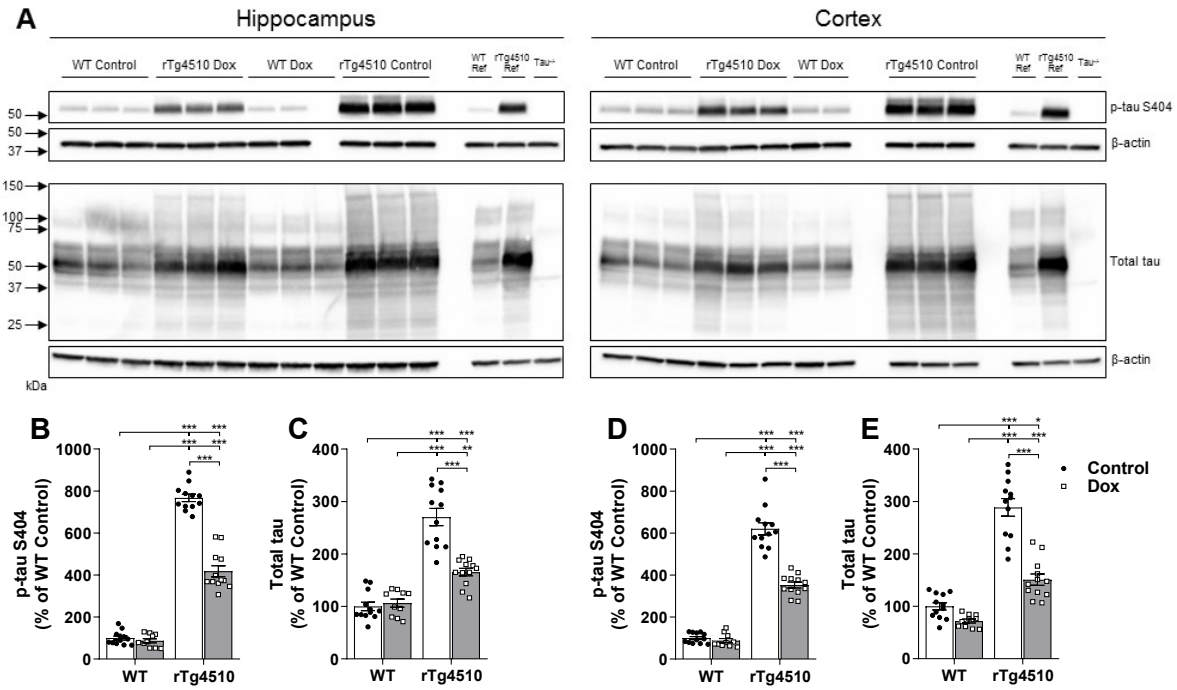

Figure 3.2. Decreased tau and phosphorylated tau levels in Dox-treated rTg4510 mice.

A, Representative western blots from the hippocampus (left) and cortex (right) probed with p-tau S404 or total tau antibodies. β-actin was used as a housekeeping protein. ***B***, ***D***, Relative p-tau S404 levels in the hippocampus (***B***) and cortex (***D***). ***C***, ***E***, Relative total tau levels in the hippocampus (***C***) and cortex (***E***). Densitometry signals were normalised to β-actin and then to the reference samples (WT Ref; rTg4510 Ref) which were loaded on every gel. Lysate from a tau knockout ($Tau^{-/-}$) mouse was used as a negative control. Data are means ± SEM and expressed as a percentage of the WT Control group. n = 10-12 per group. $^{*}P < 0.05$, $^{**}P < 0.01$, $^{***}P < 0.001$, by two-way ANOVA with Tukey's multiple comparisons test.

Dox treatment attenuated hippocampal and cortical brain atrophy

To assess the extent of neurodegeneration in the hippocampus and cortex, *ex vivo* MRI scans were performed at 6.5 months of age in a satellite group of animals. Hippocampal volume was smaller in rTg4510 mice compared with WT mice and was partly rescued by Dox treatment (Genotype: $F_{(1, 11)} = 85.47$, $P < 0.0001$; treatment: $F_{(1, 11)} = 8.677$, $P = 0.0133$; interaction: $F_{(1, 11)} = 9.385$, $P = 0.0108$, Fig. 3.3A). Comparable changes in volume were also observed in the cortex (Genotype: $F_{(1, 11)} = 75.13$, $P < 0.0001$; treatment: $F_{(1, 11)} = 8.887$, $P = 0.0125$; interaction: $F_{(1, 11)} = 21.59$, $P = 0.0007$, Fig. 3.3B), indicative of attenuated neurodegeneration with Dox treatment.

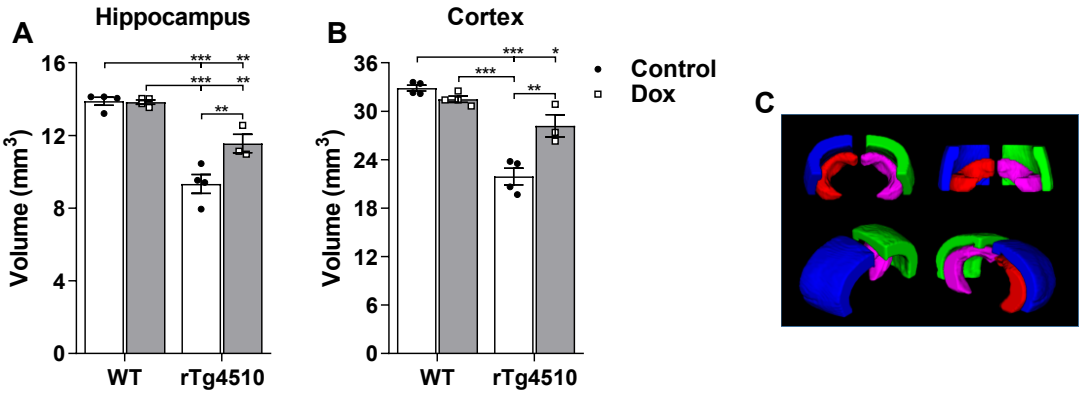

Figure 3.3. Attenuated brain atrophy in Dox-treated rTg4510 mice.

A-B, Hippocampal (***A***) and cortical (***B***) volumes as assessed by *ex vivo* MRI scans. Data are means ± SEM. n = 3-4 per group. $^{*}P < 0.05$, $^{**}P < 0.01$, $^{***}P < 0.001$, by two-way ANOVA with Tukey's multiple comparisons test. ***C***, Representative 3D images of the outlined left and right hippocampus (red and pink) and cortex (blue and green). Volume measurements were averaged across the left and right outlined regions.

rTg4510 mice exhibited microstructural alterations consistent with white matter degeneration

To investigate white matter changes, diffusion-weighted images (DWI) were acquired as part of the *ex vivo* MRI scan. FA, ADC, ADi and RD measures were obtained for the hippocampus, cortex and corpus callosum. FA was reduced in both the hippocampus (Genotype: $F_{(1, 11)} = 32.95$, $P < 0.0001$; treatment: $F_{(1, 11)} = 0.05827$, $P = 0.8127$; interaction: $F_{(1, 11)} = 0.04759$, $P = 0.8313$, Fig. 3.4A) and cortex (Genotype: $F_{(1, 11)} = 7.682$, $P = 0.0182$; treatment: $F_{(1, 11)} = 1.885$, $P = 0.1971$; interaction: $F_{(1, 11)} = 0.01631$, $P = 0.9007$, Fig. 3.4B) in rTg4510 mice compared with WT mice, but were not influenced by Dox treatment. In the corpus callosum, however, Dox treatment restored FA back to WT levels in rTg4510 mice (Genotype: $F_{(1, 10)} = 14.78$, $P = 0.0032$; treatment: $F_{(1, 10)} = 6.572$, $P = 0.0282$; interaction: $F_{(1, 10)} = 7.692$, $P = 0.0197$, Fig. 3.4C). ADC was increased in both the hippocampus (Genotype: $F_{(1, 11)} = 157.8$, $P < 0.0001$; treatment: $F_{(1, 11)} = 6.874$, $P = 0.0238$; interaction: $F_{(1, 11)} = 0.4706$, $P = 0.5069$, Fig. 3.4D) and cortex (Genotype: $F_{(1, 11)} = 21.49$, $P = 0.0007$; treatment: $F_{(1, 11)} = 6.772$, $P = 0.0246$; interaction: $F_{(1, 11)} = 0.004537$, $P = 0.9475$, Fig. 3.4E) in rTg4510 mice compared with WT mice, but were unaffected by treatment, whereas the corpus callosum exhibited no significant differences between groups (Genotype: $F_{(1, 10)} = 1.786$, $P = 0.2111$; treatment: $F_{(1, 10)} = 0.7937$, $P = 0.3939$; interaction: $F_{(1, 10)} = 1.446$, $P = 0.2568$, Fig. 3.4F). ADi was also increased in both the hippocampus (Genotype: $F_{(1, 11)} = 155.4$, $P < 0.0001$; treatment: $F_{(1, 11)} = 8.523$, $P = 0.0140$; interaction: $F_{(1, 11)} = 0.4093$, $P = 0.5354$, Fig. 3.4G) and cortex (Genotype: $F_{(1, 11)} = 21.24$, $P = 0.0008$; treatment: $F_{(1, 11)} = 6.644$, $P = 0.0257$; interaction: $F_{(1, 11)} = 0.003637$, $P = 0.9530$, Fig.

3.4H) of rTg4510 mice versus WT, but unaffected by treatment, with the corpus callosum similarly unaffected by genotype or treatment (Genotype: $F_{(1, 10)} = 0.07744$, $P = 0.7865$; treatment: $F_{(1, 10)} = 0.03795$, $P = 0.8494$; interaction: $F_{(1, 10)} = 0.0007744$, $P = 0.9783$, Fig. 3.4I). RD was increased in rTg4510 mice in the hippocampus (Genotype: $F_{(1, 11)} = 147.0$, $P < 0.0001$; treatment: $F_{(1, 11)} = 5.699$, $P = 0.0360$; interaction: $F_{(1, 11)} = 0.4641$, $P = 0.5098$, Fig. 3.4J), cortex (Genotype: $F_{(1, 11)} = 21.58$, $P = 0.0007$; treatment: $F_{(1, 11)} = 6.765$, $P = 0.0247$; interaction: $F_{(1, 11)} = 0.001726$, $P = 0.9676$, Fig. 3.4K) and corpus callosum (Genotype: $F_{(1, 10)} = 6.725$, $P = 0.0268$; treatment: $F_{(1, 10)} = 2.989$, $P = 0.1145$; interaction: $F_{(1, 10)} = 3.933$, $P = 0.0755$, Fig. 3.4L), but was not affected by treatment.

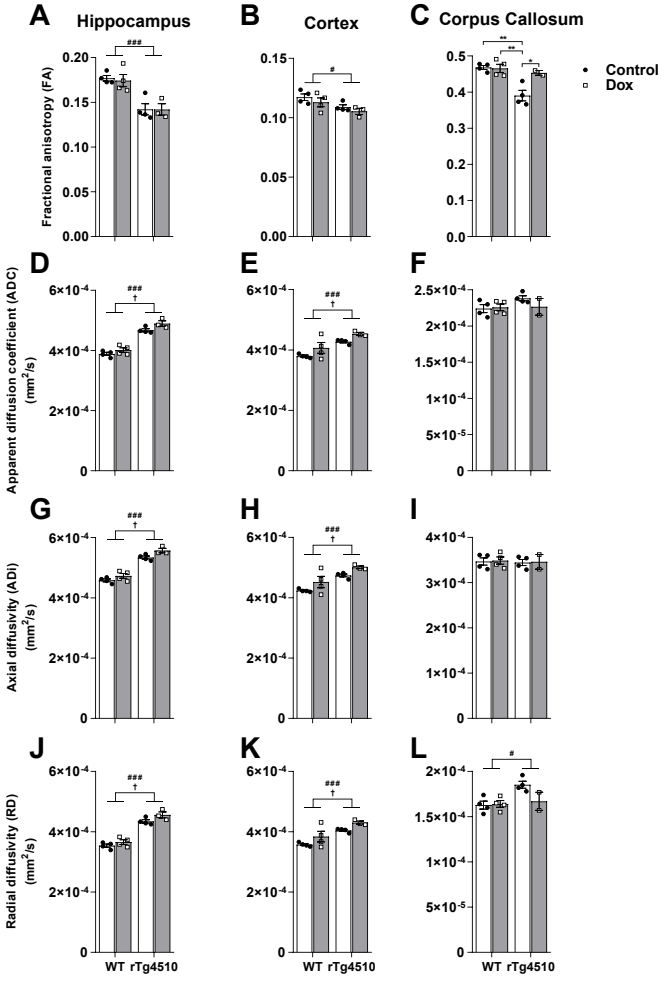

Figure 3.4. White matter changes in rTg4510 and WT mice given Dox or control diets.

A-L, Fractional anisotropy (FA) (***A-C***), apparent diffusion coefficient (ADC) (***D-F***), axial diffusivity (ADi) (***G-I***) and radial diffusivity (RD) (***J-L***) in the hippocampus, cortex and corpus callosum (from left to right), as assessed by diffusion weighted imaging (DWI). Data are means ± SEM. n = 2-4 per group. # and † denote main effects of genotype and treatment, respectively. $^{\#}P < 0.05$, $^{\#\#\#}P < 0.001$ vs. WT; $^{\dagger}P < 0.05$ vs. Control; $^{*}P < 0.05$, $^{**}P < 0.01$, by two-way ANOVA with Tukey's multiple comparisons test.

Dox treatment rescued hippocampal-dependent spatial recall deficits in the Barnes maze

To assess cognition, mice performed the Barnes maze behavioural test for hippocampal-dependent spatial memory (Barnes, 1979). Spatial recall in the final probe trial, in which the escape box had been removed, was used as the primary outcome measure. Search strategy throughout acquisition trials was also considered a reliable indicator of hippocampal function. A substantial proportion of rTg4510 mice failed to explore the maze during acquisition/probe trials and remained in the centre of the maze for the maximum time limit. Eleven out of nineteen rTg4510 Control and 6/18 rTg4510 Dox mice were excluded from the probe trial analysis due to lack of movement (Appendix III; Fig. A3.2C). With regards to acquisition search strategy, WT Control mice used the random search strategy significantly less than rTg4510 Control mice across all four days of acquisition (Fig. 3.5A). Dox treatment resulted in a decreased use of the random search strategy by day 4 in rTg4510 mice compared with Control treated mice (Fig. 3.5A). Analysis of the serial search strategy revealed a genotype effect across each day, with WT mice using the serial search strategy significantly more than rTg4510 mice on days 1 and 2 (Fig. 3.5B). Thereafter, use of the serial search strategy declined in WT mice, in favour of other strategies. Both WT Control and rTg4510 Dox mice used the spatial search strategy to accurately locate the escape box significantly more than rTg4510 Control mice by day 4 (Fig. 3.5C), indicative of greater spatial learning/acquisition.

Spatial recall in the probe trial was inferred by measuring the number of nose pokes into each individual hole on the maze relative to the target hole (Fig. 3.6). WT Control mice investigated the target hole significantly more than all other holes (except one immediately adjacent) on the maze ($F_{(5.612, 95.41)} = 7.273$, $P < 0.0001$, Fig. 3.6A), as too did WT Dox mice ($F_{(3.508, 49.11)} = 6.338$, $P = 0.0006$, Fig. 3.6B). rTg4510 Control mice displayed no overall preference for the target hole ($F_{(3.933, 27.53)} = 1.678$, $P = 0.1843$, Fig. 3.6C), whereas Dox treatment completely rescued this phenotype ($F_{(3.267, 35.94)} = 7.014$, $P = 0.0006$, Fig. 3.6D). Furthermore, upon commencement of the probe trial, WT Control, WT Dox and rTg4510 Dox mice either went directly to the target hole, or immediately adjacent to it (± 1), for 10/18, 9/15 and 8/12 trials, respectively, compared to only 1/8 for rTg4510 Control mice (Fig. 3.6E), although no statistical differences were observed between groups.

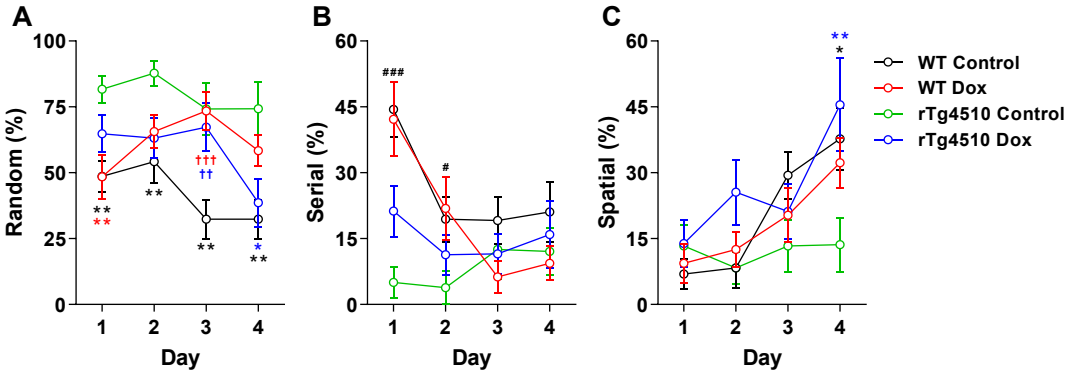

Figure 3.5. Search strategies used during Barnes maze acquisition trials.

A-C, Percentage use of the random (***A***), serial (***B***) and spatial (***C***) search strategies during Barnes maze acquisition trials in rTg4510 and WT mice administered doxycycline (Dox) or control diets. Data are means ± SEM. n = 16-18 per group. $^{*}P < 0.05$, $^{**}P < 0.01$ vs. rTg4510 Control; $^{\dagger\dagger}P < 0.01$, $^{\dagger\dagger\dagger}P < 0.001$ vs. WT Control (genotype x treatment x day); $^{\#}P < 0.05$, $^{\#\#\#}P < 0.001$ vs. rTg4510 (genotype x day) within acquisition day, by repeated measures linear mixed effects model with Tukey's multiple comparisons test.

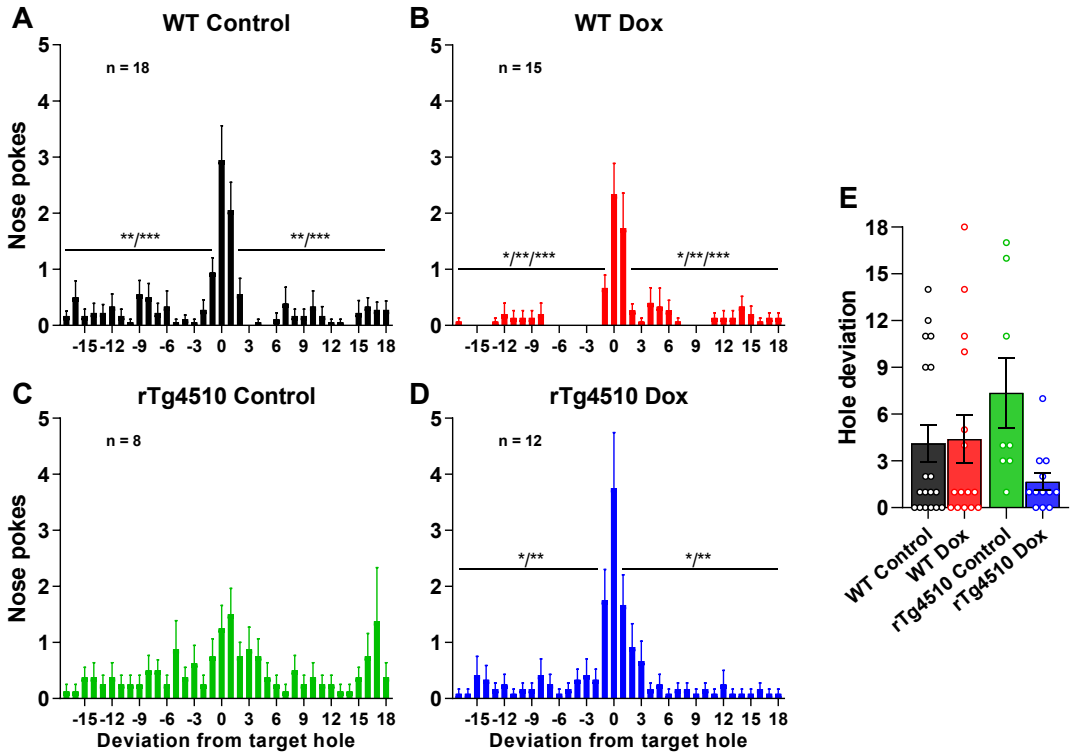

Figure 3.6. Rescue of spatial recall in the final probe trial of the Barnes maze.

A-D, Number of nose pokes into each of the 36 holes on the Barnes maze during the final probe trial, deviating from the target hole (denoted 0) by rTg4510 and WT mice administered doxycycline (Dox) or control diets. Data are means ± SEM. n = 8-18 per group. $^{*}P < 0.05$, $^{**}P < 0.01$, $^{***}P < 0.001$ vs. target hole, by one-way repeated measures ANOVA with Fisher's LSD multiple comparisons test. ***E***, Deviation between the target hole and the first hole visited during the probe trial (hole deviation of zero indicates the mouse went directly to the target hole upon trial commencement).

rTg4510 mice exhibited a hyperarousal phenotype during the active phase which was not compensated for during the inactive phase and not rescued by Dox treatment

To assess the sleep/wake phenotype of rTg4510 mice, 23 h polysomnographic recordings were performed (Fig. 3.7A-C). Parameters for the fixed effects from the repeated measures linear mixed effects model statistical analyses are summarised in Table 3.1. Significant sex effects were observed in the data, whereby the hyperarousal phenotype tended to be exacerbated in female mice and hence, data from male and female mice are graphed separately (Fig. 3.7D-L). rTg4510 mice spent significantly more time awake (Fig. 3.7A) and correspondingly less time in NREM sleep (Fig. 3.7B) compared with WT mice at numerous circadian time points during the active phase only. No genotype differences were observed during the inactive phase. An overall main effect of genotype was observed for REM sleep, whereby WT mice spent more time in REM sleep than rTg4510 mice (Fig. 3.7C). To further investigate the sleep/wake phenotype of rTg4510 mice, the average time spent in each vigilance state across the different circadian phases (active, inactive and entire recording; linear mixed effects model statistical analyses are summarised in Table 3.2) were analysed. Significant genotype effects were observed for wake time across the active phase (Fig. 3.7D) and entire recording (Fig. 3.7F), but not during the inactive phase (Fig. 3.7E), whereby rTg4510 mice spent more time awake than WT mice, indicative of a hyperarousal phenotype. This phenotype was not influenced by Dox treatment.

Given the increase in wake time, as expected, rTg4510 mice exhibited a corresponding decrease in NREM sleep time across the active phase (Fig. 3.7G) and entire recording (Fig. 3.7I), compared with WT mice. NREM sleep time was not affected by genotype, treatment or sex during the inactive phase (Fig. 3.7H), indicating rTg4510 mice slept no more than WT mice during this period, and therefore did not show a compensatory rebound from lack of sleep during the active phase.

rTg4510 mice also exhibited a decrease in REM sleep time during the active phase, compared with WT mice (Fig. 3.7C, J). During the inactive phase, a genotype and treatment interaction was observed; rTg4510 mice exhibited decreased REM sleep during this period, which was rescued by Dox treatment, predominantly in female mice (Fig. 3.7K). This effect was also evident, although less pronounced, when analysing the recording as a whole (Fig. 3.7L).

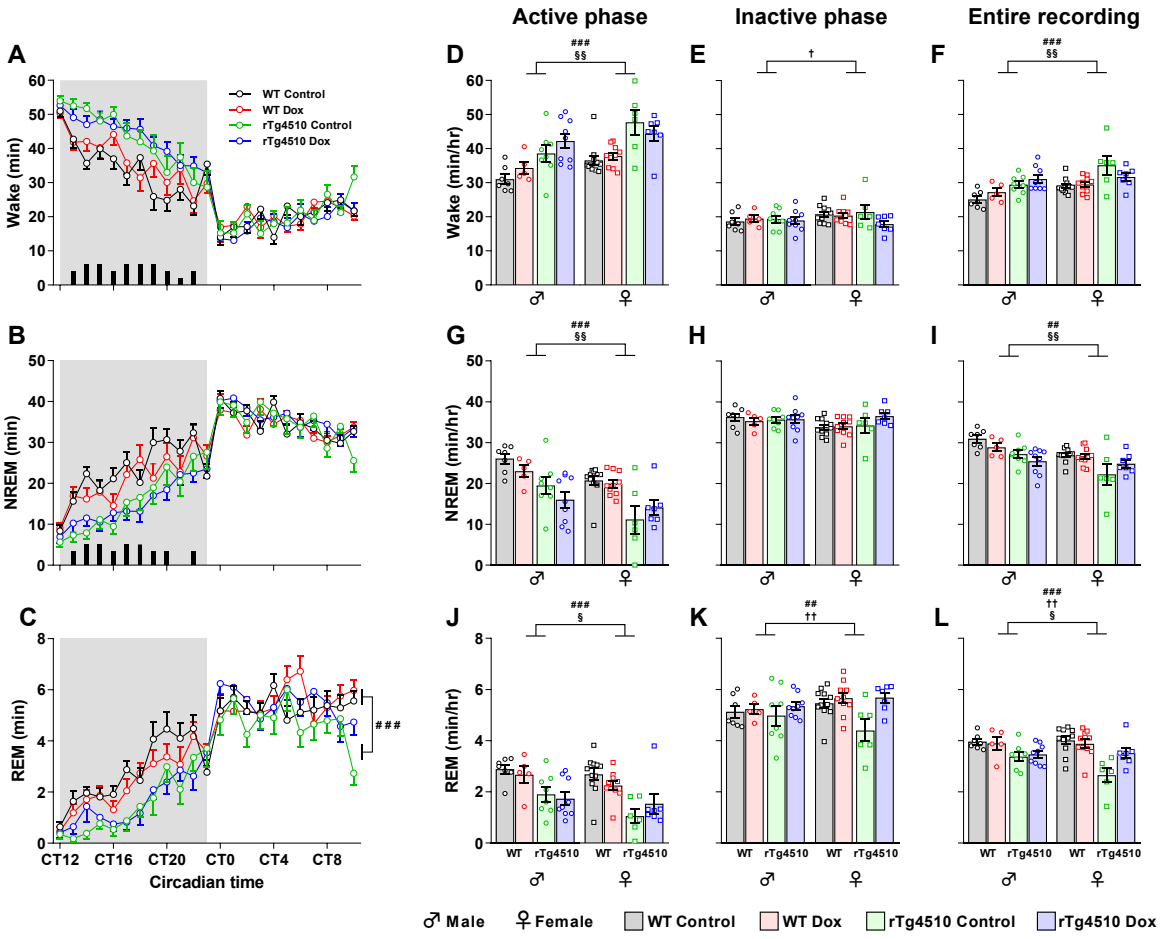

Figure 3.7. Altered sleep/wake phenotype in rTg4510 mice.

A-C, Minutes spent in wake (***A***), NREM (***B***) and REM (***C***) vigilance states per hour across a 23 h recording in rTg4510 and WT mice administered doxycycline (Dox) or control diets. Dark shade represents the active phase. Data are means ± SEM. n = 14-18 per group. Short bar: P < 0.05, medium bar: P < 0.01, tall bar: P < 0.001 vs. WT (genotype x time) within circadian time, # denotes main effect of genotype, by repeated measures linear mixed effects model with Tukey's multiple comparisons test. ***D-L***, Minutes spent in each vigilance state per hour averaged across (from left to right) the active phase, inactive phase and entire recording, for wake (***D-F***), NREM (***G-I***) and REM (***J-L***). n = 5-11 per group, per sex. #, † and § denote main effects of genotype, treatment and sex, respectively. $^{\#}$P < 0.05, $^{\#\#}$P < 0.01, $^{\#\#\#}$P < 0.001 vs. WT; †P < 0.05, ††P < 0.01 vs. Control; §P < 0.05, §§P < 0.01 vs. Female, by linear mixed effects model with Tukey's multiple comparisons test. For ***D-L***, only main effects are graphically presented, refer to Table 3.1 and 3.2 for further details.

Table 3.1. EEG recordings statistical analyses summary.

Time spent in each vigilance state across the 23 h recording were analysed by a repeated measures linear mixed effects model in R, using the *lmer* function, incorporating the factors of Genotype, Treatment, Sex and Time (repeated factor). Indented Pr(>|t|) values indicate statistical significance.

Vigilance state time															
					Wake					**NREM**					**REM**
Fixed effect	Estimate	Std. error	df	t-value	Pr(>|t|)	Estimate	Std. error	df	t-value	Pr(>|t|)	Estimate	Std. error	df	t-value	Pr(>|t|)
Genotype	-13.827	2.892	434.439	-4.781	< 0.001	12.397	2.557	396.152	4.849	< 0.001	1.429	0.468	496.700	3.054	< 0.01
Treatment	-3.081	3.170	434.439	-0.972	> 0.05	2.995	2.803	396.152	1.069	> 0.05	0.086	0.513	496.700	0.168	> 0.05
Sex	-10.285	3.078	434.439	-3.342	< 0.001	9.609	2.720	396.152	3.532	< 0.001	0.674	0.498	496.700	1.354	> 0.05
Time	-1.874	0.159	1378.000	-11.805	< 0.001	1.635	0.138	1378.000	11.823	< 0.001	0.239	0.026	1378.000	9.125	< 0.001
Genotype:Treatment	5.177	4.031	434.439	1.284	> 0.05	-4.466	3.563	396.152	-1.253	> 0.05	-0.711	0.652	496.700	-1.090	> 0.05
Genotype:Sex	2.135	4.131	434.439	0.517	> 0.05	-2.157	3.651	396.152	-0.591	> 0.05	0.022	0.668	496.700	0.033	> 0.05
Treatment:Sex	6.450	4.209	434.439	1.532	> 0.05	-6.314	3.721	396.152	-1.697	> 0.05	-0.136	0.681	496.700	-0.200	> 0.05
Genotype:Time	0.641	0.197	1378.000	3.251	< 0.01	-0.635	0.172	1378.000	-3.697	< 0.001	-0.006	0.033	1378.000	-0.180	> 0.05
Treatment:Time	-0.033	0.216	1378.000	-0.152	> 0.05	-0.032	0.188	1378.000	-0.169	> 0.05	0.065	0.036	1378.000	1.812	> 0.05
Sex:Time	0.375	0.210	1378.000	1.786	> 0.05	-0.379	0.183	1378.000	-2.070	< 0.05	0.004	0.035	1378.000	0.103	> 0.05
Genotype:Treatment:Sex	-3.646	5.921	434.439	-0.616	> 0.05	3.440	5.233	396.152	0.657	> 0.05	0.206	0.958	496.700	0.215	> 0.05
Genotype:Treatment:Time	-0.102	0.275	1378.000	-0.372	> 0.05	0.126	0.240	1378.000	0.526	> 0.05	-0.024	0.045	1378.000	-0.524	> 0.05
Genotype:Sex:Time	-0.027	0.282	1378.000	-0.097	> 0.05	0.094	0.245	1378.000	0.381	> 0.05	-0.066	0.047	1378.000	-1.426	> 0.05
Treatment:Sex:Time	-0.108	0.287	1378.000	-0.375	> 0.05	0.161	0.250	1378.000	0.644	> 0.05	-0.053	0.047	1378.000	-1.123	> 0.05
Genotype:Treatment:Sex:Time	0.013	0.404	1378.000	0.033	> 0.05	-0.067	0.352	1378.000	-0.189	> 0.05	0.053	0.067	1378.000	0.799	> 0.05

Table 3.2. Phase specific EEG recordings statistical analyses summary.

Average time spent in each vigilance state per phase were analysed by a linear mixed effects model in R, using the *lm* function, incorporating the factors of Genotype, Treatment and Sex. Indented Pr(>|t|) values indicate statistical significance.

Vigilance state time													
					Active phase				**Inactive phase**				**Entire recording**
Vigilance state	Fixed effect	Estimate	Std. error	t-value	Pr(>|t|)	Estimate	Std. error	t-value	Pr(>|t|)	Estimate	Std. error	t-value	Pr(>|t|)
Wake	Genotype	-11.189	2.833	-3.949	< 0.001	-0.610	1.498	-0.407	> 0.05	-6.130	1.661	-3.691	< 0.001
	Treatment	-3.411	3.106	-1.098	> 0.05	-3.548	1.642	-2.160	< 0.05	-3.476	1.820	-1.910	> 0.05
	Sex	-9.176	3.015	-3.043	< 0.01	-2.087	1.594	-1.309	> 0.05	-5.786	1.767	-3.274	< 0.01
	Genotype:Treatment	4.694	3.949	1.189	> 0.05	3.138	2.088	1.503	> 0.05	3.950	2.315	1.707	> 0.05
	Genotype:Sex	3.608	4.047	0.892	> 0.05	-0.155	2.140	-0.072	> 0.05	1.809	2.372	0.763	> 0.05
	Treatment:Sex	7.058	4.124	1.711	> 0.05	3.087	2.180	1.416	> 0.05	5.158	2.417	2.134	< 0.05
	Genotype:Treatment:Sex	-5.049	5.800	-0.870	> 0.05	-1.784	3.067	-0.582	> 0.05	-3.487	3.399	-1.026	> 0.05
NREM	Genotype	9.556	2.518	3.795	< 0.001	-0.449	1.308	-0.343	> 0.05	4.771	1.511	3.158	< 0.01
	Treatment	2.930	2.761	1.061	> 0.05	2.268	1.434	1.581	> 0.05	2.614	1.656	1.578	> 0.05
	Sex	8.328	2.680	3.108	< 0.01	1.509	1.392	1.084	> 0.05	5.067	1.608	3.152	< 0.01
	Genotype:Treatment	-3.772	3.510	-1.075	> 0.05	-2.062	1.824	-1.131	> 0.05	-2.954	2.106	-1.403	> 0.05
	Genotype:Sex	-2.962	3.597	-0.823	> 0.05	1.070	1.869	0.573	> 0.05	-1.033	2.158	-0.479	> 0.05
	Treatment:Sex	-6.407	3.665	-1.748	> 0.05	-2.173	1.904	-1.141	> 0.05	-4.382	2.199	-1.993	> 0.05
	Genotype:Treatment:Sex	4.176	5.155	0.810	> 0.05	0.967	2.678	0.361	> 0.05	2.641	3.093	0.854	> 0.05
REM	Genotype	1.632	0.374	4.366	< 0.001	1.060	0.360	2.944	< 0.01	1.359	0.257	5.282	< 0.001
	Treatment	0.480	0.410	1.170	> 0.05	1.280	0.395	3.242	< 0.01	0.862	0.282	3.058	< 0.01
	Sex	0.846	0.398	2.127	< 0.05	0.577	0.383	1.505	> 0.05	0.717	0.274	2.620	< 0.05
	Genotype:Treatment	-0.922	0.521	-1.769	> 0.05	-1.077	0.502	-2.146	< 0.05	-0.996	0.359	-2.779	< 0.01
	Genotype:Sex	-0.647	0.534	-1.211	> 0.05	-0.914	0.514	-1.777	> 0.05	-0.774	0.367	-2.108	< 0.05
	Treatment:Sex	-0.651	0.544	-1.195	> 0.05	-0.911	0.524	-1.739	> 0.05	-0.775	0.374	-2.071	< 0.05
	Genotype:Treatment:Sex	0.873	0.765	1.141	> 0.05	0.816	0.737	1.106	> 0.05	0.846	0.527	1.606	> 0.05

Dox treatment modulated altered rTg4510 vigilance state (wake, NREM, REM) bout numbers and bout durations

To further examine the sleep/wake architecture of rTg4510 mice, overall bout numbers and bout durations were analysed for each vigilance state: wake, NREM and REM. Statistical analyses parameters for bout numbers are summarised in Table 3.3. Significant effects of genotype, treatment and sex were observed for both wake and NREM bouts, which were particularly prominent during the active phase. rTg4510 mice exhibited fewer bouts (thus less transitions) between vigilance states than WT mice, however, this was restored to WT levels by Dox treatment for both wake (Fig. 3.8A, C) and NREM (Fig. 3.8D, F) states (Table 3.4). Analysis of REM bout numbers revealed an overall genotype effect, whereby REM bout numbers were consistently reduced in rTg4510 mice compared with WT mice, but with no significant attenuation by Dox treatment (Fig. 3.8G-I; Table 3.3, 3.4).

Vigilance state bout durations statistical analyses summary is shown in Table 3.5. Wake bout duration was influenced by genotype, treatment and sex, particularly during the active phase (Fig. 3.8J). Female mice of both genotypes (but more pronounced in rTg4510 mice) tended to display longer bouts of wake, with female rTg4510 Control mice displaying a propensity for especially long, uninterrupted bouts of wakefulness (Fig. 3.8J-L). Combined with their reduced wake bout numbers (Fig. 3.8A-C), this suggests these mice develop a persistent hyperarousal phenotype and an inability to transition normally between vigilance states. NREM sleep time during the inactive phase was nearly identical between WT and rTg4510 mice (Fig. 3.7H) given that male mice of either genotype displayed both similar NREM bout numbers and bout durations during the inactive phase. Female rTg4510 mice, however, exhibited less NREM bout numbers (Fig. 3.8E), but of longer durations (Fig. 3.8N), balancing out to an equivalent NREM sleep time, compared with WT mice. This further emphasises the rTg4510's impaired ability to regulate sleep/wake transitions, which is exacerbated in female mice. During the active phase, REM bout durations tended to be shorter in rTg4510 mice than WT mice, especially in females (Fig. 3.8P). During the inactive phase, REM bout durations were comparable or longer in rTg4510 mice (Fig. 3.8Q). Dox treatment had no notable effects on REM bout durations.

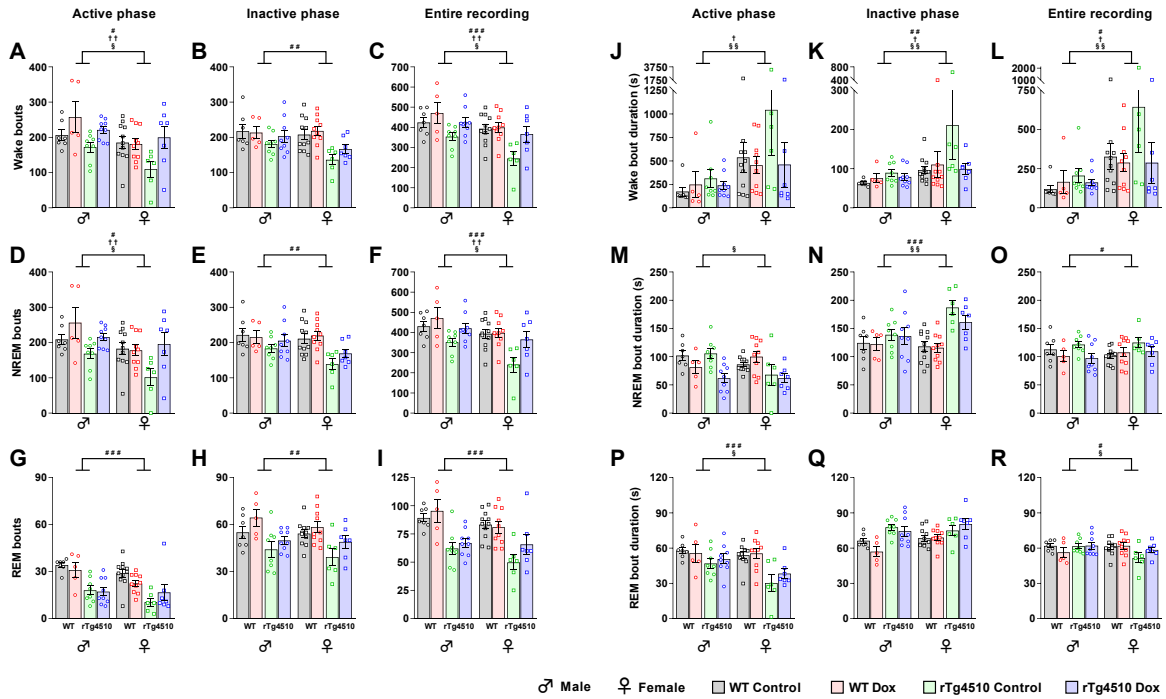

Figure 3.8. Altered sleep/wake architecture in rTg4510 mice.

A-I, Total number of wake (***A-C***), NREM (***D-F***) and REM (***G-I***) bouts averaged across (from left to right) the active phase, inactive phase and entire recording in rTg4510 and WT mice administered doxycycline (Dox) or control diets. ***J-R***, Mean wake (***J-L***), NREM (***M-O***) and REM (***P-R***) bout durations averaged across (from left to right) the active phase, inactive phase and entire recording in rTg4510 and WT mice administered Dox or control diets. Data are means ± SEM. n = 5-11 per group, per sex. #, † and § denote main effects of genotype, treatment and sex, respectively. $^{\#}P < 0.05$, $^{\#\#}P < 0.01$, $^{\#\#\#}P < 0.001$ vs. WT; $^{\dagger}P < 0.05$, $^{\dagger\dagger}P < 0.01$ vs. Control; $^{\S}P < 0.05$, $^{\S\S}P < 0.01$ vs. Female, by linear mixed effects model with Tukey's multiple comparisons test. Only main effects are graphically presented, refer to Table 3.3, 3.4 and 3.5 for further details.

Table 3.3. Vigilance state bout numbers statistical analyses summary.

Average bout numbers of each vigilance state per phase were analysed by a linear mixed effects model in R, using the *lm* function, incorporating the factors of Genotype, Treatment and Sex. Indented Pr(>|t|) values indicate statistical significance.

Vigilance state bout numbers													
		Active phase				**Inactive phase**				**Entire recording**			
Vigilance state	Fixed effect	Estimate	Std. error	t-value	Pr(>|t|)	Estimate	Std. error	t-value	Pr(>|t|)	Estimate	Std. error	t-value	Pr(>|t|)
Wake	Genotype	75.450	28.770	2.623	< 0.05	71.697	21.845	3.282	< 0.01	147.150	40.490	3.634	< 0.001
	Treatment	90.570	31.540	2.872	< 0.01	30.762	23.947	1.285	> 0.05	121.330	44.390	2.733	< 0.01
	Sex	62.370	30.620	2.037	< 0.05	44.583	23.246	1.918	> 0.05	106.960	43.090	2.482	< 0.05
	Genotype:Treatment	-94.230	40.100	-2.350	< 0.05	-19.826	30.449	-0.651	> 0.05	-114.050	56.440	-2.021	< 0.05
	Genotype:Sex	-41.540	41.090	-1.011	> 0.05	-35.376	31.200	-1.134	> 0.05	-79.920	57.830	-1.330	> 0.05
	Treatment:Sex	-41.720	41.870	-0.996	> 0.05	-9.012	31.794	-0.283	> 0.05	-50.740	58.930	-0.861	> 0.05
	Genotype:Treatment:Sex	96.890	58.900	1.645	> 0.05	-6.096	44.719	-0.136	> 0.05	90.800	82.890	1.095	> 0.05
NREM	Genotype	80.890	29.210	2.769	< 0.01	71.833	21.721	3.307	< 0.01	152.730	40.870	3.737	< 0.001
	Treatment	94.450	32.020	2.950	< 0.01	30.119	23.810	1.265	> 0.05	124.570	44.800	2.780	< 0.01
	Sex	66.670	31.080	2.145	< 0.05	44.333	23.113	1.918	> 0.05	111.000	43.490	2.552	< 0.05
	Genotype:Treatment	-98.680	40.720	-2.424	< 0.05	-21.119	30.276	-0.698	> 0.05	-119.800	56.970	-2.103	< 0.05
	Genotype:Sex	-40.680	41.720	-0.975	> 0.05	-33.762	31.023	-1.088	> 0.05	-74.440	58.380	-1.275	> 0.05
	Treatment:Sex	-47.290	42.520	-1.112	> 0.05	-8.619	31.613	-0.273	> 0.05	-55.900	59.490	-0.940	> 0.05
	Genotype:Treatment:Sex	99.000	59.800	1.656	> 0.05	-6.952	44.464	-0.156	> 0.05	92.050	83.670	1.100	> 0.05
REM	Genotype	18.591	4.362	4.262	< 0.001	14.939	5.457	2.738	< 0.01	33.530	8.062	4.159	< 0.001
	Treatment	6.241	4.782	1.300	> 0.05	9.667	5.982	1.616	> 0.05	15.881	8.838	1.797	> 0.05
	Sex	7.500	4.642	1.616	> 0.05	4.792	5.806	0.825	> 0.05	12.292	8.579	1.433	> 0.05
	Genotype:Treatment	-12.805	6.080	-2.106	< 0.05	-5.539	7.606	-0.728	> 0.05	-18.345	11.237	-1.632	> 0.05
	Genotype:Sex	-2.448	6.230	-0.393	> 0.05	-4.064	7.793	-0.522	> 0.05	-6.512	11.515	-0.566	> 0.05
	Treatment:Sex	-6.992	6.349	-1.101	> 0.05	-4.014	7.942	-0.505	> 0.05	-11.006	11.734	-0.938	> 0.05
	Genotype:Treatment:Sex	10.440	8.929	1.169	> 0.05	9.287	11.170	0.831	> 0.05	19.272	16.504	1.195	> 0.05

Table 3.4. Vigilance state bout numbers post hoc analyses summary.

Post hoc analysis of the genotype x treatment interaction from Table 3.3. Post hoc tests were conducted in R, using the *emmeans* function, with Tukey's multiple comparisons test. Indented p values indicate statistical significance.

Vigilance state bout numbers																
Interaction: Genotype x Treatment		**Active phase**					**Inactive phase**					**Entire recording**				
Vigilance state	Treatment group	Estimate	Std. error	df	t-value	p value	Estimate	Std. error	df	t-value	p value	Estimate	Std. error	df	t-value	p value
Wake	rTg4510 Control : WT Control	-54.700	20.500	55.000	-2.661	< 0.05				No significant interaction term		-108.700	28.900	55.000	-3.759	< 0.01
	rTg4510 Control : rTg4510 Dox	-69.700	20.900	55.000	-3.329	< 0.01						-96.000	29.500	55.000	-3.257	< 0.05
	rTg4510 Control : WT Dox	-78.600	21.800	55.000	-3.606	< 0.01						-136.000	30.700	55.000	-4.432	< 0.001
	WT Control : rTg4510 Dox	-15.000	19.800	55.000	-0.759	> 0.05						12.700	27.900	55.000	0.457	> 0.05
	WT Control : WT Dox	-23.900	20.700	55.000	-1.156	> 0.05						-27.300	29.100	55.000	-0.937	> 0.05
	rTg4510 Dox: WT Dox	-8.900	21.100	55.000	-0.422	> 0.05						-40.000	29.700	55.000	-1.349	> 0.05
NREM	rTg4510 Control : WT Control	-60.600	20.900	55.000	-2.903	< 0.05				No significant interaction term		-115.500	29.200	55.000	-3.957	< 0.01
	rTg4510 Control : rTg4510 Dox	-70.800	21.300	55.000	-3.331	< 0.01						-96.600	29.700	55.000	-3.248	< 0.05
	rTg4510 Control : WT Dox	-82.200	22.100	55.000	-3.713	< 0.01						-138.300	31.000	55.000	-4.467	< 0.001
	WT Control : rTg4510 Dox	-10.300	20.100	55.000	-0.510	> 0.05						18.900	28.100	55.000	0.672	> 0.05
	WT Control : WT Dox	-21.600	21.000	55.000	-1.029	> 0.05						-22.800	29.400	55.000	-0.776	> 0.05
	rTg4510 Dox: WT Dox	-11.400	21.400	55.000	-0.531	> 0.05						-41.700	30.000	55.000	-1.392	> 0.05
REM	rTg4510 Control : WT Control	-17.370	3.110	55.000	-5.575	< 0.001				No significant interaction term					No significant interaction term	
	rTg4510 Control : rTg4510 Dox	-2.720	3.170	55.000	-0.856	> 0.05										
	rTg4510 Control : WT Dox	-12.500	3.310	55.000	-3.782	< 0.01										
	WT Control : rTg4510 Dox	14.650	3.000	55.000	4.881	< 0.001										
	WT Control : WT Dox	4.870	3.140	55.000	1.550	> 0.05										
	rTg4510 Dox: WT Dox	-9.780	3.200	55.000	-3.058	> 0.05										

Table 3.5. Vigilance state bout duration statistical analyses summary.

Average bout duration of each vigilance state per phase were analysed by a linear mixed effects model in R, using the *lm* function, incorporating the factors of Genotype, Treatment and Sex. Indented Pr(>|t|) values indicate statistical significance.

Vigilance state bout duration											
		Active phase				**Inactive phase**				**Entire recording**	
Vigilance state	Fixed effect	Estimate	Std. error	t-value	Pr(>|t|)	Estimate	Std. error	t-value	Pr(>|t|)	Estimate	Std. error	t-value	Pr(>|t|)
Wake	Genotype	-507.800	257.000	-1.976	> 0.05	-115.010	41.380	-2.779	< 0.01	-319.900	147.200	-2.173	< 0.05
	Treatment	-584.600	281.800	-2.075	< 0.05	-112.340	45.360	-2.477	< 0.05	-358.700	161.400	-2.222	< 0.05
	Sex	-733.600	273.500	-2.682	< 0.01	-122.590	44.030	-2.784	< 0.01	-441.400	156.700	-2.817	< 0.01
	Genotype:Treatment	500.100	358.300	1.396	> 0.05	126.020	57.680	2.185	< 0.05	321.200	205.200	1.565	> 0.05
	Genotype:Sex	367.300	367.100	1.000	> 0.05	89.210	59.100	1.509	> 0.05	234.300	210.300	1.114	> 0.05
	Treatment:Sex	510.100	374.100	1.364	> 0.05	101.710	60.220	1.689	> 0.05	314.800	214.300	1.469	> 0.05
	Genotype:Treatment:Sex	-349.700	526.100	-0.665	> 0.05	-103.590	84.710	-1.223	> 0.05	-232.000	301.400	-0.770	> 0.05
NREM	Genotype	18.279	13.445	1.360	> 0.05	-69.150	16.040	-4.311	< 0.001	-23.534	10.869	-2.165	< 0.05
	Treatment	-6.018	14.739	-0.408	> 0.05	-26.080	17.590	-1.483	> 0.05	-15.613	11.915	-1.310	> 0.05
	Sex	37.385	14.307	2.613	< 0.05	-48.490	17.070	-2.841	< 0.01	-3.685	11.566	-0.319	> 0.05
	Genotype:Treatment	19.807	18.741	1.057	> 0.05	23.930	22.360	1.070	> 0.05	21.781	15.150	1.438	> 0.05
	Genotype:Sex	-21.932	19.203	-1.142	> 0.05	54.750	22.910	2.390	< 0.05	14.741	15.524	0.950	> 0.05
	Treatment:Sex	-37.912	19.569	-1.937	> 0.05	23.640	23.350	1.012	> 0.05	-8.474	15.819	-0.536	> 0.05
	Genotype:Treatment:Sex	3.423	27.523	0.124	> 0.05	-23.490	32.840	-0.715	> 0.05	-9.448	22.250	-0.425	> 0.05
REM	Genotype	23.743	6.302	3.767	< 0.001	-6.514	4.799	-1.357	> 0.05	9.272	3.902	2.376	< 0.05
	Treatment	8.163	6.909	1.181	> 0.05	5.523	5.261	1.050	> 0.05	6.900	4.278	1.613	> 0.05
	Sex	16.574	6.706	2.472	< 0.05	2.561	5.107	0.501	> 0.05	9.875	4.152	2.378	< 0.05
	Genotype:Treatment	-6.594	8.785	-0.751	> 0.05	-4.969	6.689	-0.743	> 0.05	-5.817	5.439	-1.069	> 0.05
	Genotype:Sex	-12.729	9.001	-1.414	> 0.05	-4.944	6.854	-0.721	> 0.05	-9.005	5.573	-1.616	> 0.05
	Treatment:Sex	-4.274	9.173	-0.466	> 0.05	-8.801	6.985	-1.260	> 0.05	-6.440	5.680	-1.134	> 0.05
	Genotype:Treatment:Sex	0.562	12.902	0.044	> 0.05	-0.965	9.824	-0.098	> 0.05	-0.168	7.988	-0.021	> 0.05

rTg4510 mice display decreased delta and theta power during sleep

To infer sleep/wakefulness quality, vigilance state-specific EEG power spectral analysis (statistical analyses summarised in Table 3.6 and 3.7) were performed. rTg4510 mice showed a general reduction in EEG power during wake compared with WT mice, predominantly in the 1-10 Hz range, but this was not affected by Dox treatment (Fig. 3.9A, D). rTg4510 mice also showed substantial decreases in delta (1-4 Hz) power during NREM sleep, particularly in the slower delta frequencies (Fig. 3.9B). Delta power deficits appeared to be slightly attenuated by Dox treatment in male, but not female rTg4510 mice, indicative of improvements in slow wave sleep quality (Fig. 3.9E). When assessing slow delta (1-2.5 Hz; Fig. 3.9G) and fast delta (2.5-4 Hz; Fig. 3.9H) power during NREM sleep separately, delta power was significantly increased in Dox-treated male rTg4510 mice, compared to controls, in the slow, but not fast frequencies. Dox treatment did not influence NREM delta power in female rTg4510 mice (Fig. 3.9E, G, H). Theta (5-9 Hz) power was also decreased in rTg4510 mice during REM sleep (Fig. 3.9C, F). Dox treatment appeared to slightly modulate theta power during REM sleep in male rTg4510 mice, although this did not reach statistical significance.

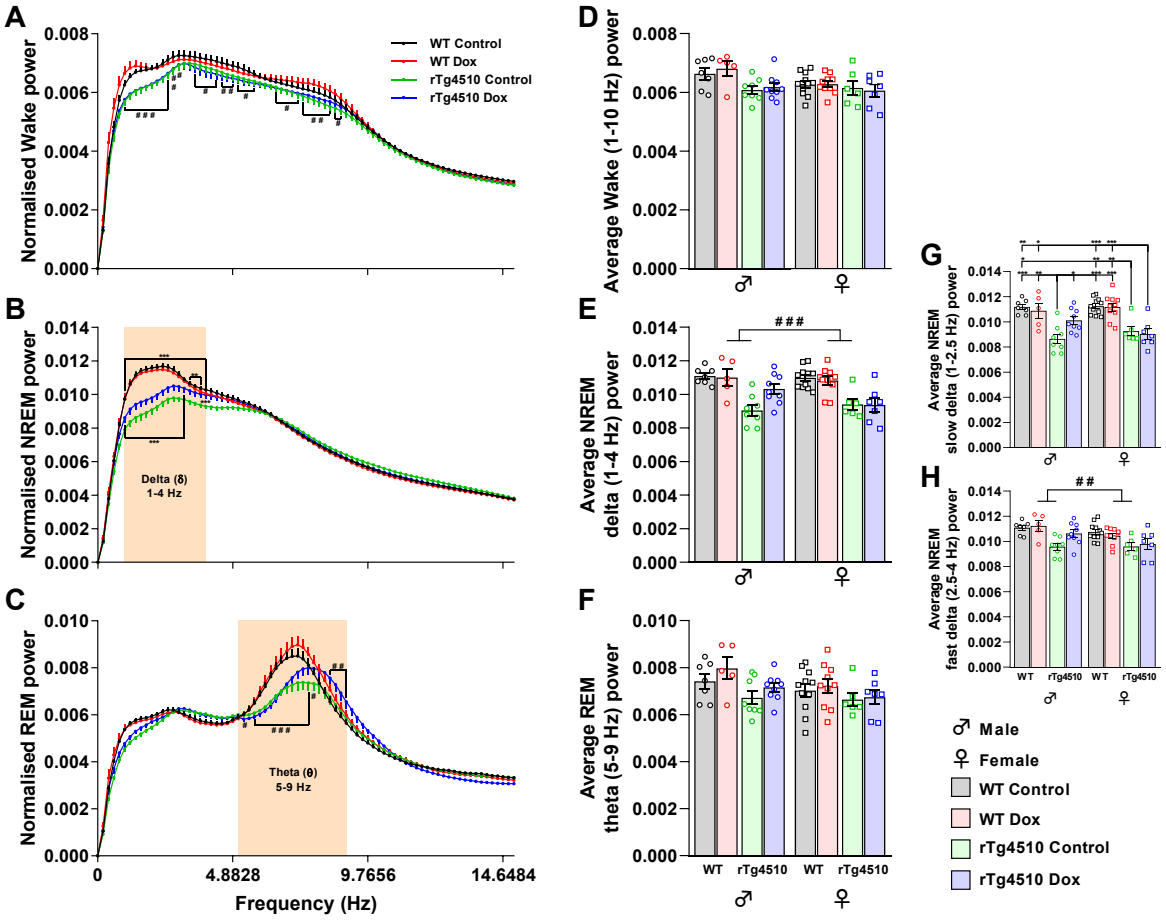

Figure 3.9. Altered EEG power in rTg4510 mice.

A-C, Vigilance state-specific normalised EEG power for wake (***A***), NREM (***B***) and REM (***C***) in rTg4510 and WT mice administered doxycycline (Dox) or control diets. Data are means ± SEM. n = 14-18 per group. $^{**}P < 0.01$, $^{***}P < 0.001$ vs. rTg4510 Control (genotype x treatment x frequency); $^{\#}P < 0.05$, $^{\#\#}P < 0.01$, $^{\#\#\#}P < 0.001$ vs. WT (genotype x frequency) within frequency band, by repeated measures linear mixed effects model with Tukey's multiple comparisons test. ***D***, Average wake power over the 1-10 Hz frequency range. ***E***, Average NREM power over the delta (1-4 Hz) frequencies. ***F***, Average REM power over the theta (5-9 Hz) frequencies. ***G***, Average NREM power over the slow delta (1-2.5 Hz) frequencies. ***H***, Average NREM power over the fast delta (2.5-4 Hz) frequencies. n = 5-11 per group, per sex. ***D-H***, # and † denote main effects of genotype and treatment, respectively. $^{\#\#\#}P < 0.001$ vs. WT; $^{\dagger}P < 0.05$ vs. Control; $^{*}P < 0.05$, $^{**}P < 0.01$, $^{***}P < 0.001$, by linear mixed effects model with Tukey's multiple comparisons test. Signals from EEG1 and EEG2 electrodes were combined. All transition epochs were excluded from power analysis. For clarity, not all statistically significant differences are graphically presented (***A-C***). Refer to Table 3.6 and 3.7 for further details.

Table 3.6. EEG power statistical analyses summary.

Vigilance state-specific normalised EEG power across the 23 h recording were analysed by a repeated measures linear mixed effects model in R, using the *lme*r function, incorporating the factors of Genotype, Treatment and Frequency (repeated factor). Indented Pr(>|t|) values indicate statistical significance.

Vigilance state-specific EEG power															
					Wake					NREM					REM
Fixed effect	Estimate	Std. error	df	t-value	Pr(>|t|)	Estimate	Std. error	df	t-value	Pr(>|t|)	Estimate	Std. error	df	t-value	Pr(>|t|)
Genotype	0.000384	0.000118	144.1	3.252	< 0.01	0.001109	0.000139	346.9	7.999	< 0.001	0.000417	0.000132	203.9	3.164	< 0.01
Treatment	0.000016	0.000121	144.1	0.133	> 0.05	0.000477	0.000142	346.9	3.346	< 0.001	0.000279	0.000135	203.9	2.063	< 0.05
Frequency (Hz)	-0.000222	0.000005	6422.0	-41.544	< 0.001	-0.000332	0.000008	6442.0	-41.336	< 0.001	-0.000154	0.000007	6442.0	-22.738	< 0.001
Genotype:Treatment	0.000100	0.000168	144.1	0.599	> 0.05	-0.000595	0.000197	346.9	-3.019	< 0.01	-0.000154	0.000187	203.9	-0.821	> 0.05
Genotype:Frequency	-0.000019	0.000007	6422.0	-2.620	< 0.01	-0.000085	0.000011	6442.0	-7.983	< 0.001	-0.000032	0.000009	6442.0	-3.584	< 0.001
Treatment:Frequency	0.000002	0.000007	6422.0	0.286	> 0.05	-0.000038	0.000011	6442.0	-3.494	< 0.001	-0.000026	0.000009	6442.0	-2.840	< 0.01
Genotype:Treatment:Frequency	-0.000012	0.000010	6422.0	-1.186	> 0.05	0.000044	0.000015	6442.0	2.855	< 0.01	0.000018	0.000013	6442.0	1.420	> 0.05

Table 3.7. EEG NREM delta power statistical analyses summary.

NREM normalised EEG power across the 23 h recording were analysed by a linear mixed effects model in R, using the *lm* function, incorporating the factors of Genotype, Treatment and Sex. Indented Pr(>|t|) values indicate statistical significance.

Vigilance state-specific EEG power										
	NREM (delta 1-4 Hz)				NREM (slow delta 1-2.5 Hz)				NREM (fast delta 2.5-4 Hz)			
Fixed effect	Estimate	Std. error	t-value	Pr(>|t|)	Estimate	Std. error	t-value	Pr(>|t|)	Estimate	Std. error	t-value	Pr(>|t|)
Genotype	0.001581	0.000423	3.739	< 0.001	0.001978	0.000481	4.111	< 0.001	0.001155	0.000399	2.896	< 0.01
Treatment	-0.000043	0.000463	-0.093	> 0.05	-0.000239	0.000527	-0.452	> 0.05	0.000195	0.000437	0.447	> 0.05
Sex	-0.000363	0.000450	-0.806	> 0.05	-0.000631	0.000512	-1.233	> 0.05	-0.000029	0.000424	-0.068	> 0.05
Genotype:Treatment	-0.000125	0.000589	-0.212	> 0.05	0.000180	0.000671	0.268	> 0.05	-0.000496	0.000556	-0.893	> 0.05
Genotype:Sex	0.000465	0.000604	0.771	> 0.05	0.000559	0.000687	0.814	> 0.05	0.000351	0.000570	0.616	> 0.05
Treatment:Sex	0.001322	0.000615	2.149	< 0.05	0.001703	0.000700	2.433	< 0.05	0.000856	0.000580	1.475	> 0.05
Genotype:Treatment:Sex	-0.001240	0.000865	-1.432	> 0.05	-0.001943	0.000985	-1.973	= 0.05	-0.000399	0.000816	-0.489	> 0.05

Dox treatment abolished the positive correlation between hyperarousal and hyperactivity in rTg4510 mice without affecting wake time

Hyperlocomotion has been previously described in rTg4510 mice (Blackmore et al., 2017). Similarly, the present study investigated locomotor activity in an open field for one hour during the active phase and detected a hyperactivity phenotype in rTg4510 mice. A main effect of genotype was observed when assessing total ambulatory distance travelled (Genotype: $F_{(1, 62)} = 17.96$, $P < 0.0001$; treatment: $F_{(1, 62)} = 3.770$, $P = 0.0567$; interaction: $F_{(1, 62)} = 3.305$, $P = 0.0739$, Fig. 3.10A). Dox treatment appeared to attenuate this phenotype, although not significantly. When assessing total ambulatory time, rTg4510 Control mice spent significantly more time ambulatory than both WT groups and Dox-treated rTg4510 mice (Genotype: $F_{(1, 62)} = 17.17$, $P < 0.0001$; treatment: $F_{(1, 62)} = 4.318$, $P = 0.0419$; interaction: $F_{(1, 62)} = 4.798$, $P = 0.0323$, Fig. 3.10B). As expected, given the hyperarousal phenotype during the active phase, a positive correlation between average wake time and ambulatory time was detected in rTg4510 Control mice ($R^2 = 0.5192$, $P = 0.0055$, Fig. 3.10C). The present study aimed to determine the dominant driving force for wakefulness in rTg4510 mice: hyperactivity or hyperarousal. Regression analysis suggested it may be hyperarousal, given that there was no association

between ambulatory time and wake duration in rTg4510 Dox-treated mice (R^2 = 0.01268, P = 0.6895, Fig. 3.10C), despite Dox treatment not altering wake time during the active phase (Fig. 3.7A, D).

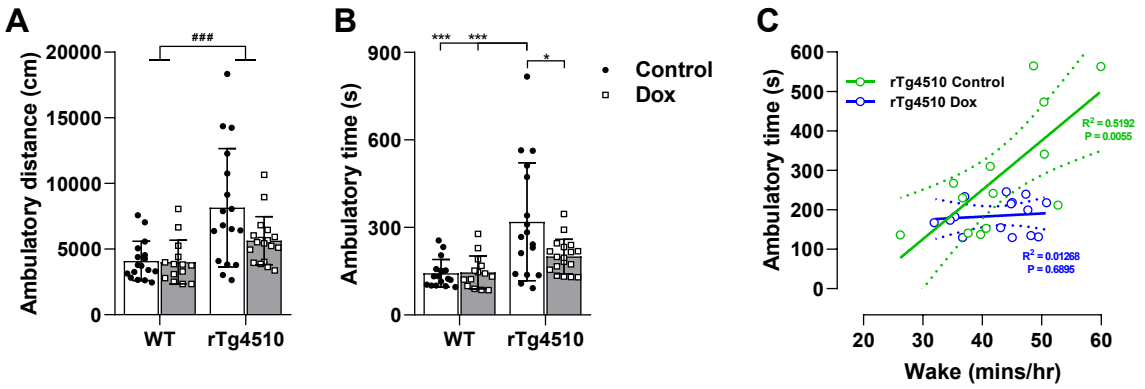

Figure 3.10. Abolished relationship between hyperarousal and hyperactivity in Dox-treated rTg4510 mice. ***A-B***, Total ambulatory distance travelled (***A***) and total time spent ambulatory (***B***) during the 1 hr open field locomotor activity assessment, conducted during the active phase of rTg4510 and WT mice administered doxycycline (Dox) or control diets. Data are means ± SEM. n = 14-17. # denotes main effect of genotype. $^{###}$P < 0.001 vs. WT; *P < 0.05, ***P < 0.001, by two-way ANOVA with Tukey's multiple comparisons test. ***C***, Correlation between total ambulatory time and average wake time per hour during the active phase. Solid lines denote the linear regression line of best fit, with 95% confidence bands (dotted curves).

3.5 Discussion

The present study examined the effects of genetically reducing tau expression on sleep/wakefulness in a mouse model overexpressing human mutant tau, in addition to the effects on the noted phenotypes of the rTg4510 mouse, which include neurodegeneration, cognitive impairments and locomotor hyperactivity. As previously reported (Ramsden et al., 2005; Santacruz et al., 2005; Blackmore et al., 2017), Dox treatment decreased tau and p-tau levels in the brain. Dox treatment also slowed or reversed the cognitive and neurodegenerative phenotype of rTg4510 mice, which attenuated brain atrophy, prevented spatial learning and recall deficits and reduced locomotor hyperactivity. rTg4510 mice exhibited a pronounced hyperarousal phenotype during the active phase, in addition to altered sleep/wake architecture and EEG power spectral deficits. Intriguingly, this sleep/wake profile was largely unaffected by Dox treatment, suggesting the arousal circuitry is affected by tau earlier and more permanently than other brain regions. Sex differences were also observed in the sleep/wake phenotype of rTg4510 mice, in general with females showing an exacerbated phenotype versus

males, certain aspects of which were corrected by Dox treatment, again particularly in female mice.

Tau and p-tau protein levels were reduced by approximately 50% in hippocampal and cortical regions in rTg4510 mice following Dox treatment. A complete abolition of transgene expression is not necessary to halt tauopathy progression or exhibit functional benefits (Blackmore et al., 2017). Furthermore, repressing tau transgene expression would likely not eliminate mutant tau that has already been deposited prior to treatment initiation. Therefore, the rescue of cognitive ability and attenuation of brain atrophy presented here is encouraging given the relative amount of hyperphosphorylated tau still present in the brains of Dox-treated rTg4510 mice. These data stress the possibility that clinical interventions for tauopathy-related diseases may not necessarily need to remove all pathological tau and that partial reductions could still be functionally beneficial, in agreement with Blackmore et al. (2017).

Dox treatment attenuates the decrease in brain weight in rTg4510 mice (Santacruz et al., 2005; Blackmore et al., 2017). Here, increased brain volume in the hippocampus and cortex of Dox-treated rTg4510 mice was documented using *ex vivo* MRI imaging. Using DWI, microstructural alterations consistent with white matter degeneration in the hippocampus, cortex and corpus callosum were also observed, which align with previous findings in rTg4510 mice (Sahara et al., 2014; Wells et al., 2015). Reduced FA and increased ADC, ADi and RD are associated with white matter degeneration (Johnstone et al., 2015; Wright et al., 2017a; Wright et al., 2017b; Wright et al., 2019). For the first time, the present study demonstrated that Dox treatment restored FA to WT levels throughout the corpus callosum, but not in the hippocampus or cortex, indicating that attenuated deterioration of long white matter tracts is within the scope of therapeutic rescue that may be achieved by reducing tau and p-tau levels. Together, these data suggest that accumulation of hyperphosphorylated tau contributes to neuronal, synaptic and axonal degeneration and that reducing tau levels can slow these processes.

Complete prevention of hippocampal-dependent spatial recall deficits in the Barnes maze were observed following Dox treatment in rTg4510 mice. Improvement in spatial memory following Dox treatment in rTg4510 mice has been previously demonstrated using the Morris water maze (Ramsden et al., 2005; Santacruz et al., 2005) and Y-maze (Blackmore et al., 2017), however, this is the first such report in the Barnes maze, further emphasising the robustness of hippocampal-dependent cognitive rescue in the model. Thus, hyperphosphorylated tau contributes to cognitive decline which may be reversible, if treated early enough.

The sleep/wake phenotype has not previously been characterised in rTg4510 mice. The present study showed that rTg4510 mice exhibit 1) a pronounced hyperarousal phenotype specifically during the active phase, 2) alterations in vigilance state bout numbers and bout durations and 3) EEG power spectral deficits, particularly during NREM and REM sleep. rTg4510 mice displayed a similar sleep/wake profile to that of PS19 mice (Holth et al., 2017b), whereby both mice exhibited increased wake time and decreased NREM and REM sleep time. Together, these data provide compelling evidence for a causative role of p-tau in altering sleep/wakefulness. This phenotype emerged rather later in PS19 mice (9-11 months) than in rTg4510 mice in the present study, although this is not surprising given the PS19's comparatively slow tauopathy progression and lower tau expression (Yoshiyama et al., 2007), compared with rTg4510 mice. Furthermore, the alterations in vigilance state bout numbers and bout durations of rTg4510 mice described here paralleled some of those reported in PS19 mice (Holth et al., 2017b). rTg4510 mice showed a decreased number of wake bouts, but of longer durations, mirroring that of 9-11-month-old PS19 mice (Holth et al., 2017b); indicating these mice are less likely to transition out of the wake state, contributing to their hyperarousal. During the inactive phase, NREM bout numbers were decreased, whereas bout durations were increased in rTg4510 mice, thus NREM time was equivalent in rTg4510 and WT mice. Again, this points to an inability to regulate sleep/wake transitions, especially out of the prevailing vigilance state. REM bout numbers were reduced in rTg4510 mice across the recording, however, bout durations varied with the phase analysed.

Substantial sex differences in the sleep/wake phenotype of rTg4510 mice were also determined in the present study, with female mice showing an exacerbated hyperarousal phenotype. Such findings align with previous reports on sex differences in rTg4510 mice, with female mice displaying a more severe phenotype due to advanced tau pathology (Yue et al., 2011). Interestingly, although rTg4510 Dox-treated mice spent as much time in wake as rTg4510 Control mice, Dox treatment partially normalised their sleep/wake architecture by increasing the number of wake bouts and decreasing wake bout duration, especially in female rTg4510 mice, such that Dox-treated mice more closely resembled their WT littermates.

Delta (δ) waves (1-4 Hz) and theta (θ) waves (5-9 Hz) are the dominant frequencies during NREM and REM sleep, respectively (Franken et al., 1998). rTg4510 mice displayed state-specific decreases in delta and theta power, in addition to a generalised reduction in wake power. Reductions in EEG power across vigilance states have also been reported in PS19 mice (Holth et al., 2017b). In the present study, wake EEG power was predominantly unaffected by Dox treatment, although the attenuation of delta power during NREM sleep, especially in the

slow delta frequencies, suggests an improvement in sleep quality. Increased delta power was not present in female rTg4510 mice, which may be attributed to their exacerbated hyperarousal and tauopathy phenotype (Yue et al., 2011), compared with males. The similar sleep/wake phenotypes of rTg4510 and PS19 mice further emphasises the concept that tau pathology alone is sufficient to drive sleep/wake changes. Interestingly, despite substantially improving the parameters discussed above, Dox treatment exhibited a much less pronounced influence on the sleep/wake phenotype of rTg4510 mice.

Several nuclei of the ascending reticular activating system (ARAS) such as the locus coeruleus (LC), tuberomammillary nucleus (TMN) and dorsal raphe nucleus (DRN) play a key role in regulating sleep and wakefulness. The ARAS, especially the LC, is particularly affected in the early development of tau pathology (Braak and Del Tredici, 2011; Braak et al., 2011; Braak and Del Tredici, 2015; Stratmann et al., 2016); this may contribute to sleep/wake changes preceding the actual onset of cognitive decline observed in neurodegenerative diseases. The tau transgene expression in rTg4510 mice is CaMKII specific, which should theoretically spare expression in the brainstem and the ARAS. However, pathological tau spreads throughout the brain and particularly to these vulnerable regions (Iba et al., 2013), especially those widely connected with the rest of the brain, such as the LC. In future work it will therefore be of interest to determine whether tau spreading to and invading these regions in rTg4510 mice contributes to the early hyperarousal phenotype. The somewhat blunted effect of Dox treatment on the sleep/wake phenotype suggests the pathological insult to these regions is more permanent than in the hippocampus or cortex. Although, in light of the recent findings from Gamache et al. (2019), it cannot be conclusively determined whether the hyperarousal phenotype of rTg4510 mice is due to non-plastic tau-induced changes in the ARAS or rather, due to consequences from non-targeted gene KO in these mice (see Chapter 6, section 6.4). However, the similar hyperarousal phenotype of PS19 mice, which do not exhibit non-targeted gene KO (Goodwin et al., 2019), supports the concept that mutant tau in particular is contributing to the hyperarousal phenotype of rTg4510 mice.

A hyperactivity phenotype has previously been reported in rTg4510 mice, which worsens with age, and is modulatable by Dox treatment (Blackmore et al., 2017). The data in the present study validates this finding and extends it to emphasise the relationship between hyperactivity and hyperarousal. It is expected that mice spending more time awake would also display more ambulatory time, and vice versa. Such a relationship indeed exists in rTg4510 mice, yet the dominant driving force is unknown. However, the abolition of this relationship in rTg4510 Dox-treated mice suggests hyperarousal is the likely dominant factor, in that Dox

treatment weakens the hyperactivity impulse yet does not affect wake time. Together these data suggest that the insult to the arousal circuitry is extensive and perhaps permanent by 4.5-6.5 months of age in rTg4510 mice.

A bidirectional relationship between sleep and neurodegenerative disease pathology has been recognised, particularly for Aβ, however, less so for tau. A key aim of the present study was to document the sleep/wake profile of tau transgenic rTg4510 mice and to determine the effects of genetically reducing mutant tau expression, after initiation of pathology, on this phenotype. In addition to altered sleep/wake architecture and diminished EEG power, rTg4510 mice exhibited a hyperarousal phenotype which was particularly prominent during the active phase and was exacerbated in female mice. This sleep/wake profile is similar to that of the tau transgenic PS19 mice (Holth et al., 2017b), which harbour a similar tau mutation to rTg4510 mice despite a dissimilar genetic construction (Yoshiyama et al., 2007; Goodwin et al., 2019), supporting the hypothesis that modified tau variants are responsible for this phenotype. Intriguingly, Dox treatment produced substantial or complete attenuation of all parameters investigated in this study, except for hyperarousal and power spectral deficits, which were only partially mitigated. These findings suggest potentially irreversible tau-mediated damage to the arousal circuitry at the ages investigated. Further work is required to investigate this hypothesis and to determine the underlying mechanisms involved. In conclusion, these findings highlight a primary role of tau pathology on early sleep/wake behaviour alterations in neurodegenerative diseases characterised by tauopathy.

Chapter 4

The Orexin Receptor 2 Antagonist MK-1064, but not Suvorexant, Improves Cognitive Performance in the rTg4510 Mouse Model of Tauopathy by Promoting Balanced Sleep

4.1 Abstract

Tau pathology contributes to the bidirectional relationship between sleep and neurodegenerative disease. Prominent sleep/wake disturbances have been reported in the rTg4510 transgenic mouse model of tauopathy, emphasising the concept that hyperphosphorylated tau may drive sleep/wake changes. The present study aimed to specifically target these sleep/wake deficits and determine whether pharmacological promotion of sleep, with orexin receptor antagonists, could improve cognition and/or slow tauopathy progression in rTg4510 mice. Four and a half-month-old male and female rTg4510 mice were treated daily for eight weeks with either 50 mg/kg/day of the dual orexin receptor antagonist (DORA) suvorexant or 40 mg/kg/day of the selective orexin receptor 2 antagonist (2-SORA) MK-1064. Vehicle-treated rTg4510 mice again demonstrated a marked hyperarousal phenotype during the active, but not inactive, phase. Suvorexant increased REM sleep in rTg4510 mice when administered during the inactive phase but did not affect cognitive ability or alter tau/phosphorylated tau levels in the brain. On the other hand, MK-1064 increased both NREM and REM sleep and attenuated the hyperarousal phenotype when administered at the beginning of the active phase in male, but not female, rTg4510 mice. MK-1064-treated male rTg4510 mice exhibited a partial improvement in hippocampal-dependent spatial recall, which correlated with the amount of MK-1064-promoted sleep. The origin of the sex-divergent responses to MK-1064 are unknown but are postulated to be due to sex differences in the hyperarousal drive of rTg4510 mice and/or functional alterations in their orexin system. Collectively, these findings highlight the therapeutic potential of sleep to correct cognitive deficits in tauopathy models and further emphasises the emerging bidirectional relationship between sleep and neurodegenerative disease.

4.2 Introduction

There is a growing recognition of the bidirectional relationship between sleep and neurological disease pathology, particularly in neurodegenerative disorders involving amyloid-β (Aβ) and/or tau pathologies (Ju et al., 2014; Lim et al., 2014; Wang and Holtzman, 2020). Much of the preclinical research conducted thus far has focused on the effects of Aβ on sleep/wakefulness (Cirrito et al., 2005; Kang et al., 2009; Bero et al., 2011; Roh et al., 2012), although emerging evidence points to a crucial involvement of tau (Chapter 3; Koss et al., 2016; Holth et al., 2017b; Zhu et al., 2018). The likely critical contribution of tau to sleep/wake phenotypes is perhaps unsurprising, since tau pathology is a major feature of neurodegenerative disorders such as Alzheimer's disease (AD) and tau-variant frontotemporal dementia (FTD-tau; Hutton et al., 1998; Blennow et al., 2006; Ballatore et al., 2007; Gotz and Ittner, 2008; Forrest et al., 2018) and patients with these disorders commonly exhibit prominent sleep/wake disturbances, which often present well before cognitive impairment (Moran et al., 2005; Anderson et al., 2009; Westerberg et al., 2012; Musiek et al., 2015). It is also plausible that in AD, Aβ and tau pathologies work synergistically to mediate sleep/wake disturbances. However, FTD patients, with little or no Aβ pathology, often experience even more severe sleep and circadian disturbances (Bonakis et al., 2014). Such observations emphasise a potentially vital role that tau may play in mediating sleep/wake disturbances in AD or FTD-tau.

Preclinical transgenic models can play an important role in answering questions about specific molecular contributions to disease symptomatology. To date, however, sleep/wake alterations in models of pure tauopathy have been published for only two tau transgenic mouse models, the $PLB2_{Tau}$ mouse (Koss et al., 2016) and the PS19 mouse, where a progressive hyperarousal phenotype was identified (Holth et al., 2017b). Given the relative scarcity of preclinical literature regarding the relationship between tauopathy mouse models and sleep, a third tau overexpression model was investigated (Chapter 3), revealing a previously unreported sleep/wake phenotype of the rTg4510 transgenic mouse model of tauopathy, which overexpresses human tau containing the P301L *MAPT* mutation (associated with FTD-tau in humans). rTg4510 mice exhibited a hyperarousal phenotype which was particularly prominent during the active phase, in addition to altered vigilance state bouts and bout durations and vigilance state-specific electroencephalography (EEG) power spectral deficits (Chapter 3). Importantly, much of the observed sleep/wake phenotype in rTg4510 mice paralleled that of the tau transgenic PS19 mouse, which harbors a similar P301S *MAPT* mutation (Holth et al., 2017b). Together, these two studies emphasise that tau pathology alone is sufficient to drive

sleep/wake changes and that these changes manifest themselves in a similar way across tauopathy models (Chapter 3; Holth et al., 2017b).

An advantage of the rTg4510 mouse is that tau transgene expression is repressible upon administration of doxycycline (Dox; Ramsden et al., 2005; Santacruz et al., 2005). Suppressing tau transgene expression with Dox from 4.5-6.5 months of age rescued the cognitive, neurodegenerative and hyperlocomotor phenotype of rTg4510 mice, but it did not prevent their altered sleep/wake phenotype (Chapter 3). In Chapter 3, a REM sleep deficit evident during the inactive phase was corrected by Dox treatment. This observation led to the hypothesis that REM sleep played a role in cognitive rescue, especially given the proposed involvement of REM sleep in the consolidation of spatial learning (Boyce et al., 2016) and the noted REM sleep disruption in AD and FTD (Prinz et al., 1982; Petit et al., 2004; Moran et al., 2005). However, despite improving REM sleep, Dox had no effect on the hyperarousal phenotype.

Sleep appears to play a key role in the consolidation of memory and learning (Diekelmann and Born, 2010). In addition, periods of extended wakefulness, or sleep deprivation, affect the extracellular release of both Aβ (Cirrito et al., 2005; Cirrito et al., 2008; Bero et al., 2011; Tabuchi et al., 2015) and tau (Pooler et al., 2013; Yamada et al., 2014; Wu et al., 2016; Wang et al., 2017a). During sleep, toxic metabolites such as Aβ and/or tau are more readily cleared from the brain in rodents (Xie et al., 2013), mediated via a glymphatic pathway (Iliff et al., 2012; Iliff et al., 2013; Iliff et al., 2014). Such findings suggest a therapeutic benefit of sleep in neurodegenerative models and/or disorders. Furthermore, it has previously been shown that sleep restriction exacerbated Aβ plaque burden in APP/PS1 mice whereas chronic treatment with the dual orexin receptor antagonist (DORA) almorexant, attenuated plaque burden (Kang et al., 2009). Tau pathology was also exacerbated following sleep restriction in tau transgenic PS19 (P301S) mice (Zhu et al., 2018), however, no studies have yet reported whether beneficial effects are accessible in a tauopathy mouse model following the enhancement of sleep or reduction of hyperarousal.

The aim of the present study was therefore to determine whether pharmacologically promoting sleep could improve cognition and/or slow tauopathy progression in rTg4510 mice by targeting the previously reported sleep/wake deficits in these mice (Chapter 3), using chronic dosing of orexin receptor antagonists to promote sleep, in an attempt to recover these insufficiencies. Orexin receptor antagonists were selected given their ability to promote both NREM and REM sleep, with DORAs in particular selectively promoting REM sleep (Mang et al., 2012; Betschart et al., 2013). Hypnotics such as non-benzodiazepine $GABA_A$ allosteric modulators tend to abolish REM sleep in rodents (Hoyer and Jacobson, 2013; Jacobson et al.,

2017; Hoyer et al., 2019). Therefore, the DORA suvorexant (Cox et al., 2010), which antagonises both orexin receptor 1 (OX_1R) and orexin receptor 2 (OX_2R) was administered during the inactive phase, with the aim of promoting REM sleep (Hoyer et al., 2013; Jacobson et al., 2014), as was previously observed following Dox treatment (Chapter 3). In a second study, the OX_2R selective orexin receptor antagonist (2-SORA) MK-1064 (Roecker et al., 2014a) was used, with the aim of promoting both NREM and REM sleep (Gotter et al., 2016). MK-1064 was administered at the beginning of the active phase, in order to mitigate the prominent hyperarousal phenotype of rTg4510 mice and replace it with balanced sleep containing both NREM and REM. The effects these treatments had on the sleep/wake profile of rTg4510 mice and their subsequent influence on cognitive ability and tau/phosphorylated tau (p-tau) levels were then assessed.

4.3 Materials and methods

Animals

Male and female rTg4510 transgenic mice and wildtype (WT) littermates controls were used (Ramsden et al., 2005; Santacruz et al., 2005). rTg4510 mice were bred in house, as previously described (Ramsden et al., 2005; Santacruz et al., 2005). In brief, FBV/N mice expressing human tau containing the P301L *MAPT* mutation (associated with FTD-tau in humans) downstream of a tetracycline operon-responsive element (TRE) were crossed with 129SVeV mice expressing a tetracycline-controlled transactivator (tTA) under control of the Ca^{2+}-calmodulin-dependent protein kinase II (CaMKII) promotor. In this mouse, constitutive expression of the tau transgene is specifically restricted to forebrain structures due to the CaMKII promotor. All mice were genotyped using a standardised polymerase chain reaction (PCR) assay for tail DNA (Transnetyx Inc., Cordova, TN, USA). rTg4510 mice and WT controls entered the studies at 4.5 months of age, based on previous studies in-house (Chapter 3). All mice were single- or group-housed in standard, transparent open-top cages (29.5 x 16 x 13 cm) on sawdust with tissue paper nesting material. Standard rodent food and water were available *ad libitum.* All experimentation was performed in accordance with the Prevention of Cruelty to Animals Act (2004), under the guidelines of the National Health and Medical Research Council Code of Practice for the Care and Use of Animals for Experimental Purposes in Australia (2013) and approved by The Florey Animal Ethics Committee (AEC number: 16-022). All efforts were made to minimise animal suffering.

Compounds and drug preparation

The DORA suvorexant (Suvo; AdooQ Bioscience) or the 2-SORA MK-1064 (Merck and Co., Inc) were used. Drugs were prepared fresh daily as suspensions. The vehicle for suvorexant was 0.5% methylcellulose (MC; Sigma-Aldrich) in water. The vehicle for MK-1064 was 20% D-α-tocopherol polyethylene glycol 1000 succinate (TPGS; Sigma-Aldrich) in water. All drugs were administered by oral gavage, daily, in a volume of 10 ml/kg.

Procedure and study design

Two separate experiments were conducted, each using a different orexin receptor antagonist. The experimental protocols were principally identical, except where noted. The experimental study design timelines are presented in Fig. 4.1. Mice were initially housed under a 12 h light/dark cycle (lights on at 0700h) until just prior to 4.5 months of age, they were then transitioned to an experimental housing area with a new lights-on time (Experiment 1: lights on 0300h; Experiment 2: lights on 2130h) ten days before treatment began, to acclimatise to the new cycle. In Experiment 1 (suvorexant; Fig. 4.1A), rTg4510 mice and WT littermates were allocated to one of four groups: WT MC; WT Suvo; rTg4510 MC or rTg4510 Suvo. In Experiment 2 (MK-1064; Fig. 4.1B), rTg4510 and WT littermates were also allocated to one of four groups: WT TPGS; WT MK-1064; rTg4510 TPGS or rTg4510 MK-1064. At 4.5 months of age, all mice began receiving their respective treatments.

For Experiment 1, mice were orally administered 50 mg/kg/day suvorexant, or MC vehicle alone. This dose was selected based on previous literature using suvorexant in C57BL/6 mice (Betschart et al., 2013) and preliminary data in-house in rTg4510 mice. All dosing occurred between 0900-1000h (Circadian time (CT)6-7). For Experiment 2, mice were orally administered 40 mg/kg/day MK-1064, or TPGS vehicle alone. This dose was selected based on previous literature using MK-1064 in C57BL/6 mice (Gotter et al., 2016) and preliminary data in-house in rTg4510 mice. All dosing occurred between 0830-0930h (CT11-12). Four weeks after treatment initiation, mice in each experiment were surgically implanted with EEG/EMG recording devices (Pinnacle Technology Inc.). Following surgery recovery and a one-week acclimatisation to recording chambers, three 23 h polysomnographic recordings were conducted over three consecutive days, then cognition was assessed in the six-day Barnes maze behavioural test. At approximately 6.4 months of age mice were culled and samples collected. Mice entered the protocol in staggered cohorts of up to nine mice at a time with treatments pseudorandomly allocated within each cohort.

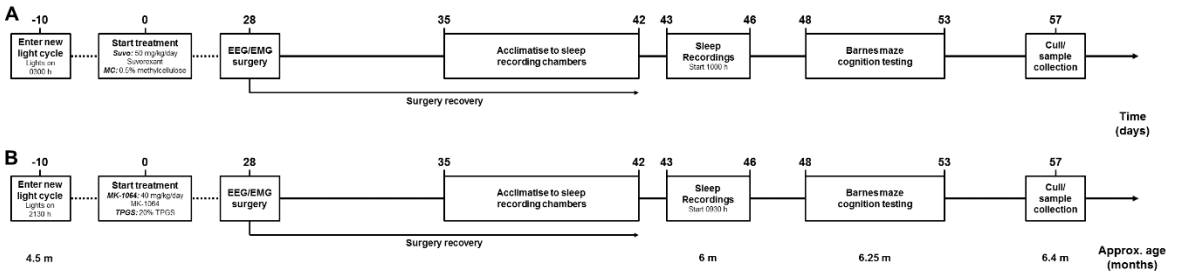

Figure 4.1. Experimental timeline schematic.

A-B*,** Schematic of the two separate study design timelines. Four and a half-month-old rTg4510 and WT littermates were acclimatised to their respective experimental light cycle ten days before treatment began. ***A, Mice were orally administered 50 mg/kg/day of suvorexant or 0.5% methylcellulose (MC) vehicle, during the inactive phase. ***B***, Mice were orally administered 40 mg/kg/day of MK-1064 or 20% D-α-tocopherol polyethylene glycol 1000 succinate (TPGS) vehicle, at the beginning of the active phase. ***A-B***, Four weeks after treatment initiation, mice were surgically implanted with EEG/EMG recording devices. Sleep/wake recordings were conducted at 6 months of age, followed by cognition testing in the Barnes maze. Mice were culled at 6.4 months of age and samples were collected. Mice entered this protocol in staggered cohorts of up to nine mice at a time.

Polysomnographic recordings and analysis

Surgery: Mice were anaesthetised with isoflurane in air (5% for induction, 2-3% for maintenance) and placed in a stereotaxic frame. Meloxicam (1-3 mg/kg, Ilium) and 500 µL of warm saline were administered subcutaneously. 50 µL of 1% lignocaine HCl (Pfizer) was administered near the incision site, then the skull was exposed and EEG/EMG preformed head mounts (Catalogue number: #8201-SS, Pinnacle Technology Inc.) were surgically implanted. EEG1 and EEG2 electrodes (screws inserted into the head mount) were positioned over the parietal and frontal lobe, respectively. Reference and ground electrodes were positioned at equivalent regions, with reference embedded in the parietal region and ground in the frontal, in addition to a non-penetrating anchor screw embedded into the skull over the motor cortex. Two EMG wires attached to the head mount were inserted into the neck musculature and sutured (7-0 Prolene, Ethicon) into place. Sutures were used to close the scalp around the head mount. Dental cement was positioned under and around the head mount using an 18G drawing-up needle and allowed to set. The mouse was removed from the stereotaxic frame and placed into a warm recovery box (30°C) until it was moving freely, then returned to its original cage.

Recordings: Mice were individually housed in transparent, cylindrical sleep recording chambers (29 cm diameter x 30 cm height) for a further week of recovery and acclimatisation. Head mounts were plugged into pre-amplifier 24 h before recordings began. Three individual 23 h recordings were then acquired over three consecutive days using Sirenia Acquisition version 1.8.0 software (Pinnacle Technology Inc.). Three channels were recorded: EEG1,

EEG2 and EMG. The sampling rate was 200 Hz. 100 Hz EEG and EMG filters were applied. For Experiment 1, recordings began at 1000h (CT7) and finished at 0900h (CT6). For Experiment 2, recordings began at 0930h (CT12) and finished at 0830h (CT11). Following EEG/EMG recordings all mice were returned to their original cages.

Analysis: Sirenia recording files (.pvfs) were exported as European Data Format (.edf) and imported into the program Somnivore™ (Allocca et al., 2019) in 4 s epochs for vigilance state and power spectral analysis. The final 23 h recording from each mouse was used for analysis, unless faulty or otherwise unavailable, in which case the recording from day two or one was used. Each recording was scored by first training the Somnivore machine learning algorithm with 101 epochs of wake, NREM and REM. The entire hypnogram was then populated using Somnivore's auto-score function. Contextual scoring rules included a minimum bout length setting of 8 s (two contiguous epochs) for both wake and NREM and 12 s (three contiguous epochs) for REM. A further 50 epochs of each state were then trained, and the auto-score function was run again. The entire recording was then manually checked and corrected. All sleep scoring was performed blinded to genotype and treatment. Vigilance state-specific (NREM or REM) normalised power spectral data were obtained from the first 5 h of recording for Experiment 1. Normalised power spectral data were obtained for the first 6 h of recordings for NREM and first 12 h for REM (due to the relative scarcity of REM sleep during the active phase) for Experiment 2, using Somnivore's built in power spectral analysis capabilities (Allocca et al., 2019). For power spectral analysis, all transition epochs were excluded and signals from EEG1 and EEG2 were averaged. Frequencies in the 0-20 Hz range were selected for statistical analysis.

Behaviour

Barnes maze

The Barnes maze (Barnes, 1979) was used to interrogate hippocampal-dependent spatial learning and memory in rTg4510 and WT mice. The Barnes maze comprised a circular platform (120 cm diameter) with 36 evenly spaced holes (5 cm diameter) around its perimeter, raised 56 cm off the ground. Two floodlights, three pedestal fans (providing ~2.2 m/s and ~1.4 m/s air speed at the edge and centre of the platform, respectively) and one additional 3D visual cue (yellow biohazard bin affixed to a steel pole) were positioned around the maze. Laminated, patterned A2 sheets (stripes or dots) were attached to the floodlight stands as further visual cues. A cylindrical container (13 cm diameter x 10 cm height) was used to hold mice in the centre of the maze at the start of each trial and was raised to the ceiling via a pulley system. A

small black container (14 x 9.5 x 5 cm) with a wire mesh ramp was used as an escape box and positioned under one hole in the maze. A camera mounted to the ceiling was positioned directly above the maze. TopScan Lite version 2.00 (CleverSys Inc.) was used for tracking analysis.

Day 0 – Habituation trials: Each mouse performed one habituation trial on day 0. All visual cues were removed for the habituation trial. The mouse was placed under the start container, the floodlights and pedestal fans switched on and the container raised using the pulley. After 15-30 s the mouse was gently guided into the escape box and allowed to remain inside for 2 min, then returned to its home cage.

Days 1-4 – Acquisition trials: Each mouse performed 3 acquisition trials per day for 4 consecutive days, with an inter-trial interval of 25-27 min. Acquisition trials were performed during the active phase. Acquisition trials began a minimum of 6 h after drug administration, to avoid excessive and potentially confounding somnolence. Mice were randomly assigned a target escape box location (hole 7, 13, 25 or 31). The escape box was positioned under this hole for every trial for that mouse. Acquisition trials lasted 4 min or until the mouse entered the escape box, if it had not entered after 4 min had elapsed, the mouse was guided inside by hand. Once the mouse was inside the escape box the floodlights and fans were immediately switched off. Mice remained inside the box for 30-60 s and were then returned to their home cage. The maze surface was wiped down with 80% ethanol between each trial.

The acquisition trial parameters measured included: *Total errors:* the number of nose pokes into a hole that was not the target hole, with consecutive dips into the same hole considered a single error. *Hole deviation:* the difference in the number of holes between the first hole the mouse visited and the target hole (range 0-18). *Latency to investigate any hole:* the time it took the mouse to move from the centre starting point and poke its nose into any hole on the maze. *Primary latency to escape hole:* the time it took the mouse to first poke its nose into the target hole. *Latency to enter escape box:* the time it took the mouse to enter the escape box. *Search strategy:* the search strategy mice used to locate the escape box. A spatial search strategy occurred when the mouse moved directly to within three holes either side of the target and then quickly located the escape box thereafter. The serial search strategy occurred when the mouse moved around the edge of the maze making errors at sequential holes before locating the escape box. The random search strategy occurred when the mouse searched the maze in an unsystematic fashion, often moving through the centre of the maze and returning to holes previously visited. *Proportion of mice requiring guidance:* the proportion of mice that had not entered the escape box after the 4 min trial limit had elapsed and hence needed to be

guided inside. *Proportion of mice failing to explore the maze:* the proportion of mice that remained in the centre of the maze for the entire 4 min trial limit (see Appendix III).

Day 5 – Probe trial: Each mouse performed one 3 min probe trial in which the escape box had been removed. The maze surface was wiped down with 80% ethanol between each probe trial. The number of times the mouse poked its nose into each hole on the maze was measured. In this case, consecutive dips into the same hole were considered as multiple nose pokes. Only the first 90 s (or second 90 s if the mouse took longer to move from the centre) of the trial were analysed. A higher number of nose pokes into the target and adjacent holes was indicative of heightened spatial recall and cognitive ability.

Cull and sample collection

All sample collection occurred within the first few hours of the active phase commencing. Mice were terminally anaesthetised with a lethal dose of sodium pentobarbitone (80 mg/kg) and perfused with approximately three times their blood volume (estimated as 7% of body weight) of 0.01M phosphate-buffered saline (PBS) containing heparin (55.6 mg/L). Brains were extracted and dissected down the midline, the right hemisphere was used to micro dissect regions containing the hippocampus and cerebral cortex, which were then immediately frozen on dry ice and stored at -80°C.

Western blotting

Tissue preparation: Brain samples were homogenised on ice using a probe sonicator (~10 s; 0.5 s on, 0.5 s off) in sodium dodecyl sulfate (SDS) lysis buffer (1:3; tissue weight (mg): buffer volume (µL)) containing 2% SDS and 10 mM Tris (pH 6.8), plus protease and phosphatase inhibitors (Roche). Homogenates were centrifuged at 13000 rpm for 30 min at 4°C. The supernatant was collected and total protein concentration was determined using the bicinchoninic acid (BCA) assay (Pierce).

Immunoblotting: Samples were diluted in SDS lysis buffer and 4X sample buffer (250 mM Tris (pH 6.8), 8% SDS, 20% Glycerol. 0.2% Bromo Blue, 10 mM Dithiothreitol (DTT)) was added to yield a final protein concentration of 1.67 µg/µL. Samples were heated at 95°C for 5-10 min, thoroughly mixed, then briefly spun down. 15 µL of sample (25 µg of protein) were added to the relevant well. Proteins were electrophoresed at 200V for 35 min on 4-20% polyacrylamide gels (BioRad) and transferred on to 0.45 µm (pore-size) nitrocellulose membranes (BioRad). Membranes were blocked in tris-buffered saline with 0.05% Tween20 (TBS-T) containing 5% skim milk powder for 1 h at room temperature. Membranes were first

incubated with mouse anti-β-actin (1:10000, catalogue number: A5441; Sigma-Aldrich) for 1 h at 4°C, then with anti-mouse secondary (1:10000, catalogue number: #7076; Cell Signaling Technology) for 1 h at room temperature. Proteins were detected using enhanced chemiluminescence (ECL; BioRad) and visualised using the ChemiDoc (BioRad). Membranes were then incubated with rabbit primary antibodies (Total tau, 1:10000, catalogue number: A0024; DAKO; phospho-tau S404, 1:4000, catalogue number: ab92676; Abcam or phospho-tau S202, 1:4000, catalogue number: #39357; Cell Signaling Technology) overnight at 4°C followed by anti-rabbit secondary (same dilution as primary, catalogue number: #7074; Cell Signaling Technology) for 2 h at room temperature. These p-tau epitopes were selected as they have been demonstrated to affect microtubule dynamics and are sites commonly phosphorylated by tau kinases cyclin-dependent kinase 5 (CDK5) and glycogen synthase kinase 3 beta (GSK-3β) in the AD state (Mandelkow et al., 1992; Baumann et al., 1993). P-tau S202 has also been associated with the increased propensity for tau to aggregate (Despres et al., 2017). All antibodies were diluted in 5% skim milk in TBS-T. All membranes were washed with TBS-T (3 x 5-10 min) before and after incubation with secondary antibodies. Proteins were detected as described above and analysed via densitometry (ImageLab version 6.0.1, BioRad). A reference sample homogenate taken from the same WT mouse, rTg4510 mouse and tau knockout ($tau^{-/-}$) mouse were loaded onto every gel. Protein levels were first normalised to β-actin and then to the reference samples. All values are expressed as a percentage of the WT vehicle (MC or TPGS) group.

Statistical analysis

Statistical analyses were performed using GraphPad Prism (version 8.0.0) or R (version 3.6.1)/RStudio (version 1.2.5001). Time spent in each vigilance state (sleep/wake data) across the 23 h recording were analysed using the *lmer* function, incorporating the factors of genotype, treatment, sex and time (repeated factor). Average bout numbers, bout durations and time spent in each vigilance state per phase were analysed by a linear mixed effects model in R, using the *lm* function, incorporating the factors of genotype, treatment and sex. Vigilance state-specific normalised EEG power were analysed using the *lmer* function, incorporating the factors of genotype, treatment and frequency (repeated factor). Only frequencies in the 0-20 Hz range were included in statistical analyses. Average EEG power per specified frequency range were analysed using the *lm* function, incorporating the factors of genotype, treatment and sex. Nose poke distributions during the Barnes maze probe trial were analysed using one-way repeated measures ANOVA followed by Fisher's LSD multiple comparisons test, versus the target hole.

Aggregate nose pokes into the target region were analysed by a linear mixed effects model in R, using the *lm* function, incorporating the factors of genotype, treatment and sex. Three mice from the rTg4510 MC, five mice from the rTg4510 Suvo, one mouse from the rTg4510 TPGS and two mice from the rTg4510 MK-1064 groups were excluded from probe trial analyses due to lack of movement. Relative tau levels (western blots) were analysed by two-way ANOVA with Tukey's multiple comparisons test. Correlations between Barnes maze parameters and total sleep time were analysed by Pearson's correlation. Akaike information criterion (AIC) was used to determine the model of best fit for all R related analyses. Where sex was a significant contributing factor data from both male and female mice are presented separately. All R related post hoc analyses were performed using the *emmeans* function, with Tukey's multiple comparisons test. For all analyses, $P < 0.05$ was considered to be statistically significant.

4.4 Results

Experiment 1

Suvorexant increased REM sleep in both rTg4510 and WT mice when administered during the inactive phase

Sleep/wake architecture of rTg4510 and WT mice were significantly altered by chronic suvorexant treatment (Fig. 4.2A-C; Table 4.1), predominantly affecting REM sleep. Suvorexant-treated WT and rTg4510 mice spent more time in REM sleep than MC-treated mice across each of the subsequent 5 hours of the inactive phase post-drug administration (Fig. 4.2C), whereas wake and NREM were not influenced by treatment (Fig. 4.2A, B). The average time spent in each vigilance state across the 1st inactive period (5 h post-suvorexant), active phase, 2nd inactive period and the entire recording were assessed (Fig. 4.2D-O; Table 4.2). Suvorexant similarly increased REM sleep in both WT and rTg4510 mice during the 1st inactive period (5 h post-suvorexant; Fig. 4.2L), compared with MC-treated mice. Less pronounced decreases in wake (Fig. 4.2D) and increases in NREM sleep (Fig. 4.2H) were also observed in suvorexant-treated mice during this period. During the active phase, main effects of genotype and sex were observed; rTg4510 mice spent more time awake (Fig. 4.2E) and subsequently less time in NREM (Fig. 4.2I) and REM (Fig. 4.2M) sleep, which was exacerbated in female rTg4510 mice, consistent with the hyperarousal phenotype previously reported in these mice (Chapter 3). No effects of genotype, treatment or sex were observed

during the 2nd inactive period, with all groups spending the same amount of time in each vigilance state (Fig. 4.2F, J, N).

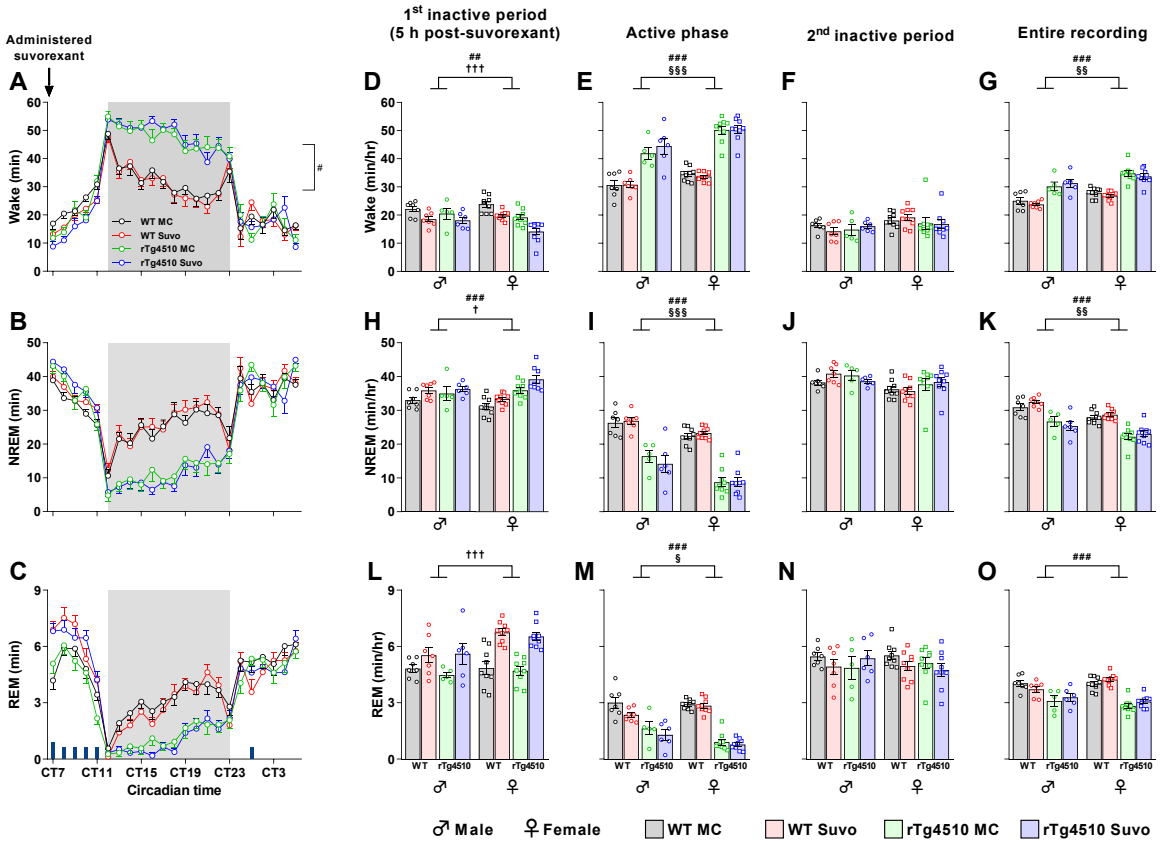

Figure 4.2. Promotion of REM sleep following suvorexant treatment in rTg4510 mice.

A-C, Minutes spent in wake (***A***), NREM (***B***) and REM (***C***) vigilance states per hour across a 23 h recording in rTg4510 and WT mice administered suvorexant (Suvo) or methylcellulose (MC) vehicle. Dark shade represents the active phase. Data are means ± SEM. n = 14-16 per group. Short bar: P < 0.01, tall bar: P < 0.001 vs. MC (treatment x time) within circadian time; # denotes main effect of genotype, by repeated measures linear mixed effects model with Tukey's multiple comparisons test. ***D-O***, Minutes spent in each vigilance state per hour averaged across (from left to right) the 1st inactive period (5 h post-suvorexant), active phase, 2nd inactive period and entire recording, for wake (***D-G***), NREM (***H-K***) and REM (***L-O***). n = 5-9 per group, per sex. #, † and § denote main effects of genotype, treatment and sex, respectively. ##P < 0.01, ###P < 0.001 vs. WT; †P < 0.05, †††P < 0.001 vs. MC; §P < 0.05, §§P < 0.01, §§§P < 0.001 vs. Female, by linear mixed effects model with Tukey's multiple comparisons test. For ***D-O***, only main effects are graphically presented, refer to Table 4.1 and 4.2 for further details.

Table 4.1. Experiment 1 (suvorexant) EEG recordings statistical analyses summary.

Time spent in each vigilance state across the 23 h recording were analysed by a repeated measures linear mixed effects model in R, using the *lmer* function, incorporating the factors of Genotype, Treatment, Sex and Time (repeated factor). Indented Pr(>|t|) values indicate statistical significance.

Vigilance state time															
					Wake					**NREM**					**REM**
Fixed effect	Estimate	Std. error	df	t-value	Pr(>|t|)	Estimate	Std. error	df	t-value	Pr(>|t|)	Estimate	Std. error	df	t-value	Pr(>|t|)
Genotype	-6.581	3.257	1387.0	-2.021	< 0.05	5.470	2.822	1387.0	1.947	> 0.05	1.083	0.519	1387.0	2.085	< 0.05
Treatment	-4.057	3.257	1387.0	-1.246	> 0.05	2.580	2.822	1387.0	0.914	> 0.05	1.477	0.519	1387.0	2.845	< 0.01
Sex	-3.886	3.854	1387.0	-1.008	> 0.05	3.594	3.340	1387.0	1.076	> 0.05	0.291	0.614	1387.0	0.474	> 0.05
Time	-0.437	0.168	1387.0	-2.602	< 0.01	0.374	0.146	1387.0	2.567	< 0.01	0.063	0.027	1387.0	2.361	< 0.05
Genotype:Treatment	0.755	4.606	1387.0	0.164	> 0.05	-0.779	3.992	1387.0	-0.195	> 0.05	0.025	0.734	1387.0	0.034	> 0.05
Genotype:Sex	1.782	5.194	1387.0	0.343	> 0.05	-1.410	4.501	1387.0	-0.313	> 0.05	-0.369	0.828	1387.0	-0.446	> 0.05
Treatment:Sex	4.920	5.302	1387.0	0.928	> 0.05	-3.758	4.595	1387.0	-0.818	> 0.05	-1.161	0.845	1387.0	-1.374	> 0.05
Genotype:Time	-0.026	0.238	1387.0	-0.109	> 0.05	0.018	0.206	1387.0	0.085	> 0.05	0.009	0.038	1387.0	0.227	> 0.05
Treatment:Time	0.248	0.238	1387.0	1.046	> 0.05	-0.145	0.206	1387.0	-0.702	> 0.05	-0.104	0.038	1387.0	-2.742	< 0.05
Sex:Time	-0.067	0.281	1387.0	-0.237	> 0.05	0.070	0.244	1387.0	0.288	> 0.05	-0.003	0.045	1387.0	-0.072	> 0.05
Genotype:Treatment:Sex	-4.529	7.236	1387.0	-0.626	> 0.05	4.478	6.270	1387.0	0.714	> 0.05	0.051	1.153	1387.0	0.044	> 0.05
Genotype:Treatment:Time	-0.062	0.336	1387.0	-0.185	> 0.05	0.064	0.291	1387.0	0.221	> 0.05	-0.002	0.054	1387.0	-0.039	> 0.05
Genotype:Sex:Time	-0.001	0.379	1387.0	-0.003	> 0.05	-0.010	0.328	1387.0	-0.032	> 0.05	0.011	0.060	1387.0	0.184	> 0.05
Treatment:Sex:Time	-0.225	0.387	1387.0	-0.583	> 0.05	0.131	0.335	1387.0	0.392	> 0.05	0.094	0.062	1387.0	1.526	> 0.05
Genotype:Treatment:Sex:Time	0.175	0.528	1387.0	0.331	> 0.05	-0.127	0.457	1387.0	-0.277	> 0.05	-0.048	0.084	1387.0	-0.571	> 0.05

Table 4.2. Experiment 1 (suvorexant) phase specific EEG recordings statistical analyses summary.

Average time spent in each vigilance state per phase were analysed by a linear mixed effects model in R, using the *lm* function, incorporating the factors of Genotype, Treatment and Sex. Indented Pr(>|t|) values indicate statistical significance.

Vigilance state time																	
		1st inactive period (5 h post-suvorexant)				**Active phase**				**2nd inactive period**				**Entire recording**			
Vigilance state	Fixed effect	Estimate	Std. error	t-value	Pr(>|t|)	Estimate	Std. error	t-value	Pr(>|t|)	Estimate	Std. error	t-value	Pr(>|t|)	Estimate	Std. error	t-value	Pr(>|t|)
Wake	Genotype	4.699	1.395	3.369	< 0.01	-15.695	1.899	-8.266	< 0.001	1.052	1.823	0.577	> 0.05	-6.893	1.211	-5.691	< 0.001
	Treatment	-5.058	1.395	-3.626	< 0.001	0.175	1.899	0.092	> 0.05	-0.263	1.823	-0.144	> 0.05	-1.077	1.211	-0.889	> 0.05
	Sex	1.288	1.651	0.780	> 0.05	-8.384	2.247	-3.732	< 0.001	-2.274	2.157	-1.054	> 0.05	-4.687	1.433	-3.271	< 0.01
	Genotype:Treatment	0.920	1.973	0.466	> 0.05	-1.052	2.685	-0.392	> 0.05	1.368	2.578	0.531	> 0.05	0.008	1.712	0.005	> 0.05
	Genotype:Sex	-3.071	2.225	-1.380	> 0.05	4.445	3.028	1.468	> 0.05	0.453	2.907	0.156	> 0.05	1.770	1.931	0.916	> 0.05
	Treatment:Sex	2.647	2.271	1.166	> 0.05	2.412	3.091	0.780	> 0.05	1.462	2.968	0.493	> 0.05	2.215	1.972	1.124	> 0.05
	Genotype:Treatment:Sex	-2.119	3.099	-0.684	> 0.05	-1.448	4.218	-0.343	> 0.05	-4.656	4.050	-1.149	> 0.05	-2.431	2.691	-0.903	> 0.05
NREM	Genotype	-4.843	1.288	-3.761	< 0.001	13.686	1.728	7.920	< 0.001	-1.462	1.571	-0.930	> 0.05	5.707	1.155	4.942	< 0.001
	Treatment	3.227	1.288	2.506	< 0.05	-0.042	1.728	-0.024	> 0.05	0.637	1.571	0.406	> 0.05	0.846	1.155	0.732	> 0.05
	Sex	-1.044	1.524	-0.685	> 0.05	7.663	2.045	3.748	< 0.001	2.546	1.859	1.369	> 0.05	4.435	1.366	3.246	< 0.01
	Genotype:Treatment	-0.995	1.821	-0.546	> 0.05	0.985	2.444	0.403	> 0.05	-1.170	2.222	-0.527	> 0.05	-0.008	1.633	-0.005	> 0.05
	Genotype:Sex	2.864	2.054	1.394	> 0.05	-3.806	2.755	-1.381	> 0.05	-0.656	2.506	-0.262	> 0.05	-1.535	1.841	-0.833	> 0.05
	Treatment:Sex	-1.953	2.096	-0.931	> 0.05	-2.197	2.813	-0.781	> 0.05	-2.348	2.558	-0.918	> 0.05	-2.183	1.880	-1.162	> 0.05
	Genotype:Treatment:Sex	2.619	2.861	0.916	> 0.05	1.817	3.839	0.473	> 0.05	5.518	3.491	1.580	> 0.05	2.957	2.565	1.153	> 0.05
REM	Genotype	0.143	0.394	0.363	> 0.05	2.007	0.236	8.506	< 0.001	0.411	0.425	0.969	> 0.05	1.186	0.190	6.253	< 0.001
	Treatment	1.831	0.394	4.636	< 0.001	-0.133	0.236	-0.564	> 0.05	-0.373	0.425	-0.879	> 0.05	0.231	0.190	1.220	> 0.05
	Sex	-0.244	0.467	-0.522	> 0.05	0.720	0.279	2.580	< 0.05	-0.270	0.502	-0.538	> 0.05	0.252	0.224	1.124	> 0.05
	Genotype:Treatment	0.075	0.558	0.134	> 0.05	0.067	0.334	0.202	> 0.05	-0.199	0.600	-0.331	> 0.05	0.000	0.268	-0.002	> 0.05
	Genotype:Sex	0.207	0.630	0.328	> 0.05	-0.638	0.376	-1.696	> 0.05	0.200	0.677	0.295	> 0.05	-0.236	0.302	-0.780	> 0.05
	Treatment:Sex	-0.694	0.643	-1.080	> 0.05	-0.215	0.384	-0.561	> 0.05	0.886	0.691	1.281	> 0.05	-0.032	0.309	-0.104	> 0.05
	Genotype:Treatment:Sex	-0.500	0.877	-0.570	> 0.05	-0.369	0.524	-0.704	> 0.05	-0.860	0.943	-0.912	> 0.05	-0.526	0.421	-1.248	> 0.05

Suvorexant promoted REM sleep by increasing bout numbers without affecting bout duration

Vigilance state bout numbers and bout durations were significantly altered by chronic suvorexant treatment (Fig. 4.3, 4.4; Table 4.3, 4.4). Wake (Fig. 4.3A) and NREM (Fig. 4.3E) bout numbers were unaffected by suvorexant treatment during the 1st inactive period. During the active phase, wake and NREM bout numbers were generally decreased in female mice, especially female rTg4510 mice, but with no effect of suvorexant treatment (Fig. 4.3B, F). Wake and NREM bout numbers appeared to somewhat normalise during the 2nd inactive period (Fig. 4.3C, G). Suvorexant increased REM bout numbers in both WT and rTg4510 mice during the 1st inactive period (Fig. 4.3I). REM bout numbers were reduced thereafter during the active phase (Fig. 4.3J) and 2nd inactive period (Fig. 4.3K) in rTg4510 mice, compared with WT, but with no effect of suvorexant.

Wake bout durations were attenuated by suvorexant treatment in the 1st inactive period (Fig. 4.4A). Thereafter, wake durations tended to be longer in rTg4510 mice, consistent with previous findings and the hyperarousal phenotype of these mice (Chapter 3; Fig. 4.4B-D). NREM bout durations were also increased in rTg4510 mice throughout the 1st and 2nd inactive period (Fig. 4.4E, G), but were reduced during the active phase (Fig. 4.4F), compared with WT mice. During the 1st inactive period, REM bout durations were increased in rTg4510 mice, compared with WT mice, however, with no influence of suvorexant treatment (Fig. 4.4I). REM bout durations were thereafter decreased during the active phase (Fig. 4.4J) but increased again during the 2nd inactive period (Fig. 4.4K) in rTg4510 mice, consistent with previous findings (Chapter 3).

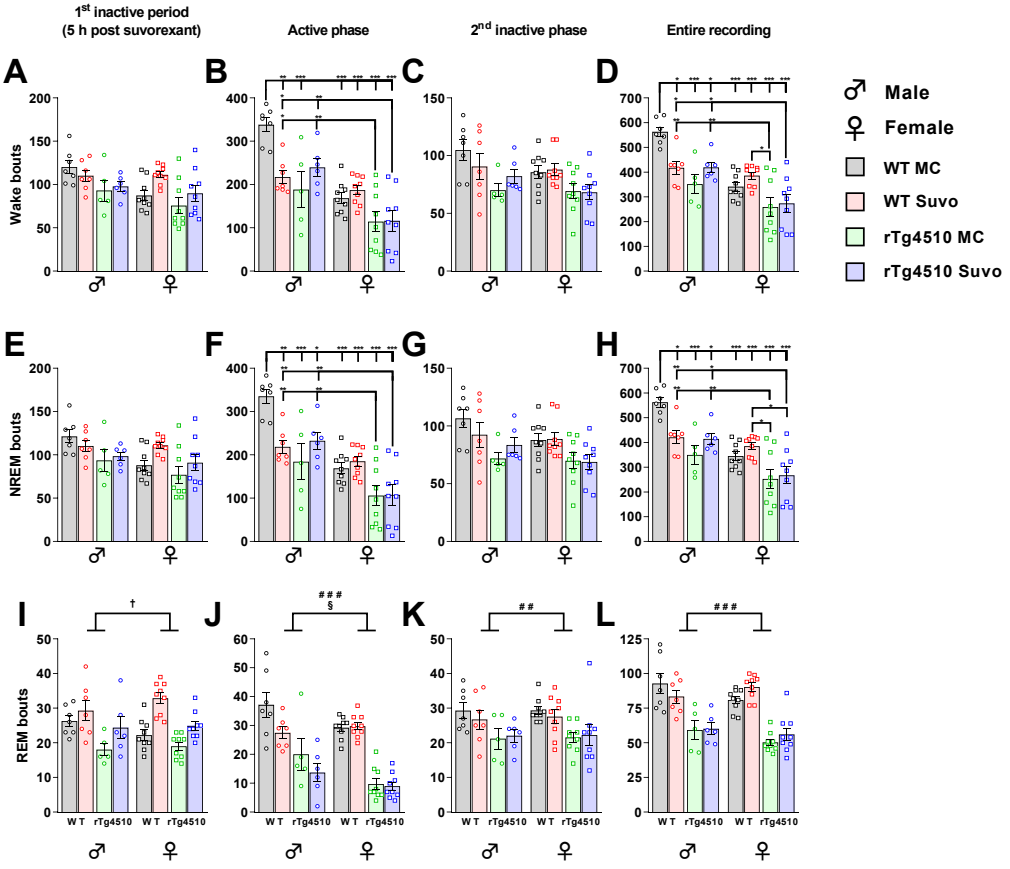

Figure 4.3. Increased REM bouts following suvorexant treatment in rTg4510 mice.

A-L, Total number of wake (***A-D***), NREM (***E-H***) and REM (***I-L***) bouts averaged across (from left to right) the 1st inactive period (5 h post-suvorexant), active phase, 2nd inactive period and entire recording in rTg4510 and WT mice administered suvorexant (Suvo) or methylcellulose (MC) vehicle. Data are means ± SEM. n = 5-9 per group, per sex. #, † and § denote main effects of genotype, treatment and sex, respectively. $^{\#\#}P < 0.01$, $^{\#\#\#}P < 0.001$ vs. WT; $^{\dagger}P < 0.05$ vs. MC; $^{\S}P < 0.05$, vs. Female; $^{*}P < 0.05$ $^{**}P < 0.01$, $^{***}P < 0.001$, by linear mixed effects model with Tukey's multiple comparisons test. Refer to Table 4.3 for further details.

Table 4.3. Experiment 1 (suvorexant) vigilance state bout numbers statistical analyses summary.

Average bout numbers of each vigilance state per phase were analysed by a linear mixed effects model in R, using the *lm* function, incorporating the factors of Genotype, Treatment and Sex. Indented Pr(>|t|) values indicate statistical significance.

Vigilance state bout numbers															
		1st inactive period (5 h post suvorexant)				**Active phase**				**2nd inactive period**				**Entire recording**			
Vigilance state	Fixed effect	Estimate	Std. error	t-value	Pr(>|t|)	Estimate	Std. error	t-value	Pr(>|t|)	Estimate	Std. error	t-value	Pr(>|t|)	Estimate	Std. error	t-value	Pr(>|t|)
Wake	Genotype	11.667	9.950	1.173	> 0.05	54.333	26.450	2.054	< 0.05	16.333	9.191	1.777	> 0.05	82.330	36.330	2.266	< 0.05
	Treatment	14.222	9.950	1.429	> 0.05	1.667	26.450	0.063	> 0.05	-1.000	9.191	-0.109	> 0.05	14.890	36.330	0.410	> 0.05
	Sex	17.333	11.773	1.472	> 0.05	73.422	31.297	2.346	< 0.05	0.667	10.875	0.061	> 0.05	91.420	42.980	2.127	< 0.05
	Genotype:Treatment	9.667	14.071	0.687	> 0.05	17.000	37.406	0.454	> 0.05	3.222	12.998	0.248	> 0.05	29.890	51.380	0.582	> 0.05
	Genotype:Sex	15.333	15.866	0.966	> 0.05	95.181	42.179	2.257	< 0.05	18.524	14.656	1.264	> 0.05	129.040	57.930	2.227	< 0.05
	Treatment:Sex	-9.556	16.197	-0.590	> 0.05	49.633	43.058	1.153	> 0.05	13.167	14.962	0.880	> 0.05	53.240	59.140	0.900	> 0.05
	Genotype:Treatment:Sex	-24.333	22.105	-1.101	> 0.05	-189.014	58.763	-3.217	< 0.01	-29.675	20.419	-1.453	> 0.05	-243.020	80.710	-3.011	< 0.01
NREM	Genotype	11.111	10.111	1.099	> 0.05	63.000	26.585	2.370	< 0.05	18.000	9.243	1.947	> 0.05	92.110	36.630	2.514	< 0.05
	Treatment	14.111	10.111	1.396	> 0.05	1.444	26.585	0.054	> 0.05	-1.000	9.243	-0.108	> 0.05	14.560	36.630	0.397	> 0.05
	Sex	16.600	11.964	1.388	> 0.05	77.978	31.456	2.479	< 0.05	1.911	10.937	0.175	> 0.05	96.490	43.340	2.226	< 0.05
	Genotype:Treatment	8.778	14.299	0.614	> 0.05	14.667	37.597	0.390	> 0.05	1.889	13.072	0.145	> 0.05	25.330	51.810	0.489	> 0.05
	Genotype:Sex	16.575	16.124	1.028	> 0.05	87.800	42.394	2.071	< 0.05	16.771	14.739	1.138	> 0.05	121.150	58.410	2.074	< 0.05
	Treatment:Sex	-9.378	16.460	-0.570	> 0.05	46.689	43.278	1.079	> 0.05	12.700	15.047	0.844	> 0.05	50.010	59.630	0.839	> 0.05
	Genotype:Treatment:Sex	-24.511	22.463	-1.091	> 0.05	-179.371	59.063	-3.037	< 0.01	-27.732	20.535	-1.350	> 0.05	-231.610	81.380	-2.846	< 0.01
REM	Genotype	3.222	2.435	1.324	> 0.05	19.556	3.269	5.983	< 0.001	7.778	2.875	2.705	< 0.01	30.556	5.741	5.323	< 0.001
	Treatment	5.889	2.435	2.419	< 0.05	-0.778	3.269	-0.238	> 0.05	0.667	2.875	0.232	> 0.05	5.778	5.741	1.006	> 0.05
	Sex	-1.000	2.881	-0.347	> 0.05	10.222	3.868	2.643	< 0.05	-0.356	3.402	-0.105	> 0.05	8.867	6.792	1.305	> 0.05
	Genotype:Treatment	4.778	3.443	1.388	> 0.05	1.333	4.623	0.288	> 0.05	-2.444	4.066	-0.601	> 0.05	3.667	8.118	0.452	> 0.05
	Genotype:Sex	5.064	3.882	1.304	> 0.05	-2.413	5.213	-0.463	> 0.05	0.308	4.585	0.067	> 0.05	2.959	9.154	0.323	> 0.05
	Treatment:Sex	0.444	3.963	0.112	> 0.05	-5.556	5.321	-1.044	> 0.05	0.133	4.681	0.028	> 0.05	-4.978	9.345	-0.533	> 0.05
	Genotype:Treatment:Sex	-8.111	5.409	-1.500	> 0.05	-4.714	7.262	-0.649	> 0.05	-0.927	6.388	-0.145	> 0.05	-13.752	12.754	-1.078	> 0.05

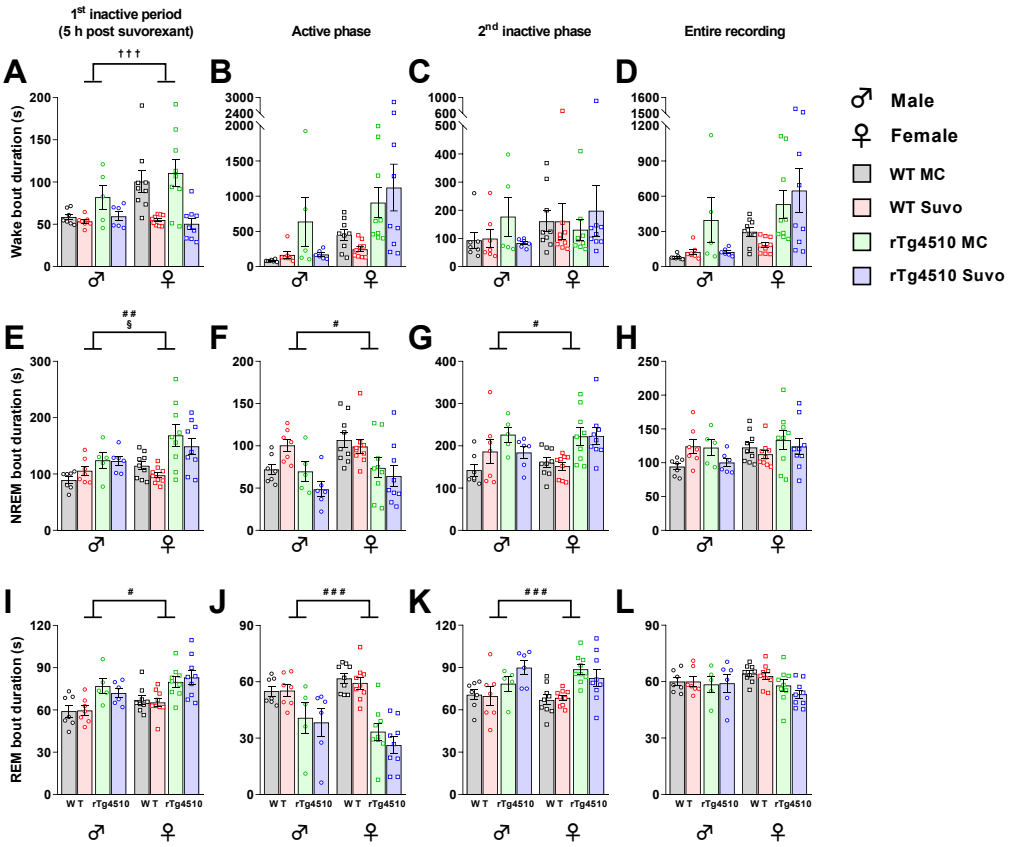

Figure 4.4. Unchanged REM bout duration following suvorexant treatment in rTg4510 mice.

A-L, Mean wake (***A-D***), NREM (***E-H***) and REM (***I-L***) bout durations averaged across (from left to right) the 1st inactive period (5 h post-suvorexant), active phase, 2nd inactive period and entire recording in rTg4510 and WT mice administered suvorexant (Suvo) or methylcellulose (MC) vehicle. Data are means ± SEM. n = 5-9 per group, per sex. #, † and § denote main effects of genotype, treatment and sex, respectively. $^{\#}P < 0.05$, $^{\#\#}P < 0.01$, $^{\#\#\#}P < 0.001$ vs. WT; $^{\dagger\dagger\dagger}P < 0.001$ vs. MC; $^{\S}P < 0.05$, vs. Female, by linear mixed effects model with Tukey's multiple comparisons test. Refer to Table 4.4 for further details.

Table 4.4. Experiment 1 (suvorexant) vigilance state bout duration statistical analyses summary.

Average bout duration of each vigilance state per phase were analysed by a linear mixed effects model in R, using the *lm* function, incorporating the factors of Genotype, Treatment and Sex. Indented Pr(>|t|) values indicate statistical significance.

Vigilance state bout durations		1st inactive period (5 h post suvorexant)				Active phase				2nd inactive period				Entire recording			
Vigilance state	Fixed effect	Estimate	Std. error	t-value	Pr(>|t|)	Estimate	Std. error	t-value	Pr(>|t|)	Estimate	Std. error	t-value	Pr(>|t|)	Estimate	Std. error	t-value	Pr(>|t|)
Wake	Genotype	-10.168	12.805	-0.794	> 0.05	-463.180	244.440	-1.895	> 0.05	30.280	71.940	0.421	> 0.05	-235.970	136.750	-1.725	> 0.05
	Treatment	-60.267	12.805	-4.706	< 0.001	213.540	244.440	0.874	> 0.05	67.590	71.940	0.940	> 0.05	115.940	136.750	0.848	> 0.05
	Sex	-28.673	15.151	-1.892	> 0.05	-271.510	289.230	-0.939	> 0.05	46.740	85.130	0.549	> 0.05	-135.700	161.810	-0.839	> 0.05
	Genotype:Treatment	14.790	18.109	0.817	> 0.05	-414.670	345.690	-1.200	> 0.05	-68.220	101.750	-0.671	> 0.05	-230.930	193.400	-1.194	> 0.05
	Genotype:Sex	-13.288	20.420	-0.651	> 0.05	-92.910	389.790	-0.238	> 0.05	-114.560	114.730	-0.999	> 0.05	-81.250	218.070	-0.373	> 0.05
	Treatment:Sex	37.660	20.845	1.807	> 0.05	-681.740	397.920	-1.713	> 0.05	-161.810	117.120	-1.382	> 0.05	-389.710	222.620	-1.751	> 0.05
	Genotype:Treatment:Sex	2.507	28.449	0.088	> 0.05	965.570	543.060	1.778	> 0.05	168.560	159.840	1.055	> 0.05	548.290	303.820	1.805	> 0.05
NREM	Genotype	-54.058	15.639	-3.456	< 0.01	33.029	13.192	2.504	< 0.05	-61.978	23.325	-2.657	< 0.05	-10.688	13.106	-0.815	> 0.05
	Treatment	-19.617	15.639	-1.254	> 0.05	-9.732	13.192	-0.738	> 0.05	0.917	23.325	0.039	> 0.05	-9.103	13.106	-0.695	> 0.05
	Sex	-44.733	18.505	-2.417	< 0.05	-4.357	15.609	-0.279	> 0.05	3.511	27.599	0.127	> 0.05	-11.082	15.508	-0.715	> 0.05
	Genotype:Treatment	2.533	22.118	0.115	> 0.05	1.984	18.656	0.106	> 0.05	-9.783	32.987	-0.297	> 0.05	-0.967	18.535	-0.052	> 0.05
	Genotype:Sex	19.148	24.939	0.768	> 0.05	-30.768	21.036	-1.463	> 0.05	-22.054	37.195	-0.593	> 0.05	-17.644	20.900	-0.844	> 0.05
	Treatment:Sex	18.609	25.459	0.731	> 0.05	-11.446	21.475	-0.533	> 0.05	-43.163	37.971	-1.137	> 0.05	-13.186	21.336	-0.618	> 0.05
	Genotype:Treatment:Sex	14.909	34.745	0.429	> 0.05	47.811	29.308	1.631	> 0.05	96.135	51.820	1.855	> 0.05	53.264	29.118	1.829	> 0.05
REM	Genotype	-12.883	5.112	-2.520	< 0.05	28.344	5.700	4.972	< 0.001	-21.774	5.861	-3.715	< 0.001	6.307	3.580	1.762	> 0.05
	Treatment	3.198	5.112	0.626	> 0.05	-7.166	5.700	-1.257	> 0.05	-6.201	5.861	-1.058	> 0.05	-4.661	3.580	-1.302	> 0.05
	Sex	-3.059	6.048	-0.506	> 0.05	7.414	6.745	1.099	> 0.05	-10.442	6.935	-1.506	> 0.05	0.479	4.236	0.113	> 0.05
	Genotype:Treatment	-4.918	7.229	-0.680	> 0.05	4.769	8.062	0.592	> 0.05	7.693	8.289	0.928	> 0.05	3.426	5.063	0.677	> 0.05
	Genotype:Sex	-4.921	8.151	-0.604	> 0.05	-14.230	9.090	-1.565	> 0.05	14.008	9.347	1.499	> 0.05	-4.840	5.709	-0.848	> 0.05
	Treatment:Sex	-8.192	8.321	-0.985	> 0.05	4.667	9.280	0.503	> 0.05	17.590	9.541	1.843	> 0.05	5.242	5.828	0.900	> 0.05
	Genotype:Treatment:Sex	10.406	11.356	0.916	> 0.05	-1.932	12.664	-0.153	> 0.05	-20.073	13.022	-1.541	> 0.05	-3.982	7.954	-0.501	> 0.05

Suvorexant attenuated theta power deficits during REM sleep in male but not female rTg4510 mice

To assess the effects of suvorexant on EEG power during sleep, vigilance state-specific power spectral analyses over the 1st inactive period immediately after dosing were performed (Fig. 4.5; Table 4.5, 4.6). Consistent with previous findings, rTg4510 mice exhibited deficits in delta (1-4 Hz) power during NREM sleep (Fig 4.5A, C). Suvorexant appeared to modulate delta power in male, but not female, rTg4510 mice, although this did not reach statistical significance (Fig. 4.5C; Table 4.6). rTg4510 mice also exhibited substantial deficits in theta (5-9 Hz) power during REM sleep (Fig. 4.5B), which was slightly attenuated by suvorexant treatment, but only in male rTg4510 mice (Fig. 4.5D). Theta power in WT mice was not affected (Fig. 4.5D).

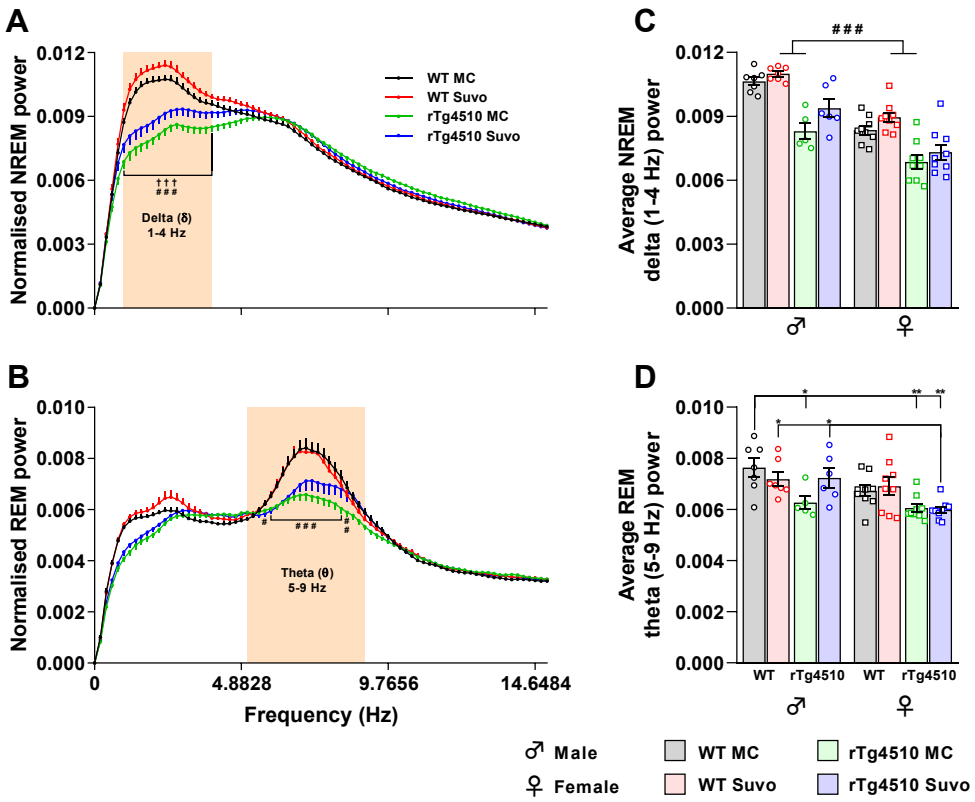

Figure 4.5. Altered EEG power following suvorexant treatment in rTg4510 mice.

A-B, Vigilance state-specific normalised EEG power during NREM (***A***) and REM (***B***) sleep in rTg4510 and WT mice administered suvorexant (Suvo) or methylcellulose (MC) vehicle. Data are means ± SEM. n = 14-16 per group. #P < 0.05, ##P < 0.01, ###P < 0.001 vs. WT (genotype x frequency); †††P < 0.001 vs. MC (treatment x frequency) within frequency band, by repeated measures linear mixed effects model with Tukey's multiple comparisons test. ***C***, Average NREM power over the delta (1-4 Hz) frequencies. ***D***, Average REM power over the theta (5-9 Hz) frequencies. n = 5-9 per group, per sex. ***C-D***, # denotes main effect of genotype. ###P < 0.001 vs. WT; *P < 0.05 **P < 0.01, by linear mixed effects model with Tukey's multiple comparisons test. Signals from EEG1 and EEG2 electrodes were combined. All transition epochs were excluded from power analysis. For clarity, not all statistically significant differences are graphically presented. Refer to Table 4.5 and 4.6 for further details.

Table 4.5. Experiment 1 (suvorexant) EEG power statistical analyses summary.

Vigilance state-specific normalised EEG power during the 1st inactive period were analysed by a repeated measures linear mixed effects model in R, using the *lmer* function, incorporating the factors of Genotype, Treatment and Frequency (repeated factor). Indented Pr(>|t|) values indicate statistical significance.

Vigilance state-specific EEG power										
					NREM					**REM**
Fixed effect	Estimate	Std. error	df	t-value	Pr(>|t|)	Estimate	Std. error	df	t-value	Pr(>|t|)
Genotype	0.001053	0.000138	363.9	7.638	< 0.001	0.000738	0.000130	180.9	5.672	< 0.001
Treatment	0.000526	0.000140	363.9	3.754	< 0.001	0.000254	0.000132	180.9	1.926	> 0.05
Frequency (Hz)	-0.000281	0.000008	6218.0	-35.576	< 0.001	-0.000127	0.000006	6218.0	-20.007	< 0.001
Genotype:Treatment	-0.000067	0.000193	363.9	-0.344	> 0.05	-0.000118	0.000182	180.9	-0.649	> 0.05
Genotype:Frequency	-0.000086	0.000011	6218.0	-7.964	< 0.001	-0.000054	0.000009	6218.0	-6.179	< 0.001
Treatment:Frequency	-0.000044	0.000011	6218.0	-4.021	< 0.001	-0.000016	0.000009	6218.0	-1.855	> 0.05
Genotype:Treatment:Frequency	0.000014	0.000015	6218.0	0.903	> 0.05	0.000009	0.000012	621.8	0.720	> 0.05

Table 4.6. Experiment 1 (suvorexant) NREM delta and REM theta statistical analyses summary.

Summed NREM delta and REM theta normalised EEG power during the 1st inactive period were analysed by a linear mixed effects model in R, using the *lm* function, incorporating the factors of Genotype, Treatment and Sex. Indented Pr(>|t|) values indicate statistical significance.

Vigilance state-specific EEG power								
			NREM (delta 1-4 Hz)				**REM (theta 5-9 Hz)**	
Fixed effect	Estimate	Std. error	t-value	Pr(>|t|)	Estimate	Std. error	t-value	Pr(>|t|)
Genotype	0.001753	0.000423	4.414	< 0.001	0.000666	0.000351	1.900	> 0.05
Treatment	0.000536	0.000423	1.266	> 0.05	-0.000071	0.000351	-0.201	> 0.05
Sex	0.000300	0.000501	0.599	> 0.05	0.000205	0.000415	0.493	> 0.05
Genotype:Treatment	0.000159	0.000599	0.266	> 0.05	0.000252	0.000496	0.508	> 0.05
Genotype:Sex	0.000587	0.000675	0.870	> 0.05	0.000709	0.000559	1.268	> 0.05
Treatment:Sex	0.000547	0.000689	0.794	> 0.05	0.001041	0.000571	1.823	> 0.05
Genotype:Treatment:Sex	-0.000890	0.000940	-0.947	> 0.05	-0.001676	0.000779	-2.150	< 0.05

Suvorexant did not rescue hippocampal-dependent spatial recall deficits

Spatial recall was well-preserved in WT MC mice, investigating the target hole significantly more than all others (except those immediately adjacent) on the maze ($F_{(5.377, 80.66)} = 6.071$, $P < 0.0001$, Fig. 4.6A), as too did WT suvorexant-treated mice ($F_{(6.665, 93.31)} = 5.242$, $P < 0.0001$, Fig. 4.6B). rTg4510 MC mice exhibited no preference for the target hole ($F_{(4.919, 44.27)} = 1.004$, $P = 0.4258$, Fig. 4.6C), with no prevention of this phenotype in rTg4510 mice following suvorexant treatment ($F_{(5.623, 44.99)} = 1.498$, $P = 0.2039$, Fig. 4.6D).

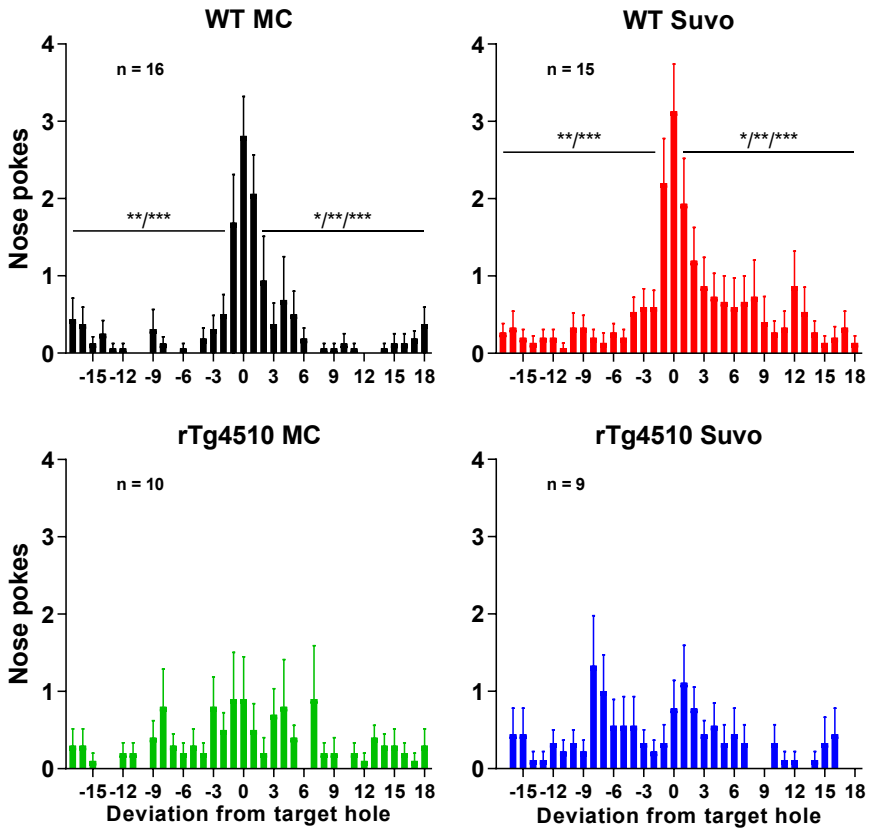

Figure 4.6. Spatial recall in the probe trial of the Barnes maze following suvorexant treatment.

A-D, Number of nose pokes into each of the 36 holes on the Barnes maze during the final probe trial, deviating from the target hole (denoted 0) by rTg4510 and WT mice administered suvorexant (Suvo) or methylcellulose (MC) vehicle. Data are means ± SEM. n = 9-16 per group. $^{*}P < 0.05$, $^{**}P < 0.01$, $^{***}P < 0.001$ vs. target hole, by one-way repeated measures ANOVA with Fisher's LSD multiple comparisons test.

Suvorexant did not alter tau or phosphorylated tau levels in the hippocampus or cortex

Tau expression in the hippocampus and cortex was assessed by western blot (Fig. 4.7A). P-tau S404 levels were 12.75-fold higher in the hippocampus and 7.80-fold higher in the cortex of rTg4510 MC mice compared with WT MC mice (Fig. 4.7B, D). Suvorexant treatment did not affect p-tau S404 levels in rTg4510 or WT mice in the hippocampus (Genotype: $F_{(1, 42)} = 405.1$, $P < 0.0001$; treatment: $F_{(1, 42)} = 0.7588$, $P = 0.3887$; interaction: $F_{(1, 42)} = 1.153$, $P = 0.2891$, Fig. 4.7B) or cortex (Genotype: $F_{(1, 42)} = 580.8$, $P < 0.0001$; treatment: $F_{(1, 42)} = 0.7735$, $P = 0.3841$; interaction: $F_{(1, 42)} = 2.138$, $P = 0.1511$, Fig. 4.7D). Total tau levels were 2.43-fold higher in the hippocampus and 3.51-fold higher in the cortex of rTg4510 MC mice compared with WT MC mice (Fig. 4.7C, E). Suvorexant treatment did not affect total tau levels in rTg4510 or WT mice in the hippocampus (Genotype: $F_{(1, 42)} = 240.5$, $P < 0.0001$; treatment: $F_{(1, 42)} = 1.118$, $P = 0.2963$; interaction: $F_{(1, 42)} = 0.1318$, $P = 0.7184$, Fig. 4.7C) or cortex (Genotype: $F_{(1, 42)} = 77.25$,

P < 0.0001; treatment: $F_{(1, 42)} = 0.05176$, P = 0.8211; interaction: $F_{(1, 42)} = 0.03514$, P = 0.8522, Fig. 4.7E).

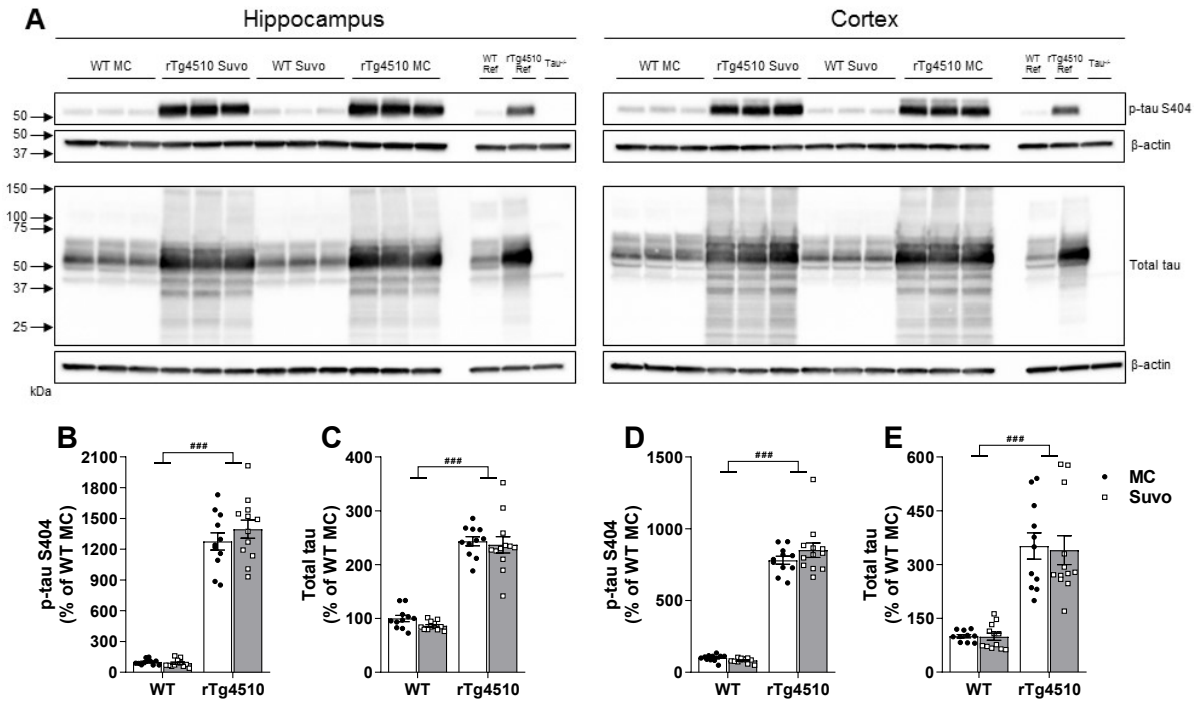

Figure 4.7. Tau and phosphorylated tau levels in rTg4510 mice following suvorexant treatment.

A, Representative western blots from the hippocampus (left) and cortex (right) probed with p-tau S404 or total tau antibodies. β-actin was used as a housekeeping protein. ***B***, ***D***, Relative p-tau S404 levels in the hippocampus (***B***) and cortex (***D***). ***C***, ***E***, Relative total tau levels in the hippocampus (***C***) and cortex (***E***). Densitometry signals were normalised to β-actin and then to the reference samples (WT Ref; rTg4510 Ref) which were loaded across every gel. Lysate from a tau knockout ($Tau^{-/-}$) mouse was used as a negative control. Data are means ± SEM and expressed as a percentage of the WT MC group. n = 11-12 per group. # denotes main effect of genotype. $^{###}P < 0.001$ vs. WT; $^{*}P < 0.05$, $^{**}P < 0.01$, $^{***}P < 0.001$, by two-way ANOVA with Tukey's multiple comparisons test.

Experiment 2

MK-1064 increased NREM/REM sleep and attenuated hyperarousal in male but not female rTg4510 mice when administered during the active phase

Sleep/wake architecture of rTg4510 and WT mice were significantly altered by chronic MK-1064 treatment (Fig. 4.8A-C; Table 4.7), influencing all three vigilance states. Genotype, treatment, sex and circadian time had a profound effect on the amount of time spent in each vigilance state (Fig. 4.8A-C; Table 4.7). Due to the particularly striking sex difference in response to MK-1064 treatment in rTg4510 mice, data from both male and female mice are presented separately over the 23 h recording (Fig. 4.8A-C). Male rTg4510 mice responded

robustly to MK-1064 treatment, with consistent reductions in wake time and increases in NREM and REM sleep time for several hours post administration (Fig. 4.8A-C). Female MK-1064-treated rTg4510 mice, however, displayed a similar sleep/wake profile to that of their female TPGS-treated controls, indicating an ineffectiveness of MK-1064 at promoting sleep in female rTg4510 mice (Fig. 4.8A-C).

The average time spent in each vigilance state across the first half of the active phase (6 h), complete active phase (12 h), inactive phase and the entire recording were assessed (Fig. 4.8D-O; Table 4.8). Summated data indicated that wake, NREM and REM sleep time were all influenced by genotype, treatment and sex during the first 6 and 12 h of the active phase (Fig. 4.8D, E, H, I, L, M; Table 4.8). During the active phase (6 h), wake time was reduced to WT levels in male rTg4510 mice. MK-1064 treatment also decreased wake time in female WT mice (Fig. 4.8D). However, female rTg4510 mice exhibited no decrease in wake time following MK-1064 treatment (Fig. 4.8D). The data indicated the lack of response to MK-1064 was sex- and genotype-dependent, and not just specific to female mice in general (Fig. 4.8D, E). As seen in previous studies (Chapter 3), there was no effect of genotype and therefore nor of treatment in the inactive phase (Fig. 4.8F), although genotype and sex effects were present over the entire 23 h summated recording (Fig. 4.8G; Table 4.8).

In male rTg4510 mice, MK-1064 increased both NREM and REM sleep to WT levels and was efficacious in WT females but again, no effect was observed in female rTg4510 mice (Fig. 4.8H, L). Some sex differences were also observed in male and female WT mice in that female WT mice spent more time in wake and less time in NREM sleep than WT males following TPGS treatment, and therefore exhibited a correspondingly larger response to MK-1064 than males. The responses of these mice to MK-1064 treatment may thus point to potential ceiling/floor effects in the background mouse strain (FBV/N x 129SVeV; Fig. 4.8D, H, L). Similar effects were observed, as discussed above, when analysing the complete active phase (12 h), although less pronounced, presumably as the drug cleared from the brain and circulation (Fig. 4.8E, I, M). During the inactive phase, no significant differences were observed across all vigilance states, consistent with previous findings (Chapter 3; Fig. 4.8F, J, N).

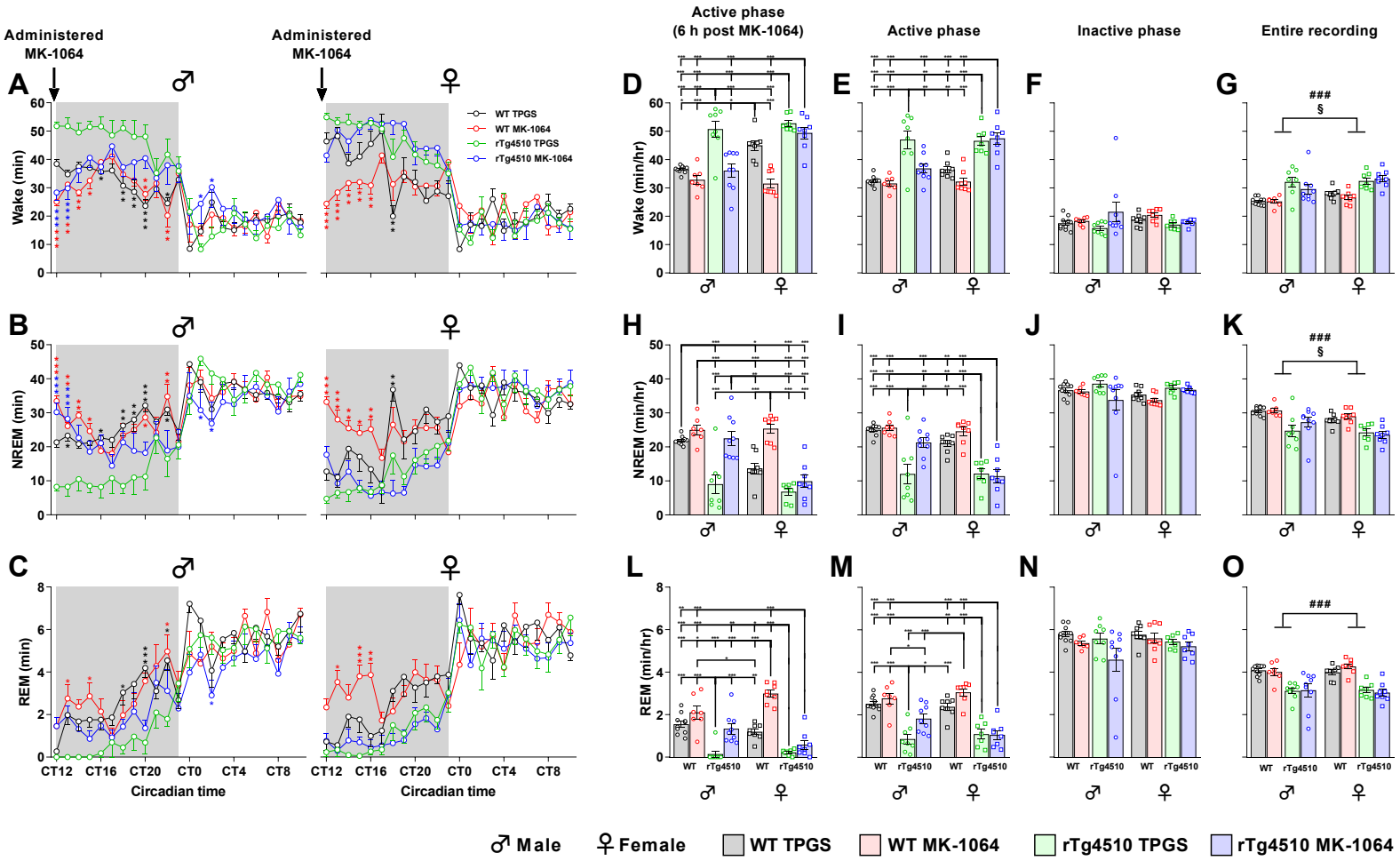

Figure 4.8. Promotion of NREM/REM sleep following MK-1064 treatment in rTg4510 mice.

A-C, Minutes spent in wake (***A***), NREM (***B***) and REM (***C***) vigilance states per hour across a 23 h recording in rTg4510 and WT mice administered MK-1064 or TPGS vehicle. Dark shade represents the active phase. Data are means ± SEM. n = 7-10 per group, per sex. $^{*}P < 0.05$, $^{**}P < 0.01$, $^{***}P < 0.001$ vs. rTg4510 TPGS, by repeated measures linear mixed effects model with Tukey's multiple comparisons test. For clarity, not all statistically significant differences are graphically presented. Continued over page…

…continued from previous: ***D-O***, Minutes spent in each vigilance state per hour averaged across (from left to right) the active phase (6 h post-MK-1064), complete active phase (12 h), inactive phase and entire recording, for wake (***D-G***), NREM (***H-K***) and REM (***L-O***). n = 7-10 per group, per sex. # and § denote main effects of genotype and sex, respectively. ###P < 0.001 vs. WT; §P < 0.05 vs. Female; *P < 0.05, **P < 0.01, ***P < 0.001, by linear mixed effects model with Tukey's multiple comparisons test. Refer to Table 4.7 and 4.8 for further details.

Table 4.7. Experiment 2 (MK-1064) EEG recordings statistical analyses summary.

Time spent in each vigilance state across the 23 h recording were analysed by a repeated measures linear mixed effects model in R, using the *lmer* function, incorporating the factors of Genotype, Treatment, Sex and Time (repeated factor). Indented Pr(>|t|) values indicate statistical significance.

Vigilance state time															
					Wake					**NREM**					**REM**
Fixed effect	Estimate	Std. error	df	t-value	Pr(>|t|)	Estimate	Std. error	df	t-value	Pr(>|t|)	Estimate	Std. error	df	t-value	Pr(>|t|)
Genotype	-22.298	2.782	407.328	-8.014	< 0.001	19.779	2.480	387.590	7.976	< 0.001	2.516	0.426	461.328	5.912	< 0.001
Treatment	1.117	2.880	407.328	0.388	> 0.05	-0.869	2.567	387.590	-0.339	> 0.05	-0.249	0.441	461.328	-0.564	> 0.05
Sex	-15.825	2.704	407.328	-5.852	< 0.001	14.844	2.410	387.590	6.159	< 0.001	0.979	0.414	461.328	2.368	< 0.05
Time	-1.998	0.132	1422.000	-15.127	< 0.001	1.709	0.117	1422.000	14.636	< 0.001	0.289	0.021	1421.999	14.038	< 0.001
Genotype:Treatment	8.141	4.005	407.328	2.033	< 0.05	-7.186	3.569	387.590	-2.013	< 0.05	-0.954	0.613	461.328	-1.557	> 0.05
Genotype:Sex	16.196	3.950	407.328	4.100	< 0.001	-14.576	3.521	387.590	-4.140	< 0.001	-1.619	0.604	461.328	-2.679	< 0.01
Treatment:Sex	16.153	3.950	407.328	4.089	< 0.001	-14.767	3.521	387.590	-4.194	< 0.001	-1.383	0.604	461.328	-2.288	< 0.05
Genotype:Time	1.302	0.187	1422.000	6.969	< 0.001	-1.195	0.165	1422.000	-7.235	< 0.001	-0.107	0.029	1421.999	-3.677	< 0.001
Treatment:Time	-0.162	0.193	1422.000	-0.838	> 0.05	0.131	0.171	1422.000	0.765	> 0.05	0.031	0.030	1421.999	1.035	> 0.05
Sex:Time	1.004	0.182	1422.000	5.527	< 0.001	-0.930	0.161	1422.000	-5.795	< 0.001	-0.074	0.028	1421.999	-2.597	< 0.01
Genotype:Treatment:Sex	-22.818	5.556	407.328	-4.107	< 0.001	20.606	4.952	387.590	4.161	< 0.001	2.209	0.850	461.328	2.599	< 0.01
Genotype:Treatment:Time	-0.497	0.269	1422.000	-1.847	> 0.05	0.451	0.238	1422.000	1.896	> 0.05	0.046	0.042	1421.999	1.092	> 0.05
Genotype:Sex:Time	-1.154	0.265	1422.000	-4.351	< 0.001	1.049	0.234	1422.000	4.475	< 0.001	0.105	0.041	1421.999	2.532	< 0.05
Treatment:Sex:Time	-1.065	0.265	1422.000	-4.014	< 0.001	0.962	0.234	1422.000	4.104	< 0.001	0.102	0.041	1421.999	2.476	< 0.05
Genotype:Treatment:Sex:Time	1.513	0.373	1422.000	4.056	< 0.001	-1.371	0.330	1422.000	-4.159	< 0.001	-0.142	0.058	1421.999	-2.438	< 0.05

Table 4.8. Experiment 2 (MK-1064) phase specific EEG recordings statistical analyses summary.

Average time spent in each vigilance state per phase were analysed by a linear mixed effects model in R, using the *lm* function, incorporating the factors of Genotype, Treatment and Sex. Indented Pr(>|t|) values indicate statistical significance.

Vigilance state time																	
			Active phase (6 h post MK-1064)				**Active phase**				**Inactive phase**				**Entire recording**			
Vigilance state	Fixed effect	Estimate	Std. error	t-value	Pr(>|t|)	Estimate	Std. error	t-value	Pr(>|t|)	Estimate	Std. error	t-value	Pr(>|t|)	Estimate	Std. error	t-value	Pr(>|t|)
Wake	Genotype	-17.897	2.606	-6.867	< 0.001	-15.236	2.405	-6.335	< 0.001	2.665	2.155	1.237	> 0.05	-6.675	1.648	-4.051	< 0.001
	Treatment	3.444	2.698	1.277	> 0.05	-0.829	2.490	-0.333	> 0.05	-0.824	2.231	-0.370	> 0.05	-0.827	1.706	-0.485	> 0.05
	Sex	-13.444	2.533	-5.257	< 0.001	-10.647	2.337	-4.555	< 0.001	3.706	2.094	1.770	> 0.05	-3.782	1.601	-2.362	< 0.05
	Genotype:Treatment	10.088	3.751	2.689	< 0.01	5.071	3.462	1.465	> 0.05	-0.968	3.101	-0.312	> 0.05	2.183	2.372	0.920	> 0.05
	Genotype:Sex	14.628	3.700	3.953	< 0.001	9.949	3.415	2.913	< 0.01	-5.947	3.060	-1.944	> 0.05	2.346	2.340	1.003	> 0.05
	Treatment:Sex	11.189	3.700	3.024	< 0.01	11.008	3.415	3.224	< 0.01	-4.952	3.060	-1.619	> 0.05	3.375	2.340	1.443	> 0.05
	Genotype:Treatment:Sex	-21.018	5.204	-4.039	< 0.001	-14.399	4.803	-2.998	< 0.01	5.966	4.303	1.386	> 0.05	-4.660	3.291	-1.416	> 0.05
NREM	Genotype	15.479	2.425	6.383	< 0.001	13.220	2.194	6.025	< 0.001	-3.039	1.859	-1.635	> 0.05	5.444	1.491	3.651	< 0.001
	Treatment	-3.078	2.510	-1.226	> 0.05	0.787	2.271	0.346	> 0.05	0.606	1.924	0.315	> 0.05	0.700	1.544	0.454	> 0.05
	Sex	12.570	2.357	5.334	< 0.001	9.876	2.132	4.631	< 0.001	-3.067	1.806	-1.698	> 0.05	3.686	1.449	2.543	< 0.05
	Genotype:Treatment	-8.642	3.490	-2.476	< 0.05	-4.336	3.158	-1.373	> 0.05	1.014	2.675	0.379	> 0.05	-1.777	2.146	-0.828	> 0.05
	Genotype:Sex	-12.977	3.443	-3.769	< 0.001	-8.887	3.115	-2.853	< 0.01	5.543	2.639	2.100	< 0.05	-1.986	2.117	-0.938	> 0.05
	Treatment:Sex	-10.364	3.443	-3.010	< 0.01	-10.004	3.115	-3.211	< 0.01	4.180	2.639	1.584	> 0.05	-3.220	2.117	-1.521	> 0.05
	Genotype:Treatment:Sex	18.931	4.843	3.909	< 0.001	12.952	4.381	2.956	< 0.01	-5.448	3.712	-1.468	> 0.05	4.152	2.978	1.395	> 0.05
REM	Genotype	2.417	0.270	8.937	< 0.001	2.015	0.278	7.234	< 0.001	0.374	0.392	0.956	> 0.05	1.230	0.242	5.074	< 0.001
	Treatment	-0.366	0.280	-1.308	> 0.05	0.042	0.288	0.145	> 0.05	0.218	0.405	0.537	> 0.05	0.126	0.251	0.502	> 0.05
	Sex	0.744	0.263	2.832	< 0.01	0.770	0.271	2.844	< 0.01	-0.638	0.381	-1.678	> 0.05	0.096	0.236	0.408	> 0.05
	Genotype:Treatment	-1.444	0.389	-3.710	< 0.001	-0.733	0.401	-1.829	> 0.05	-0.045	0.564	-0.080	> 0.05	-0.404	0.349	-1.158	> 0.05
	Genotype:Sex	-1.649	0.384	-4.296	< 0.001	-1.061	0.395	-2.683	< 0.01	0.403	0.556	0.725	> 0.05	-0.361	0.344	-1.048	> 0.05
	Treatment:Sex	-0.822	0.384	-2.140	< 0.05	-1.001	0.395	-2.532	< 0.05	0.772	0.556	1.388	> 0.05	-0.153	0.344	-0.445	> 0.05
	Genotype:Treatment:Sex	2.082	0.540	3.856	< 0.001	1.444	0.556	2.597	< 0.05	-0.518	0.782	-0.662	> 0.05	0.506	0.484	1.045	> 0.05

MK-1064 promoted NREM/REM sleep in male rTg4510 mice by increasing both bout numbers and bout durations

Vigilance state bout numbers and bout durations were significantly altered by chronic MK-1064 treatment (Fig. 4.9, 4.10; Table 4.9, 4.10). During the active phase (6 h), wake, NREM and REM bout numbers were influenced by genotype, treatment and sex (Fig. 4.9; Table 4.9). Male TPGS-treated WT mice exhibited a significantly higher number of wake and NREM bouts compared with their female WT equivalents (Fig. 4.9A, E), consistent with the sex differences observed in WT mice here (Fig. 4.8D, H). MK-1064 normalised these bout numbers across the WT sexes by decreasing them in male mice and increasing them in female mice (Fig. 4.9A, E). Male rTg4510 mice exhibited a striking reduction in the number of wake and NREM bouts relative to WT males (Fig. 4.9A, E). MK-1064 treatment increased wake and NREM bout numbers in male rTg4510 mice but had no effect on bout numbers in female rTg4510 mice (Fig. 4.9A, E).

REM bout numbers were increased in all groups following MK-1064 treatment except for female rTg4510 mice, with male rTg4510 bout numbers restored to WT levels (Fig. 4.9I). Similar, although less pronounced effects, were observed when analysing the complete active phase (12 h; Fig. 4.9B, F, J). During the inactive phase a main effect of genotype only was observed, whereby rTg4510 mice exhibited less bout numbers across all three vigilance states (Fig. 4.9C, G, K).

Bout duration during the active phase was significantly affected by genotype, treatment and sex (Fig. 4.10; Table 4.10). Female TPGS-treated WT mice exhibited particularly long wake bout durations (Fig. 4.10A, B). MK-1064 decreased wake bout duration in female WT mice, but not in female rTg4510 mice (Fig. 4.10A, B). NREM (Fig. 4.10E, F) and REM (Fig. 4.10I, J) bout durations were increased to WT levels in male rTg4510 mice following MK-1064 treatment across the active phase but were unaffected in female rTg4510 mice. During the inactive phase, NREM (Fig. 4.10G) and REM (Fig. 4.10K) bout durations were increased in rTg4510 mice, but with no effect of treatment or sex, consistent with previous findings (Chapter 3).

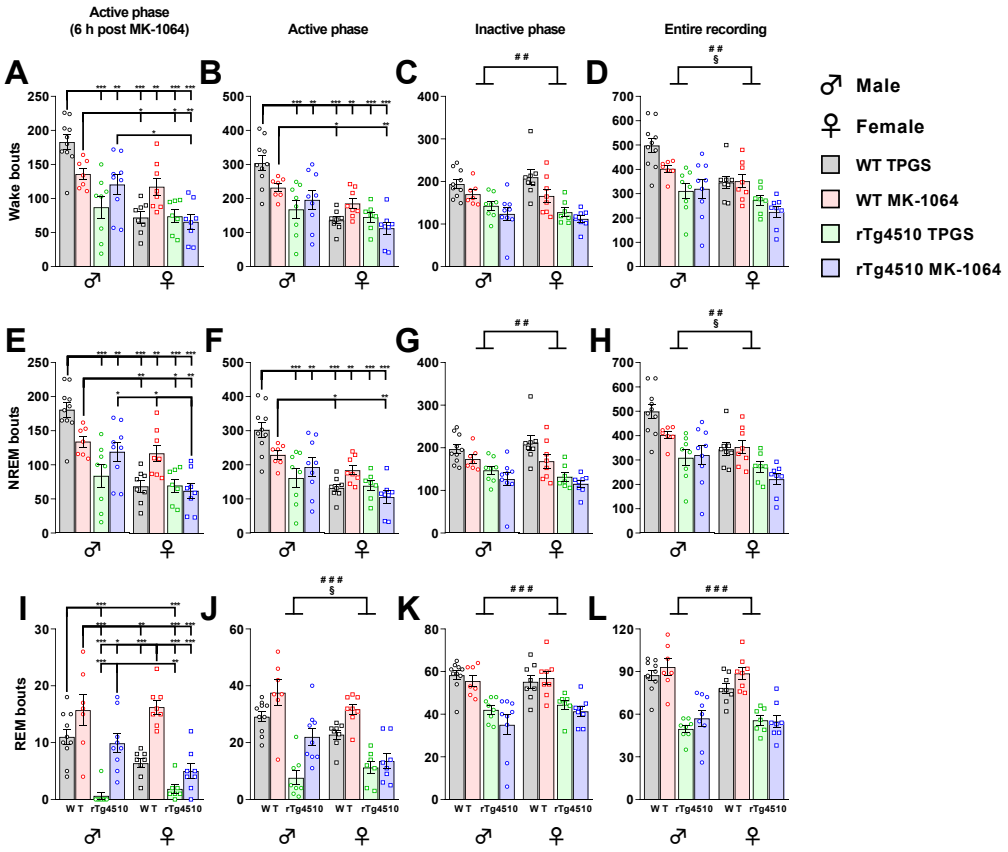

Figure 4.9. Increased NREM/REM bout numbers following MK-1064 treatment in rTg4510 mice.

A-L, Total number of wake (***A-D***), NREM (***E-H***) and REM (***I-L***) bouts averaged across (from left to right) the active phase (6 h post-MK-1064), complete active phase (12 h), inactive phase and entire recording in rTg4510 and WT administered MK-1064 or TPGS vehicle. Data are means ± SEM. n = 7-10 per group, per sex. # and § denote main effects of genotype and sex, respectively. $^{\#\#}P < 0.01$, $^{\#\#\#}P < 0.001$ vs. WT; $^{\S}P < 0.05$ vs. Female; $^{*}P < 0.05$ $^{**}P < 0.01$, $^{***}P < 0.001$, by linear mixed effects model with Tukey's multiple comparisons test. Refer to Table 4.9 for further details.

Table 4.9. Experiment 2 (MK-1064) vigilance state bout numbers statistical analyses summary.

Average bout numbers of each vigilance state per phase were analysed by a linear mixed effects model in R, using the *lm* function, incorporating the factors of Genotype, Treatment and Sex. Indented Pr(>|t|) values indicate statistical significance.

Vigilance state bout numbers																	
		Active phase (6 h post MK-1064)				**Active phase**				**Inactive phase**				**Entire recording**			
Vigilance state	Fixed effect	Estimate	Std. error	t-value	Pr(>|t|)	Estimate	Std. error	t-value	Pr(>|t|)	Estimate	Std. error	t-value	Pr(>|t|)	Estimate	Std. error	t-value	Pr(>|t|)
Wake	Genotype	51.625	16.941	3.047	< 0.01	72.870	28.760	2.534	< 0.05	53.750	18.146	2.962	< 0.01	126.620	41.180	3.075	< 0.01
	Treatment	8.268	17.535	0.471	> 0.05	33.000	29.770	1.109	> 0.05	15.518	18.783	0.826	> 0.05	48.520	42.630	1.138	> 0.05
	Sex	54.569	16.463	3.315	< 0.01	83.220	27.950	2.978	< 0.01	11.264	17.635	0.639	> 0.05	94.490	40.020	2.361	< 0.05
	Genotype:Treatment	-53.518	24.382	-2.195	< 0.05	-82.250	41.390	-1.987	> 0.05	28.482	26.117	1.091	> 0.05	-53.770	59.270	-0.907	> 0.05
	Genotype:Sex	-36.212	24.053	-1.506	> 0.05	-37.100	40.830	-0.909	> 0.05	-7.353	25.764	-0.285	> 0.05	-44.450	58.470	-0.760	> 0.05
	Treatment:Sex	-41.462	24.053	-1.724	> 0.05	-60.970	40.830	-1.493	> 0.05	3.468	25.764	0.135	> 0.05	-57.500	58.470	-0.983	> 0.05
	Genotype:Treatment:Sex	133.955	33.827	3.960	< 0.001	182.320	57.420	3.175	< 0.01	-23.954	36.235	-0.661	> 0.05	158.370	82.230	1.926	> 0.05
NREM	Genotype	55.250	16.941	3.261	< 0.01	79.000	29.050	2.719	< 0.01	53.375	18.408	2.900	< 0.01	132.370	41.820	3.165	< 0.01
	Treatment	7.982	17.535	0.455	> 0.05	33.250	30.070	1.106	> 0.05	16.786	19.054	0.881	> 0.05	50.040	43.290	1.156	> 0.05
	Sex	57.125	16.463	3.470	< 0.001	87.810	28.230	3.110	< 0.01	10.833	17.889	0.606	> 0.05	98.640	40.640	2.427	< 0.05
	Genotype:Treatment	-56.482	24.382	-2.317	< 0.05	-85.370	41.810	-2.042	< 0.05	26.214	26.493	0.989	> 0.05	-59.160	60.190	-0.983	> 0.05
	Genotype:Sex	-40.107	24.052	-1.667	> 0.05	-43.560	41.250	-1.056	> 0.05	-6.137	26.135	-0.235	> 0.05	-49.690	59.380	-0.837	> 0.05
	Treatment:Sex	-40.107	24.052	-1.792	> 0.05	-65.310	41.250	-1.583	> 0.05	4.006	26.135	0.153	> 0.05	-61.300	59.380	-1.032	> 0.05
	Genotype:Treatment:Sex	138.264	33.827	4.087	< 0.001	190.630	58.010	3.286	< 0.01	-23.777	36.757	-0.647	> 0.05	166.850	83.510	1.998	> 0.05
REM	Genotype	11.250	2.044	5.504	< 0.001	18.250	3.698	4.935	< 0.001	15.625	4.230	3.694	< 0.001	33.875	6.222	5.445	< 0.001
	Treatment	-3.143	2.116	-1.486	> 0.05	-2.214	3.828	-0.578	> 0.05	3.054	4.378	0.697	> 0.05	0.839	6.440	0.130	> 0.05
	Sex	4.889	1.986	2.461	< 0.05	8.500	3.594	2.365	< 0.05	-6.375	4.111	-1.551	> 0.05	2.125	6.046	0.351	> 0.05
	Genotype:Treatment	-6.732	2.942	-2.289	< 0.05	-6.661	5.323	-1.251	> 0.05	-4.804	6.088	-0.789	> 0.05	-11.464	8.955	-1.280	> 0.05
	Genotype:Sex	-5.425	2.902	-1.869	> 0.05	-2.679	5.251	-0.510	> 0.05	4.946	6.005	0.824	> 0.05	2.268	8.834	0.257	> 0.05
	Treatment:Sex	-6.121	2.902	-2.109	< 0.05	-12.161	5.251	-2.316	< 0.05	3.946	6.005	0.657	> 0.05	-8.214	8.834	-0.930	> 0.05
	Genotype:Treatment:Sex	11.282	4.081	2.764	< 0.01	12.564	7.385	1.701	> 0.05	0.532	8.446	0.063	> 0.05	13.096	12.424	1.054	> 0.05

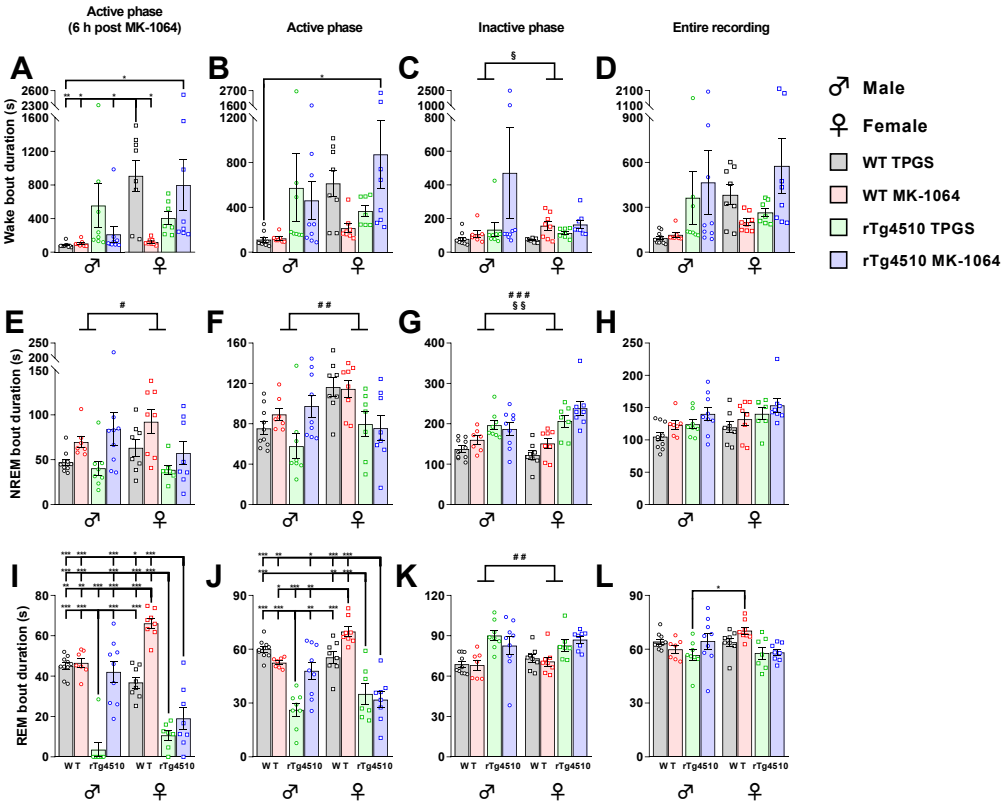

Figure 4.10. Increased NREM/REM bout durations following MK-1064 treatment in rTg4510 mice.

A-L*,** Mean wake (A-D***), NREM (***E-H***) and REM (***I-L***) bout durations averaged across (from left to right) the active phase (6 h post-MK-1064), complete active phase (12 h), inactive phase and entire recording in rTg4510 and WT administered MK-1064 or TPGS vehicle. Data are means ± SEM. n = 7-10 per group, per sex. # and § denote main effects of genotype and sex, respectively. $^{\#}P < 0.05$, $^{\#\#}P < 0.01$, $^{\#\#\#}P < 0.001$ vs. WT; $^{\S}P < 0.05$, $^{\S\S}P < 0.01$ vs. Female; $^{*}P < 0.05$ $^{**}P < 0.01$, $^{***}P < 0.001$, by linear mixed effects model with Tukey's multiple comparisons test. Refer to Table 4.10 for further details.

Table 4.10. Experiment 2 (MK-1064) vigilance state bout duration statistical analyses summary.

Average bout duration of each vigilance state per phase were analysed by a linear mixed effects model in R, using the *lm* function, incorporating the factors of Genotype, Treatment and Sex. Indented Pr(>|t|) values indicate statistical significance.

Vigilance state bout durations															
		Active phase (6 h post MK-1064)				**Active phase**				**Inactive phase**				**Entire recording**			
Vigilance state	Fixed effect	Estimate	Std. error	t-value	Pr(>|t|)	Estimate	Std. error	t-value	Pr(>|t|)	Estimate	Std. error	t-value	Pr(>|t|)	Estimate	Std. error	t-value	Pr(>|t|)
Wake	Genotype	-678.000	227.300	-2.982	< 0.01	-659.400	244.600	-2.695	< 0.01	-7.601	154.784	-0.049	> 0.05	-347.657	173.882	-1.999	> 0.05
	Treatment	-393.400	235.300	-1.672	> 0.05	-505.500	253.200	-1.996	> 0.05	-50.206	160.216	-0.313	> 0.05	-287.764	179.985	-1.599	> 0.05
	Sex	-587.900	220.900	-2.661	< 0.05	-411.900	237.700	-1.732	> 0.05	306.592	150.423	2.038	< 0.05	-68.267	168.983	-0.404	> 0.05
	Genotype:Treatment	1180.200	327.200	3.607	< 0.001	905.300	352.100	2.571	< 0.05	-33.995	222.772	-0.153	> 0.05	456.068	250.259	1.822	> 0.05
	Genotype:Sex	569.400	322.800	1.764	> 0.05	320.400	347.300	0.922	> 0.05	-356.284	219.764	-1.621	> 0.05	-3.239	246.881	-0.013	> 0.05
	Treatment:Sex	737.200	322.800	2.284	< 0.05	617.800	347.300	1.779	> 0.05	-287.836	219.764	-1.310	> 0.05	184.669	246.881	0.748	> 0.05
	Genotype:Treatment:Sex	-1543.900	454.000	-3.401	< 0.01	-1029.600	488.500	-2.108	< 0.05	343.382	309.075	1.111	> 0.05	-372.973	347.212	-1.074	> 0.05
NREM	Genotype	34.900	15.800	2.209	< 0.05	39.003	14.310	2.726	< 0.01	-87.226	18.529	-4.707	< 0.001	-21.368	12.520	-1.707	> 0.05
	Treatment	-18.860	16.350	-1.153	> 0.05	4.046	14.813	0.273	> 0.05	-31.659	19.180	-1.651	> 0.05	-13.030	12.960	-1.005	> 0.05
	Sex	26.500	15.350	1.726	> 0.05	21.847	13.907	1.571	> 0.05	-51.549	18.007	-2.863	< 0.01	-13.256	12.168	-1.089	> 0.05
	Genotype:Treatment	-10.160	22.730	-0.447	> 0.05	-2.326	20.596	-0.113	> 0.05	2.978	26.668	0.112	> 0.05	0.211	18.020	0.012	> 0.05
	Genotype:Sex	-49.220	22.430	-2.194	< 0.05	-47.279	20.318	-2.327	< 0.05	60.104	26.308	2.285	< 0.05	4.078	17.777	0.229	> 0.05
	Treatment:Sex	-24.790	22.430	-1.105	> 0.05	-43.814	20.318	-2.156	< 0.05	41.185	26.308	1.565	> 0.05	-3.162	17.777	-0.178	> 0.05
	Genotype:Treatment:Sex	31.240	31.540	0.990	> 0.05	28.328	28.575	0.991	> 0.05	-34.887	37.000	-0.943	> 0.05	-1.906	25.001	-0.076	> 0.05
REM	Genotype	47.156	5.069	9.303	< 0.001	38.036	5.214	7.295	< 0.001	-16.175	5.617	-2.880	< 0.01	12.109	3.914	3.094	< 0.01
	Treatment	-8.410	5.247	-1.603	> 0.05	3.192	5.397	0.591	> 0.05	-4.358	5.814	-0.750	> 0.05	-0.419	4.051	-0.104	> 0.05
	Sex	22.992	4.926	4.667	< 0.001	16.015	5.067	3.161	< 0.01	-4.456	5.459	-0.816	> 0.05	6.224	3.803	1.637	> 0.05
	Genotype:Treatment	-20.992	7.295	-2.871	< 0.01	-17.594	7.504	-2.345	< 0.05	6.667	8.084	0.825	> 0.05	-5.991	5.633	-1.064	> 0.05
	Genotype:Sex	-42.669	7.197	-5.929	< 0.001	-33.522	7.403	-4.528	< 0.001	1.703	7.975	0.214	> 0.05	-16.675	5.557	-3.001	< 0.01
	Treatment:Sex	-30.096	7.197	-4.182	< 0.001	-24.961	7.403	-3.372	< 0.01	11.836	7.975	1.484	> 0.05	-7.363	5.557	-1.325	> 0.05
	Genotype:Treatment:Sex	57.972	10.121	5.728	< 0.001	46.916	10.411	4.506	< 0.001	-13.509	11.216	-1.204	> 0.05	18.017	7.815	2.306	< 0.05

MK-1064 attenuated EEG power deficits in the slow delta and theta frequencies during NREM and REM sleep in male but not female rTg4510 mice

To assess the effects of MK-1064 on EEG power during sleep, vigilance state-specific power spectral analysis over the first 6 (NREM) or 12 h (REM) post-administration were performed (Fig. 4.11; Table 4.11, 4.12). As in Experiment 1, rTg4510 mice exhibited deficits in delta power during NREM sleep (Fig. 4.11A, C) and theta power during REM sleep (Fig. 4.11B, D). MK-1064 treatment increased delta power during NREM sleep in the slow (1-2.5 Hz; Fig. 4.11E), but not fast (2.5-4 Hz; Fig. 4.11F) delta frequency band in male, but not female rTg4510 mice, with a significant treatment x sex interaction observed for slow delta waves (Fig. 4.11E; Table 4.12). Theta power during REM sleep was similarly reduced in rTg4510 versus WT mice particularly in the fast theta band (Fig. 4.11B; Table 4.12). Sex differences were also evident with increased slow (5-7.5 Hz; Fig. 4.11G), but not fast (7.5-9 Hz; Fig. 4.11H), REM sleep theta in male, but not female rTg4510 mice. There was no effect of MK-1064 in WT mice of either sex (Fig. 4.11).

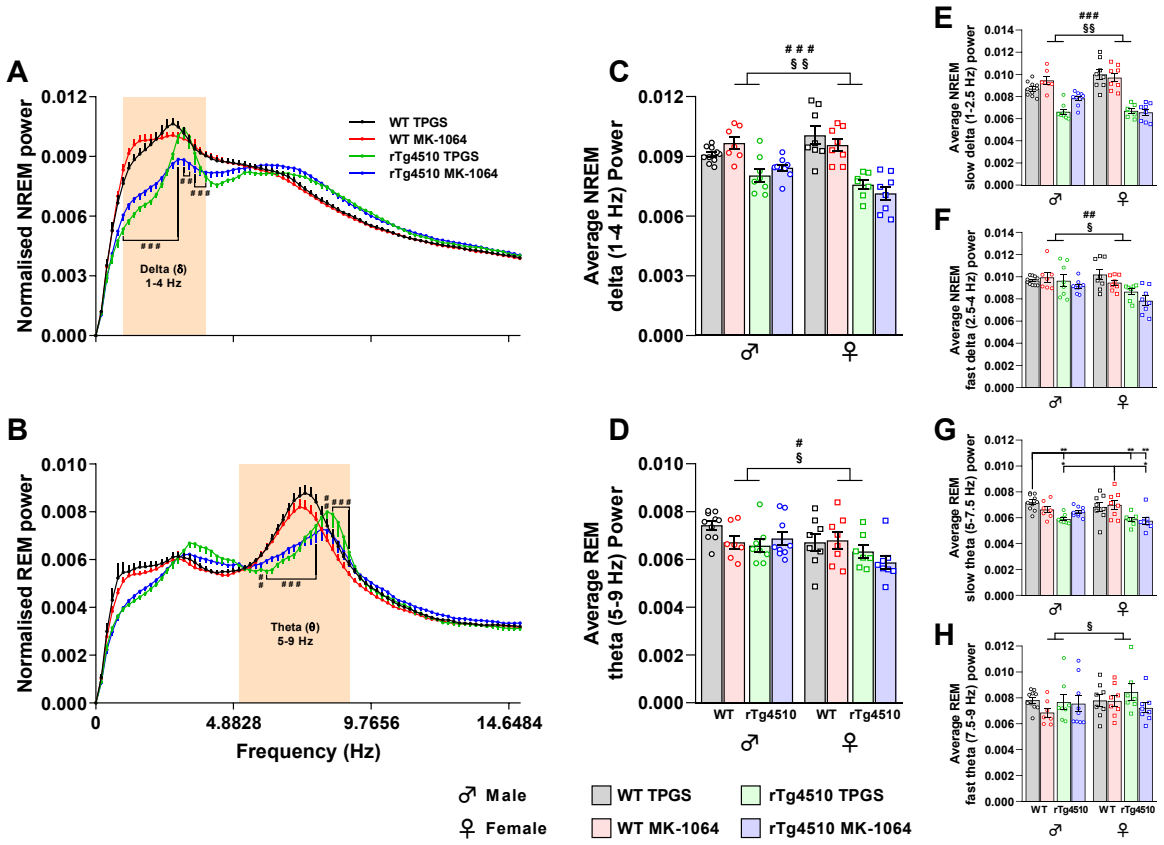

Figure 4.11. Altered EEG power following MK-1064 treatment in rTg4510 mice.

A-B, Vigilance state-specific normalised EEG power during NREM (***A***) and REM (***B***) sleep in rTg4510 and WT mice administered MK-1064 or TPGS vehicle. Data are means ± SEM. n = 15-18 per group. $^{\#\#}P < 0.01$, $^{\#\#\#}P < 0.001$ vs. WT (genotype x frequency) within frequency band, by repeated measures linear mixed effects model with Tukey's multiple comparisons test. ***C***, Average NREM power over the delta (1-4 Hz) frequencies. ***D***, Average REM power over the theta (5-9 Hz) frequencies. ***E-F***, Average NREM power over the slow (1-2.5 Hz) (***E***) and fast (2.5-4 Hz) (***F***) delta frequencies. ***G-H***, Average REM power over the slow (5-7.5 Hz) (***G***) and fast (7.5-9 Hz) (***H***) theta frequencies. n = 7-10 per group, per sex. # and § denote main effect of genotype and sex, respectively. $^{\#}P < 0.05$, $^{\#\#}P < 0.01$, $^{\#\#\#}P < 0.001$ vs. WT; $^{\S}P < 0.05$, $^{\S\S}P < 0.01$ vs. Female; $^{*}P < 0.05$ $^{**}P < 0.01$, by linear mixed effects model with Tukey's multiple comparisons test. Signals from EEG1 and EEG2 electrodes were combined. All transition epochs were excluded from power analysis. For clarity, not all statistically significant differences are graphically presented. Refer to Table 4.11 and 4.12 for further details.

Table 4.11. Experiment 2 (MK-1064) EEG power statistical analyses summary.

Vigilance state-specific normalised EEG power across the first 6 (NREM) or 12 h (REM) of the recording were analysed by a repeated measures linear mixed effects model in R, using the *lmer* function, incorporating the factors of Genotype, Treatment and Frequency (repeated factor). Indented Pr(>|t|) values indicate statistical significance.

Vigilance state-specific EEG power										
					NREM					**REM**
Fixed effect	Estimate	Std. error	df	t-value	Pr(>|t|)	Estimate	Std. error	df	t-value	Pr(>|t|)
Genotype	0.000908	0.000142	248.1	6.413	< 0.001	0.000397	0.000131	207.8	3.028	< 0.01
Treatment	-0.000203	0.000142	248.1	-1.434	> 0.05	0.000081	0.000131	207.8	0.615	> 0.05
Frequency (Hz)	-0.000251	0.000007	6626.0	-36.271	< 0.001	-0.000128	0.000006	6626.0	-20.970	< 0.001
Genotype:Treatment	0.000163	0.000199	248.1	0.818	> 0.05	0.000217	0.000184	207.8	1.177	> 0.05
Genotype:Frequency	-0.000081	0.000010	6626.0	-7.979	< 0.001	-0.000045	0.000009	6626.0	-5.005	< 0.001
Treatment:Frequency	0.000014	0.000010	6626.0	1.362	> 0.05	-0.000013	0.000009	6626.0	-1.502	> 0.05
Genotype:Treatment:Frequency	-0.000008	0.000014	6626.0	-0.538	> 0.05	-0.000002	0.000013	6626.0	-0.124	> 0.05

Table 4.12. Experiment 2 (MK-1064) NREM delta and REM theta statistical analyses summary.

Summed NREM delta and REM theta normalised EEG power were analysed by a linear mixed effects model in R, using the *lm* function, incorporating the factors of Genotype, Treatment and Sex. Indented Pr(>|t|) values indicate statistical significance.

Vigilance state-specific EEG power											
					NREM						**REM**
Frequency	Fixed effect	Estimate	Std. error	t-value	Pr(>|t|)	Frequency		Estimate	Std. error	t-value	Pr(>|t|)
Delta (1-4 Hz)	Genotype	0.002432	0.000416	5.844	< 0.001	**Theta (5-9 Hz)**	Genotype	0.000931	0.000410	2.272	< 0.05
	Treatment	0.000441	0.000431	1.023	> 0.05		Treatment	0.000460	0.000424	1.085	> 0.05
	Sex	0.001289	0.000404	3.187	< 0.01		Sex	0.001002	0.000398	2.516	< 0.05
	Genotype:Treatment	0.000046	0.000599	0.077	> 0.05		Genotype:Treatment	-0.000550	0.000590	-0.933	> 0.05
	Genotype:Sex	-0.001188	0.000591	-2.011	< 0.05		Genotype:Sex	-0.001088	0.000582	-1.871	> 0.05
	Treatment:Sex	-0.000829	0.000591	-1.403	> 0.05		Treatment:Sex	-0.000757	0.000582	-1.302	> 0.05
	Genotype:Treatment:Sex	-0.000251	0.000831	-0.302	> 0.05		Genotype:Treatment:Sex	0.001562	0.000818	1.909	> 0.05
Slow delta (1-2.5 Hz)	Genotype	0.003135	0.000431	7.278	< 0.001	**Slow theta (5-7.5 Hz)**	Genotype	0.001226	0.000346	3.542	< 0.001
	Treatment	0.000135	0.000446	0.302	> 0.05		Treatment	0.000111	0.000358	0.310	> 0.05
	Sex	0.001243	0.000419	2.969	< 0.01		Sex	0.000679	0.000337	2.017	< 0.05
	Genotype:Treatment	0.000157	0.000620	0.253	> 0.05		Genotype:Treatment	-0.000272	0.000498	-0.547	> 0.05
	Genotype:Sex	-0.001509	0.000612	-2.468	< 0.05		Genotype:Sex	-0.001055	0.000492	-2.146	< 0.05
	Treatment:Sex	-0.001340	0.000612	-2.192	< 0.05		Treatment:Sex	-0.000668	0.000492	-1.358	> 0.05
	Genotype:Treatment:Sex	0.000293	0.000860	0.340	> 0.05		Genotype:Treatment:Sex	0.001385	0.000691	2.003	< 0.05
Fast delta (2.5-4 Hz)	Genotype	0.001628	0.000504	3.233	< 0.01	**Fast theta (7.5-9 Hz)**	Genotype	0.000451	0.000622	0.725	> 0.05
	Treatment	0.000817	0.000521	1.568	> 0.05		Treatment	0.001027	0.000644	1.595	> 0.05
	Sex	0.001299	0.000489	2.654	< 0.05		Sex	0.001527	0.000605	2.525	< 0.05
	Genotype:Treatment	-0.000082	0.000725	-0.122	> 0.05		Genotype:Treatment	-0.001001	0.000895	-1.118	> 0.05
	Genotype:Sex	-0.000826	0.000715	-1.115	> 0.05		Genotype:Sex	-0.001142	0.000883	-1.293	> 0.05
	Treatment:Sex	-0.000322	0.000715	-0.450	> 0.05		Treatment:Sex	-0.000903	0.000883	-1.023	> 0.05
	Genotype:Treatment:Sex	-0.000710	0.001006	-0.706	> 0.05		Genotype:Treatment:Sex	0.001849	0.001242	1.488	> 0.05

MK-1064 improved hippocampal-dependent spatial recall deficits in the Barnes maze in male but not female rTg4510 mice

Paralleling the striking sex differences in the sleep/wake response to MK-1064, sex differences in cognitive performance following MK-1064 treatment in rTg4510 mice were similarly observed. Hence data from both male and female mice are presented in separate graphs (Fig. 4.12A-H). WT TPGS-treated mice exhibited a significant preference for the target region (target ± 1) in both male ($F_{(4.508, 40.57)} = 5.949$, $P = 0.0005$, Fig. 4.12A) and female mice ($F_{(4.494, 31.46)} = 3.413$, $P = 0.0167$, Fig. 4.12B). WT MK-1064 mice also showed preference for the target region however, the ANOVA did not quite reach significance in either male ($F_{(4.717, 37.74)} =$

1.758, P = 0.1485, Fig. 4.12C) or female mice ($F_{(3.137, 21.96)} = 2.207$, P = 0.1137, Fig. 4.12D). rTg4510 TPGS mice exhibited no preference for the target region in either male ($F_{(3.746, 26.22)} = 1.307$, P = 0.2934, Fig. 4.12E) or female mice ($F_{(4.672, 28.03)} = 0.9971$, P = 0.4339, Fig. 4.12F). Male rTg4510 MK-1064-treated mice showed evidence of a partial rescue of spatial recall although the ANOVA was not significant ($F_{(3.320, 19.92)} = 2.821$, P = 0.0607, Fig. 4.12G). However, female rTg4510 mice showed complete failure to respond to MK-1064 in the probe trial ($F_{(3.898, 31.18)} = 0.9652$, P = 0.4387, Fig. 4.12H), which was not unexpected given the lack of response to MK-1064 in female rTg4510 mice in sleep/wake parameters (Fig. 4.8). The lack of ANOVA significance in male rTg4510 mice may be attributed to the spread of nose poke distribution over the entire target region, rather than the target hole specifically. Aggregate nose pokes across the target region were also assessed, which was restored to WT levels in male MK-1064-treated rTg4510 mice, albeit not significantly, likely due to behavioural variation in the data (Fig. 4.12I).

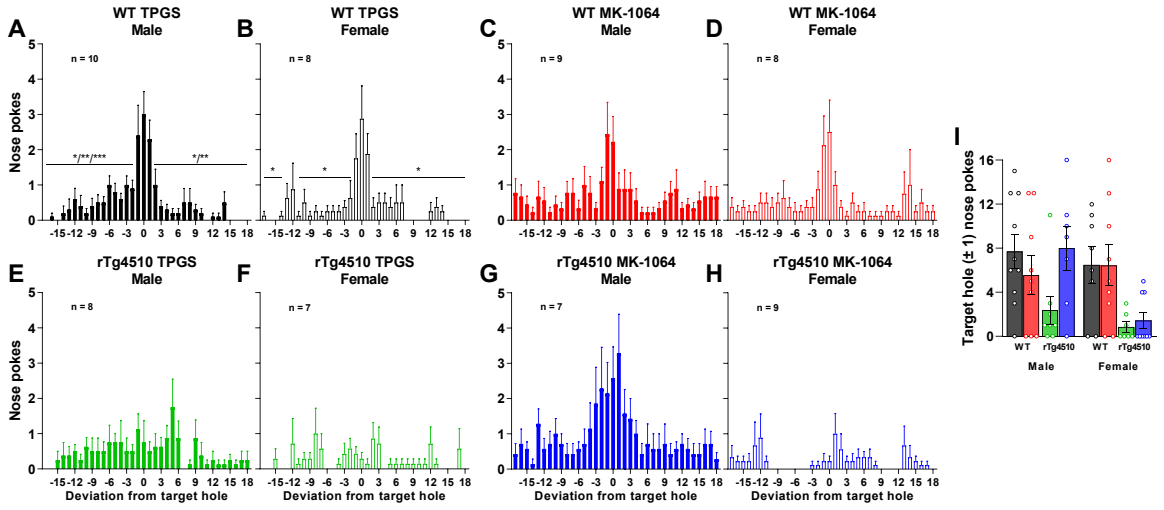

Figure 4.12. Improved spatial recall in the final probe trial of the Barnes maze following MK-1064 treatment. ***A-H***, Number of nose pokes into each of the 36 holes on the Barnes maze during the final probe trial, deviating from the target hole (denoted 0) by rTg4510 and WT mice administered MK-1064 or TPGS vehicle. Data are means ± SEM. n = 7-10 per group, per sex. $^{*}P < 0.05$, $^{**}P < 0.01$, $^{***}P < 0.001$ vs. target hole, by one-way repeated measures ANOVA with Fisher's LSD multiple comparisons test. ***I***, Total number of nose pokes into the target region (target hole ± 1).

Cognitive performance in the Barnes maze correlated with MK-1064 promoted sleep

In order to further evaluate whether the partial rescue of spatial recall was likely due to the drug intervention, correlative analyses of key outcome measures from both the acquisition phase (average primary latency during the 4th day of acquisition) and the recall/probe phase (aggregate target region nose pokes) of the Barnes maze, against summed MK-1064-promoted NREM/REM sleep time in the first 6 h post-drug administration were analysed. When assessing the experimental cohort as a whole, a negative correlation was observed between average primary latency and total sleep time, whereby mice that located the target hole faster tended to sleep more during the specified period ($R^2 = 0.3072$, $P < 0.0001$, Fig. 4.13A). This relationship was still evident when assessing all rTg4510 mice ($R^2 = 0.1931$, $P = 0.0171$, Fig. 4.13B) and the MK-1064-treated rTg4510 mice alone ($R^2 = 0.4733$, $P = 0.0046$, Fig. 4.13C). Furthermore, a positive correlation between total target region nose pokes and total sleep time was detected, whereby mice that poked their nose into the target region more frequently, indicative of greater spatial recall, tended to sleep more during the specified period ($R^2 = 0.2240$, $P = 0.0001$, Fig. 4.13D). Similarly, as above, these relationships were maintained when assessing rTg4510 mice ($R^2 = 0.2316$, $P = 0.0082$, Fig. 4.13E) and MK-1064-treated rTg4510 mice alone ($R^2 = 0.3195$, $P = 0.0281$, Fig. 4.13F).

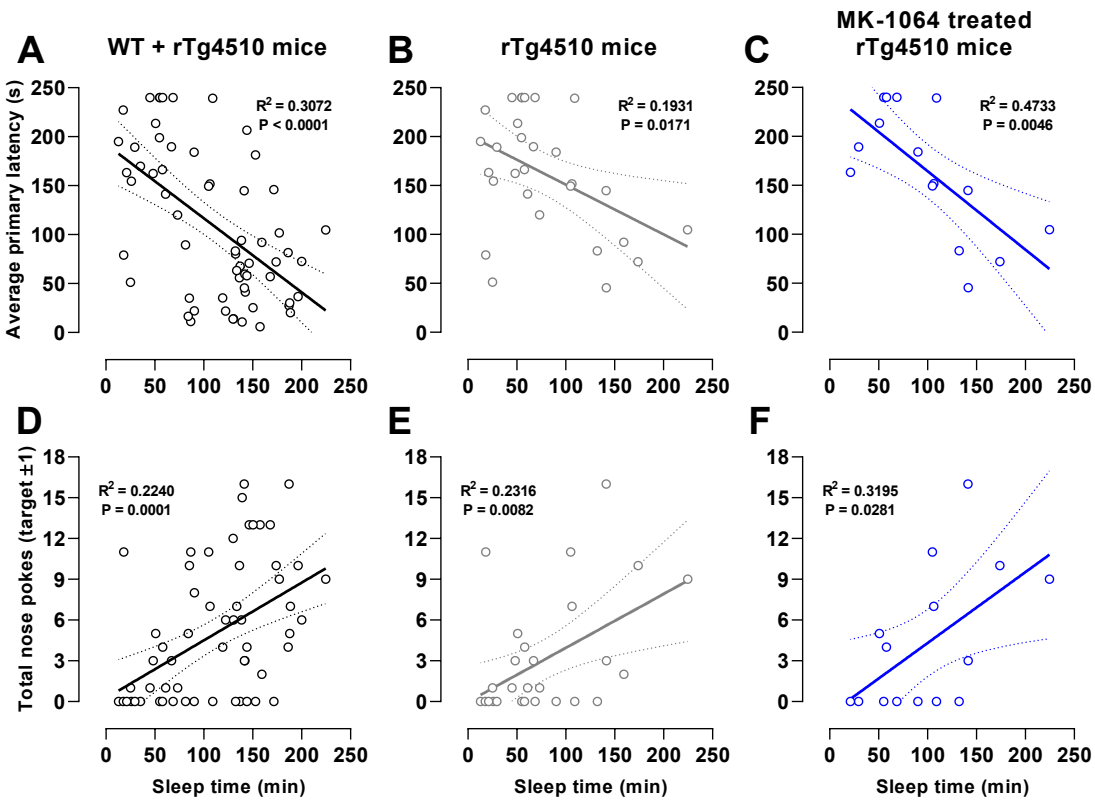

Figure 4.13. Correlation between Barnes maze performance and MK-1064-promoted sleep.
A-C, Average primary latency during the 4th day of acquisition trials plotted against aggregate MK-1064-promoted NREM+REM sleep during the first 6 h post-drug administration, in all experimental mice (***A***), rTg4510 mice alone (***B***) and MK-1064-treated rTg4510 mice alone (***C***). ***D-F***, Total target region (target hole ± 1) nose pokes during the probe/recall trial plotted against aggregate MK-1064-promoted NREM+REM sleep during the first 6 h post-drug administration, in all experimental mice (***D***), rTg4510 mice alone (***E***) and MK-1064-treated rTg4510 mice alone (***F***). n = 62 (all mice), 29 (rTg4510 mice) and 15 (MK-1064-treated rTg4510 mice). Solid lines denote the linear regression line of best fit, with 95% confidence bands (dotted curves).

MK-1064 reduced phosphorylated tau levels at the serine-404 but not serine-202 epitope without affecting total tau levels

Tau expression in the hippocampus and cortex was assessed by western blot (Fig. 4.14A). P-tau S404 levels were 12.40-fold higher in the hippocampus and 8.02-fold higher in the cortex of rTg4510 TPGS mice compared with WT TPGS mice (Fig. 4.14B, E). MK-1064 treatment reduced p-tau S404 levels by 10.06% in rTg4510 mice without affecting p-tau S404 levels in WT mice, in the hippocampus (Genotype: $F_{(1, 41)} = 1185$, $P < 0.0001$; treatment: $F_{(1, 41)} = 2.452$, $P = 0.1251$; interaction: $F_{(1, 41)} = 6.114$, $P = 0.0176$, Fig. 4.14B) and by 8.45% in the cortex (Genotype: $F_{(1, 41)} = 2121$, $P < 0.0001$; treatment: $F_{(1, 41)} = 5.146$, $P = 0.0286$; interaction: $F_{(1, 41)} = 5.819$, $P = 0.0204$, Fig. 4.14E), hence the reduction was relatively consistent across both brain regions analysed.

A second phosphorylated epitope was probed to determine whether the effects were generalised across more than one epitope. P-tau S202 levels were 8.34-fold higher in the hippocampus and 5.34-fold higher in the cortex of rTg4510 TPGS mice compared with WT TPGS mice (Fig. 4.14C, F). MK-1064 treatment did not affect p-tau S202 levels in rTg4510 or WT mice in the hippocampus (Genotype: $F_{(1, 41)} = 2411$, $P < 0.0001$; treatment: $F_{(1, 41)} = 0.8004$, $P = 0.3762$; interaction: $F_{(1, 41)} = 2.222$, $P = 0.1437$, Fig. 4.14C) or cortex (Genotype: $F_{(1, 41)} = 646.4$, $P < 0.0001$; treatment: $F_{(1, 41)} = 2.055$, $P = 0.1593$; interaction: $F_{(1, 41)} = 2.332$, $P = 0.1344$, Fig. 4.14F). Total levels were 2.37-fold higher in the hippocampus and 2.51-fold higher in the cortex of rTg4510 TPGS mice compared with WT TPGS mice (Fig. 4.14D, G). MK-1064 treatment did not affect total tau levels in rTg4510 or WT mice in the hippocampus (Genotype: $F_{(1, 41)} = 478.5$, $P < 0.0001$; treatment: $F_{(1, 41)} = 0.03302$, $P = 0.8567$; interaction: $F_{(1, 41)} = 3.348$, $P = 0.0746$, Fig. 4.14D) or cortex (Genotype: $F_{(1, 41)} = 293.4$, $P < 0.0001$; treatment: $F_{(1, 41)} = 0.5030$, $P = 0.4822$; interaction: $F_{(1, 41)} = 0.3279$, $P = 0.5700$, Fig. 4.14G).

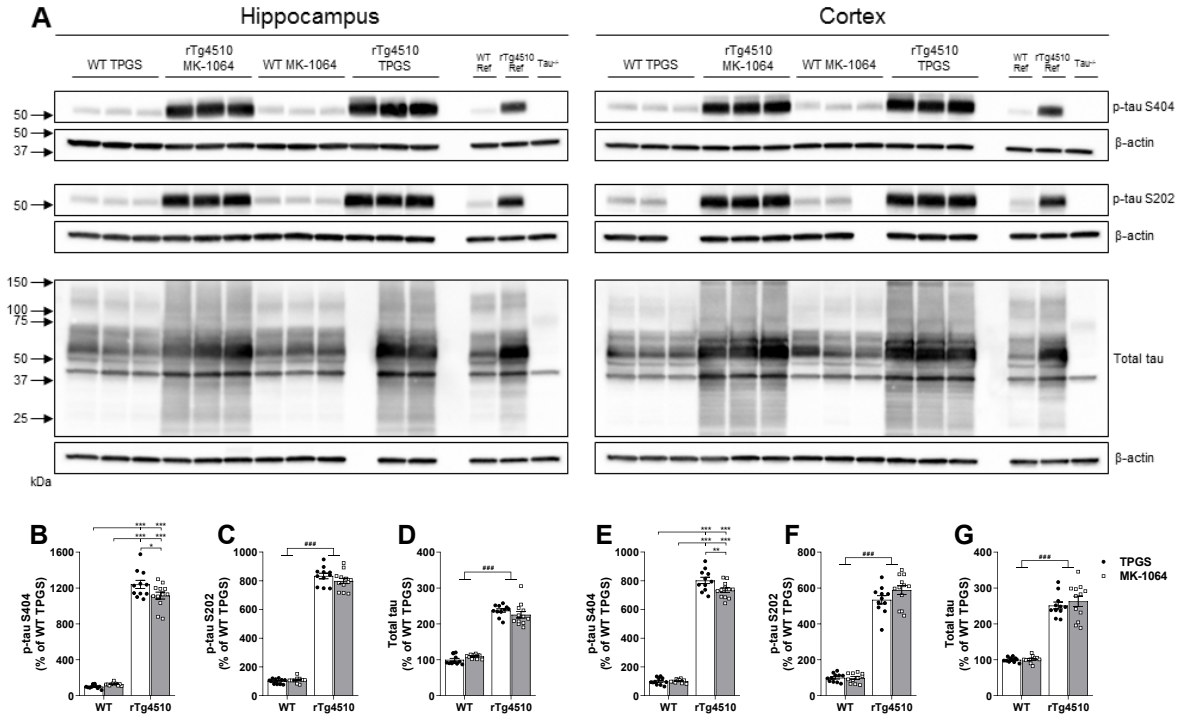

Figure 4.14. Tau and phosphorylated tau levels in rTg4510 mice following suvorexant treatment.

A, Representative western blots from the hippocampus (left) and cortex (right) probed with p-tau S404, p-tau S202 or total tau antibodies. β-actin was used as a housekeeping protein. ***B***, ***E***, Relative p-tau S404 levels in the hippocampus (***B***) and cortex (***E***). ***C***, ***F***, Relative p-tau S202 levels in the hippocampus (***C***) and cortex (***F***). ***D***, ***G***, Relative total tau levels in the hippocampus (***D***) and cortex (***G***). Densitometry signals were normalised to β-actin and then to the reference samples (WT Ref; rTg4510 Ref) which were loaded across every gel. Lysate from a tau knockout ($Tau^{-/-}$) mouse was used as a negative control. Data are means ± SEM and expressed as a percentage of the WT TPGS group. n = 11-12 per group. # denotes main effect of genotype. $^{###}P < 0.001$ vs. WT; $^{*}P < 0.05$, $^{**}P < 0.01$, $^{***}P < 0.001$, by two-way ANOVA with Tukey's multiple comparisons test.

4.5 Discussion

The present study examined the effects of promoting sleep, through chronic treatment with orexin receptor antagonists, in the rTg4510 mouse which overexpresses human mutant tau (Ramsden et al., 2005; Santacruz et al., 2005). The DORA suvorexant was used as it selectively increases REM sleep (Hoyer et al., 2013; Hoyer and Jacobson, 2013), in contrast to the 2-SORA MK-1064, which increases both NREM and REM sleep in a proportional manner (Roecker et al., 2014a; Gotter et al., 2016; Jacobson et al., 2017). Specific and marked sleep/wake deficits in rTg4510 mice previously reported (Chapter 3), which are characterised by a massive increase in time spent awake and decrease in NREM and REM sleep during the active phase, were replicated in the present study, testimony to the robustness of this phenotype. The present data show that suvorexant dosed during the late inactive phase increased REM sleep in rTg4510 mice but did not restore cognitive ability or alter tau/p-tau levels in the brain. By contrast, MK-1064 dosed in the early dark phase, markedly increased both NREM and REM sleep and attenuated wake time in male rTg4510 mice. Male rTg4510 mice also exhibited a partial improvement in hippocampal-dependent spatial recall which importantly, correlated with the amount of MK-1064-promoted sleep. Surprisingly, MK-1064 was largely devoid of effects on sleep/wake states in female rTg4510 mice, despite producing robust effects in female WT mice, nor did it correct cognitive deficits in female rTg4510 mice.

In Experiment 1, the aim was to target the phenotypic REM sleep deficits previously observed during the inactive phase in rTg4510 mice (Chapter 3). Suvorexant predominantly promoted REM sleep in both WT and rTg4510 mice, by increasing REM bout numbers without affecting average bout duration. Subtle increases in delta power during NREM sleep and theta power during REM sleep were also observed, predominantly in male rTg4510 mice. However, increased REM sleep following suvorexant treatment did not translate to improved cognitive ability, as suvorexant-treated rTg4510 mice exhibited similarly impaired hippocampal-dependent spatial recall compared with their MC-treated controls. It is important to note that spatial recall was unaffected in suvorexant-treated WT mice, further supporting the concept that orexin receptor antagonists promote sleep without impairing normal functioning and/or memory consolidation (Dietrich and Jenck, 2010; Morairty et al., 2014; Tannenbaum et al., 2016).

Suvorexant treatment did not alter tau or p-tau levels in the brains of rTg4510 mice, which was perhaps not surprising given the lack of effect on Barnes maze cognitive performance. It has previously been demonstrated that an approximate 50% reduction in tau levels following Dox treatment in rTg4510 mice was associated with complete rescue of

cognitive deficits and a restoration of REM sleep in the late inactive phase (Chapter 3). Data from Experiment 1 thus indicated that REM sleep was not associated with either spatial recall or tau levels. The release and clearance of Aβ and/or tau is proposed to be regulated by sleep/wakefulness (Kang et al., 2009; Roh et al., 2012; Holth et al., 2019) and therefore the amount or type of sleep promoted in the present study by suvorexant was probably insufficient to aid in the clearance of any considerable amount of tau. With regard to amount, REM sleep represents a minor proportion of overall sleep/wake states and during the inactive phase the range of response available may have been insufficient in mice that were already sleeping. With regard to the type of sleep, Xie et al. (2013) proposed that sleep, whether natural or pharmacologically enhanced with anaesthetics (which typically abolish REM sleep in rodents (Pal et al., 2011; Pick et al., 2011; Scharf and Kelz, 2013)) was important for glymphatic clearance. The present data may therefore support the premise that NREM sleep is more important for the clearance of p-tau than REM, given the lack of effect of enhancing REM sleep on tau levels following chronic suvorexant treatment. Any improvement in REM sleep-enhanced consolidation of spatial memory (Boyce et al., 2016) that suvorexant may have afforded was evidently insufficient to overcome the substantial tau-mediated cognitive burden in rTg4510 mice.

In Experiment 1, during the active phase, a prominent hyperarousal phenotype which was particularly exacerbated in female rTg4510 mice was observed. Therefore, Experiment 2 directly targeted this phenotype using MK-1064 to replace the excessive wakefulness with a proportional increase of both NREM and REM sleep, a feature accessible with OX_2R antagonists but not DORAs (Dugovic et al., 2009; Dugovic et al., 2014; Gotter et al., 2016; Jacobson et al., 2017). Accordingly, MK-1064 promoted both NREM and REM sleep and decreased wake time during the active phase, particularly during the first 6 hours post-administration, but only in male and not female rTg4510 mice. In male rTg4510 mice, MK-1064 restored time spent in all three vigilance states to WT levels, whereas in female rTg4510 mice no changes were observed. MK-1064 promoted sleep in male rTg4510 mice by increasing both NREM/REM bout numbers and average bout durations. Neither bout numbers nor bout durations were influenced by MK-1064 in female rTg4510 mice. Female WT mice responded robustly to MK-1064 treatment, indicating the ineffectiveness in rTg4510 mice is likely tau mediated/dependent. Nevertheless, the exact mechanisms behind these striking sex differences in response to MK-1064 are currently unknown. Much of the preclinical literature with orexin receptor antagonists have used only male rodents (Brisbare-Roch et al., 2007; Mang et al., 2012; Betschart et al., 2013; Hoyer et al., 2013; Dugovic et al., 2014; Roecker et al., 2014a;

Gotter et al., 2016) and sex differences in clinical settings have not been reported thus far, further supporting the concept that overexpression of mutant tau is contributing to this lack of response.

Sex differences in the hyperarousal phenotype of rTg4510 mice have been observed, which may be attributable to the sex differences in pathology onset previously reported, which occurs earlier in female than male rTg4510 mice (Yue et al., 2011). This may provide a possible explanation for the lack of response to MK-1064 in female rTg4510 mice. This may not be the case in male rTg4510 mice, given their comparatively lower hyperarousal impulse. However, female rTg4510 mice did respond very acutely to MK-1064 indicating their orexin system functioning is somewhat intact, however, after 1-2 hours the hyperarousal drive appears to have overridden any sleep pressure imposed by the drug. The observation that female rTg4510 mice responded equally as well as male rTg4510 mice to suvorexant suggests that timing of dosing may also be an important factor in the lack of response to MK-1064. Given the hyperarousal phenotype of rTg4510 mice is only present during the active phase there would be no hyperarousal drive to counter the effects of suvorexant when administered during the late inactive phase.

Another contributing factor to the differential responses of male and female rTg4510 mice to MK-1064 could be related to potential differences in orexin system function between male and female rTg4510 mice, for example, at the orexin peptide or receptor expression level. Suvorexant is a DORA which antagonises both OX_1R and OX_2R and evidence suggests that the enhanced promotion of REM sleep over NREM sleep by DORAs is predominantly driven by the blockade of OX_1R in the presence of OX_2R antagonism (Smith et al., 2003; Mieda et al., 2011; Morairty et al., 2012; Dugovic et al., 2014; Schwartz et al., 2016), especially given the almost exclusive expression of OX_1R in the REM-suppressing locus coeruleus (LC). MK-1064 however, is an OX_2R selective SORA. The lack of effect of MK-1064, but not suvorexant, suggests a potential enhanced dysregulation in OX_2R but not OX_1R function in female compared with male rTg4510 mice. Further work is required to determine the exact mechanisms involved.

Male, in contrast to female rTg4510 mice, exhibited improved cognitive performance in the Barnes maze following MK-1064 treatment, which correlated with the amount of MK-1064-promoted sleep. This is the first study to demonstrate attenuated cognitive impairment in a tauopathy mouse model, using sleep as a therapeutic approach. Orexin receptor antagonists were used to promote sleep with specific types of sleep architecture to investigate this premise. However, it is not clear whether effects observed were due to orexin receptor antagonists

themselves or effects on sleep, *per se*. It would therefore be of interest to test other hypnotic principles to examine this. However, the adverse effects on memory of several non-orexin receptor antagonist hypnotics suggests that the pharmacological modality used to enhance sleep is important. Zolpidem, for example, promotes substantial increases in NREM sleep but also causes memory impairments (Mattila et al., 1998; Mintzer and Griffiths, 1999; Verster et al., 2002; Otmani et al., 2008; Hall-Porter et al., 2014), confounding any potential sleep-induced cognitive benefit. This feature of non-benzodiazepine $GABA_A$ receptor modulators makes them inappropriate therapeutic candidates in neurodegenerative disorders where cognitive deficits are prevalent. In preclinical work, Morairty et al. (2014) demonstrated that zolpidem promoted NREM sleep to a greater extent than the DORA almorexant in rats. Cognitive performance in the Morris water maze was impaired by zolpidem, but not by almorexant (Morairty et al., 2014). A decline in Barnes maze performance was not observed in MK-1064-treated WT mice in the present study, which further supports the concept that orexin receptor antagonists promote sleep without negatively affecting memory. The lack of improvement in WT mice following MK-1064 may reflect ceiling effects, whereby WT mice of this background strain are already performing at their maximum cognitive faculty.

Given that the aim of the Barnes maze is for the mouse to locate the target hole in order to escape the aversive, brightly lit, windy open platform the relationship between cognitive behaviour, motivation to complete the task, and/or anxiety/fear should be considered. Across experiments in Chapter 3 and 4, it was observed that some rTg4510 mice failed to engage in the Barnes maze acquisition or probe trials and thus remained in the centre of the maze for the duration of the trial time limit. This behaviour may be attributable to a lack of motivation to complete the task, or alternatively, to an anxiety-like response to the Barnes maze environment. Anxiety and fear-like responses have previously been examined in a battery of behavioural tests in the rTg4510 mouse (Cook et al., 2014). Interestingly, by 6 months of age, approximately the same age as that investigated in the present research, rTg4510 mice displayed a hyper-exploratory phenotype, with greater distance travelled in the open field, more time spent in the open arms (and higher ratio of open arm exploration time/duration) in the elevated plus maze and more time spent in the light chamber in the light/dark exploration task (Cook et al., 2014). These data suggest an anxiolytic phenotype of rTg4510 mice. However, it was also noted that rTg4510 mice had an increased tendency to freeze once out in the open arms or light compartment (Cook et al., 2014), which aligns with the apparent freezing or lack of engagement behaviour observed in the present experiments. These data could suggest that

the lack of engagement in the Barnes maze task may be mediated by innate anxiety/fear, although the potential role of decreased motivation cannot be ruled out either.

The orexin system has also been implicated in anxiety and panic behaviour, with a proposed involvement of OX_1R (Gotter et al., 2012; Li et al., 2014; Chen et al., 2015). This is currently being evaluated in clinical studies with the OX_1R antagonist JNJ-61393215 (Salvadore et al., 2020). Johnson et al. (2015) assessed CO_2-induced anxiety-like behaviours in rats and observed that a DORA or 1-SORA, but not a 2-SORA, attenuated anxiety-like behaviour. Additionally, administration of a 1-SORA prevented nicotine-induced anxiogenic-like effects in C57BL/6 mice (Plaza-Zabala et al., 2010). It would be of interest to ascertain whether the reduced expression of OX_1R in the LC determined in Chapter 2 of this thesis aligns with the 1-SORA anxiolytic effects in these studies and the aforementioned interpretation of anxiolysis as a cause of hyper-exploratory activity in rTg4510 mice. Nevertheless, results may suggest that the OX_2R selective MK-1064 would likely not play a role in modulating any potential innate anxiety of the rTg4510 mouse in the present experiments (even the DORA suvorexant did not affect freezing or lack of engagement behaviour), and support the claim that improved performance in the final probe trial was indeed driven by enhanced cognition, rather than an alleviation of anxiety. Future work assessing rTg4510 behaviour in tasks assessing innate anxiety (see Jacobson et al., 2007), contextually conditioned fear and cognitive tasks (in addition to the Barnes maze), following dosing of various orexin receptor antagonists would be warranted to further assess anxiety versus cognitive behaviour in these mice, and the potential effects of orexin receptor antagonism.

Tau pathology was largely unaffected in rTg4510 mice following MK-1064 treatment, except for a subtle reduction in p-tau S404 levels in the hippocampus and cortex. rTg4510 mice express high levels of p-tau (Ramsden et al., 2005; Santacruz et al., 2005; Song et al., 2015) and thus it is possible that any clearance of tau afforded by the improved sleep may not have been detected by western blot for the soluble tau species measured here. Kang et al. (2009) showed that chronic treatment with the DORA almorexant for eight weeks attenuated Aβ burden in the brains of APP/PS1 mice. It was subsequently confirmed that the effects orexin receptor antagonism has on sleep, rather than orexin signalling itself, influenced the plaque load of Aβ (Roh et al., 2012; Roh et al., 2014). The decrease in wake time observed in Kang et al. (2009) following almorexant treatment was comparable to the decrease in wake time observed following MK-1064 treatment in the present study. Nevertheless, the different strains (APP/PS1 vs. rTg4510), proteins investigated (Aβ vs. tau) and methods used (immunohistochemistry (IHC) vs. western blot) make direct comparisons about the influence

of sleep on pathology challenging. IHC studies for tau in rTg4510 mice following sleep restoration are an important next step to further examine the effects of sleep on tau pathology. In addition, cognitive performance was also not assessed by Kang and colleagues (Kang et al., 2009), so whether reduced Aβ burden translated to a cognitive benefit is unknown, although, Aβ burden and cognitive decline in AD patients are not well correlated (Nelson et al., 2012).

Interestingly, treatment with the antiepileptic drug levetiracetam in an AD mouse model expressing human APP (hAPPJ20) was able to reduce abnormal spike activity, reverse behavioural abnormalities, improve memory/learning and reverse synaptic deficits in the hippocampus, however, it had no effect on the levels of hAPP, Aβ or Aβ deposition (Sanchez et al., 2012). Reducing hyperactivity with levetiracetam in humans with amnestic mild cognitive impairment (aMCI) also improved cognition (Bakker et al., 2012). These studies suggest that levetiracetam's influence on network activity restores normal hippocampal functioning leading to a recovery of cognitive functions, irrespective of its effects on protein pathology (Sanchez et al., 2012). In the current study, MK-1064 was effective at reducing wakefulness and increasing sleep. It remains possible that attenuating hyperarousal may be having a similarly positive influence on hippocampal/cognitive function, and irrespective of tau pathology. In addition, MK-1064 treatment increased slow delta (1-2.5 Hz) power during NREM sleep in male, but not female rTg4510 mice. In humans, lower frequency slow waves have been associated with increased memory consolidation (Marshall et al., 2006; Diekelmann and Born, 2010; Chauvette et al., 2012). Furthermore, it was demonstrated that transcranial stimulation of slow oscillations (1.33-1.5 Hz) enhanced memory consolidation in rats (Binder et al., 2014). Therefore, heightened NREM slow waves promoted by MK-1064 may be contributing to improved cognitive performance in the current study, irrespective of the effects on tau pathology. Nevertheless, it is also plausible that increased sleep and attenuated hyperarousal may have had effects on other tau species not investigated here.

Overall, however, the fact that MK-1064 was able to improve cognitive ability in a model of tauopathy as aggressive as the rTg4510 mouse is promising. Though, the recently discovered genetic limitations of the rTg4510 mouse model (Gamache et al., 2019) must also be taken into consideration here. As highlighted, potential therapies could improve tauopathy-like phenotypes (e.g. hyperarousal and cognitive deficits) by incidentally correcting effects resulting from non-targeted gene KO, without modifying the intended target (Gamache et al., 2019). Studies using sleep as a therapeutic approach in the similar PS19 mouse, which does not exhibit non-targeted gene KO (Goodwin et al., 2019), are warranted. These data, however,

provide an encouraging proof of principle for the therapeutic benefit of sleep, which will hopefully be taken forward into more advanced preclinical studies.

The aim of the current study was to use orexin receptor antagonists to correct sleep/wake deficits in the rTg4510 mouse, and to assess their downstream effects on cognition and tau pathology. The DORA suvorexant promoted REM sleep in both WT and rTg4510 mice when administered during the inactive phase, but did not correct their hyperarousal phenotype, nor did it translate into improved cognition or reduced tau/p-tau levels. By contrast, the 2-SORA MK-1064 increased both NREM and REM sleep and attenuated the hyperarousal phenotype of male, but not female rTg4510 mice. These divergent responses may be attributable to sex differences in the hyperarousal drive of rTg4510 mice and/or potential alterations in their orexin system function. Male rTg4510 mice exhibited a partial restoration of hippocampal-dependent spatial recall which importantly, correlated with the amount of MK-1064-promoted sleep. In conclusion, these findings highlight the therapeutic potential of sleep at restoring cognitive deficits in tauopathy models and further emphasises the emerging bidirectional relationship between sleep and neurodegenerative disease.

Chapter 5

Differential Sleep/wake Response and Sex Effects Following Acute Suvorexant, MK-1064 and Zolpidem Administration in the rTg4510 Mouse Model of Tauopathy

5.1 Abstract

Tau transgenic mouse models of tauopathy display prominent sleep/wake disturbances which manifest primarily as a hyperarousal phenotype during the active phase. These findings support the concept that tau pathology contributes to sleep/wake changes, however, no study has yet investigated the responses of tauopathy mouse models to sleep-promoting compounds. Such information has implications for the use of hypnotics as potential therapeutic tools in tauopathy-related disorders. The present study examined polysomnographic recordings in 6-6.5-month-old male and female rTg4510 mice following acute administration of either 50 mg/kg suvorexant, 30 mg/kg MK-1064 or 10 mg/kg zolpidem, administered at the commencement of the active phase. Suvorexant, a dual orexin receptor antagonist, similarly and exclusively promoted REM sleep in male and female rTg4510 mice, without affecting wake or NREM sleep. On the other hand, MK-1064, a selective orexin receptor 2 antagonist, effectively attenuated the hyperarousal phenotype of male rTg4510 mice by decreasing wake and increasing NREM sleep, whereas female rTg4510 mice exhibited a blunted response to MK-1064 compared with male rTg4510 mice. Zolpidem, a $GABA_A$ receptor positive allosteric modulator, decreased wake and increased NREM sleep equally in both male and female rTg4510 mice. Of the three compounds, MK-1064 appeared to promote the most physiologically normal sleep with regard to NREM and REM sleep architecture. Collectively, these findings indicate that hyperphosphorylated tau accumulation does not significantly alter the ability of the rTg4510 mouse model of tauopathy to respond to sleep-promoting compounds. However, the noted sex differences observed in the sleep/wake response of rTg4510 mice to MK-1064, but not suvorexant or zolpidem, raises questions about therapeutic implications for the use of OX_2R selective antagonists in human neurodegenerative disorders.

5.2 Introduction

The bidirectional relationship between sleep and neurological disease pathology (Ju et al., 2014; Lim et al., 2014; Wang and Holtzman, 2020) is being recognised, particularly for neurodegenerative disorders such as Alzheimer's disease (AD) and tau-variant frontotemporal dementia (FTD-tau), driven by amyloid-β (Aβ) and/or tau pathologies. Much of the preclinical research conducted thus far has focused on the effects of Aβ on sleep/wakefulness (Cirrito et al., 2005; Kang et al., 2009; Bero et al., 2011; Roh et al., 2012), although recently, attention has also turned to the involvement of tau (Chapter 3 and 4; Koss et al., 2016; Holth et al., 2017b; Zhu et al., 2018). Periods of extended wakefulness, or sleep deprivation, regulate the extracellular release of both Aβ (Cirrito et al., 2005; Cirrito et al., 2008; Bero et al., 2011; Tabuchi et al., 2015) and tau (Pooler et al., 2013; Yamada et al., 2014; Wu et al., 2016; Wang et al., 2017a). Conversely, it has been demonstrated in rodent models that the clearance of toxic metabolites such as Aβ and/or tau is enhanced during sleep (Xie et al., 2013). Combined with the proposed role that sleep plays in the consolidation of memory and learning (Diekelmann and Born, 2010), sleep therefore presents as a potentially viable therapeutic target in neurodegenerative models and/or disorders.

Studies investigating the bidirectional relationship between tauopathy mouse models and sleep are currently limited. The sleep/wake phenotype of the rTg4510 transgenic mouse model of tauopathy, which overexpresses human tau containing the P301L *MAPT* mutation (associated with FTD-tau in humans), was recently characterised (Chapter 3). rTg4510 mice exhibit a disrupted sleep/wake profile which manifests primarily as a hyperarousal phenotype particularly prominent during the active phase (Chapter 3). The sleep/wake phenotype of rTg4510 mice phenocopies that of the tau transgenic PS19 mouse, which harbors the similar P301S *MAPT* mutation (Holth et al., 2017b), albeit controlled by different promotors and with different transgene insertion points (Yoshiyama et al., 2007; Goodwin et al., 2019). Together, these studies indicate that tau pathology alone is sufficient to drive sleep/wake changes and that these changes manifest themselves in a similar way across tauopathy models (Chapter 3; Holth et al., 2017b). Despite this, no study has yet investigated whether mutant tau expression also influences the ability of these mice to respond to hypnotic agents, including more recent treatment modalities, such as orexin receptor antagonists. Such information may warrant further investigations into the use of sleep-promoting hypnotics as potential therapeutic tools in tauopathy-related disorders.

The aim of the current study was therefore to assess the sleep/wake response of rTg4510 mice following acute administration of three different sleep-promoting compounds: the dual

orexin receptor antagonist (DORA) suvorexant (Cox et al., 2010), the selective orexin receptor 2 (OX_2R) antagonist (2-SORA) MK-1064 (Roecker et al., 2014a) and the $GABA_A$ receptor positive allosteric modulator zolpidem (Arbilla et al., 1985). Two of these compounds (suvorexant and zolpidem) are marketed for the treatment of insomnia, whereas various 2-SORAs are in late stage clinical development (Hoyer et al., 2019). Zolpidem was selected as a standard and well-established hypnotic and a member of the "Z-drugs" family of compounds. These compounds increase total sleep time primarily by promoting NREM sleep, but suppress REM sleep in rodents (Hoyer et al., 2019). Orexin receptor antagonists are a relatively new addition to the hypnotic field. DORAs such as suvorexant and almorexant robustly induce sleep in rodents (Mang et al., 2012; Betschart et al., 2013; Hoyer and Jacobson, 2013) and patients (reviewed in Jacobson et al., 2014), primarily by increasing REM sleep without affecting NREM sleep to any great extent. Conversely, 2-SORAs increase sleep by modulating both NREM and REM sleep in a proportional, physiological-like manner (Betschart et al., 2013; Hoyer and Jacobson, 2013; Jacobson et al., 2017). A single dose of suvorexant, MK-1064 or zolpidem was given to rTg4510 mice and wildtype (WT) littermates at the commencement of the active phase, when the rTg4510 hyperarousal phenotype is prominent, and the subsequent sleep/wake profile relative to within-subject vehicle-treated controls was assessed.

5.3 Materials and methods

Animals

Male and female rTg4510 transgenic mice and WT littermate controls were used (Ramsden et al., 2005; Santacruz et al., 2005). rTg4510 mice were bred in house, as previously described (Ramsden et al., 2005; Santacruz et al., 2005). In brief, FBV/N background mice expressing human tau containing the P301L *MAPT* mutation (associated with FTD-tau in humans) downstream of a tetracycline operon-responsive element (TRE), were crossed with 129SVeV mice expressing a tetracycline-controlled transactivator (tTA) under control of the Ca^{2+}-calmodulin-dependent protein kinase II (CaMKII) promotor. In this mouse, constitutive expression of the tau transgene is specifically restricted to forebrain structures due to the CaMKII promotor. All mice were genotyped using a standardised tail DNA polymerase chain reaction (PCR) assay (Transnetyx Inc., Cordova, TN, USA). Mice used in this study were between 6-6.5 months of age during experimental sleep recordings. This age was selected to align with the age of rTg4510 mice during sleep recordings from previous reports (Chapter 3

and 4). All mice were single- or group-housed in standard, transparent open-top cages (29.5 x 16 x 13 cm) with sawdust and tissue paper nesting material. Standard rodent food and water were available *ad libitum.* All experimentation was performed in accordance with the Prevention of Cruelty to Animals Act (2004), under the guidelines of the National Health and Medical Research Council Code of Practice for the Care and Use of Animals for Experimental Purposes in Australia (2013) and approved by The Florey Animal Ethics Committee (AEC number: 16-022). All efforts were made to minimise animal suffering.

Compounds and drug preparation

The DORA suvorexant (Suvo; AdooQ Bioscience), 2-SORA MK-1064 (Merck and Co., Inc) or the $GABA_A$ positive allosteric modulator zolpidem (Zolp; Sapphire Bioscience) were used. Drugs were prepared fresh as suspensions on the day of administration. The vehicle for suvorexant and zolpidem was 0.5% methylcellulose (MC; Sigma-Aldrich) in water. The vehicle for MK-1064 was 20% D-α-tocopherol polyethylene glycol 1000 succinate (TPGS; Sigma-Aldrich) in water. All drugs were administered by oral gavage in a volume of 10 ml/kg.

Experimental study design

All mice were initially housed on a 12 h light/dark cycle (lights on at 0700h) before being moved into a new housing area with their respective experimental light cycle (lights on at 0300h), ten days before EEG/EMG surgery. The experimental protocol involved three consecutive 23 h polysomnographic recordings commencing at the start of the active phase (Circadian time (CT)12). On Day 1, mice were administered water (10 ml/kg, *per os*) to habituate to oral gavage. On Day 2, they received vehicle (MC or TPGS, 10 ml/kg, *per os*). On Day 3, 50 mg/kg suvorexant, 30 mg/kg MK-1064 or 10 mg/kg zolpidem were administered *per os*. Administration of compounds was performed within a time window of 5-15 min before the start of the recordings. Some mice received two or all three active compounds, with their own respective water and vehicle recordings, and a minimum one-week wash-out period between experiments.

Polysomnographic recordings and analysis

Surgery: Mice were anaesthetised with isoflurane in air (5% for induction, 2-3% for maintenance) and placed in a stereotaxic frame. Meloxicam (1-3 mg/kg, Ilium) and 500 µL of warm saline were administered subcutaneously. 50 µL of 1% lignocaine HCl (Pfizer) was administered near the incision site, then the skull was exposed and EEG/EMG preformed head mounts (Catalogue number: #8201-SS, Pinnacle Technology Inc.) were surgically implanted. EEG1 and EEG2 electrodes (screws inserted into the head mount) were positioned over the parietal and frontal lobe, respectively. Reference and ground electrodes were positioned at equivalent regions, with reference embedded in the parietal region and ground in the frontal, in addition to a non-penetrating anchor screw embedded into the skull over the motor cortex. Two EMG wires attached to the head mount were inserted into the neck musculature and sutured (7-0 Prolene, Ethicon) into place. Sutures were used to close the scalp around the head mount. Dental cement was positioned under and around the head mount using an 18G drawing-up needle and allowed to set. The mouse was removed from the stereotaxic frame and placed into a warm recovery box (30°C) until it was moving freely, then returned to its original cage.

Recordings: Mice were individually housed in transparent, cylindrical sleep recording chambers (29 cm diameter x 30 cm height) for a further week of recovery and acclimatisation. Head mounts were plugged into the pre-amplifier 24 h before recordings began. Sirenia Acquisition version 1.8.0 software (Pinnacle Technology Inc.) was used for EEG/EMG acquisition. Three channels were recorded: EEG1, EEG2 and EMG. The sampling rate was 200 Hz. 100 Hz EEG and EMG filters were applied. Recordings began at 1500h (CT12) and finished at 1400h (CT11). Following EEG/EMG recordings all mice were returned to their original cages.

Analysis: Sirenia recording files (.pvfs) were exported as European Data Format (.edf) and imported into the program Somnivore™ (Allocca et al., 2019) in 4 s epochs. Each recording was scored by first training the Somnivore machine learning algorithm with 101 epochs of wake, NREM and REM. The entire hypnogram was then populated using Somnivore's auto-score function. Contextual scoring rules included a minimum bout length setting of 8 s (two contiguous epochs) for both wake and NREM and 12 s (three contiguous epochs) for REM. A further 50 epochs of each state were then trained, and the auto-score function was run again. The entire recording was then manually checked and corrected. All sleep scoring was performed blinded to genotype and treatment.

Statistical analysis

Statistical analyses were performed using GraphPad Prism (version 8.0.0) or R (version 3.6.1)/RStudio (version 1.2.5001). Time spent in each vigilance state across the 23 h recording was analysed by a repeated measures linear mixed effects model in R, using the *lmer* function. Data for each compound were analysed within genotype and sex, versus the respective vehicle. Post hoc analyses were performed using the *emmeans* function, with Tukey's multiple comparisons test. REM as a percentage of total sleep, average bout numbers, bout durations and time spent in each vigilance state per phase were analysed by Student's paired t-test between compound and respective vehicle. For all analyses, $P < 0.05$ was considered to be statistically significant.

5.4 Results

Suvorexant similarly increased REM sleep in male and female WT and rTg4510 mice without affecting wake or NREM sleep

Sleep/wake architecture of rTg4510 and WT mice were significantly altered by suvorexant (Fig. 5.1A-C; Table 5.1), whereby REM sleep was enhanced in the absence of effects on either wake or NREM. No effect of suvorexant treatment was observed in either rTg4510 or WT mice for wake (Fig. 5.1A) or NREM (Fig. 5.1B) vigilance states. Male and female WT mice spent significantly more time in REM sleep following suvorexant administration for each of the first two and four hours, respectively, compared with the corresponding vehicle treatment (Fig. 5.1C). Similar effects were observed with male rTg4510 mice, which spent significantly more time in REM sleep for each of the first two hours post suvorexant administration. Suvorexant-treated female rTg4510 mice, however, exhibited a substantial increase in REM sleep during the first hour of treatment, compared with their respective vehicle (Fig. 5.1C).

The average time spent in each vigilance state across the first half of the active phase (6 h post-suvorexant), full active phase, inactive phase and the entire recording were assessed. When administered at the beginning of the active phase, suvorexant did not significantly alter average time spent in the wake or NREM states in male or female WT or rTg4510 mice, across any of the periods analysed (Fig. 5.1D-K). During the first 6 hours following suvorexant administration, however, average REM time was significantly increased in WT (Male: $t_{(6)} = 6.077$, $P = 0.0009$; female: $t_{(10)} = 6.709$, $P < 0.0001$) and rTg4510 mice (Male: $t_{(6)} = 3.735$, $P = 0.0097$; female: $t_{(5)} = 3.249$, $P = 0.0227$) of either sex, compared with their respective vehicle

treatment (Fig. 5.1L). Across the entire active phase, REM sleep was increased in both male ($t_{(6)} = 2.595$, P = 0.041) and female rTg4510 mice ($t_{(5)} = 3.547$, P = 0.0164), but only in female WT mice ($t_{(10)} = 2.557$, P = 0.0285; Fig. 5.1M). During the inactive phase, male WT mice exhibited a slight rebound effect, whereby REM sleep was decreased compared with vehicle ($t_{(6)} = 3.718$, P = 0.0099; Fig. 5.1N). When assessing the entire 23 h recording, only female WT mice exhibited an overall increase in REM sleep ($t_{(10)} = 2.294$, P = 0.0447; Fig. 5.1O).

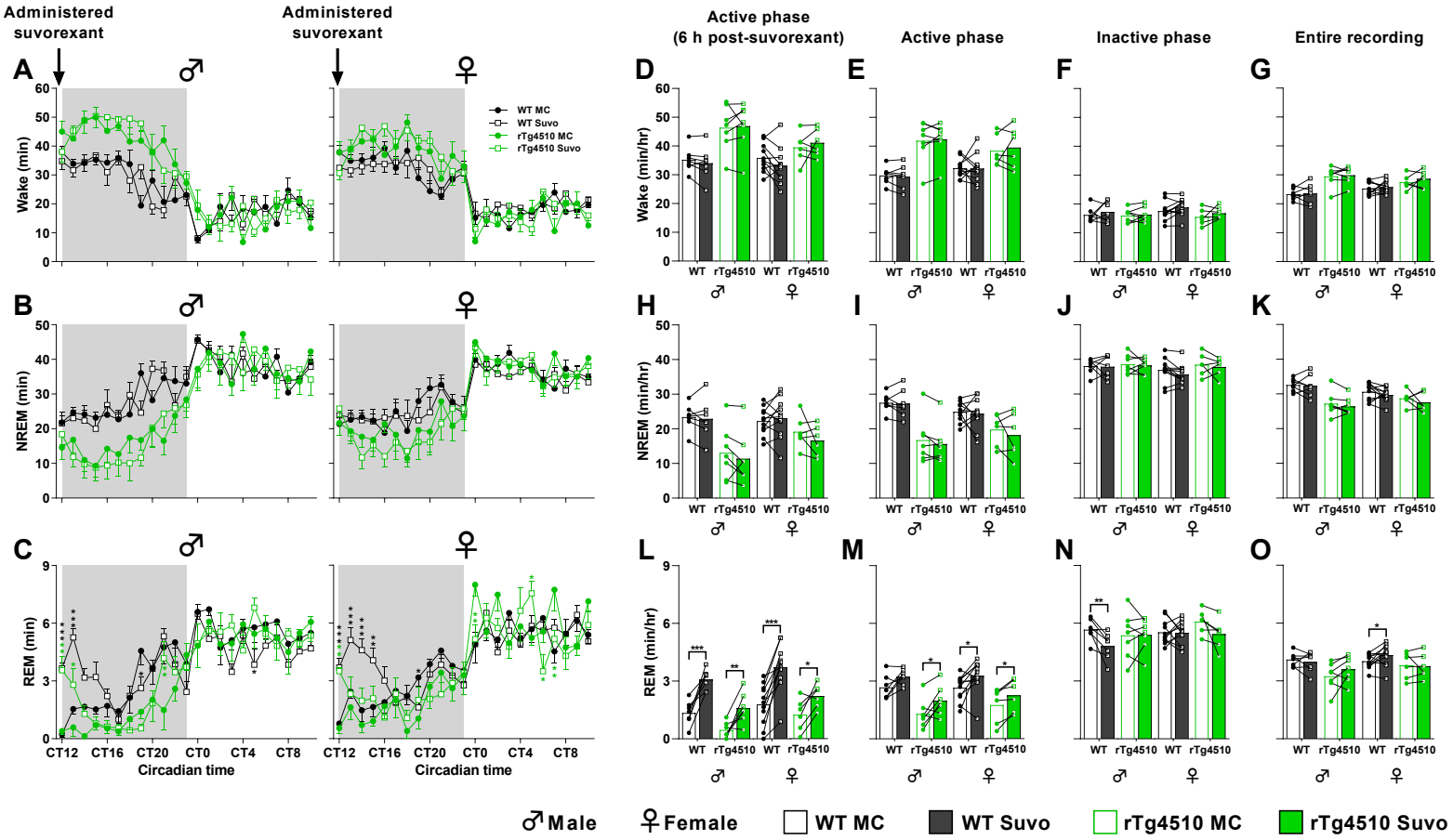

Figure 5.1. Promotion of REM sleep following acute suvorexant administration in rTg4510 mice.

A-C, Minutes spent in wake (***A***), NREM (***B***) and REM (***C***) vigilance states per hour across a 23 h recording in rTg4510 and WT mice administered 50 mg/kg suvorexant (Suvo) or methylcellulose (MC) vehicle. Dark shade represents the active phase. Data are means ± SEM. n = 6-11 per group, per sex. $^{*}P < 0.05$, $^{**}P < 0.01$, $^{***}P < 0.001$ vs. respective vehicle, by repeated measures linear mixed effects model with Tukey's multiple comparisons test. ***D-O***, Minutes spent in each vigilance state per hour averaged across (from left to right) the active phase (6 h post-suvorexant), full active phase (12 h), inactive phase and entire recording, for wake (***D-G***), NREM (***H-K***) and REM (***L-O***). n = 6-11 per group, per sex. $^{*}P < 0.05$, $^{**}P < 0.01$, $^{***}P < 0.001$ vs. vehicle, by Student's paired t-test.

Table 5.1. EEG recordings statistical analyses summary (suvorexant).

Time spent in each vigilance state across the 23 h recording were analysed by a repeated measures linear mixed effects model in R, using the *lmer* function, incorporating the factors of Treatment and Time (repeated factor). Indented Pr(>|t|) values indicate statistical significance.

Vigilance state time																
						Wake					NREM					REM
Group	Fixed effect	Estimate	Std. error	df	t-value	Pr(>|t|)	Estimate	Std. error	df	t-value	Pr(>|t|)	Estimate	Std. error	df	t-value	Pr(>|t|)
WT Male	Treatment	-1.4666	2.3537	312.000	-0.623	> 0.05	-0.2666	2.0548	312.000	-0.129	> 0.05	1.7317	0.4463	312.000	3.880	< 0.001
	Time	-1.0179	0.1214	312.000	-8.386	< 0.001	0.7756	0.1060	312.000	7.319	< 0.001	0.2423	0.0230	312.000	10.525	< 0.001
	Treatment: Time	0.1492	0.1717	312.000	0.869	> 0.05	0.0056	0.1499	312.000	0.037	> 0.05	-0.1547	0.0326	312.000	-4.752	< 0.001
WT Female	Treatment	-1.8361	2.0387	492.000	-0.901	> 0.05	0.3317	1.7927	492.000	0.185	> 0.05	1.5045	0.3658	492.000	4.113	< 0.001
	Time	-1.0700	0.1051	492.000	-10.178	< 0.001	0.8415	0.0925	492.000	9.101	< 0.001	0.2286	0.0189	492.000	12.115	< 0.001
	Treatment: Time	0.2001	0.1487	492.000	1.346	> 0.05	-0.1010	0.1308	492.000	-0.772	> 0.05	-0.0991	0.0267	492.000	-3.714	< 0.001
rTg4510 Male	Treatment	0.2343	2.9499	312.000	0.079	> 0.05	-1.4599	2.6107	312.000	-0.559	> 0.05	1.2250	0.4710	312.000	2.601	< 0.01
	Time	-1.8720	0.1521	312.000	-12.305	< 0.001	1.5635	0.1346	312.000	11.613	< 0.001	0.3084	0.0243	312.000	12.697	< 0.001
	Treatment: Time	0.0144	0.2151	312.000	0.067	> 0.05	0.0571	0.1904	312.000	0.300	> 0.05	-0.0715	0.0344	312.000	-2.082	< 0.05
rTg4510 Female	Treatment	0.9795	2.7956	267.000	0.350	> 0.05	-2.1596	2.4439	267.000	-0.884	> 0.05	1.1802	0.4993	267.000	2.364	< 0.05
	Time	-1.5165	0.1442	267.000	-10.518	< 0.001	1.2119	0.1260	267.000	9.616	< 0.001	0.3045	0.0258	267.000	11.825	< 0.001
	Treatment: Time	0.0192	0.2039	267.000	0.094	> 0.05	0.0832	0.1782	267.000	0.467	> 0.05	-0.1024	0.0364	267.000	-2.811	< 0.01

Suvorexant promoted REM sleep predominantly by increasing bout numbers in WT mice and bout duration in rTg4510 mice

Suvorexant administration increased wake bouts in female, but not male mice, compared with the respective vehicle treatment across both the first half (WT: $t_{(10)} = 4.684$, $P = 0.0009$; rTg4510: $t_{(5)} = 3.319$, $P = 0.021$; Fig. 5.2A) and full active phase (WT: $t_{(10)} = 2.982$, $P = 0.0138$; rTg4510: $t_{(5)} = 2.682$, $P = 0.0437$; Fig. 5.2B). Suvorexant similarly increased NREM bouts in female, but not male mice, compared with their respective vehicle treatment across the first half (WT: $t_{(10)} = 4.700$, $P = 0.0008$; rTg4510: $t_{(5)} = 3.354$, $P = 0.0202$; Fig. 5.2E) and entire active phase (WT: $t_{(10)} = 2.922$, $P = 0.0153$; rTg4510: $t_{(5)} = 2.730$, $P = 0.0413$; Fig. 5.2F). During the first 6 hours following suvorexant administration, REM bouts were significantly increased in WT mice (Male: $t_{(6)} = 3.526$, $P = 0.0124$; female: $t_{(10)} = 6.938$, $P < 0.0001$; Fig. 5.2I). The majority of male and female rTg4510 mice also exhibited an increase in REM bouts following suvorexant administration compared with vehicle during this period, however, this did not reach overall statistical significance (Fig. 5.2I). Similar to both wake and NREM bouts, only female mice exhibited increased REM bouts across the entire active phase (WT: $t_{(10)} = 3.696$, $P = 0.0041$; rTg4510: $t_{(5)} = 3.058$, $P = 0.0282$; Fig. 5.2J). During the inactive phase, male WT mice exhibited decreased REM bouts compared with vehicle ($t_{(6)} = 4.355$, $P = 0.0048$; Fig. 5.2K), aligning with the REM rebound observed (Fig. 5.1N). When assessing the 23 h recording as a whole, only female WT mice exhibited an overall increase in REM bouts ($t_{(10)} = 3.469$, $P = 0.006$; Fig. 5.2L).

Wake bout duration was largely unaffected by suvorexant treatment (Fig. 5.3A-D) except for a decreased duration in female WT mice across the active phase ($t_{(10)} = 2.591$, $P =$

0.0269; Fig. 5.3B) and entire recording ($t_{(10)}$ = 2.347, P = 0.0409; Fig. 5.3D). During the first half of the active phase, suvorexant decreased NREM bout duration in male ($t_{(6)}$ = 4.376, P = 0.047) and female rTg4510 mice ($t_{(5)}$ = 3.941, P = 0.0109), but only in female WT mice ($t_{(10)}$ = 2.792, P = 0.019; Fig. 5.3E). Interestingly, this effect persisted across the full active phase in only male rTg4510 mice ($t_{(6)}$ = 2.778, P = 0.0321; Fig. 5.3F). During the first 6 hours following suvorexant administration, REM bout duration was significantly increased in male ($t_{(6)}$ = 3.209, P = 0.0184) and female rTg4510 mice ($t_{(5)}$ = 3.850, P = 0.012; Fig. 5.3I). The majority of male and female WT mice also exhibited an increase in REM bout duration following suvorexant administration compared with vehicle during this period, however, this did not reach overall statistical significance (Fig. 5.3I). When assessing the 23 h recording as a whole, only female rTg4510 mice exhibited an overall increase in REM bout duration ($t_{(5)}$ = 3.032, P = 0.029; Fig. 5.3L).

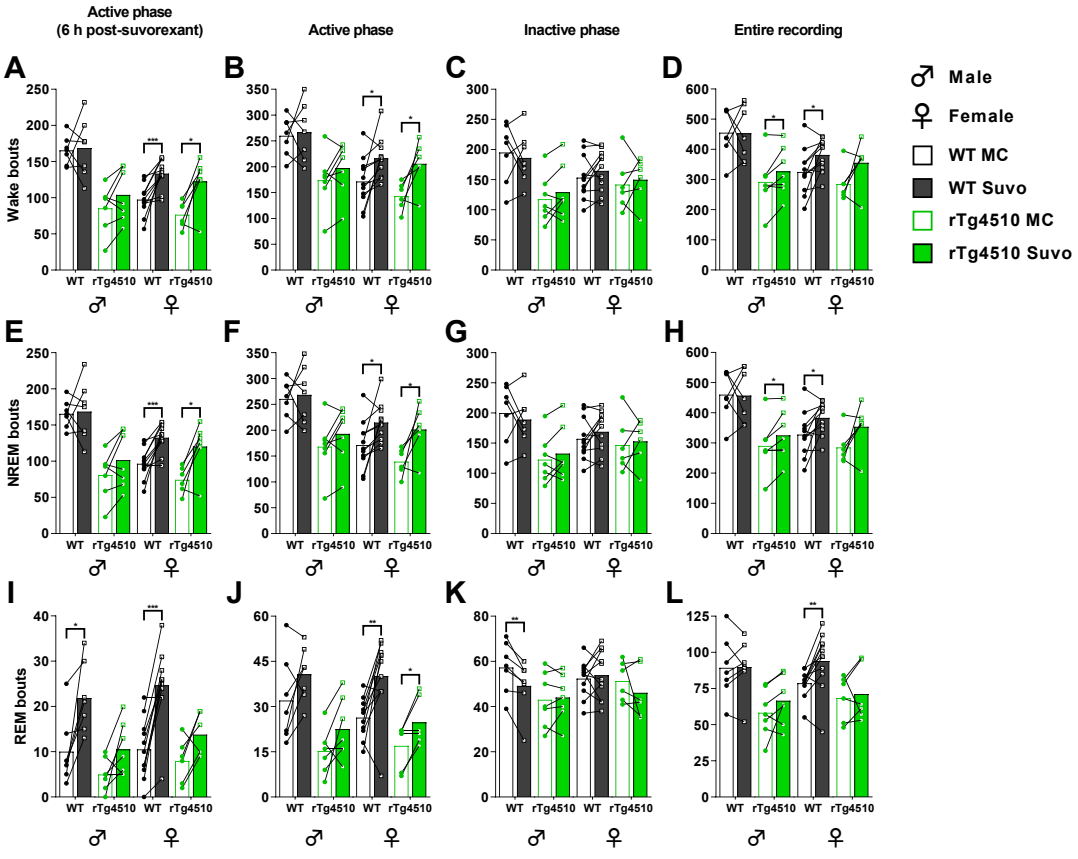

Figure 5.2. Effects of acute suvorexant administration on bout numbers in rTg4510 mice.

A-L, Total number of wake (***A-D***), NREM (***E-H***) and REM (***I-L***) bouts averaged across (from left to right) the active phase (6 h post-suvorexant), full active phase (12 h), inactive phase and entire recording in rTg4510 and WT mice administered 50 mg/kg suvorexant (Suvo) or methylcellulose (MC) vehicle. Data are means ± SEM. n = 6-11 per group, per sex. *P < 0.05 **P < 0.01, ***P < 0.001 vs. vehicle, by Student's paired t-test.

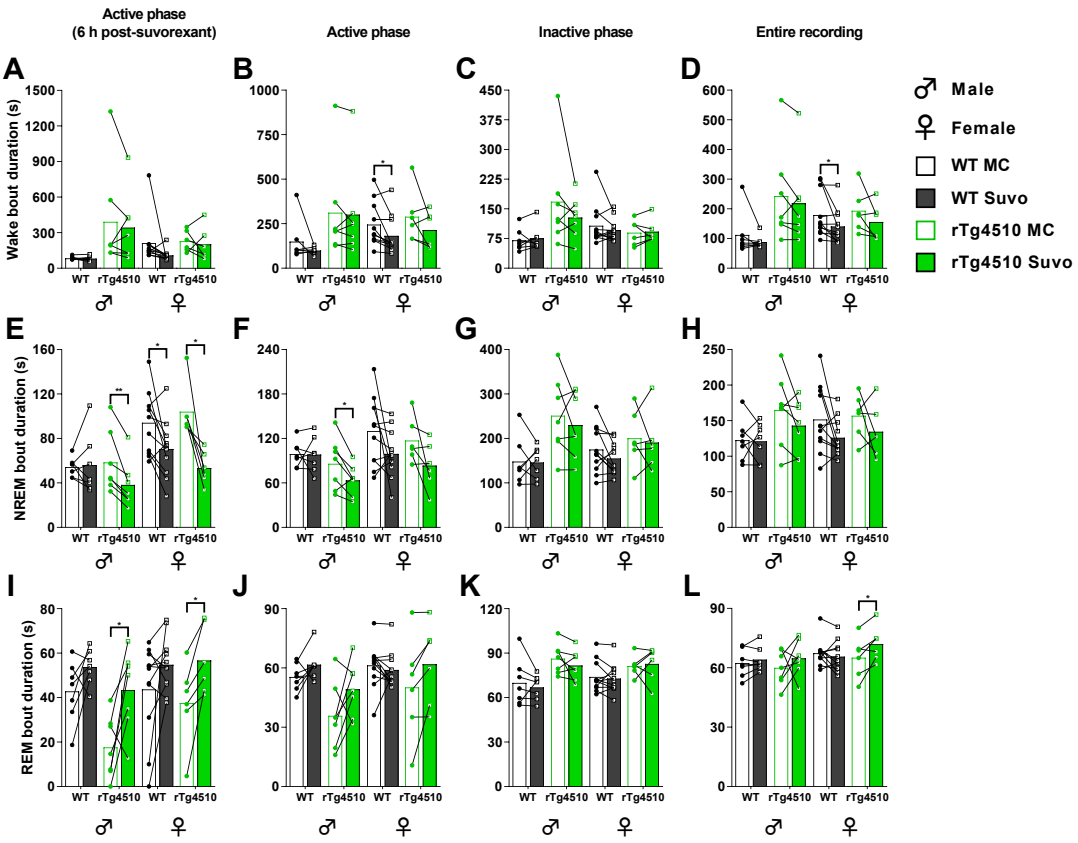

Figure 5.3. Effects of acute suvorexant administration on bout duration in rTg4510 mice.

A-L, Mean wake (***A-D***), NREM (***E-H***) and REM (***I-L***) bout durations averaged across (from left to right) the active phase (6 h post-suvorexant), full active phase (12 h), inactive phase and entire recording in rTg4510 and WT mice administered 50 mg/kg suvorexant (Suvo) or methylcellulose (MC) vehicle. Data are means ± SEM. n = 6-11 per group, per sex. $^{*}P < 0.05$ $^{**}P < 0.01$ vs. vehicle, by Student's paired t-test.

Female rTg4510 mice exhibited a blunted sleep/wake response to MK-1064 compared with male rTg4510 mice

Sleep/wake architecture of rTg4510 and WT mice were significantly altered by MK-1064 (Fig. 5.4A-C; Table 5.2), predominantly influencing both wake and NREM vigilance states. Male rTg4510 and WT mice spent significantly less time in the wake state following MK-1064 administration, across each of the first four and five hours, respectively, compared with their corresponding vehicle treatment (Fig. 5.4A). Female rTg4510 and WT mice, however, exhibited a decrease in wake time during only the first hour post MK-1064 administration, compared with the respective vehicle treatment (Fig. 5.4A). Male rTg4510 and WT mice correspondingly also spent significantly more time in NREM sleep following MK-1064 administration, across each of the first four and five hours, respectively, compared with their

corresponding vehicle (Fig. 5.4B). Female rTg4510 mice exhibited an increase in NREM sleep during the first hour post MK-1064 administration, with female WT mice exhibiting increased NREM sleep for each of the first two hours, compared with their respective vehicle (Fig. 5.4B). No significant changes in REM sleep were observed at any individual time point, compared with vehicle (Fig. 5.4C).

Examining the first 6 hours following MK-1064 administration, it was apparent that average wake time was significantly decreased in WT (Male: $t_{(7)} = 15.32$, $P < 0.0001$; female: $t_{(6)} = 4.140$, $P = 0.0061$) and rTg4510 mice (Male: $t_{(7)} = 7.560$, $P = 0.0001$; female: $t_{(6)} = 2.716$, $P = 0.0348$) of either sex, compared with their respective vehicle, with a larger effect size in male mice (Fig. 5.4D). This effect persisted across the full active phase in male mice of either genotype (WT: $t_{(7)} = 3.571$, $P = 0.0091$; rTg4510: $t_{(7)} = 3.389$, $P = 0.0116$), but not in female mice of either genotype (Fig. 5.4E). During the first 6 hours following MK-1064 administration, average NREM sleep time was significantly increased in WT mice (Male: $t_{(7)} = 12.54$, $P < 0.0001$; female: $t_{(6)} = 4.950$, $P = 0.0026$) and rTg4510 mice (Male: $t_{(7)} = 8.043$, $P < 0.0001$; Female: $t_{(6)} = 2.535$, $P = 0.0444$) of either sex, compared with their respective vehicle, again with a stronger effect in male mice (Fig. 5.4H). The increase in NREM sleep persisted across the full active phase in WT mice of either sex (Male: $t_{(7)} = 4.014$, $P = 0.0051$; Female: $t_{(6)} = 2.636$, $P = 0.0388$) and in male rTg4510 mice ($t_{(7)} = 3.518$, $P = 0.0097$) , but not in female rTg4510 mice (Fig. 5.4I). Female rTg4510 mice also displayed a rebound of NREM sleep during the inactive phase, exhibiting a decrease compared with vehicle ($t_{(6)} = 3.004$, $P = 0.0239$; Fig. 5.4J). During the first 6 hours following MK-1064 administration, average REM sleep was significantly increased in only male WT mice ($t_{(7)} = 9.399$, $P < 0.0001$; Fig. 5.4L).

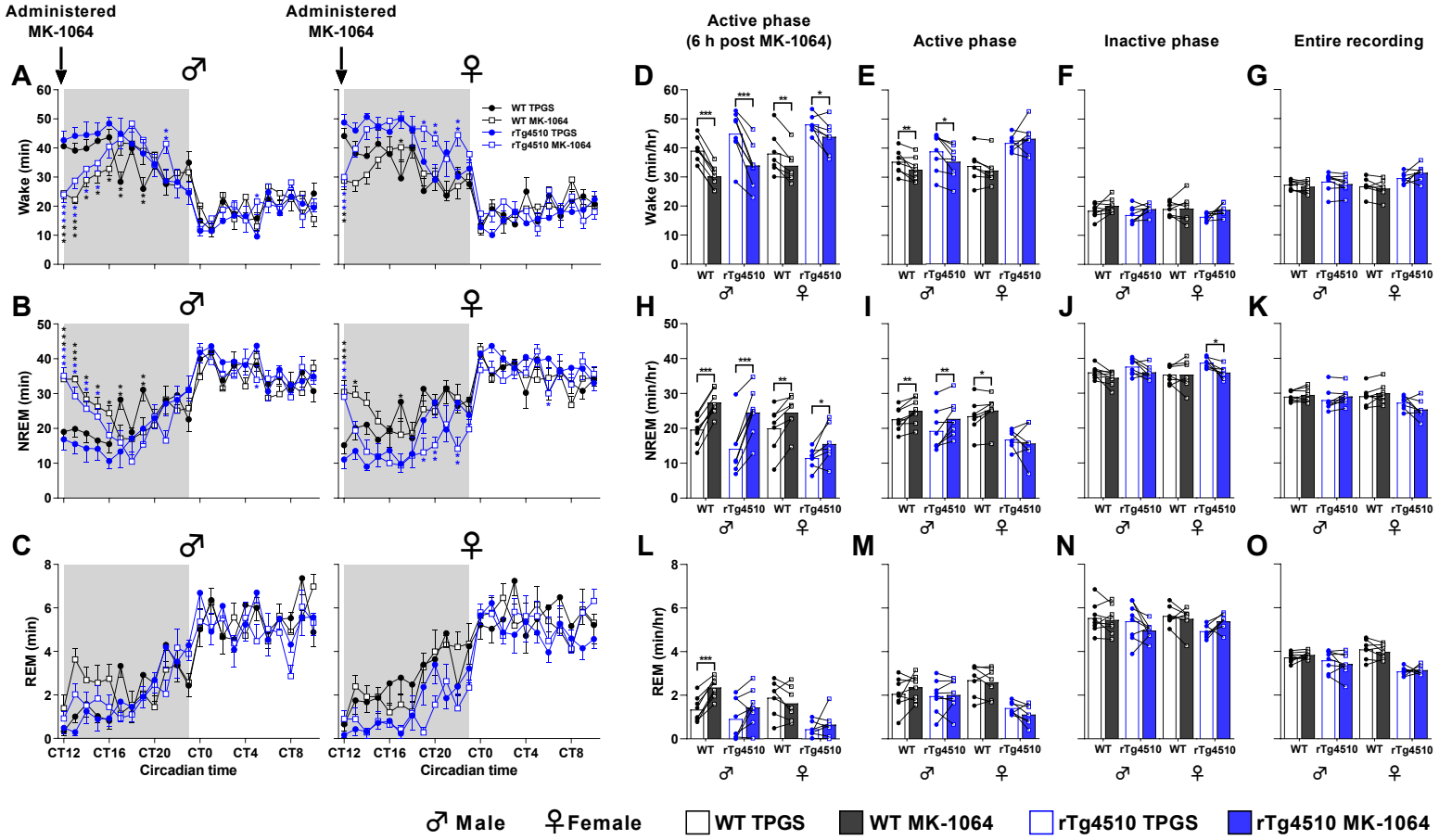

Figure 5.4. Blunted sleep/wake response following acute MK-1064 administration in female rTg4510 mice.

A-C, Minutes spent in wake (***A***), NREM (***B***) and REM (***C***) vigilance states per hour across a 23 h recording in rTg4510 and WT mice administered 40 mg/kg MK-1064 or TPGS vehicle. Dark shade represents the active phase. Data are means ± SEM. n = 7-8 per group, per sex. $^{*}P < 0.05$, $^{**}P < 0.01$, $^{***}P < 0.001$ vs. respective vehicle, by repeated measures linear mixed effects model with Tukey's multiple comparisons test. ***D-O***, Minutes spent in each vigilance state per hour averaged across (from left to right) the active phase (6 h post-MK-1064), full active phase (12 h), inactive phase and entire recording, for wake (***D-G***), NREM (***H-K***) and REM (***L-O***). n = 7-8 per group, per sex. $^{*}P < 0.05$, $^{**}P < 0.01$, $^{***}P < 0.001$ vs. vehicle, by Student's paired t-test.

Table 5.2. EEG recordings statistical analyses summary (MK-1064).

Time spent in each vigilance state across the 23 h recording were analysed by a repeated measures linear mixed effects model in R, using the *lmer* function, incorporating the factors of Treatment and Time (repeated factor). Indented Pr(>|t|) values indicate statistical significance.

Vigilance state time																
						Wake					NREM					REM
Group	Fixed effect	Estimate	Std. error	df	t-value	Pr(>|t|)	Estimate	Std. error	df	t-value	Pr(>|t|)	Estimate	Std. error	df	t-value	Pr(>|t|)
WT Male	Treatment	6.8341	2.3905	357.000	2.859	< 0.01	-6.0213	2.0694	357.000	-2.910	< 0.01	-0.8118	0.4234	364.000	-1.917	> 0.05
	Time	-0.6674	0.1233	357.000	-5.413	< 0.001	0.4553	0.1067	357.000	4.266	< 0.001	0.2121	0.0218	364.000	9.712	< 0.001
	Treatment: Time	-0.5172	0.1743	357.000	-2.966	< 0.01	0.4590	0.1509	357.000	3.041	< 0.01	0.0581	0.0309	364.000	1.882	> 0.05
WT Female	Treatment	4.3219	2.4989	312.000	1.729	> 0.05	-4.3442	2.1838	312.000	-1.989	< 0.05	2.1470	0.4485	312.000	0.048	> 0.05
	Time	-0.8065	0.1289	312.000	-6.258	< 0.001	0.5818	0.1126	312.000	5.166	< 0.001	2.2460	0.0231	312.000	9.711	< 0.001
	Treatment: Time	-0.2982	0.1823	312.000	-1.636	> 0.05	0.2904	0.1593	312.000	1.823	> 0.05	7.7897	0.0327	312.000	0.241	> 0.05
rTg4510 Male	Treatment	8.3701	2.5396	357.000	3.296	< 0.01	-7.9411	2.2489	357.000	-3.531	< 0.001	-0.4289	0.4072	357.000	-1.053	> 0.05
	Time	-0.9512	0.1310	357.000	-7.262	< 0.001	0.7336	0.1160	357.000	6.325	< 0.001	0.2176	0.0210	357.000	10.360	< 0.001
	Treatment: Time	-0.6248	0.1852	357.000	-3.374	< 0.001	0.5745	0.1640	357.000	3.503	< 0.001	0.0503	0.0297	357.000	1.694	> 0.05
rTg4510 Female	Treatment	1.0646	2.6201	312.000	0.406	> 0.05	-1.5170	2.3097	312.000	-0.657	> 0.05	0.4526	0.4155	318.000	1.089	> 0.05
	Time	-1.5802	0.1351	312.000	-11.695	< 0.001	1.2826	0.1191	312.000	10.768	< 0.001	0.2975	0.0214	318.000	13.883	< 0.001
	Treatment: Time	-0.2460	0.1911	312.000	-1.287	> 0.05	0.2885	0.1685	312.000	1.712	> 0.05	-0.0426	0.0303	318.000	-1.404	> 0.05

MK-1064 increased NREM bout numbers and bout durations in male but not female rTg4510 mice

Analysis of summed data during the first 6 hours of the active phase revealed that MK-1064 administration significantly increased both wake ($t_{(7)}$ = 2.416, P = 0.0463; Fig. 5.5A) and NREM ($t_{(7)}$ = 2.522, P = 0.0397; Fig. 5.5E) bouts compared with vehicle, in male rTg4510 mice, but not in female rTg4510 mice. During the inactive phase, wake ($t_{(6)}$ = 2.949, P = 0.0256; Fig. 5.5C) and NREM ($t_{(6)}$ = 3.125, P = 0.0204; Fig. 5.5G) bouts were decreased in only female WT mice, compared with vehicle. REM bouts were significantly increased in only male WT mice, compared with vehicle, across the first half of the active phase ($t_{(7)}$ = 13.34, P < 0.0001; Fig. 5.5I), full active phase ($t_{(7)}$ = 2.511, P = 0.0403; Fig. 5.5J) and the entire recording ($t_{(7)}$ = 2.639, P = 0.0335; Fig. 5.5L).

Wake bout duration was not significantly affected by MK-1064 administration (Fig. 6A-D), in part due to larger variation in this parameter. Across the first 6 hours following MK-1064 administration, NREM bout duration was significantly increased, compared with vehicle, in male mice of either genotype (WT: $t_{(7)}$ = 2.745, P = 0.0287; rTg4510: $t_{(7)}$ = 3.306, P = 0.013), but not in female mice of either genotype (Fig. 5.6E). When assessing the entire 23 h recording, female rTg4510 mice exhibited a decrease in NREM bout duration following MK-1064 administration ($t_{(6)}$ = 2.568, P = 0.0425; Fig. 5.6H), probably in part due to rebound reduction in NREM sleep during the inactive phase in these mice (Fig. 5.4J). Male rTg4510 mice also exhibited an increase in REM bout duration across the first half of the active phase ($t_{(7)}$ = 2.395, P = 0.0478; Fig. 5.6I) and the entire recording ($t_{(7)}$ = 2.800, P = 0.0265; Fig. 5.6L), compared with vehicle. This effect was absent in female rTg4510 mice (Fig. 5.6I, L).

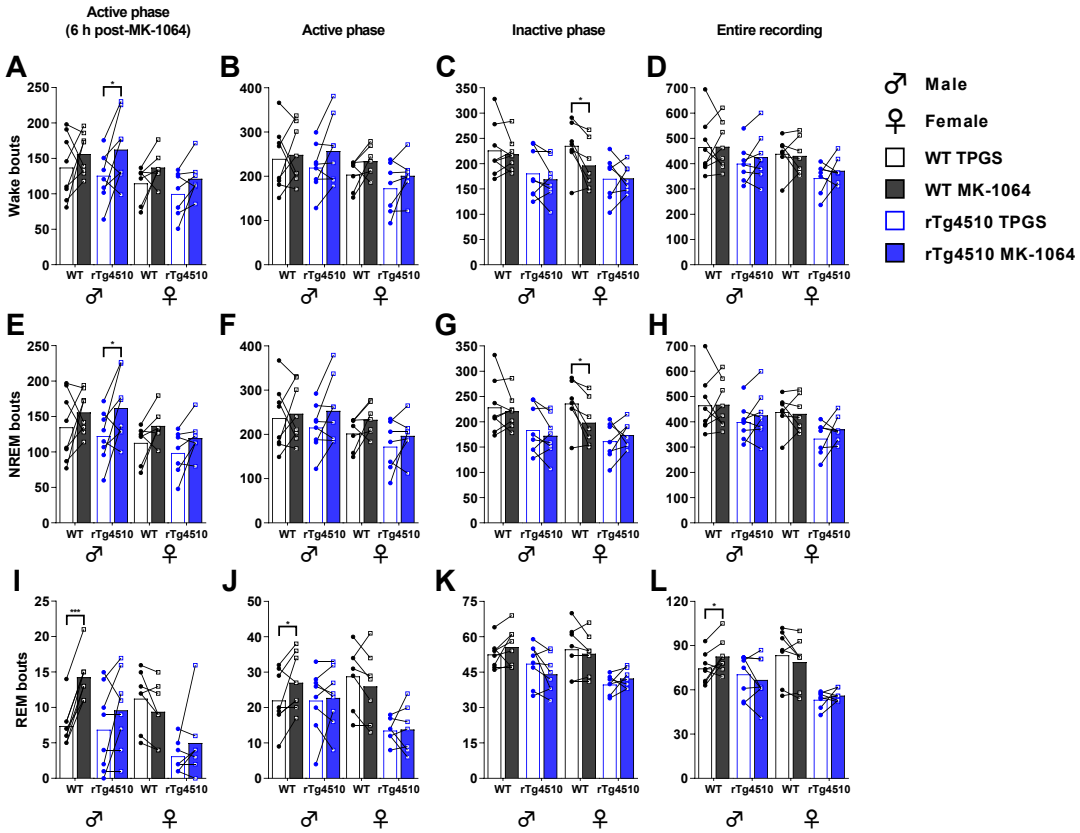

Figure 5.5. Effects of acute MK-1064 administration on bout numbers in rTg4510 mice.

A-L, Total number of wake (***A-D***), NREM (***E-H***) and REM (***I-L***) bouts averaged across (from left to right) the active phase (6 h post-MK-1064), full active phase (12 h), inactive phase and entire recording in rTg4510 and WT mice administered 40 mg/kg MK-1064 or TPGS vehicle. Data are means ± SEM. n = 7-8 per group, per sex. $^{*}P < 0.05$, $^{***}P < 0.001$ vs. vehicle, by Student's paired t-test.

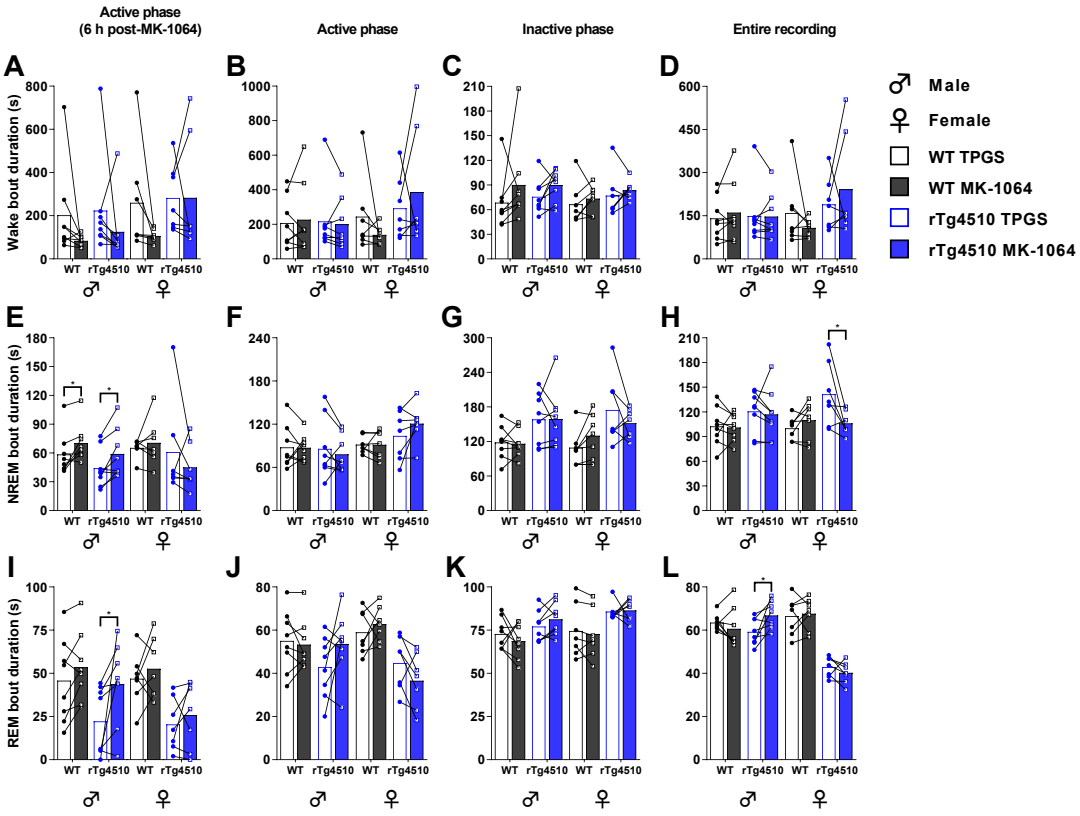

Figure 5.6. Effects of acute MK-1064 administration on bout duration in rTg4510 mice.

A-L*,** Mean wake (A-D***), NREM (***E-H***) and REM (***I-L***) bout durations averaged across (from left to right) the active phase (6 h post-MK-1064), full active phase (12 h), inactive phase and entire recording in rTg4510 and WT mice administered 40 mg/kg MK-1064 or TPGS vehicle. Data are means ± SEM. n = 7-8 per group, per sex. $^{*}P < 0.05$ vs. vehicle, by Student's paired t-test.

Zolpidem similarly increased NREM sleep and decreased wake in male and female WT and rTg4510 mice

Sleep/wake architecture of rTg4510 and WT were significantly altered by zolpidem (Fig. 5.7A-C; Table 5.3), predominantly influencing both wake and NREM vigilance states. Male and female WT mice spent significantly less time in the wake state for each of the first two hours following zolpidem administration, compared with the corresponding vehicle treatment (Fig. 5.7A). Male rTg4510 mice exhibited a decrease in wake time during only the first hour, with female mice exhibiting a decrease for hours one, two and four, following zolpidem administration, compared with their respective vehicle (Fig. 5.7A). Male and female WT mice spent significantly more time in NREM sleep for each of the first two hours following zolpidem administration, compared with their respective vehicle (Fig. 5.7B). Male rTg4510 mice exhibited an increase in NREM sleep during only the first hour, with female mice exhibiting an increase for hours one, two and four, following zolpidem administration, compared with

their respective vehicle (Fig. 5.7B). No significant changes in REM sleep were observed at any individual time point, compared with vehicle (Fig. 5.7C), although the level of REM sleep at this CT time is typically very low.

Analysis of summed data during the first 6 hours following zolpidem administration revealed that average wake time was significantly decreased in WT (Male: $t_{(6)} = 13.27$, $P < 0.0001$; Female: $t_{(8)} = 2.802$, $P = 0.0231$) and rTg4510 mice (Male: $t_{(6)} = 13.64$, $P < 0.0001$; Female: $t_{(5)} = 3.110$, $P = 0.0266$; Fig. 5.7D) of either sex. This effect persisted across the full active phase in male mice of either genotype (WT: $t_{(6)} = 3.576$, $P = 0.0117$; rTg4510: $t_{(6)} = 4.514$, $P = 0.004$), but not in female mice of either genotype (Fig. 5.7E). No statistical differences were observed during the inactive phase (Fig. 5.7F), however, when assessing the 23 h recording as a whole, all four groups of mice exhibited decreases in average wake time, compared with their respective vehicle (Male WT: $t_{(6)} = 2.829$, $P = 0.03$; male rTg4510: $t_{(6)} = 2.858$, $P = 0.0289$; female WT: $t_{(8)} = 3.001$, $P = 0.0171$; female rTg4510: $t_{(5)} = 2.645$, $P = 0.0457$; Fig. 5.7G). During the first 6 hours following zolpidem administration, average NREM sleep time was significantly increased in WT (Male: $t_{(6)} = 12.52$, $P < 0.0001$; female: $t_{(8)} = 3.298$, $P = 0.0109$) and rTg4510 mice (Male: $t_{(6)} = 13.89$, $P < 0.0001$; female: $t_{(5)} = 3.050$, $P = 0.0284$) of either sex, compared with their respective vehicle (Fig. 5.7H). The increase in NREM sleep persisted across the full active phase in male mice of either genotype (WT: $t_{(6)} = 3.700$, $P = 0.0101$; rTg4510: $t_{(6)} = 4.850$, $P = 0.0029$) and female WT mice ($t_{(8)} = 2.598$, $P = 0.0317$), but not female rTg4510 mice (Fig. 5.7I). No statistical differences were observed during the inactive phase (Fig. 5.7J), however, when assessing the 23 h recording as a whole, WT mice of either sex (Male: $t_{(6)} = 3.146$, $P = 0.0199$; female: $t_{(8)} = 3.169$, $P = 0.0132$) and male ($t_{(6)} = 3.200$, $P = 0.0186$), but not female rTg4510 mice exhibited increased NREM sleep, compared with their respective vehicle (Fig. 5.7K). Average REM time was not significantly affected by zolpidem across the first 6 hours (Fig. 5.7L), however, female WT mice exhibited a significant decrease across the full active phase ($t_{(8)} = 4.375$, $P = 0.0024$; Fig. 5.7M) and the entire recording ($t_{(8)} = 2.655$, $P = 0.029$; Fig. 5.7O), compared with their respective vehicle, while male WT mice exhibited decreased REM sleep during the inactive phase ($t_{(6)} = 3.095$, $P = 0.0213$; Fig. 5.7N).

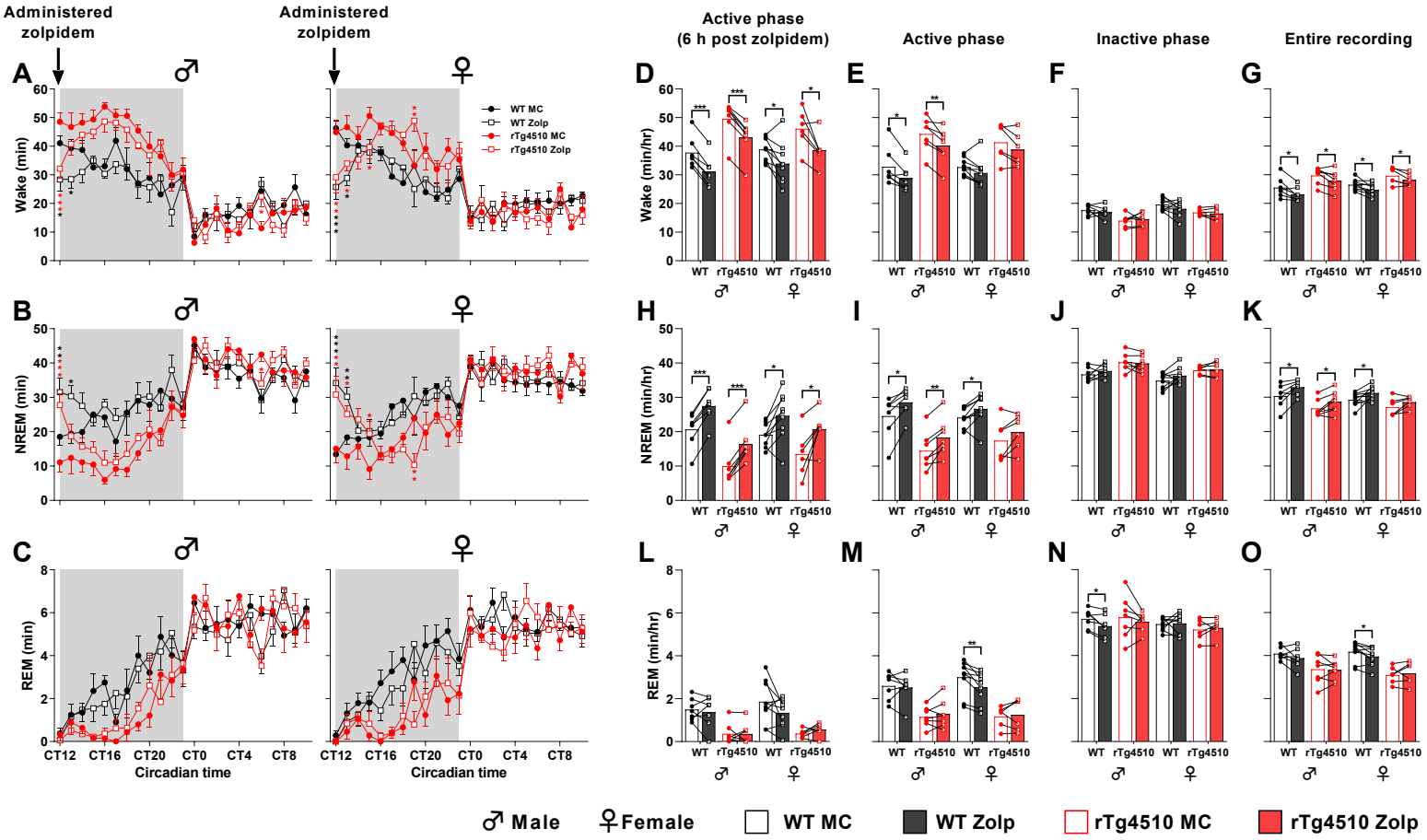

Figure 5.7. Promotion of NREM sleep and attenuation of wakefulness following acute zolpidem administration in rTg4510 mice.

A-C, Minutes spent in wake (***A***), NREM (***B***) and REM (***C***) vigilance states per hour across a 23 h recording in rTg4510 and WT mice administered 10 mg/kg zolpidem or methylcellulose (MC) vehicle. Dark shade represents the active phase. Data are means ± SEM. n = 6-9 per group, per sex. $^{*}P < 0.05$, $^{**}P < 0.01$, $^{***}P < 0.001$ vs. respective vehicle, by repeated measures linear mixed effects model with Tukey's multiple comparisons test. ***D-O***, Minutes spent in each vigilance state per hour averaged across (from left to right) the active phase (6 h post-zolpidem), full active phase (12 h), inactive phase and entire recording, for wake (***D-G***), NREM (***H-K***) and REM (***L-O***). n = 6-9 per group, per sex. $^{*}P < 0.05$, $^{**}P < 0.01$, $^{***}P < 0.001$ vs. vehicle, by Student's paired t-test.

Table 5.3. EEG recordings statistical analyses summary (zolpidem).

Time spent in each vigilance state across the 23 h recording were analysed by a repeated measures linear mixed effects model in R, using the *lmer* function, incorporating the factors Treatment and Time (repeated factor). Indented Pr(>|t|) values indicate statistical significance.

Vigilance state time																
						Wake					NREM					REM
Group	Fixed effect	Estimate	Std. error	df	t-value	Pr(>|t|)	Estimate	Std. error	df	t-value	Pr(>|t|)	Estimate	Std. error	df	t-value	Pr(>|t|)
WT Male	Treatment	-5.9249	2.4926	312.000	-2.377	< 0.05	6.1126	2.1951	312.000	2.785	< 0.01	-0.1895	0.4330	312.000	-0.438	> 0.05
	Time	-1.0950	0.1285	312.000	-8.518	< 0.001	0.8467	0.1132	312.000	7.480	< 0.001	0.2482	0.0223	312.000	11.114	< 0.001
	Treatment: Time	0.2973	0.1818	312.000	1.636	> 0.05	-0.2962	0.1601	312.000	-1.850	> 0.05	-0.0010	0.0316	312.000	-0.031	> 0.05
WT Female	Treatment	-4.5513	2.3432	402.000	-1.942	> 0.05	5.1911	2.0677	402.000	2.511	< 0.05	-0.6396	0.3985	402.000	-1.605	> 0.05
	Time	-1.0720	0.1208	402.000	-8.872	< 0.001	0.8650	0.1066	402.000	8.112	< 0.001	0.2070	0.0206	402.000	10.072	< 0.001
	Treatment: Time	0.2301	0.1709	402.000	1.347	> 0.05	-0.2650	0.1508	402.000	-1.757	> 0.05	0.0348	0.0291	402.000	1.198	> 0.05
rTg4510 Male	Treatment	-6.6405	2.6785	312.000	-2.479	< 0.05	6.6295	2.3664	312.000	2.802	< 0.01	0.0114	0.4418	312.000	0.026	> 0.05
	Time	-2.1283	0.1381	312.000	-15.407	< 0.001	1.7990	0.1220	312.000	14.741	< 0.001	0.3293	0.0228	312.000	14.452	< 0.001
	Treatment: Time	0.3997	0.1953	312.000	2.046	< 0.05	-0.3960	0.1726	312.000	-2.295	< 0.05	-0.0037	0.0322	312.000	-0.114	> 0.05
rTg4510 Female	Treatment	-5.4443	2.7873	267.000	-1.953	> 0.05	5.3080	2.5156	267.000	2.110	< 0.05	0.1369	0.4196	267.000	0.326	> 0.05
	Time	-1.7460	0.1437	267.000	-12.147	< 0.001	1.4448	0.1297	267.000	11.137	< 0.001	0.3011	0.0216	267.000	13.913	< 0.001
	Treatment: Time	0.3284	0.2033	267.000	1.615	> 0.05	-0.3234	0.1835	267.000	-1.763	> 0.05	-0.0051	0.0306	267.000	-0.167	> 0.05

Zolpidem decreased REM bout duration predominantly in female WT mice

Wake bout numbers were largely unaffected by zolpidem administration (Fig. 5.8A-D), except for a small decrease in total wake bouts across the entire 23 h recording in male WT mice, compared with vehicle ($t_{(6)}$ = 2.518, P = 0.0454; Fig. 5.8D). NREM bouts were similarly unaffected (Fig. 5.8E-H), except for a significant decrease in male WT mice across the inactive phase ($t_{(6)}$ = 2.596, P = 0.0409; Fig. 5.8G) and entire recording ($t_{(6)}$ = 2.495, P = 0.0469; Fig. 5.8H), compared with vehicle. REM bouts were also not significantly altered (Fig. 5.8I-L), except for an increase in REM bouts in female WT mice during the inactive phase ($t_{(8)}$ = 2.718; P = 0.0263; Fig. 5.8K).

Wake bout duration was not significantly affected by zolpidem administration across any of the periods analysed (Fig. 5.9A-D). Across the first 6 hours post zolpidem administration, NREM bout duration was significantly increased in male mice of either genotype (Male: $t_{(6)}$ = 4.307, P = 0.0051; rTg4510: $t_{(6)}$ = 3.623, P = 0.0111), but not in female mice of either genotype, compared with their respective vehicle (Fig. 5.9E). Male WT mice exhibited an overall increase in NREM bout duration across the 23 h recording ($t_{(6)}$ = 2.710, P = 0.0351; Fig. 5.9H). REM bout duration was significantly decreased in only female WT mice across the first half of the active phase ($t_{(8)}$ = 3.866, P = 0.0048; Fig. 5.9I), full active phase ($t_{(8)}$ = 3.126, P = 0.0141; Fig. 5.9J) and the entire recording ($t_{(8)}$ = 4.831, P = 0.0013; Fig. 5.9L), compared with vehicle.

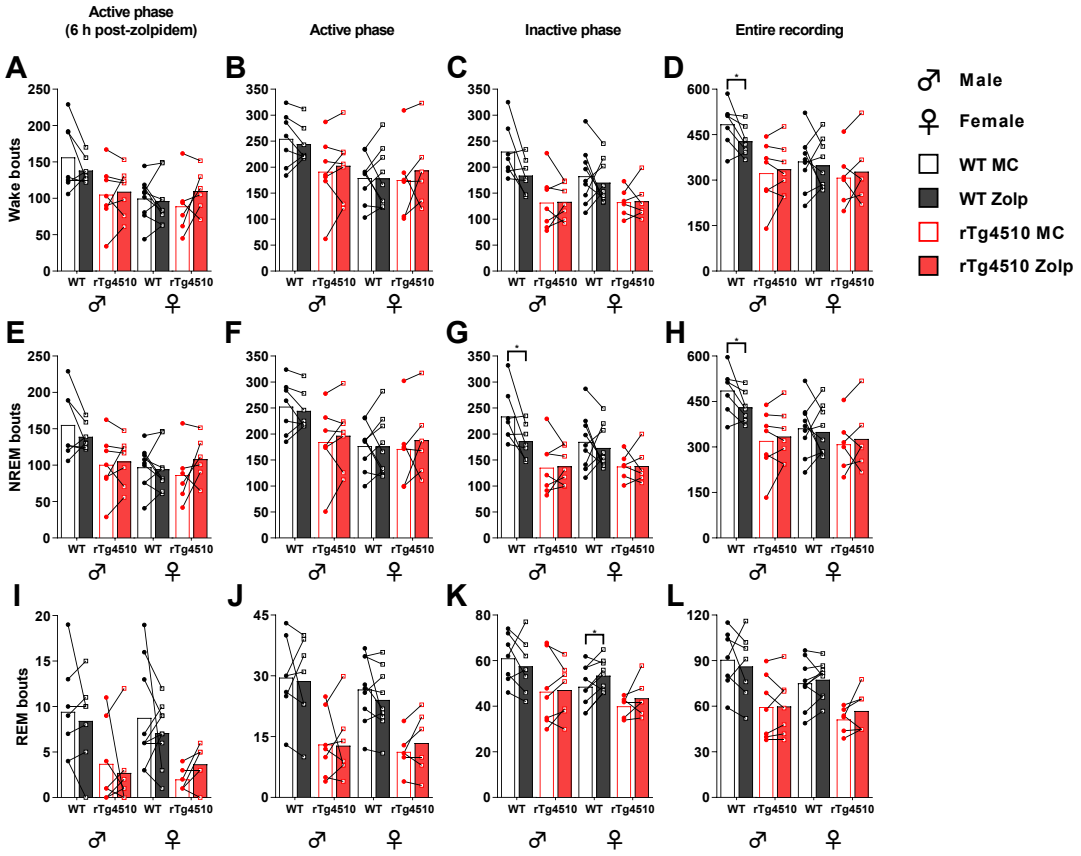

Figure 5.8. Effects of acute zolpidem administration on bout numbers in rTg4510 mice.

A-L, Total number of wake (***A-D***), NREM (***E-H***) and REM (***I-L***) bouts averaged across (from left to right) the active phase (6 h post-zolpidem), full active phase (12 h), inactive phase and entire recording in rTg4510 and WT mice administered 10 mg/kg zolpidem or methylcellulose (MC) vehicle. Data are means ± SEM. n = 6-9 per group, per sex. $^{*}P < 0.05$ vs. vehicle, by Student's paired t-test.

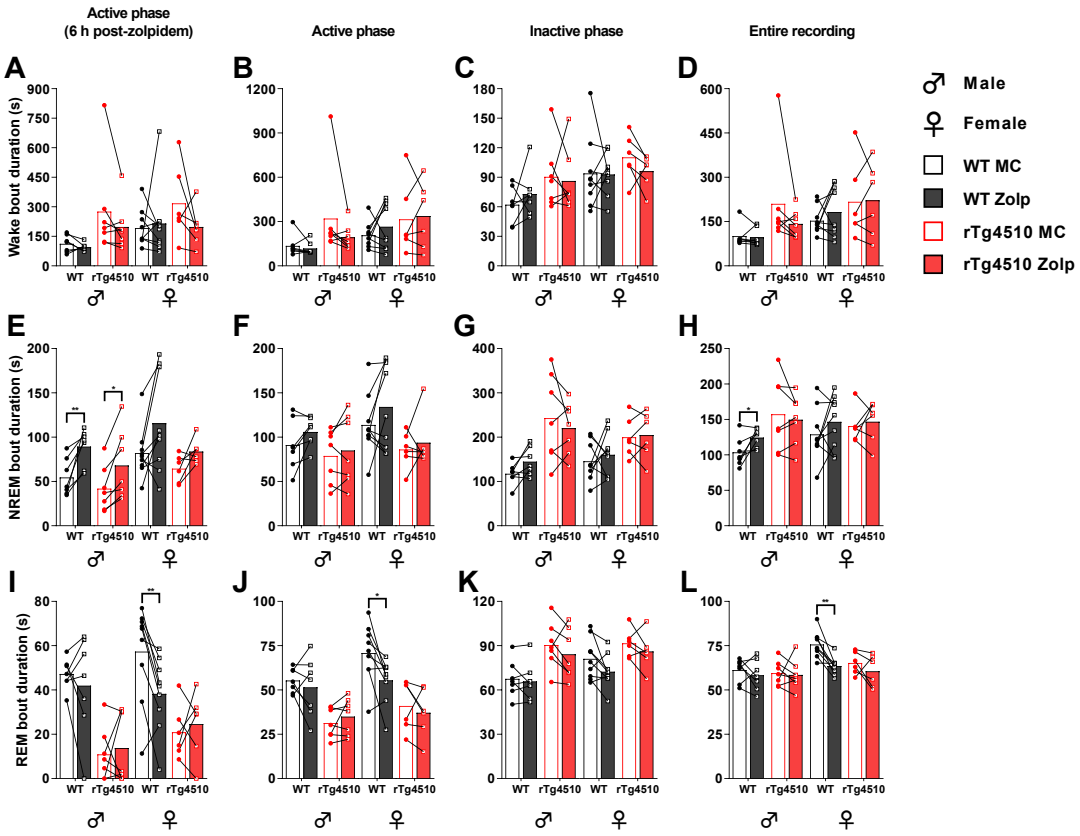

Figure 5.9. Effects of acute zolpidem administration on bout duration in rTg4510 mice.

A-L, Mean wake (***A-D***), NREM (***E-H***) and REM (***I-L***) bout durations averaged across (from left to right) the active phase (6 h post-zolpidem), full active phase (12 h), inactive phase and entire recording in rTg4510 and WT mice administered 10 mg/kg zolpidem or methylcellulose (MC) vehicle. Data are means ± SEM. n = 6-9 per group, per sex. $^{*}P < 0.05$, $^{**}P < 0.01$ vs. vehicle, by Student's paired t-test.

Differential effects of suvorexant, MK-1064 and zolpidem on REM as a proportion of total sleep

Given the previously reported differences of DORAs, 2-SORAs and Z-drugs such as zolpidem on the relative proportions of REM sleep, REM as a proportion of total sleep across the active phase was assessed (Fig. 5.10). Suvorexant significantly increased REM as a proportion of total sleep in WT ($t_{(17)} = 5.061$, $P < 0.0001$) and rTg4510 mice ($t_{(12)} = 3.770$, $P = 0.0027$), compared with vehicle (Fig. 5.10A). MK-1064 did not affect this parameter in either WT or rTg4510 mice (Fig. 5.10B). Zolpidem significantly decreased REM as a proportion of total sleep in WT ($t_{(15)} = 3.285$, $P = 0.005$), but not rTg4510 mice (Fig. 5.10C).

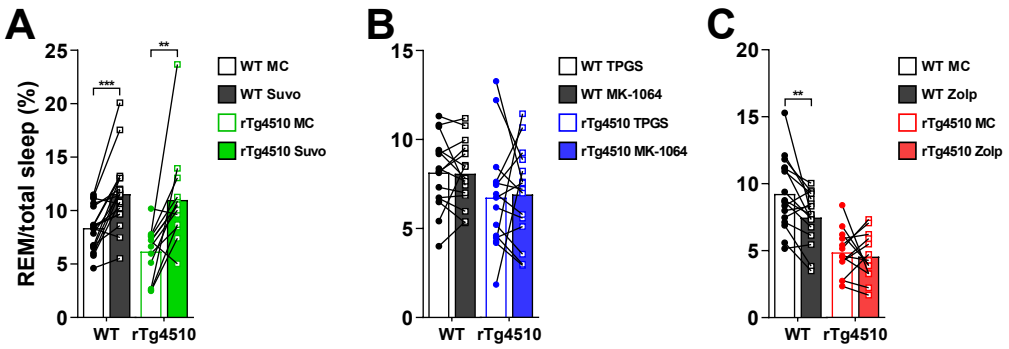

Figure 5.10. Effects of acute suvorexant, MK-1064 or zolpidem administration on REM as a proportion of total sleep.

A-C, REM as a percentage of total sleep during the active phase following acute suvorexant (***A***), MK-1064 (***B***) or zolpidem (***C***) administration in rTg4510 and WT mice. Data are means ± SEM. n = 13-18 per genotype. $^{**}P < 0.01$, $^{***}P < 0.001$ vs. vehicle, by Student's paired t-test.

5.5 Discussion

Recent evidence has demonstrated that mutant tau overexpression contributes to sleep/wake disruptions in the form of hyperarousal in tauopathy mouse models (Chapter 3 and 4; Koss et al., 2016; Holth et al., 2017b; Zhu et al., 2018). Whether this phenotype influences sleep/wake responses to sleep hypnotics has not been previously investigated. The present study therefore examined the sleep/wake response of rTg4510 versus WT mice following acute administration of suvorexant, MK-1064 or zolpidem at the commencement of the active phase, when a prominent hyperarousal phenotype is evident in rTg4510 mice (Chapter 3 and 4). Suvorexant promoted REM sleep in both male and female rTg4510 mice, without overly affecting wake or NREM sleep, as previously reported in non-transgenic mice (Betschart et al., 2013; Hoyer et al., 2013). On the other hand, MK-1064 effectively attenuated the hyperarousal phenotype of male rTg4510 mice by decreasing wake and increasing NREM sleep, in alignment with previous preclinical studies using 2-SORAs (Roecker et al., 2014a; Gotter et al., 2016). Female rTg4510 mice, however, exhibited a blunted response to MK-1064 administration, compared with male rTg4510 mice, an effect that has not been reported previously in non-transgenic mice. Zolpidem, on the other hand, decreased wake and increased NREM sleep equally in both male and female rTg4510 mice.

Suvorexant similarly increased REM sleep for several hours post-dose in male and female WT and rTg4510 mice, without significantly affecting wake or NREM sleep. As a

consequence, suvorexant did not attenuate the hyperarousal phenotype of rTg4510 mice. The promotion of REM sleep in the present study parallels that observed by Betschart et al. (2013), in which 50 mg/kg suvorexant administration at the beginning of the active phase significantly increased REM sleep for up to five hours post-dose, compared with vehicle, in C57BL/6 mice, with minimal effects on NREM sleep. These data indicate that the selective promotion of REM sleep by DORAs such as suvorexant is not diminished in the rTg4510 tauopathy mouse model, regardless of sex. In terms of REM sleep architecture, REM bout number and duration were typically higher in all mice following suvorexant treatment compared with vehicle, however, suvorexant increased REM sleep in WT mice predominantly by increasing REM bouts, without significantly altering REM bout duration. Conversely, the promotion of REM sleep in rTg4510 mice was driven primarily by an increase in REM bout duration, but not total REM bouts. These data suggest that hyperphosphorylated tau accumulation and the sleep/wake phenotype of rTg4510 mice somewhat influences the response to suvorexant, but only to a limited extent.

MK-1064 effectively decreased wake time and increased NREM sleep time, compared with vehicle, for several hours post-dose in WT mice and male rTg4510 mice, consistent with previous observations in C57BL/6 mice (Roecker et al., 2014a; Gotter et al., 2016). Female rTg4510 mice, however, exhibited a more transient and blunted response to MK-1064 administration. Unlike suvorexant, which antagonises both orexin receptor 1 (OX_1R) and OX_2R, MK-1064 is OX_2R selective and the presence of OX_2R is necessary for the sleep promoting effects of MK-1064 (Gotter et al., 2016), and orexin receptor antagonists in general (Mang et al., 2012). The diminished response following MK-1064, but not suvorexant, administration in female rTg4510 mice suggests potential differences in OX_2R function and/or expression. In Chapter 2 it was demonstrated that male rTg4510 mice exhibited altered OX_1R mRNA expression in the locus coeruleus (LC) but no changes in OX_2R expression, which aligns with the robust response to the OX_2R selective antagonist MK-1064 in male rTg4510 mice. Female rTg4510 mice, however, were not examined in Chapter 2. Investigations into OX_2R function and/or expression in female rTg4510 mice are warranted. Nevertheless, the initial prominent, although transient, response in female rTg4510 mice suggests that OX_2R function is still at least partially intact. An exacerbated hyperarousal phenotype has been identified in female rTg4510 mice compared with males (Chapter 3 and 4), and hence the blunted response may be attributable to an inability to overcome this heightened hyperarousal drive. To further investigate this concept, the sleep/wake response of rTg4510 mice following acute zolpidem administration was also assessed, which promotes sleep via $GABA_A$ receptor positive allosteric modulation and not orexin receptors.

Male and female WT and rTg4510 mice exhibited a proportionally similar decrease in wake and increase in NREM sleep following zolpidem administration. Zolpidem promotes sleep via a global suppression of CNS activity, through modulation of $GABA_A$ receptors, without affecting orexin receptors. Ablation of dense orexin receptor expressing LC or tuberomammillary nucleus (TMN) neurons in rats attenuated almorexant-mediated promotion of REM sleep, but had no influence on the efficacy of zolpidem in promoting sleep (Schwartz et al., 2016), indicating zolpidem does not act via orexin receptors. This suggests that the contribution of the heightened hyperarousal drive of female rTg4510 mice to the blunted effect of MK-1064 is likely negligible, at least with respect to the GABAergic system, and again, points to sex-dependent differences in OX_2R function in rTg4510 mice. Conversely, the transient response of MK-1064 may indicate differences in the pharmacokinetics and/or metabolism of MK-1064, but not suvorexant or zolpidem, in female rTg4510 mice, compared with males. Currently, such differences have not been reported in rodents or humans administered MK-1064, although pharmacokinetic differences have been reported for suvorexant in obese women (reviewed in Jacobson et al., 2014). Hence, there is clearly inherent differences in female rTg4510 mice that contributes to the diminished response to MK-1064. The exact mechanisms involved remain to be elucidated but may relate to previously reported sex differences in rTg4510 mice, in which female mice have more advanced tau pathology than males, by the same age (Yue et al., 2011). Overall, such differences reinforce the importance of investigating both sexes in rodent preclinical studies, as previously recommended (Docherty et al., 2019).

REM as a proportion of total sleep during the active phase was assessed following acute suvorexant, MK-1064 or zolpidem administration. The DORA suvorexant increased sleep predominantly by disproportionately promoting REM sleep, as previously reported (Betschart et al., 2013; Hoyer et al., 2013), whilst the 2-SORA MK-1064 produced a balanced increase of both NREM and REM sleep in WT and rTg4510 mice. Zolpidem, however, preferentially promoted NREM sleep and suppressed REM sleep albeit only in WT mice. REM as proportion of total sleep remained quite stable in rTg4510 mice following zolpidem administration, which is most probably due to the limited time that rTg4510 mice spend in REM sleep during the active phase, as a result of their hyperarousal phenotype. These data further reinforce the concept that OX_2R selective antagonists promote a more physiological type of sleep (Betschart et al., 2013; Hoyer and Jacobson, 2013; Jacobson et al., 2017; Hoyer et al., 2019), even in a mouse model of neurodegenerative tauopathy. Furthermore, although zolpidem increased NREM sleep in both male and female rTg4510 mice without overtly suppressing REM sleep,

it is not an ideal candidate for neurodegenerative tauopathy-related disorders. Prominent disadvantages of benzodiazepines or Z-drugs such as zolpidem include adverse drug-drug interactions, negative effects on cognition and balance leading to falls and overall general inhibition of brain function (Winrow and Renger, 2014; Kales et al., 2015); hence contraindicating them for promoting sleep in neurodegenerative disorders. A 2-SORA therefore appears to be the most suitable compound as a potential therapeutic targeting sleep in neurodegenerative disorders (Hoyer et al., 2019), although based on the present data, investigations into potential sex effects on the response to MK-1064 in tauopathy-related disorders in a clinical setting are warranted.

In summary, the aim of the current study was to assess the sleep/wake response of rTg4510 mice following acute administration of sleep-promoting compounds during the active phase, when a hyperarousal phenotype is evident. The DORA suvorexant similarly promoted REM sleep in rTg4510 mice, without attenuating hyperarousal. The OX_2R selective antagonist MK-1064 effectively attenuated the hyperarousal phenotype by decreasing wake time and increasing NREM sleep particularly in male, but with blunted efficacy in female rTg4510 mice, whereas zolpidem effectively promoted NREM sleep and decreased wake equivalently in both male and female rTg4510 mice. These data reveal sex differences in the response of rTg4510 mice to MK-1064, highlighting potential alterations in OX_2R function and/or expression in females in response to tau overexpression. The proportionally similar increase in NREM and REM sleep following MK-1064, but not suvorexant or zolpidem, reinforces the notion that OX_2R selective antagonists promote a more ideal sleep architecture in both WT mice and a tau transgenic model of neurodegenerative tauopathy. In conclusion, these data indicate that rTg4510 mice respond to sleep-promoting therapeutics despite a noted hyperarousal phenotype and dysregulation of REM sleep balance. Noted sex differences suggest further investigations into sex-specific effects of hyperphosphorylated tau on OX_2R pharmacology are warranted.

Chapter 6

General Discussion

The experiments described in this thesis demonstrate a key role for hyperphosphorylated tau in mediating sleep/wake and cognitive disruptions in the rTg4510 transgenic mouse model of tauopathy, and further support the conclusion that a bidirectional relationship between sleep and tauopathy exists, in the context of Alzheimer's disease (AD) and frontotemporal dementia (FTD).

Initial work revealed similar phenotypes at a molecular level regarding orexin receptor 1 (OX_1R) expression in the sleep/wake-regulating locus coeruleus (LC), in both rTg4510 and tau knockout (KO) mice. The comparable decrease in OX_1R expression in the LC may hence contribute to similar functional consequences – hyperarousal and sleep/wake fragmentation – and suggests that orexinergic input to the LC is modulated by altered or loss of tau function.

Subsequent work involved functional and behavioural studies in rTg4510 mice and demonstrated that hyperphosphorylated tau accumulation contributes to exacerbated neurodegeneration, sleep/wake disruptions, cognitive deficits and behavioural abnormalities. With the exception of the sleep/wake phenotype, these phenotypes were slowed or reversed by repressing tau transgene expression with doxycycline (Dox), suggesting that tau-mediated damage to the sleep/wake regulating circuitry is perhaps more permanent or even irreversible compared with other brain circuits.

Subsequent experiments revealed that rTg4510 mice respond to common hypnotic therapeutics and that the promotion of physiological/balanced sleep, using orexin receptor antagonists, to replace the hyperarousal observed in these mice resulted in a proportional improvement in cognitive function. The partial or complete recovery of cognition using independent, different interventions that targeted the reduction of mutant tau or the increase of sleep, further reinforces the bidirectional relationship between sleep and neurodegenerative disease and enabled the identification of key factors underlying cognitive restoration in rTg4510 mice.

Together, these studies demonstrate that hyperphosphorylated tau contributes to sleep/wake and cognitive deficits in neurodegenerative tauopathies and that reducing

hyperphosphorylated tau accumulation and/or promoting sleep may be viable and effective therapeutic strategies for the treatment of AD and FTD.

6.1 Potential mechanisms driving sleep/wake disruptions in rTg4510 mice

Prior to the research outlined in this thesis, the sleep/wake phenotype of rTg4510 mice had not been previously reported. As discussed in Chapter 3, rTg4510 mice exhibit a disrupted sleep/wake phenotype including a prominent hyperarousal phenotype during the active phase, altered vigilance state bout numbers and bout durations, and electroencephalography (EEG) power spectral deficits during sleep. The following section discusses the potential mechanisms which may contribute to these sleep/wake disturbances, based on current knowledge of the rTg4510 mouse. Further insights into potential mechanisms highlighted by the data generated in this thesis will also be considered.

6.1.1 Current evidence – tau-induced neuronal hyperexcitability

There is a distinct paucity of research examining the sleep/wake phenotype of pure tauopathy mouse models (Koss et al., 2016; Holth et al., 2017b). More extensive electrophysiological recordings, however, have been conducted using neurons from rTg4510 mice (Rocher et al., 2010; Crimins et al., 2011; Crimins et al., 2012; Menkes-Caspi et al., 2015). Hence, influences of mutant tau on the activity of the broader neural network contributing to sleep and wakefulness, may be inferred to some degree based on the properties of these individual neurons.

Electrophysiological studies using layer 3 frontal cortical pyramidal cells from rTg4510 mice demonstrated that rTg4510 neurons exhibit a depolarised resting membrane potential, compared with wildtype (WT) controls, which lead to hyperexcitability and heightened action potential (AP) firing rates (Rocher et al., 2010; Crimins et al., 2012). Rheobase (i.e., the amount of current required to elicit an AP) is also significantly reduced in rTg4510 neurons, compared with WT controls, in both the early (1-3 months) and advanced (9-13 months) stages of the tauopathy mouse model (Crimins et al., 2012). Morphological changes revealed differences including truncated apical tufts, diminished dendritic arbours and decreased spine density in rTg4510 neurons (Rocher et al., 2010; Crimins et al., 2012), particularly in the advanced stages (Crimins et al., 2012). Intriguingly, these changes were observed regardless of the presence of mature neurofibrillary tangles (NFTs) in the recorded neurons. Together, these findings suggest that non-fibrillar tau species can have detrimental effects on the function of neurons before the development of mature NFTs (Rocher et al., 2010; Crimins et al., 2012); hence contributing to

functional changes before any advanced aggregated pathology or neurodegeneration occurs. It was further demonstrated that compensatory changes due to neuronal/synaptic atrophy may result in the increased excitability of surviving neurons, which attempt to maintain normal network function (Crimins et al., 2011). Such changes result in increased AP-dependent neurotransmitter release from presynaptic terminals (Crimins et al., 2011). Importantly, lifelong Dox treatment was able to completely abolish both the structural and functional changes in rTg4510 neurons, which become indistinguishable from WT neurons, hence emphasising the involvement of tau overexpression in mediating these effects (Crimins et al., 2012).

As discussed in Chapter 1, tau pathology appears to initially and selectively develop in brain regions comprising the ascending reticular activating system (ARAS; Braak and Braak, 1991b; Braak and Braak, 1995; Iba et al., 2013; Braak and Del Tredici, 2015; Theofilas et al., 2015; Stratmann et al., 2016). Tau-induced hyperexcitability of neurons in these regions may plausibly lead to the increased release of neurotransmitters (that is, monoamines such as noradrenaline, dopamine, histamine and serotonin) and drive elevated wakefulness. In this way, increased hyperexcitability of nuclei in the ARAS, which promote wakefulness, may hence contribute to the hyperarousal phenotype of rTg4510 mice. Taken together, these electrophysiological findings from rTg4510 neurons provide support for a potential mechanism by which non-fibrillar tau species may elicit functional neuronal changes and therefore sleep/wake disruptions, before any substantial neurodegeneration is observed.

Although the studies described above may explain how hyperexcitability at the neuronal level leads to global network alterations and hyperarousal, they do not necessarily explain why the hyperarousal phenotype of rTg4510 mice is restricted only to the active, and not the inactive, phase. One of the most interesting findings in the present work is that despite the hyperarousal phenotype during the active phase, these mice do not exhibit any rebound sleep during the inactive phase, hence they are chronically sleep-deprived compared with WT controls. A potential explanation for this observation may involve the orexin system. As discussed in Chapter 1, orexin neurons fire actively during wakefulness and become virtually silent during sleep (Sakurai, 2007). Monoaminergic nuclei in the ARAS receive dense orexinergic input, and the activity of these nuclei is largely dependent on the balance of inhibitory signals from sleep promoting regions (e.g. ventrolateral preoptic nucleus (VLPO)) and excitatory signals from orexin neurons (Gotter et al., 2012). Electrophysiological studies discussed above demonstrated that rTg4510 cortical neurons are hyperexcitable and require less input to elicit increased firing rates. Therefore, during the active phase, when orexin levels

are at their peak and orexin neurons are actively firing, this input to the ARAS may result in a non-proportional heightened output of ARAS activity, due to tau-induced hyperexcitability in these nuclei. This elevated ARAS activity would then lead to hyperarousal during the active phase. During the inactive phase, however, orexin neurons are firing less or are completely silent; hence, there is no orexinergic input to drive the ARAS, thus resulting in a relatively normal sleep/wake phenotype during the inactive phase in rTg4510 mice.

It is interesting to note that the active, but not inactive, phase hyperarousal phenotype of rTg4510 mice thus also suggests that the signals that induce the silencing of orexin neurons during the sleep-dominant inactive phase appear to be preserved in rTg4510 mice. These would include the wake-off and sleep-on neuronal systems (e.g. VLPO) that drive inactivity and orexin neuron silencing during the inactive phase, as supported by the observation that the circadian rhythm and baseline timing of sleep-on/wake-off systems in rTg4510 mice also appeared normal. It is therefore interesting to speculate about the status of sleep homeostasis systems in rTg4510 mice, given their lack of sleep rebound from hyperarousal. Investigating how tau transgenic mice respond to sleep deprivation in terms of their subsequent sleep/wake profile is therefore of interest in future studies. Overall, these observations point to a tau-dependent dysregulation of the wake-active components of the ARAS, and particularly orexin neurons, as the major driver of the active phase hyperarousal in rTg4510 mice.

6.1.2 New insights – tau-mediated changes in the locus coeruleus and the orexin system

Tau-induced hyperexcitability in ARAS nuclei leading to enhanced activity and neurotransmitter release is a plausible mechanism for the hyperarousal phenotype in rTg4510 mice. Data generated in this thesis build on and offer new insights into these mechanisms, in particular by highlighting the potential importance of tau-mediated alterations in the LC and the orexin system.

In situ hybridisation (ISH) studies (Chapter 2) revealed decreased OX_1R mRNA expression in the LC of both rTg4510 and tau KO mice. In rTg4510 mice, the expression of the tau transgene is driven by a Ca^{2+}-calmodulin-dependent protein kinase II (CaMKII) promotor and hence forebrain specific; therefore, the tau transgene should theoretically spare expression in the LC. However, given the selective vulnerability of the LC (Iba et al., 2013), it is hypothesised that tau may be invading the LC from transgene overexpression regions and is contributing to the decrease in OX_1R expression observed. Although near identical results were observed in tau KO mice, the same mechanism cannot be proposed at a surface level given the

absence of tau. Nevertheless, tau KO mice similarly exhibit a hyperarousal phenotype and fragmented sleep/wake transitions (Cantero et al., 2010). Further work is required to elucidate the exact mechanisms involved; however, there are proposals that tau hyperphosphorylation may act as a loss of tau function, as soluble tau is sequestered into aggregates, although evidence for a toxic gain of phosphorylated tau (p-tau) also exists (reviewed in Ittner and Ittner, 2018). It is of course plausible that loss- or gain-of-function may co-exist in a complex system, depending on which function is being evaluated. Certainly, from the present data, it appears that altered/lost tau function modulates orexinergic input to the LC, resulting in similar molecular (OX_1R mRNA expression) and hence, functional (hyperarousal) consequences.

Why are LC neurons especially vulnerable to developing tau pathology? The selective vulnerability of ARAS nuclei, such as the LC, highlights the concept that tau pathology spreads through the brain via synaptically and functionally connected regions, rather than by proximity. The LC innervates virtually the entire cortex with long and thin axons which are poorly myelinated. Such properties leave the LC vulnerable to retrograde propagation of tau and the increased risk of developing NFTs (Satoh and Iijima, 2019). LC processes are further highly exposed to the blood circulation and cerebrospinal fluid (CSF), thus increasing the risk of coming into contact with harmful metabolites and toxins such as tau (Braak and Del Tredici, 2015; Satoh and Iijima, 2019). LC neurons are also tonically active and have a high bioenergetic demand, especially during wakefulness (Satoh and Iijima, 2019). This may further put LC neurons at risk and expose them to the activity-dependent release of tau (Pooler et al., 2013; Yamada et al., 2014; Wu et al., 2016; Wang et al., 2017a) and/or Aβ (Cirrito et al., 2005; Cirrito et al., 2008; Bero et al., 2011; Tabuchi et al., 2015).

The overactivity of LC, as well as orexinergic, neurons during periods of extended wakefulness leading to activity-dependent release of tau is potentially problematic in a neurodegenerative state. The phosphorylation state of tau is mediated by the activity of various kinases including glycogen synthase kinase 3β (GSK-3β; Mandelkow et al., 1992; Hong et al., 1997) and cyclin-dependent kinase 5 (CDK5; Baumann et al., 1993), and phosphatases such as protein phosphatase 2A (PP2A), which accounts for the majority of tau phosphatase activity *in vivo* (Liu et al., 2005; Qian et al., 2010). In AD, the expression of GSK-3β is increased (Leroy et al., 2007), whereas PP2A activity and expression is decreased (Gong et al., 1993; Vogelsberg-Ragaglia et al., 2001). The activity-dependent release of tau in this environment may thus increase the likelihood of tau becoming hyperphosphorylated and developing into pathological aggregates. This highlights the need for adequate neuronal ‘down-time’ during sleep and the enhanced clearance of metabolites such as tau (and Aβ) during this process (Xie

et al., 2013). In the rTg4510 model, levels of the PP2A(A) subunit are decreased, thus likely contributing to heightened p-tau levels (McKenzie-Nickson et al., 2018). Exactly how sleep/wake regulation affects the activity of tau kinases and phosphatases in humans or rodent models, however, is currently unknown. Variations in the phosphorylation state of tau are regulated during sleep/wake states, mediated primarily via natural alterations in temperature during sleep (Guisle et al., 2019), although the changes in kinase/phosphatase activity across sleep/wake states has not been fully elucidated. A better understanding of exactly how sleep/wake function regulates tau dynamics is imperative.

Given that the activation of orexin receptors promotes wakefulness, it appears contradictory that a decrease in OX_1R expression in the wake-promoting LC would lead to hyperarousal. There are several possible explanations for these observations. In humans, CSF orexin levels are commonly increased in moderate to severe stages of AD (Dauvilliers et al., 2014b; Liguori et al., 2014b; Liguori et al., 2016; Gabelle et al., 2017; Heywood et al., 2018) and often correlate with tau and p-tau levels (Deuschle et al., 2014; Liguori et al., 2014b; Liguori et al., 2016; Osorio et al., 2016). Analyses of orexin levels in CSF taken from rTg4510 mice is therefore imperative. Given the presence of extensive tau pathology, it is anticipated that rTg4510 mice would indeed exhibit elevated CSF orexin levels compared with WT mice. Should this be the case, elevated orexin levels could potentially be contributing to the hyperarousal phenotypes of both rTg4510 and tau KO mice, while reduced OX_1R expression in the LC may reflect a compensatory down-regulation of orexin receptor signalling to combat rising orexin levels.

In addition, neurodegenerative disorders have been associated with LC neuronal loss in both humans (Bondareff et al., 1982; Bondareff et al., 1987; German et al., 1987; German et al., 1992; Manaye et al., 1995) and rodent models (O'Neil et al., 2007; Liu et al., 2008b; Manaye et al., 2013). The death of LC neurons may hence result in increased activity of surviving neurons, attempting to maintain normal function, as observed in the electrophysiology of rTg4510 neurons (Crimins et al., 2011) and discussed above. Furthermore, periods of extended wakefulness and sleep deprivation have been demonstrated to cause LC cell loss even in WT mice (Zhang et al., 2014; Zhu et al., 2016), hence plausibly explaining LC neuronal death and subsequent hyperactivity in tau KO mice; devoid of any tau pathology.

6.2 Key factors underlying cognitive restoration in rTg4510 mice

Based on the findings from the three chronic studies in rTg4510 mice using Dox, suvorexant and MK-1064 (Chapter 3 and 4), possible key factors potentially contributing to the recovery of cognitive function in rTg4510 mice can be identified.

First and foremost, perhaps the most obvious factor was a substantial reduction in both tau and p-tau levels in the brains of rTg4510 mice following Dox treatment (Chapter 3). Given that the neurodegenerative phenotype of rTg4510 mice is driven by the overexpression of mutant tau, it is not particularly surprising that a reduction in tau levels would result in positive cognitive outcomes, as previously reported (Ramsden et al., 2005; Santacruz et al., 2005; Blackmore et al., 2017). Perhaps more pertinent to discuss, is the timing and magnitude of the effects observed following Dox treatment (Chapter 3). Dox treatment initiation began at 4.5 months in rTg4510 mice, an age at which modified variants of tau and tangle-like inclusions have already begun to develop, whereas extensive neurodegeneration has yet to occur (Ramsden et al., 2005). In terms of subsequent protein levels in the hippocampus and cortex nine weeks later, p-tau levels were reduced by approximately 50% compared with rTg4510 Control mice, yet were still 3-4 times higher than in the WT mice. Given that modified variants of tau had been developing for 4.5 months before Dox treatment began, it was not expected that tau levels would be entirely reverted to WT levels. Nevertheless, a complete prevention of cognitive deficits was observed, despite the relatively high amount of p-tau still present in the brains of rTg4510 Dox-treated mice. In agreement with previous findings (Blackmore et al., 2017), this has clinical implications for tauopathy-related disorders and potential anti-tau therapeutics. These data emphasise the concept that the complete removal of all pathological tau is not necessary and that partial reductions can still be functionally beneficial (Blackmore et al., 2017), provided interventions are commenced early enough, before any substantial neuronal and synaptic loss has already occurred. Furthermore, given that the primary effect of Dox is to prevent the generation of new tau and p-tau, which by nature is more likely to be soluble than older, aggregated p-tau in the brain, it also supports the well-defined notion that soluble tau species are inherently more toxic than that which has aggregated (Mirbaha et al., 2018).

The second key factor appeared to be the attenuated neurodegeneration of hippocampal and cortical neurons, as well as white matter tracts, especially through the corpus callosum. As with tau protein, brain volumes of rTg4510 mice treated with Dox were not restored to WT levels; however, Dox treatment was evidently initiated early enough to allow sufficient survival of neurons/synapses necessary for full recovery of cognitive function. The prevention of

cognitive decline, attenuation of neurodegeneration and mitigation of locomotor hyperactivity following Dox treatment, but not the abolition of the hyperarousal phenotype, suggests that pathological insults to the cortex, hippocampus and corpus callosum are more responsive to treatment that the ARAS, at the investigated ages. Tau-driven insult to the ARAS is perhaps more permanent and/or irreversible compared with other brain regions, which would align with the selective vulnerability of these nuclei to developing tau pathology. Dox treatment may therefore need to be initiated much earlier than 4.5 months of age to potentially prevent the sleep/wake disturbances present in rTg4510 mice, although some restoration of power spectrum and sleep/wake architecture was observed with transgene inactivation (discussed below).

Reductions in tau levels evidently play a key role in mediating cognitive restoration in rTg4510 mice. But what about the effects of restoring sleep? Based on the proposed bidirectional relationship between sleep and disease pathology, it was expected that promoting sleep would enhance cognitive function and memory consolidation and/or aid in the clearance of hyperphosphorylated tau species. In Chapter 3, an increase in REM sleep during the inactive phase was observed in rTg4510 mice following Dox treatment. This observation led to the hypothesis that REM sleep may have played a role in cognitive recall, especially given the proposed role that REM sleep plays in the consolidation of spatial memory (Boyce et al., 2016) and the defects in REM sleep observed in AD and FTD patients (Prinz et al., 1982; Petit et al., 2004; Moran et al., 2005). However, selectively promoting REM sleep with the dual orexin receptor antagonist (DORA) suvorexant during the inactive phase in rTg4510 mice did not improve cognitive function or reduce tau levels (Chapter 4). Dox-induced reduction in tau levels by 50% was sufficient to completely restore cognitive function (Chapter 3). Hence, the lack of effect of suvorexant on spatial recall suggested tau levels were not modulated either, as was the case.

Since the release and clearance of tau is proposed to be regulated by sleep and wakefulness, the amount and type of sleep promoted by suvorexant was likely insufficient to aid in the clearance of amounts of tau that are detectable at the resolution of a western blot. This may be because REM sleep comprises a minor proportion of overall vigilance states and suvorexant was administered during the inactive phase, when rTg4510 mice exhibit most of their REM sleep anyway. It may also be because REM sleep may not promote clearance of metabolites from the brain in comparison to balanced physiological sleep, which includes NREM sleep, via glymphatic pathways (Xie et al., 2013). Acute administration of suvorexant during the active phase, however, did not affect wake or NREM sleep to any extent in rTg4510

mice (Chapter 5), suggesting the timing of dosing with suvorexant in rTg4510 mice has no impact on the promotion of NREM sleep. Either way, any improvement in the consolidation of spatial memory that suvorexant may have afforded was evidently insufficient to overcome the substantial tau-mediated cognitive burden in rTg4510 mice. Together, these data suggest that the previously observed rescue of cognitive ability following Dox treatment (Chapter 3) was driven almost exclusively by reductions in tau levels. The prevention of REM deficits was likely a downstream effect of attenuated hyperphosphorylated tau, rather than the other way around, and indicated that the actual increase in REM sleep time observed likely contributed minimally to cognitive improvement. Taken together, these results further reinforce the concept that reductions in tau levels are a critical contributing factor underlying cognitive restoration in rTg4510 mice.

The orexin receptor 2 (OX_2R) selective orexin receptor antagonist (2-SORA) MK-1064 effectively promoted NREM and REM sleep and attenuated hyperarousal, albeit in only male rTg4510 mice, which resulted in a partial but distinct improvement of spatial recall (Chapter 4). Tau levels, however, were largely unaffected in both the hippocampus and cortex, except for a subtle reduction in p-tau S404 levels. As discussed in Chapter 4, any additional clearance of tau afforded by increased sleep, or reduced release afforded by decreased arousal, was likely insufficient to overcome the very high levels of tau overexpression. It therefore appears plausible that the effects of MK-1064 on sleep and neuronal network function may have contributed to improved cognitive faculty perhaps irrespectively of the effects on tau pathology. In addition to MK-1064's general effect on the amount of time spent in wake and NREM/REM sleep, it also increased slow delta power in the 1-2.5 Hz frequency range in male, but not female, rTg4510 mice. In humans, lower frequency slow waves have been associated with increased memory consolidation (Marshall et al., 2006; Diekelmann and Born, 2010; Chauvette et al., 2012) and importantly, transcranial stimulation of slow oscillations (1.33-1.5 Hz), within the same frequency range enriched by MK-1064, enhanced memory consolidation in rats (Binder et al., 2014). These data provide a foundation from which to explain the effects of MK-1064 on improved spatial recall in male rTg4510 mice, irrespective of its effects on tau pathology. To further reinforce this point, rTg4510 mice similarly exhibited an overall increase in delta power (1-4 Hz) during NREM sleep following Dox treatment. Intriguingly, when assessing only slow delta waves (1-2.5 Hz), associated with memory consolidation, an almost indistinguishable result was observed following either Dox or MK-1064 treatment (Chapter 3 and 4). That nearly identical outcomes following completely independent and differing interventions were observed is highly interesting. Further work is required to elucidate the

exact mechanisms involved, however, elevated slow delta power during NREM sleep presents as a third key factor likely underlying cognitive restoration in rTg4510 mice.

Furthermore, a recent study by Vasselli et al. (2017) reported that *Hcrt* (orexin) KO mice exhibited specific deficits in delta power, predominantly affecting slow rather than fast delta waves. These mice hence exhibit a significantly elevated fast/slow delta wave ratio compared with their WT controls (Vassalli and Franken, 2017). The similar deficits in slow delta power observed in rTg4510 and orexin KO mice further supports the concept that the orexin system is dysregulated in rTg4510 mice. Further work is required to confirm this hypothesis.

Although not directly examined in the present work, the potential impact of the relationship between impaired sleep and microglia-mediated neuroinflammation deserves consideration (Green et al., 2020). In WT mice, sleep loss has been shown to induce microglial activation, predisposing the brain to subsequent damage (Bellesi et al., 2017). Additionally, sleep disturbance in mice resulted in hippocampal neuroinflammation, which impaired hippocampal-dependent learning and memory (Zhu et al., 2012). Microglia activation has also been implicated in tau propagation and subsequent synapse loss and neurodegeneration in tauopathies (Asai et al., 2015; Hong et al., 2016; Liddelow et al., 2017; Shi et al., 2017; Rajendran and Paolicelli, 2018). Furthermore, Zhu et al. (2018) demonstrated that chronic sleep disruption was associated with advanced progression of tauopathy, and importantly, with greater microglia activation in the hippocampus of tau transgenic PS19 mice when exposed to chronic sleep disruption, compared to rested controls. In the present work, it would be of interest to examine whether improved sleep following MK-1064 administration conferred protection against microglia-mediated neuroinflammation, resulting in reduced neurodegeneration in the hippocampus and hence, improved hippocampus-dependent spatial recall. Experiments assessing microglia-specific immunoreactivity in the hippocampus of MK-1064 treated rTg4510 mice are thus warranted. The role of neuroinflammation may serve as another mechanism of injury in tauopathies, potentially exacerbating neurodegeneration and cognitive impairments, and further contributing to sleep/wake disruptions.

In summary, the combination of reduced tau and p-tau levels, attenuated brain atrophy including rescued white matter functionality and increased slow delta power during NREM sleep are associated with the restoration of cognitive function, especially in male rTg4510 mice, which typically exhibit enhanced cognitive performance compared with females. Interestingly, female rTg4510 mice did not display the increase in delta power following Dox treatment, which may be related to their exacerbated tau pathology and/or hyperarousal drive compared

with males, or to sex-specific effects. Nevertheless, in the few female rTg4510 mice in which cognitive deficits were prevented by Dox, this was likely driven by reductions in tau levels and attenuated neurodegeneration, as discussed above. In contrast, the partial restoration of cognitive ability following MK-1064 appears predominantly driven by attenuation of hyperarousal and increased slow delta power during NREM sleep, with minimal effects on tau levels, hence potentially explaining the discrepancy in the effect size when compared with Dox treatment.

6.3 Sex differences in rTg4510 mice

rTg4510 mice exhibit sex differences in terms of tau pathology and subsequent memory decline (Yue et al., 2011). The exacerbated hyperarousal drive of female rTg4510 mice (Chapter 3 and 4) may in part be attributed to their more advanced pathology of certain tau species compared with same-aged males, although no differences in soluble tau levels were observed in the present studies. In contrast, stark differences in responses to OX_2R antagonists between the sexes were observed. The data from Chapter 4 and 5 in this thesis revealed rTg4510 sex differences in terms of the sleep/wake response to orexin receptor antagonists. This information warrants investigations into the use of orexin receptor antagonists as potential therapeutics in tauopathy-related neurodegenerative disorders to determine whether sex-specific effects observed here translates to a clinical setting.

Female rTg4510 mice, but not female WT mice, exhibited a blunted response to both chronic (Chapter 4) and acute (Chapter 5) administration of MK-1064, compared with male rTg4510 mice. The similarly blunted response following only one dose of MK-1064 indicated that the lack of response observed following chronic treatment was not due to tachyphylaxis from repeated dosing. These observations imply that there are inherent differences in female rTg4510 mice which contribute to this impaired response. Following either acute or chronic administration of MK-1064, female rTg4510 mice displayed a quite prominent, although transient response, before their sleep/wake profile quickly resembled that of their vehicle-treated controls. Initially, this led to the hypothesis that the heightened drive to remain awake during the active phase is potentially too strong to be alleviated by the urge to sleep induced by MK-1064 in female, but not male, rTg4510 mice. However, the similar promotion of NREM sleep by zolpidem (Chapter 5) suggest this hypothesis is incorrect and that the contribution of the exacerbated hyperarousal phenotype is negligible, at least with respect to the GABAergic system.

Suvorexant was also equally effective in both male and female rTg4510 mice in promoting REM sleep. Given that suvorexant antagonises both OX_1R and OX_2R, whereas MK-1064 selectively targets OX_2R, this highlights potential differences in OX_2R function and/or expression in female rTg4510 mice. In Chapter 2, it was demonstrated that the mutant tau overexpression of the rTg4510 mouse indeed influenced orexin receptor expression. In that experiment, however, only male mice were used, and female mice were not examined. Further investigations into potential differences in OX_2R expression and/or function in female rTg4510 mice are thus warranted. It is hypothesised that if female rTg4510 mice indeed exhibit alterations in OX_2R function, perhaps the basis of sleep/wake sex differences in pharmacology may originate in the dense OX_2R-expressing tuberomammillary nucleus (TMN), which plays a key role in regulating arousal and NREM sleep (Willie et al., 2003; Sakurai, 2007). Nevertheless, the initial transient response in female rTg4510 mice suggests that OX_2R function is still at least partially intact. These data also suggest that potential sex differences in the pharmacokinetics and/or metabolism of MK-1064 should be examined, although the equipotency of suvorexant and zolpidem in all four groups of mice rule out a generalised disruption in metabolism of female rTg4510 mice, *per se*.

Although the effectiveness of suvorexant and zolpidem, but not MK-1064, for promoting sleep indicates OX_2R dysregulation in female rTg4510 mice, it is also necessary to consider the potential effects of the interaction between tau pathology and sex/hormonal differences in rTg4510 mice. Sex hormones have been proposed to affect sleep-dependent memory consolidation (see Baker et al., 2019 for review), however, in Chapter 4, it was demonstrated that female WT mice responded robustly to chronic MK-1064 treatment and exhibited comparable spatial recall to males in the Barnes maze, suggesting the more generalised effects of sex hormone differences on sleep and memory alone (Paul et al., 2006; Mong et al., 2011) cannot explain the lack of sleep/wake response or cognitive improvement in female rTg4510 mice. Notable sex differences are present in AD and other dementias (although little is currently known regarding tau-variant frontotemporal dementia (FTD-tau)) in humans (Seshadri et al., 1997; Podcasy and Epperson, 2016; Laws et al., 2018), where incidence rates are more prevalent in the female population (Seshadri et al., 1997). These findings support that sex and hormonal differences in females may increase the risk of developing and/or accelerate neurodegenerative disease pathology (Seshadri et al., 1997).

In this context, estrogen and progesterone receptors are expressed in sleep/wake regulating nuclei such as the LC, dorsal raphe nucleus (DRN) and basal forebrain (Curran-Rauhut and Petersen, 2002; Baker et al., 2019). As discussed above (section 6.1.1), tau-induced

hyperexcitability of these nuclei may underlie the hyperarousal phenotype of rTg4510 mice. In female mice at the age investigated, these nuclei will also receive additional input from sex hormones that differ from male mice. In female rats, estradiol suppressed the activity of the sleep-promoting VLPO (Hadjimarkou et al., 2008). Furthermore, when estrogen and progesterone levels were at their peak, NREM and REM sleep were significantly decreased and wake time was increased during the active, but not inactive, phase (Hadjimarkou et al., 2008). It would therefore be of interest to assess estrogen and progesterone levels in female rTg4510 versus WT mice, to determine whether this may contribute to the exacerbated hyperarousal phenotype during the active phase in female rTg4510 mice and to the blunted response to MK-1064.

Indeed, previous studies have demonstrated that gonadal steroids regulate the expression of OX_1R and OX_2R in various organs (Johren et al., 2003; Silveyra et al., 2007a) and CNS tissue, including in the hypothalamus (Silveyra et al., 2007b; Silveyra et al., 2009). The expression levels of OX_1R and OX_2R were highest when sex hormones such as progesterone, estradiol, prolactin, luteinising hormone (LH) and follicle stimulating hormone (FSH) were at their peak (Silveyra et al., 2007b; Silveyra et al., 2009) and importantly, these effects were abolished in ovariectomised female rats, but were restored following estradiol administration (Silveyra et al., 2009). Despite the general effects of sex hormones on sleep/wake architecture and orexin receptor expression, it is evident from the present studies that the lack of response of female rTg4510 mice to MK-1064 is both sex- and tau-dependent.

It is worth noting, however, since MK-1064 selectively antagonises only orexin receptors, it does not have direct impact on estrogen/progesterone receptors. Therefore, in the presence of MK-1064, the activation of ARAS nuclei to promote hyperarousal could be mediated by sex hormone expression, their receptors, or down-stream signalling pathways of steroid receptors and/or OX_2R. Robust sleep responses were indeed observed in male mice of either genotype and in female WT mice following MK-1064, further implicating the dependence on tau for these sex-divergent effects.

The concept of estrogen/progesterone-mediated activation of the ARAS may align with the transient response to MK-1064 in female rTg4510 mice. It is hypothesised that the initial brain concentration of MK-1064 was sufficient to outweigh estrogen/progesterone-mediated ARAS activity. This activity may have quickly overridden the sleep-promoting effects of MK-1064 leading to the observed restoration of hyperarousal within 1-2 hours post-administration. The influence of female sex hormones and receptors on sleep and wakefulness further aligns with the comparable sleep-promoting effects of zolpidem in both male and female rTg4510

mice; given that zolpidem promotes sleep via a global suppression of all CNS activity via the $GABA_A$ receptor. The similar response to suvorexant in both male and female rTg4510 mice also aligns with the concept of heightened ARAS drive in female rTg4510 mice, since acute suvorexant administration during the active phase did not affect wake or NREM sleep (Chapter 5). Suvorexant disproportionately promoted REM sleep but did not affect overall sleep time, thus the hyperarousal drive of rTg4510 mice of either sex was not affected.

In summary, previous literature and the data presented within this thesis (Chapter 4 and 5) demonstrate that the 2-SORA MK-1064 promoted a more physiologically normal sleep in terms of NREM and REM sleep architecture, and did not negatively affect memory or global function, unlike the noted effects of benzodiazepines or Z-drugs such as zolpidem. Whatever the underlying cause of the blunted responses of female rTg4510 mice to MK-1064, it will be of interest to determine if these divergent sex effects translate to human tauopathy-related disorders. Hence, clinical trials and preclinical research must be performed in both sexes.

6.4 Limitations of the rTg4510 mouse model

Transgenic mouse models have been immensely valuable for accessibly investigating certain aspects of human disease/disorders. These models never fully recapitulate the complexity of the human disease but nevertheless play a vital role in advancing the understanding of some of the key mechanisms involved. All transgenic mouse models invariably have their own drawbacks and limitations, which limit the conclusions that can be drawn from findings. In mid-2019, a study (Gamache et al., 2019) identified drawbacks in the genetic construction of rTg4510 mice and cast some doubt over the validity of the neurodegenerative phenotype of the rTg4510 mouse in particular, and thus subsequent conclusions drawn from the extensive work previously carried out using this mouse model.

The rTg4510 mouse harbours two inserted transgenes: 1) human tau containing the P301L *MAPT* mutation which is downstream of a tetracycline operon-responsive element (TRE) and 2) the tetracycline-controlled transactivator (tTA) which is under control of the CaMKII promotor. The fact that tTA activity and tau expression are intrinsically linked in this mouse model precludes conclusively elucidating the individual impacts of each transgene on the phenotype of the rTg4510 mouse (Gamache et al., 2019). Gamache and colleagues report that when this mouse model was first generated the insertion of the transgenes disrupted/replaced other genes in the genome. The tau transgene insertion resulted in a ~250 kb pair deletion of the first exons and promotor regions of fibroblast growth factor 14 (*Fgf14*) and the tTA transgene insertion deleted ~500 kb pairs, disrupting another five genes (Gamache

et al., 2019). The authors conclude that the disruption of these genes, and particularly the disruption of *Fgf14*, contributes to the exacerbated neurodegenerative phenotype of rTg4510 mice.

A new transgenic mouse model was generated, designated rT2/T2, harbouring the same transgenes as rTg4510 mice, but without the disrupted *Fgf14* gene (Gamache et al., 2019). The temporal progression of neurodegeneration and brain atrophy commonly observed in rTg4510 mice was shifted in rT2/T2 mice, with these mice exhibiting comparable forebrain mass loss to 7-month-old rTg4510 mice only after 12 months of age, which for both transgenic models was markedly smaller than WT mice (Gamache et al., 2019). This finding suggests that a functional impact from the disruption of the *Fgf14* gene, other than the overexpression of the tau transgene, contributes to the premature brain atrophy observed in rTg4510 mice (Gamache et al., 2019). Despite occurring later than in rTg4510 mice, it should be noted that the rT2/T2 mouse still displays profound tau-dependent neurodegeneration (12 months onwards), demonstrating an important role for tau in this phenomenon. The hemizygous rT2 line (which contain the tTA transgene but with only modest overexpression of the tau transgene compared with rT2/T2 mice (58% of rT2/T2 as determined by qRT-PCR)) did not exhibit overt brain atrophy even by 18 months, nor did they develop the same level of tau histopathology as rT2/T2 or rTg4510 mice, as expected. Thus, these data indicate that tau overexpression is still a critically important contributor to the rTg4510 phenotype (Gamache et al., 2019).

The attenuation of the cognitive and neurodegenerative phenotype of rTg4510 mice following Dox treatment (which was scarcely discussed in Gamache et al., 2019) observed previously (Ramsden et al., 2005; Santacruz et al., 2005; Blackmore et al., 2017) and in this thesis (Chapter 3), further highlights the key contribution of mutant tau. Dox treatment effectively suppresses the expression of the tau transgene without restoring the function of the lost *Fgf14* gene or other disrupted genes. Therefore, even in the absence of *Fgf14*, the decrease in tau expression (and subsequent tau pathology) leads to significant physiological and functional improvements in rTg4510 mice. It should, however, be noted that Gamache and colleagues point out that it has not yet been conclusively proven whether the phenotype of rTg4510 (and rT2/T2) mice and their subsequent functional improvement following Dox treatment is specifically due to the high levels of mutant tau in particular, or rather to the extreme overexpression of an exogenous gene in general (Gamache et al., 2019). However, experiments with transgenic lines such as reporter mouse lines, for example, would suggest that overexpression of just any gene in general is not sufficient to drive neurodegeneration *per se* (Thakker et al., 2004; Ch'ng and Lawrence, 2015). In addition, the very similar sleep/wake

phenotype of both rTg4510 and PS19 mice (Holth et al., 2017b), which do not have extreme transgene overexpression (Yoshiyama et al., 2007) or exhibit non-targeted gene KO (Goodwin et al., 2019), supports the notion that mutant tau is essential to the rTg4510 hyperarousal phenotype.

In conclusion, it must be acknowledged that factors other than the overexpression of mutant tau and the development of tau pathology are contributing to the phenotype of rTg4510 mice. Nevertheless, the newly generated rT2/T2 mouse and phenotypic outcomes following Dox treatment in rTg4510 mice suggest that tau pathology contributes (and very substantially) to the phenotype of rTg4510 mice. The authors further state they are not asserting that any hypotheses regarding tau pathology generated from rTg4510 mouse studies are necessarily incorrect, simply that other factors must also be accounted for and considered (Gamache et al., 2019).

6.5 Summary and future directions

The research described in this thesis highlights the pivotal role that hyperphosphorylated tau plays in driving sleep/wake and cognitive disruptions in the rTg4510 transgenic mouse model of tauopathy. These data further support a bidirectional relationship between sleep and neurodegenerative pathology, particularly with regards to tau proteinopathies, and highlight the therapeutic potential of sleep in such neurodegenerative disorders.

rTg4510 males and tau KO mice exhibited decreased OX_1R mRNA expression in the sleep/wake-regulating LC, which may contribute to the hyperarousal phenotype observed in both these mouse models.

rTg4510 mice exhibited elevated tau and p-tau levels in the hippocampus and cortex, significant brain atrophy as assessed by MRI scanning, substantial spatial recall deficits in the Barnes maze and locomotor hyperactivity. Dox treatment approximately halved tau and p-tau protein levels, and all other parameters measured, with the exception of sleep, were substantially attenuated following tau transgene suppression with Dox from 4.5 months of age. rTg4510 mice further exhibited a disrupted sleep/wake phenotype which manifested primarily as a hyperarousal phenotype during the active phase. This phenotype may be a result of tau-induced hyperexcitability in wake-promoting nuclei, driven by orexinergic activity. The blunted effect of Dox on this phenotype indicates that tau-mediated insult to the arousal circuitry may be potentially irreversible by 4.5 months of age in rTg4510 mice.

The promotion of REM sleep during the inactive phase using the DORA suvorexant corrected the observed phenotypic deficit in this parameter but did not alter tau pathology or

improve cognition in rTg4510 mice. By contrast, attenuating the hyperarousal phenotype of these mice during the active phase using the 2-SORA MK-1064 resulted in a partial recovery of spatial recall, but only in male rTg4510 mice, which importantly correlated with MK-1064-promoted sleep time. Taken together, these data enabled the identification of key factors underlying cognitive restoration in rTg4510 mice: 1) substantial reductions in tau and p-tau levels in the hippocampus and cortex, 2) attenuation of hippocampal and cortical brain atrophy and white matter tracts through the corpus callosum, and 3) increased slow delta (1-2.5 Hz) power during NREM sleep associated with enhanced memory consolidation. These data are therefore the first to demonstrate the therapeutic potential of sleep in a neurodegenerative tauopathy mouse model.

The exacerbated hyperarousal phenotype of female rTg4510 mice combined with their blunted sleep/wake response to MK-1064, but not suvorexant or zolpidem, revealed striking sex differences in the rTg4510 model. These data highlight potential dysregulated OX_2R function and/or expression, altered pharmacokinetic or metabolism properties and/or sex hormone/receptor-mediated influences on the sleep/wake phenotype of female rTg4510 mice, which bear further investigation.

In light of the recent study by Gamache et al. (2019), additional limitations of the rTg4510 mouse model were discussed; however, they do not necessarily negate the relevance or validity of the findings contained within this thesis, especially given the important contribution of tau overexpression to the rTg4510 phenotype and the attenuation of tauopathy-like phenotypes following tau transgene suppression with Dox. The similar sleep/wake phenotype of rTg4510 and PS19 mice, further supports the concept that mutant tau contributes to the rTg4510 phenotype.

The findings arising from the present work reveal numerous questions that warrant further experiments. These experiments include:

1) Sleep/wake studies in rTg4510 mice following lifelong Dox treatment. Combined with the electrophysiological data from Crimins et al. (2012), where lifelong Dox treatment abolished all structural and functional alterations in rTg4510 neurons, it is hypothesised such treatment would indeed eradicate the disrupted sleep/wake phenotype of rTg4510 mice. Turning the transgene off at different time points to determine by which age the hyperarousal phenotype becomes permanent is also of interest.

2) Additional advanced sleep/wake studies in rTg4510 mice with similar designs to those from Chapter 4, however, including different treatment lengths and/or initiation points to help discern the range of cognitive improvement available using sleep as a therapeutic

approach. The use of zolpidem would also be interesting to investigate in similar sleep/wake studies, given the increase in NREM sleep achieved with this compound, despite the negative effects on memory. Assessing the effects of promoting sleep on the cognitive and tauopathy phenotype of the similar PS19, or newly generated rT2/T2 mouse, would also be a valuable experiment to cross-validate the therapeutic potential of sleep in another tauopathy model.

3) Given the evident absence of response of female rTg4510 mice to MK-1064, detailed studies assessing OX_2R function and expression in both male and female rTg4510 mice would be highly informative.

4) Pharmacokinetic studies following dosing of MK-1064 in both sexes in rTg4510 mice would help to discern the potential contribution of pharmacokinetics to the blunted response to MK-1064 and may help to rule out this effect as a contributing factor.

5) Assessment of sex hormone and estrogen/progesterone receptor differences in rTg4510 mice and their influence on tau- and sex-dependent responses to MK-1064 given the potential contribution of these systems to the exacerbated hyperarousal in female rTg4510 mice. Assessing whether ovariectomised female rTg4510 mice respond to MK-1064 treatment would also be of interest. If the response to MK-1064 is enhanced following ovariectomy in female rTg4510 mice, this would warrant further investigations into the sleep-promoting effects of MK-1064 in postmenopausal women with tauopathies.

6) Assess how sleep/wake function influences the temporal patterns of tau and p-tau, and the activity of GSK-3β and PP2A, thus further elucidating how sleep/wake states regulate tau dynamics.

Such experiments will hopefully aid in developing the understanding of how tau pathology contributes to development of sleep/wake and cognitive disruptions in neurodegenerative tauopathies and further highlight avenues for restoring normal sleep as a viable therapeutic treatment strategy for these devastating disorders.

References

Adamantidis AR, Zhang F, Aravanis AM, Deisseroth K, de Lecea L (2007) Neural substrates of awakening probed with optogenetic control of hypocretin neurons. Nature 450:420-424.

Akbari E, Naghdi N, Motamedi F (2006) Functional inactivation of orexin 1 receptors in CA1 region impairs acquisition, consolidation and retrieval in Morris water maze task. Behav Brain Res 173:47-52.

Allocca G et al. (2019) Validation of 'Somnivore', a Machine Learning Algorithm for Automated Scoring and Analysis of Polysomnography Data. Front Neurosci 13:207.

Alonso Adel C, Mederlyova A, Novak M, Grundke-Iqbal I, Iqbal K (2004) Promotion of hyperphosphorylation by frontotemporal dementia tau mutations. The Journal of biological chemistry 279:34873-34881.

Ancoli-Israel S, Clopton P, Klauber MR, Fell R, Mason W (1997) Use of wrist activity for monitoring sleep/wake in demented nursing-home patients. Sleep 20:24-27.

Ancoli-Israel S, Gehrman P, Martin JL, Shochat T, Marler M, Corey-Bloom J, Levi L (2003) Increased light exposure consolidates sleep and strengthens circadian rhythms in severe Alzheimer's disease patients. Behav Sleep Med 1:22-36.

Ancoli-Israel S, Palmer BW, Cooke JR, Corey-Bloom J, Fiorentino L, Natarajan L, Liu L, Ayalon L, He F, Loredo JS (2008) Cognitive effects of treating obstructive sleep apnea in Alzheimer's disease: a randomized controlled study. J Am Geriatr Soc 56:2076-2081.

Anderson KN, Hatfield C, Kipps C, Hastings M, Hodges JR (2009) Disrupted sleep and circadian patterns in frontotemporal dementia. Eur J Neurol 16:317-323.

Andreasen N, Minthon L, Davidsson P, Vanmechelen E, Vanderstichele H, Winblad B, Blennow K (2001) Evaluation of CSF-tau and CSF-A beta 42 as diagnostic markers for Alzheimer disease in clinical practice. Arch Neurol 58:373-379.

Arbilla S, Depoortere H, George P, Langer SZ (1985) Pharmacological profile of the imidazopyridine zolpidem at benzodiazepine receptors and electrocorticogram in rats. Naunyn Schmiedebergs Arch Pharmacol 330:248-251.

Asai H, Ikezu S, Tsunoda S, Medalla M, Luebke J, Haydar T, Wolozin B, Butovsky O, Kugler S, Ikezu T (2015) Depletion of microglia and inhibition of exosome synthesis halt tau propagation. Nat Neurosci 18:1584-1593.

Asayama K, Yamadera H, Ito T, Suzuki H, Kudo Y, Endo S (2003) Double blind study of melatonin effects on the sleep-wake rhythm, cognitive and non-cognitive functions in Alzheimer type dementia. J Nippon Med Sch 70:334-341.

Aston-Jones G, Bloom FE (1981) Activity of norepinephrine-containing locus coeruleus neurons in behaving rats anticipates fluctuations in the sleep-waking cycle. J Neurosci 1:876-886.

Auld DS, Kornecook TJ, Bastianetto S, Quirion R (2002) Alzheimer's disease and the basal forebrain cholinergic system: relations to beta-amyloid peptides, cognition, and treatment strategies. Prog Neurobiol 68:209-245.

Avila J, Lucas JJ, Perez M, Hernandez F (2004) Role of tau protein in both physiological and pathological conditions. Physiological reviews 84:361-384.

Backhaus J, Born J, Hoeckesfeld R, Fokuhl S, Hohagen F, Junghanns K (2007) Midlife decline in declarative memory consolidation is correlated with a decline in slow wave sleep. Learn Mem 14:336-341.

Baker FC, Sattari N, de Zambotti M, Goldstone A, Alaynick WA, Mednick SC (2019) Impact of sex steroids and reproductive stage on sleep-dependent memory consolidation in women. Neurobiol Learn Mem 160:118-131.

Baker TL, Foutz AS, McNerney V, Mitler MM, Dement WC (1982) Canine model of narcolepsy: genetic and developmental determinants. Exp Neurol 75:729-742.

Bakker A, Krauss GL, Albert MS, Speck CL, Jones LR, Stark CE, Yassa MA, Bassett SS, Shelton AL, Gallagher M (2012) Reduction of hippocampal hyperactivity improves cognition in amnestic mild cognitive impairment. Neuron 74:467-474.

Balkin TJ, O'Donnell VM, Wesensten N, McCann U, Belenky G (1992) Comparison of the daytime sleep and performance effects of zolpidem versus triazolam. Psychopharmacology (Berl) 107:83-88.

Ballard C, Gauthier S, Corbett A, Brayne C, Aarsland D, Jones E (2011) Alzheimer's disease. Lancet 377:1019-1031.

Ballatore C, Lee VM, Trojanowski JQ (2007) Tau-mediated neurodegeneration in Alzheimer's disease and related disorders. Nat Rev Neurosci 8:663-672.

Barnes CA (1979) Memory deficits associated with senescence: a neurophysiological and behavioral study in the rat. J Comp Physiol Psychol 93:74-104.

Bartus RT, Dean RL, 3rd, Beer B, Lippa AS (1982) The cholinergic hypothesis of geriatric memory dysfunction. Science 217:408-414.

Bateman RJ, Munsell LY, Morris JC, Swarm R, Yarasheski KE, Holtzman DM (2006) Human amyloid-beta synthesis and clearance rates as measured in cerebrospinal fluid in vivo. Nat Med 12:856-861.

Bathgate D, Snowden JS, Varma A, Blackshaw A, Neary D (2001) Behaviour in frontotemporal dementia, Alzheimer's disease and vascular dementia. Acta Neurol Scand 103:367-378.

Baumann K, Mandelkow EM, Biernat J, Piwnica-Worms H, Mandelkow E (1993) Abnormal Alzheimer-like phosphorylation of tau-protein by cyclin-dependent kinases cdk2 and cdk5. FEBS Lett 336:417-424.

Beauchamp LC, Chan J, Hung LW, Padman BS, Vella LJ, Liu XM, Coleman B, Bush AI, Lazarou M, Hill AF, Jacobson L, Barnham KJ (2018) Ablation of tau causes an olfactory deficit in a murine model of Parkinson's disease. Acta Neuropathol Commun 6:57.

Bellesi M, de Vivo L, Chini M, Gilli F, Tononi G, Cirelli C (2017) Sleep Loss Promotes Astrocytic Phagocytosis and Microglial Activation in Mouse Cerebral Cortex. J Neurosci 37:5263-5273.

Benedict C, Byberg L, Cedernaes J, Hogenkamp PS, Giedratis V, Kilander L, Lind L, Lannfelt L, Schioth HB (2015) Self-reported sleep disturbance is associated with Alzheimer's disease risk in men. Alzheimers Dement 11:1090-1097.

Bernard-Valnet R, Yshii L, Queriault C, Nguyen XH, Arthaud S, Rodrigues M, Canivet A, Morel AL, Matthys A, Bauer J, Pignolet B, Dauvilliers Y, Peyron C, Liblau RS (2016) CD8 T cell-mediated killing of orexinergic neurons induces a narcolepsy-like phenotype in mice. Proceedings of the National Academy of Sciences of the United States of America 113:10956-10961.

Bernardis LL, Bellinger LL (1993) The lateral hypothalamic area revisited: neuroanatomy, body weight regulation, neuroendocrinology and metabolism. Neurosci Biobehav Rev 17:141-193.

Bero AW, Yan P, Roh JH, Cirrito JR, Stewart FR, Raichle ME, Lee JM, Holtzman DM (2011) Neuronal activity regulates the regional vulnerability to amyloid-beta deposition. Nat Neurosci 14:750-756.

Bero AW, Bauer AQ, Stewart FR, White BR, Cirrito JR, Raichle ME, Culver JP, Holtzman DM (2012) Bidirectional relationship between functional connectivity and amyloid-beta deposition in mouse brain. J Neurosci 32:4334-4340.

Betschart C, Hintermann S, Behnke D, Cotesta S, Fendt M, Gee CE, Jacobson LH, Laue G, Ofner S, Chaudhari V, Badiger S, Pandit C, Wagner J, Hoyer D (2013) Identification of a novel series of orexin receptor antagonists with a distinct effect on sleep architecture for the treatment of insomnia. Journal of medicinal chemistry 56:7590-7607.

Bettica P, Squassante L, Groeger JA, Gennery B, Winsky-Sommerer R, Dijk DJ (2012a) Differential effects of a dual orexin receptor antagonist (SB-649868) and zolpidem on sleep initiation and consolidation, SWS, REM sleep, and EEG power spectra in a model of situational insomnia. Neuropsychopharmacology 37:1224-1233.

Bettica P, Squassante L, Zamuner S, Nucci G, Danker-Hopfe H, Ratti E (2012b) The orexin antagonist SB-649868 promotes and maintains sleep in men with primary insomnia. Sleep 35:1097-1104.

Bettica P, Nucci G, Pyke C, Squassante L, Zamuner S, Ratti E, Gomeni R, Alexander R (2012c) Phase I studies on the safety, tolerability, pharmacokinetics and pharmacodynamics of SB-649868, a novel dual orexin receptor antagonist. J Psychopharmacol 26:1058-1070.

Beuckmann CT, Sinton CM, Williams SC, Richardson JA, Hammer RE, Sakurai T, Yanagisawa M (2004) Expression of a poly-glutamine-ataxin-3 transgene in orexin neurons induces narcolepsy-cataplexy in the rat. J Neurosci 24:4469-4477.

Biernat J, Gustke N, Drewes G, Mandelkow EM, Mandelkow E (1993) Phosphorylation of Ser(262) Strongly Reduces Binding of Tau-Protein to Microtubules - Distinction between Phf-Like Immunoreactivity and Microtubule-Binding. Neuron 11:153-163.

Binder S, Berg K, Gasca F, Lafon B, Parra LC, Born J, Marshall L (2014) Transcranial slow oscillation stimulation during sleep enhances memory consolidation in rats. Brain Stimul 7:508-515.

Bingham S, Davey PT, Babbs AJ, Irving EA, Sammons MJ, Wyles M, Jeffrey P, Cutler L, Riba I, Johns A, Porter RA, Upton N, Hunter AJ, Parsons AA (2001) Orexin-A, an hypothalamic peptide with analgesic properties. Pain 92:81-90.

Blackmore T, Meftah S, Murray TK, Craig PJ, Blockeel A, Phillips K, Eastwood B, O'Neill MJ, Marston H, Ahmed Z, Gilmour G, Gastambide F (2017) Tracking progressive pathological and functional decline in the rTg4510 mouse model of tauopathy. Alzheimers Res Ther 9:77.

Blackwell T, Yaffe K, Ancoli-Israel S, Scheider JL, Cauley JA, Hillier TA, Fink HA, Stone KL, Grp SOF (2006) Poor sleep is associated with impaired cognitive function in older women: The Study of Osteoporotic Fractures. J Gerontol a-Biol 61:405-410.

Blennow K, Hampel H (2003) CSF markers for incipient Alzheimer's disease. Lancet Neurol 2:605-613.

Blennow K, Vanmechelen E, Hampel H (2001) CSF total tau, a beta 42 and phosphorylated tau protein as biomarkers for Alzheimer's disease. Mol Neurobiol 24:87-97.

Blennow K, de Leon MJ, Zetterberg H (2006) Alzheimer's disease. Lancet 368:387-403.

Blennow K, Hampel H, Weiner M, Zetterberg H (2010) Cerebrospinal fluid and plasma biomarkers in Alzheimer disease. Nat Rev Neurol 6:131-144.

Boespflug EL, Iliff JJ (2018) The Emerging Relationship Between Interstitial Fluid-Cerebrospinal Fluid Exchange, Amyloid-beta, and Sleep. Biol Psychiatry 83:328-336.

Boland E, Goldschmied J, Kayser MS, Gehrman PR (2019) Precision Medicine for Insomnia. Sleep Med Clin 14:291-+.

Bonakis A, Economou NT, Paparrigopoulos T, Bonanni E, Maestri M, Carnicelli L, Di Coscio E, Ktonas P, Vagiakis E, Theodoropoulos P, Papageorgiou SG (2014) Sleep in frontotemporal dementia is equally or possibly more disrupted, and at an earlier stage, when compared to sleep in Alzheimer's disease. J Alzheimers Dis 38:85-91.

Bonanni E, Maestri M, Tognoni G, Fabbrini M, Nucciarone B, Manca ML, Gori S, Iudice A, Murri L (2005) Daytime sleepiness in mild and moderate Alzheimer's disease and its relationship with cognitive impairment. J Sleep Res 14:311-317.

Bonaventure P, Shelton J, Yun S, Nepomuceno D, Sutton S, Aluisio L, Fraser I, Lord B, Shoblock J, Welty N, Chaplan SR, Aguilar Z, Halter R, Ndifor A, Koudriakova T, Rizzolio M, Letavic M, Carruthers NI, Lovenberg T, Dugovic C (2015) Characterization of JNJ-42847922, a Selective Orexin-2 Receptor Antagonist, as a Clinical Candidate for the Treatment of Insomnia. J Pharmacol Exp Ther 354:471-482.

Bondareff W, Mountjoy CQ, Roth M (1982) Loss of neurons of origin of the adrenergic projection to cerebral cortex (nucleus locus ceruleus) in senile dementia. Neurology 32:164-168.

Bondareff W, Mountjoy CQ, Roth M, Rossor MN, Iversen LL, Reynolds GP, Hauser DL (1987) Neuronal degeneration in locus ceruleus and cortical correlates of Alzheimer disease. Alzheimer Dis Assoc Disord 1:256-262.

Bourgin P, Huitron-Resendiz S, Spier AD, Fabre V, Morte B, Criado JR, Sutcliffe JG, Henriksen SJ, de Lecea L (2000) Hypocretin-1 modulates rapid eye movement sleep through activation of locus coeruleus neurons. J Neurosci 20:7760-7765.

Boyce R, Glasgow SD, Williams S, Adamantidis A (2016) Causal evidence for the role of REM sleep theta rhythm in contextual memory consolidation. Science 352:812-816.

Braak H, Braak E (1991a) Alzheimers-Disease Affects Limbic Nuclei of the Thalamus. Acta Neuropathol 81:261-268.

Braak H, Braak E (1991b) Neuropathological Staging of Alzheimer-Related Changes. Acta Neuropathol 82:239-259.

Braak H, Braak E (1995) Staging of Alzheimer's disease-related neurofibrillary changes. Neurobiol Aging 16:271-278.

Braak H, Braak E (1997) Frequency of stages of Alzheimer-related lesions in different age categories. Neurobiol Aging 18:351-357.

Braak H, Del Tredici K (2004) Alzheimer's disease: intraneuronal alterations precede insoluble amyloid-beta formation. Neurobiol Aging 25:713-718; discussion 743-716.

Braak H, Del Tredici K (2011) The pathological process underlying Alzheimer's disease in individuals under thirty. Acta Neuropathol 121:171-181.

Braak H, Del Tredici K (2015) The preclinical phase of the pathological process underlying sporadic Alzheimer's disease. Brain 138:2814-2833.

Braak H, Braak E, Bohl J, Reintjes R (1996) Age, neurofibrillary changes, A beta-amyloid and the onset of Alzheimer's disease. Neurosci Lett 210:87-90.

Braak H, Thal DR, Ghebremedhin E, Del Tredici K (2011) Stages of the pathologic process in Alzheimer disease: age categories from 1 to 100 years. J Neuropathol Exp Neurol 70:960-969.

Braak H, Alafuzoff I, Arzberger T, Kretzschmar H, Del Tredici K (2006) Staging of Alzheimer disease-associated neurofibrillary pathology using paraffin sections and immunocytochemistry. Acta Neuropathol 112:389-404.

Branch AF, Navidi W, Tabuchi S, Terao A, Yamanaka A, Scammell TE, Diniz Behn C (2016) Progressive Loss of the Orexin Neurons Reveals Dual Effects on Wakefulness. Sleep 39:369-377.

Branger P, Arenaza-Urquijo EM, Tomadesso C, Mezenge F, Andre C, de Flores R, Mutlu J, de La Sayette V, Eustache F, Chetelat G, Rauchs G (2016) Relationships between sleep quality and brain volume, metabolism, and amyloid deposition in late adulthood. Neurobiol Aging 41:107-114.

Brayet P, Petit D, Frauscher B, Gagnon JF, Gosselin N, Gagnon K, Rouleau I, Montplaisir J (2016) Quantitative EEG of Rapid-Eye-Movement Sleep: A Marker of Amnestic Mild Cognitive Impairment. Clin EEG Neurosci 47:134-141.

Brenner RP, Ulrich RF, Spiker DG, Sclabassi RJ, Reynolds CF, 3rd, Marin RS, Boller F (1986) Computerized EEG spectral analysis in elderly normal, demented and depressed subjects. Electroencephalogr Clin Neurophysiol 64:483-492.

Brisbare-Roch C, Dingemanse J, Koberstein R, Hoever P, Aissaoui H, Flores S, Mueller C, Nayler O, van Gerven J, de Haas SL, Hess P, Qiu C, Buchmann S, Scherz M, Weller T, Fischli W, Clozel M, Jenck F (2007) Promotion of sleep by targeting the orexin system in rats, dogs and humans. Nat Med 13:150-155.

Brody DL, Magnoni S, Schwetye KE, Spinner ML, Esparza TJ, Stocchetti N, Zipfel GJ, Holtzman DM (2008) Amyloid-beta dynamics correlate with neurological status in the injured human brain. Science 321:1221-1224.

Bron R, Yin L, Russo D, Furness JB (2013) Expression of the ghrelin receptor gene in neurons of the medulla oblongata of the rat. J Comp Neurol 521:2680-2702.

Bron R, Wood RJ, Brock JA, Ivanusic JJ (2014) Piezo2 expression in corneal afferent neurons. J Comp Neurol 522:2967-2979.

Brown BM, Rainey-Smith SR, Villemagne VL, Weinborn M, Bucks RS, Sohrabi HR, Laws SM, Taddei K, Macaulay SL, Ames D, Fowler C, Maruff P, Masters CL, Rowe CC, Martins RN, Group AR (2016) The Relationship between Sleep Quality and Brain Amyloid Burden. Sleep 39:1063-1068.

Brown RE, Sergeeva O, Eriksson KS, Haas HL (2001) Orexin A excites serotonergic neurons in the dorsal raphe nucleus of the rat. Neuropharmacology 40:457-459.

Buckner RL, Andrews-Hanna JR, Schacter DL (2008) The brain's default network - Anatomy, function, and relevance to disease. In: Year in Cognitive Neuroscience 2008 (Kingstone A, Miller MB, eds), pp 1-38. Malden: Wiley-Blackwell.

Buckner RL, Snyder AZ, Shannon BJ, LaRossa G, Sachs R, Fotenos AF, Sheline YI, Klunk WE, Mathis CA, Morris JC, Mintun MA (2005) Molecular, structural, and functional characterization of Alzheimer's disease: evidence for a relationship between default activity, amyloid, and memory. J Neurosci 25:7709-7717.

Buee L, Bussiere T, Buee-Scherrer V, Delacourte A, Hof PR (2000) Tau protein isoforms, phosphorylation and role in neurodegenerative disorders. Brain Res Brain Res Rev 33:95-130.

Burke SL, Hu T, Spadola CE, Burgess A, Li T, Cadet T (2019) Treatment of Sleep Disturbance May Reduce the Risk of Future Probable Alzheimer's Disease. J Aging Health 31:322-342.

Busche MA, Wegmann S, Dujardin S, Commins C, Schiantarelli J, Klickstein N, Kamath TV, Carlson GA, Nelken I, Hyman BT (2019) Tau impairs neural circuits, dominating amyloid-beta effects, in Alzheimer models in vivo. Nat Neurosci 22:57-64.

Busser J, Geldmacher DS, Herrup K (1998) Ectopic cell cycle proteins predict the sites of neuronal cell death in Alzheimer's disease brain. J Neurosci 18:2801-2807.

Buysse DJ (2013) Insomnia. Jama 309:706-716.

Cagnin A, Fragiacomo F, Camporese G, Turco M, Busse C, Ermani M, Montagnese S (2017) Sleep-Wake Profile in Dementia with Lewy Bodies, Alzheimer's Disease, and Normal Aging. J Alzheimers Dis 55:1529-1536.

Callander GE, Olorunda M, Monna D, Schuepbach E, Langenegger D, Betschart C, Hintermann S, Behnke D, Cotesta S, Fendt M, Laue G, Ofner S, Briard E, Gee CE, Jacobson LH, Hoyer D (2013) Kinetic properties of "dual" orexin receptor antagonists at OX1R and OX2R orexin receptors. Front Neurosci 7:230.

Campbell IG (2009) EEG recording and analysis for sleep research. Curr Protoc Neurosci Chapter 10:Unit10 12.

Cantero JL, Hita-Yanez E, Moreno-Lopez B, Portillo F, Rubio A, Avila J (2010) Tau protein role in sleep-wake cycle. J Alzheimers Dis 21:411-421.

Carmona S, Hardy J, Guerreiro R (2018) The genetic landscape of Alzheimer disease. Handb Clin Neurol 148:395-408.

Carter ME, Brill J, Bonnavion P, Huguenard JR, Huerta R, de Lecea L (2012) Mechanism for Hypocretin-mediated sleep-to-wake transitions. Proceedings of the National Academy of Sciences of the United States of America 109:E2635-2644.

Carter ME, Yizhar O, Chikahisa S, Nguyen H, Adamantidis A, Nishino S, Deisseroth K, de Lecea L (2010) Tuning arousal with optogenetic modulation of locus coeruleus neurons. Nat Neurosci 13:1526-1533.

Cedernaes J, Osorio RS, Varga AW, Kam K, Schioth HB, Benedict C (2017) Candidate mechanisms underlying the association between sleep-wake disruptions and Alzheimer's disease. Sleep Med Rev 31:102-111.

Ch'ng SS, Lawrence AJ (2015) Distribution of the orexin-1 receptor (OX1R) in the mouse forebrain and rostral brainstem: A characterisation of OX1R-eGFP mice. J Chem Neuroanat 66-67:1-9.

Chauvette S, Seigneur J, Timofeev I (2012) Sleep oscillations in the thalamocortical system induce long-term neuronal plasticity. Neuron 75:1105-1113.

Chemelli RM, Willie JT, Sinton CM, Elmquist JK, Scammell T, Lee C, Richardson JA, Williams SC, Xiong Y, Kisanuki Y, Fitch TE, Nakazato M, Hammer RE, Saper CB, Yanagisawa M (1999) Narcolepsy in orexin knockout mice: molecular genetics of sleep regulation. Cell 98:437-451.

Chen CP, Eastwood SL, Hope T, McDonald B, Francis PT, Esiri MM (2000) Immunocytochemical study of the dorsal and median raphe nuclei in patients with Alzheimer's disease prospectively assessed for behavioural changes. Neuropathol Appl Neurobiol 26:347-355.

Chen DW, Wang J, Zhang LL, Wang YJ, Gao CY (2018) Cerebrospinal Fluid Amyloid-beta Levels are Increased in Patients with Insomnia. J Alzheimers Dis 61:645-651.

Chen Q, de Lecea L, Hu Z, Gao D (2015) The hypocretin/orexin system: an increasingly important role in neuropsychiatry. Med Res Rev 35:152-197.

Cirrito JR, Kang JE, Lee J, Stewart FR, Verges DK, Silverio LM, Bu G, Mennerick S, Holtzman DM (2008) Endocytosis is required for synaptic activity-dependent release of amyloid-beta in vivo. Neuron 58:42-51.

Cirrito JR, Yamada KA, Finn MB, Sloviter RS, Bales KR, May PC, Schoepp DD, Paul SM, Mennerick S, Holtzman DM (2005) Synaptic activity regulates interstitial fluid amyloid-beta levels in vivo. Neuron 48:913-922.

Colby-Milley J, Cavanagh C, Jego S, Breitner JC, Quirion R, Adamantidis A (2015) Sleep-Wake Cycle Dysfunction in the TgCRND8 Mouse Model of Alzheimer's Disease: From Early to Advanced Pathological Stages. PLoS One 10:e0130177.

Coleman PJ, Cox CD, Roecker AJ (2011) Discovery of dual orexin receptor antagonists (DORAs) for the treatment of insomnia. Curr Top Med Chem 11:696-725.

Coleman PJ et al. (2012) Discovery of [(2R,5R)-5-{[(5-fluoropyridin-2-yl)oxy]methyl}-2-methylpiperidin-1-yl][5-methyl-2 -(pyrimidin-2-yl)phenyl]methanone (MK-6096): a dual orexin receptor antagonist with potent sleep-promoting properties. ChemMedChem 7:415-424, 337.

Connor K, Budd K, Snavely D, Liu K, Hutzel-Mann J, Benca R, Krystal A, Roth T, Michelson D, Herring WJ (2012) Efficacy and safety of suvorexant, an orexin receptor antagonist, in patients with primary insomnia: a 3-month phase 3 trial (trial #1). J Sleep Res 21:97-97.

Cook C, Dunmore JH, Murray ME, Scheffel K, Shukoor N, Tong J, Castanedes-Casey M, Phillips V, Rousseau L, Penuliar MS, Kurti A, Dickson DW, Petrucelli L, Fryer JD (2014) Severe amygdala dysfunction in a MAPT transgenic mouse model of frontotemporal dementia. Neurobiol Aging 35:1769-1777.

Cortelli P, Gambetti P, Montagna P, Lugaresi E (1999) Fatal familial insomnia: clinical features and molecular genetics. J Sleep Res 8 Suppl 1:23-29.

Cox CD et al. (2010) Discovery of the dual orexin receptor antagonist [(7R)-4-(5-chloro-1,3-benzoxazol-2-yl)-7-methyl-1,4-diazepan-1-yl][5-methyl-2-(2H -1,2,3-triazol-2-yl)phenyl]methanone (MK-4305) for the treatment of insomnia. Journal of medicinal chemistry 53:5320-5332.

Coyle JT, Price DL, Delong MR (1983) Alzheimers-Disease - a Disorder of Cortical Cholinergic Innervation. Science 219:1184-1190.

Craig-Schapiro R, Fagan AM, Holtzman DM (2009) Biomarkers of Alzheimer's disease. Neurobiol Dis 35:128-140.

Crimins JL, Rocher AB, Luebke JI (2012) Electrophysiological changes precede morphological changes to frontal cortical pyramidal neurons in the rTg4510 mouse model of progressive tauopathy. Acta Neuropathol 124:777-795.

Crimins JL, Rocher AB, Peters A, Shultz P, Lewis J, Luebke JI (2011) Homeostatic responses by surviving cortical pyramidal cells in neurodegenerative tauopathy. Acta Neuropathol 122:551-564.

Crocker A, Espana RA, Papadopoulou M, Saper CB, Faraco J, Sakurai T, Honda M, Mignot E, Scammell TE (2005) Concomitant loss of dynorphin, NARP, and orexin in narcolepsy. Neurology 65:1184-1188.

Crowley K (2011) Sleep and sleep disorders in older adults. Neuropsychol Rev 21:41-53.

Cummings JL, Morstorf T, Zhong K (2014) Alzheimer's disease drug-development pipeline: few candidates, frequent failures. Alzheimers Res Ther 6:37.

Curran-Rauhut MA, Petersen SL (2002) The distribution of progestin receptor mRNA in rat brainstem. Brain Res Gene Expr Patterns 1:151-157.

Daulatzai MA (2016) Dysfunctional Sensory Modalities, Locus Coeruleus, and Basal Forebrain: Early Determinants that Promote Neuropathogenesis of Cognitive and Memory Decline and Alzheimer's Disease. Neurotoxicity research 30:295-337.

Dauvilliers Y, Siegel JM, Lopez R, Torontali ZA, Peever JH (2014a) Cataplexy--clinical aspects, pathophysiology and management strategy. Nat Rev Neurol 10:386-395.

Dauvilliers YA, Lehmann S, Jaussent I, Gabelle A (2014b) Hypocretin and brain beta-amyloid peptide interactions in cognitive disorders and narcolepsy. Front Aging Neurosci 6:119.

Davies J, Chen J, Pink R, Carter D, Saunders N, Sotiriadis G, Bai B, Pan Y, Howlett D, Payne A, Randeva H, Karteris E (2015) Orexin receptors exert a neuroprotective effect in Alzheimer's disease (AD) via heterodimerization with GPR103. Sci Rep 5:12584.

Davies P, Maloney AJF (1976) Selective Loss of Central Cholinergic Neurons in Alzheimers-Disease. Lancet 2:1403-1403.

Dawson HN, Ferreira A, Eyster MV, Ghoshal N, Binder LI, Vitek MP (2001) Inhibition of neuronal maturation in primary hippocampal neurons from tau deficient mice. J Cell Sci 114:1179-1187.

de Lecea L (2015) Optogenetic control of hypocretin (orexin) neurons and arousal circuits. Curr Top Behav Neurosci 25:367-378.

de Lecea L, Carter ME, Adamantidis A (2012) Shining light on wakefulness and arousal. Biol Psychiatry 71:1046-1052.

de Lecea L, Kilduff TS, Peyron C, Gao X, Foye PE, Danielson PE, Fukuhara C, Battenberg EL, Gautvik VT, Bartlett FS, 2nd, Frankel WN, van den Pol AN, Bloom FE, Gautvik KM, Sutcliffe JG (1998) The hypocretins: hypothalamus-specific peptides with neuroexcitatory activity. Proceedings of the National Academy of Sciences of the United States of America 95:322-327.

De Strooper B, Karran E (2016) The Cellular Phase of Alzheimer's Disease. Cell 164:603-615.

Defrancesco M, Marksteiner J, Fleischhacker WW, Blasko I (2015) Use of Benzodiazepines in Alzheimer's Disease: A Systematic Review of Literature. Int J Neuropsychopharmacol 18:pyv055.

Despres C, Byrne C, Qi H, Cantrelle FX, Huvent I, Chambraud B, Baulieu EE, Jacquot Y, Landrieu I, Lippens G, Smet-Nocca C (2017) Identification of the Tau phosphorylation pattern that drives its aggregation. Proceedings of the National Academy of Sciences of the United States of America 114:9080-9085.

Deuschle M, Schilling C, Leweke FM, Enning F, Pollmacher T, Esselmann H, Wiltfang J, Frolich L, Heuser I (2014) Hypocretin in cerebrospinal fluid is positively correlated with Tau and pTau. Neurosci Lett 561:41-45.

Di Meco A, Joshi YB, Pratico D (2014) Sleep deprivation impairs memory, tau metabolism, and synaptic integrity of a mouse model of Alzheimer's disease with plaques and tangles. Neurobiol Aging 35:1813-1820.

Dickson DW (1997) The pathogenesis of senile plaques. J Neuropathol Exp Neurol 56:321-339.

Diekelmann S, Born J (2010) The memory function of sleep. Nat Rev Neurosci 11:114-126.

Dietrich H, Jenck F (2010) Intact learning and memory in rats following treatment with the dual orexin receptor antagonist almorexant. Psychopharmacology (Berl) 212:145-154.

Diniz Behn CG, Klerman EB, Mochizuki T, Lin SC, Scammell TE (2010) Abnormal sleep/wake dynamics in orexin knockout mice. Sleep 33:297-306.

Docherty JR, Stanford SC, Panattieri RA, Alexander SPH, Cirino G, George CH, Hoyer D, Izzo AA, Ji Y, Lilley E, Sobey CG, Stanley P, Stefanska B, Stephens G, Teixeira M, Ahluwalia A (2019) Sex: A change in our guidelines to authors to ensure that this is no longer an ignored experimental variable. Br J Pharmacol 176:4081-4086.

Dowling GA, Hubbard EM, Mastick J, Luxenberg JS, Burr RL, Van Someren EJ (2005) Effect of morning bright light treatment for rest-activity disruption in institutionalized patients with severe Alzheimer's disease. Int Psychogeriatr 17:221-236.

Dowling GA, Burr RL, Van Someren EJ, Hubbard EM, Luxenberg JS, Mastick J, Cooper BA (2008) Melatonin and bright-light treatment for rest-activity disruption in institutionalized patients with Alzheimer's disease. J Am Geriatr Soc 56:239-246.

Drieu C, Zugaro M (2019) Hippocampal Sequences During Exploration: Mechanisms and Functions. Front Cell Neurosci 13:232.

Dugovic C, Shelton JE, Yun S, Bonaventure P, Shireman BT, Lovenberg TW (2014) Orexin-1 receptor blockade dysregulates REM sleep in the presence of orexin-2 receptor antagonism. Front Neurosci 8:28.

Dugovic C, Shelton JE, Aluisio LE, Fraser IC, Jiang X, Sutton SW, Bonaventure P, Yun S, Li X, Lord B, Dvorak CA, Carruthers NI, Lovenberg TW (2009) Blockade of orexin-1 receptors attenuates orexin-2 receptor antagonism-induced sleep promotion in the rat. J Pharmacol Exp Ther 330:142-151.

Duncan MJ, Smith JT, Franklin KM, Beckett TL, Murphy MP, St Clair DK, Donohue KD, Striz M, O'Hara BF (2012) Effects of aging and genotype on circadian rhythms, sleep, and clock gene expression in APPxPS1 knock-in mice, a model for Alzheimer's disease. Exp Neurol 236:249-258.

Duxon MS, Stretton J, Starr K, Jones DNC, Holland V, Riley G, Jerman J, Brough S, Smart D, Johns A, Chan W, Porter RA, Upton N (2001) Evidence that orexin-A-evoked grooming in the rat is mediated by orexin-1 (OX1) receptors, with downstream 5-HT2C receptor involvement. Psychopharmacology 153:203-209.

Eriksson KS, Sergeeva O, Brown RE, Haas HL (2001) Orexin/hypocretin excites the histaminergic neurons of the tuberomammillary nucleus. J Neurosci 21:9273-9279.

Estabrooke IV, McCarthy MT, Ko E, Chou TC, Chemelli RM, Yanagisawa M, Saper CB, Scammell TE (2001) Fos expression in orexin neurons varies with behavioral state. J Neurosci 21:1656-1662.

Everson CA, Henchen CJ, Szabo A, Hogg N (2014) Cell injury and repair resulting from sleep loss and sleep recovery in laboratory rats. Sleep 37:1929-1940.

Fagan AM, Holtzman DM (2010) Cerebrospinal fluid biomarkers of Alzheimer's disease. Biomark Med 4:51-63.

Fagan AM, Mintun MA, Mach RH, Lee SY, Dence CS, Shah AR, LaRossa GN, Spinner ML, Klunk WE, Mathis CA, DeKosky ST, Morris JC, Holtzman DM (2006) Inverse relation between in vivo amyloid imaging load and cerebrospinal fluid Abeta42 in humans. Ann Neurol 59:512-519.

Feld GB, Wilhelm I, Ma Y, Groch S, Binkofski F, Molle M, Born J (2013) Slow wave sleep induced by GABA agonist tiagabine fails to benefit memory consolidation. Sleep 36:1317-1326.

Feng Z, Qin C, Chang Y, Zhang JT (2006) Early melatonin supplementation alleviates oxidative stress in a transgenic mouse model of Alzheimer's disease. Free Radic Biol Med 40:101-109.

Fetveit A, Bjorvatn B (2005) Bright-light treatment reduces actigraphic-measured daytime sleep in nursing home patients with dementia: a pilot study. Am J Geriatr Psychiatry 13:420-423.

Fetveit A, Skjerve A, Bjorvatn B (2003) Bright light treatment improves sleep in institutionalised elderly--an open trial. Int J Geriatr Psychiatry 18:520-526.

Forrest SL, Kril JJ, Stevens CH, Kwok JB, Hallupp M, Kim WS, Huang Y, McGinley CV, Werka H, Kiernan MC, Gotz J, Spillantini MG, Hodges JR, Ittner LM, Halliday GM (2018) Retiring the term FTDP-17 as MAPT mutations are genetic forms of sporadic frontotemporal tauopathies. Brain 141:521-534.

Foutz AS, Mitler MM, Cavalli-Sforza LL, Dement WC (1979) Genetic factors in canine narcolepsy. Sleep 1:413-421.

Fox SV, Gotter AL, Tye SJ, Garson SL, Savitz AT, Uslaner JM, Brunner JI, Tannenbaum PL, McDonald TP, Hodgson R, Yao L, Bowlby MR, Kuduk SD, Coleman PJ, Hargreaves R, Winrow CJ, Renger JJ (2013) Quantitative electroencephalography within sleep/wake states differentiates GABAA modulators eszopiclone and zolpidem from dual orexin receptor antagonists in rats. Neuropsychopharmacology 38:2401-2408.

Franken P, Malafosse A, Tafti M (1998) Genetic variation in EEG activity during sleep in inbred mice. Am J Physiol-Regul Integr Comp Physiol 275:R1127-1137.

Friedman LF, Zeitzer JM, Lin L, Hoff D, Mignot E, Peskind ER, Yesavage JA (2007) In Alzheimer disease, increased wake fragmentation found in those with lower hypocretin-1. Neurology 68:793-794.

Fronczek R, van Geest S, Frolich M, Overeem S, Roelandse FW, Lammers GJ, Swaab DF (2012) Hypocretin (orexin) loss in Alzheimer's disease. Neurobiol Aging 33:1642-1650.

Fujiki N, Yoshida Y, Ripley B, Honda K, Mignot E, Nishino S (2001) Changes in CSF hypocretin-1 (orexin A) levels in rats across 24 hours and in response to food deprivation. Neuroreport 12:993-997.

Gabelle A, Jaussent I, Hirtz C, Vialaret J, Navucet S, Grasselli C, Robert P, Lehmann S, Dauvilliers Y (2017) Cerebrospinal fluid levels of orexin-A and histamine, and sleep profile within the Alzheimer process. Neurobiol Aging 53:59-66.

Galasko D, Chang L, Motter R, Clark CM, Kaye J, Knopman D, Thomas R, Kholodenko D, Schenk D, Lieberburg I, Miller B, Green R, Basherad R, Kertiles L, Boss MA, Seubert P (1998) High cerebrospinal fluid tau and low amyloid beta 42 levels in the clinical diagnosis of Alzheimer disease and relation to apolipoprotein E genotype. Arch Neurol 55:937-945.

Gamache J, Benzow K, Forster C, Kemper L, Hlynialuk C, Furrow E, Ashe KH, Koob MD (2019) Factors other than hTau overexpression that contribute to tauopathy-like phenotype in rTg4510 mice. Nat Commun 10:2479.

Garcia-Mesa Y, Gimenez-Llort L, Lopez LC, Venegas C, Cristofol R, Escames G, Acuna-Castroviejo D, Sanfeliu C (2012) Melatonin plus physical exercise are highly neuroprotective in the 3xTg-AD mouse. Neurobiol Aging 33:1124 e1113-1129.

Gehrman PR, Connor DJ, Martin JL, Shochat T, Corey-Bloom J, Ancoli-Israel S (2009) Melatonin fails to improve sleep or agitation in double-blind randomized placebo-controlled trial of institutionalized patients with Alzheimer disease. Am J Geriatr Psychiatry 17:166-169.

German DC, White CL, Sparkman DR (1987) Alzheimers-Disease - Neurofibrillary Tangles in Nuclei That Project to the Cerebral-Cortex. Neuroscience 21:305-312.

German DC, Manaye KF, White CL, 3rd, Woodward DJ, McIntire DD, Smith WK, Kalaria RN, Mann DM (1992) Disease-specific patterns of locus coeruleus cell loss. Ann Neurol 32:667-676.

Geula C, Nagykery N, Nicholas A, Wu CK (2008) Cholinergic neuronal and axonal abnormalities are present early in aging and in Alzheimer disease. J Neuropathol Exp Neurol 67:309-318.

Glenner GG, Wong CW (1984) Alzheimers-Disease - Initial Report of the Purification and Characterization of a Novel Cerebrovascular Amyloid Protein. Biochem Bioph Res Co 120:885-890.

Goate A, Chartier-Harlin MC, Mullan M, Brown J, Crawford F, Fidani L, Giuffra L, Haynes A, Irving N, James L, et al. (1991) Segregation of a missense mutation in the amyloid precursor protein gene with familial Alzheimer's disease. Nature 349:704-706.

Goedert M, Spillantini MG (2006) A century of Alzheimer's disease. Science 314:777-781.

Goedert M, Ghetti B, Spillantini MG (2012) Frontotemporal dementia: implications for understanding Alzheimer disease. Cold Spring Harb Perspect Med 2:a006254.

Goedert M, Spillantini MG, Jakes R, Rutherford D, Crowther RA (1989) Multiple Isoforms of Human Microtubule-Associated Protein-Tau - Sequences and Localization in Neurofibrillary Tangles of Alzheimers-Disease. Neuron 3:519-526.

Goldgaber D, Lerman MI, Mcbride OW, Saffiotti U, Gajdusek DC (1987) Characterization and Chromosomal Localization of a Cdna-Encoding Brain Amyloid of Alzheimers-Disease. Science 235:877-880.

Gomez-Isla T, Hollister R, West H, Mui S, Growdon JH, Petersen RC, Parisi JE, Hyman BT (1997) Neuronal loss correlates with but exceeds neurofibrillary tangles in Alzheimer's disease. Ann Neurol 41:17-24.

Gompf HS, Aston-Jones G (2008) Role of orexin input in the diurnal rhythm of locus coeruleus impulse activity. Brain Res 1224:43-52.

Gong CX, Singh TJ, Grundke-Iqbal I, Iqbal K (1993) Phosphoprotein phosphatase activities in Alzheimer disease brain. J Neurochem 61:921-927.

Goodwin LO, Splinter E, Davis TL, Urban R, He H, Braun RE, Chesler EJ, Kumar V, van Min M, Ndukum J, Philip VM, Reinholdt LG, Svenson K, White JK, Sasner M, Lutz C, Murray SA (2019) Large-scale discovery of mouse transgenic integration sites reveals frequent structural variation and insertional mutagenesis. Genome Res 29:494-505.

Gotter AL, Webber AL, Coleman PJ, Renger JJ, Winrow CJ (2012) International Union of Basic and Clinical Pharmacology. LXXXVI. Orexin receptor function, nomenclature and pharmacology. Pharmacol Rev 64:389-420.

Gotter AL, Forman MS, Harrell CM, Stevens J, Svetnik V, Yee KL, Li X, Roecker AJ, Fox SV, Tannenbaum PL, Garson SL, Lepeleire ID, Calder N, Rosen L, Struyk A, Coleman PJ, Herring WJ, Renger JJ, Winrow CJ (2016) Orexin 2 Receptor Antagonism is Sufficient to Promote NREM and REM Sleep from Mouse to Man. Sci Rep 6:27147.

Gotz J, Ittner LM (2008) Animal models of Alzheimer's disease and frontotemporal dementia. Nat Rev Neurosci 9:532-544.

Gotz J, Gladbach A, Pennanen L, van Eersel J, Schild A, David D, Ittner LM (2010) Animal models reveal role for tau phosphorylation in human disease. Biochim Biophys Acta-Mol Basis Dis 1802:860-871.

Gozzi A, Turrini G, Piccoli L, Massagrande M, Amantini D, Antolini M, Martinelli P, Cesari N, Montanari D, Tessari M, Corsi M, Bifone A (2011) Functional magnetic resonance imaging reveals different neural substrates for the effects of orexin-1 and orexin-2 receptor antagonists. PLoS One 6:e16406.

Green TRF, Ortiz JB, Wonnacott S, Williams RJ, Rowe RK (2020) The Bidirectional Relationship Between Sleep and Inflammation Links Traumatic Brain Injury and Alzheimer's Disease. Front Neurosci 14:894.

Greicius MD, Srivastava G, Reiss AL, Menon V (2004) Default-mode network activity distinguishes Alzheimer's disease from healthy aging: evidence from functional MRI. Proceedings of the National Academy of Sciences of the United States of America 101:4637-4642.

Grinberg LT, Rüb U, Ferretti REL, Nitrini R, Farfel JM, Polichiso L, Gierga K, Jacob-Filho W, Heinsen H (2009) The dorsal raphe nucleus shows phospho-tau neurofibrillary changes before the transentorhinal region in Alzheimer's disease. A precocious onset? Neuropathology and Applied Neurobiology 35:406-416.

Grudzien A, Shaw P, Weintraub S, Bigio E, Mash DC, Mesulam MM (2007) Locus coeruleus neurofibrillary degeneration in aging, mild cognitive impairment and early Alzheimer's disease. Neurobiol Aging 28:327-335.

Guisle I, Gratuze M, Petry S, Morin F, Keraudren R, Whittington RA, Hebert SS, Mongrain V, Planel E (2019) Circadian and sleep/wake-dependent variations in tau phosphorylation are driven by temperature. Sleep.

Guo Q, Wang Z, Li H, Wiese M, Zheng H (2012) APP physiological and pathophysiological functions: insights from animal models. Cell Res 22:78-89.

Hadjimarkou MM, Benham R, Schwarz JM, Holder MK, Mong JA (2008) Estradiol suppresses rapid eye movement sleep and activation of sleep-active neurons in the ventrolateral preoptic area. Eur J Neurosci 27:1780-1792.

Hagan JJ et al. (1999) Orexin A activates locus coeruleus cell firing and increases arousal in the rat. Proceedings of the National Academy of Sciences of the United States of America 96:10911-10916.

Hahn EA, Wang HX, Andel R, Fratiglioni L (2014) A change in sleep pattern may predict Alzheimer disease. Am J Geriatr Psychiatry 22:1262-1271.

Hall-Porter JM, Schweitzer PK, Eisenstein RD, Ahmed HA, Walsh JK (2014) The effect of two benzodiazepine receptor agonist hypnotics on sleep-dependent memory consolidation. J Clin Sleep Med 10:27-34.

Hara J, Beuckmann CT, Nambu T, Willie JT, Chemelli RM, Sinton CM, Sugiyama F, Yagami K, Goto K, Yanagisawa M, Sakurai T (2001) Genetic ablation of orexin neurons in mice results in narcolepsy, hypophagia, and obesity. Neuron 30:345-354.

Hardy J (2009) The amyloid hypothesis for Alzheimer's disease: a critical reappraisal. J Neurochem 110:1129-1134.

Hardy J, Selkoe DJ (2002) The amyloid hypothesis of Alzheimer's disease: progress and problems on the road to therapeutics. Science 297:353-356.

Hardy J, Bogdanovic N, Winblad B, Portelius E, Andreasen N, Cedazo-Minguez A, Zetterberg H (2014) Pathways to Alzheimer's disease. J Intern Med 275:296-303.

Hardy JA, Higgins GA (1992) Alzheimers-Disease - the Amyloid Cascade Hypothesis. Science 256:184-185.

Harris GC, Wimmer M, Aston-Jones G (2005) A role for lateral hypothalamic orexin neurons in reward seeking. Nature 437:556-559.

Hassainia F, Petit D, Nielsen T, Gauthier S, Montplaisir J (1997) Quantitative EEG and statistical mapping of wakefulness and REM sleep in the evaluation of mild to moderate Alzheimer's disease. Eur Neurol 37:219-224.

He Z, Guo JL, McBride JD, Narasimhan S, Kim H, Changolkar L, Zhang B, Gathagan RJ, Yue C, Dengler C, Stieber A, Nitla M, Coulter DA, Abel T, Brunden KR, Trojanowski JQ, Lee VM (2018) Amyloid-beta plaques enhance Alzheimer's brain tau-seeded pathologies by facilitating neuritic plaque tau aggregation. Nat Med 24:29-38.

Heneka MT, Nadrigny F, Regen T, Martinez-Hernandez A, Dumitrescu-Ozimek L, Terwel D, Jardanhazi-Kurutz D, Walter J, Kirchhoff F, Hanisch UK, Kummer MP (2010) Locus ceruleus controls Alzheimer's disease pathology by modulating microglial functions through norepinephrine. Proceedings of the National Academy of Sciences of the United States of America 107:6058-6063.

Heneka MT, Ramanathan M, Jacobs AH, Dumitrescu-Ozimek L, Bilkei-Gorzo A, Debeir T, Sastre M, Galldiks N, Zimmer A, Hoehn M, Heiss WD, Klockgether T, Staufenbiel M (2006) Locus ceruleus degeneration promotes Alzheimer pathogenesis in amyloid precursor protein 23 transgenic mice. J Neurosci 26:1343-1354.

Herring WJ, Ceesay P, Snyder E, Bliwise D, Budd K, Hutzelmann J, Stevens J, Michelson D (2019) 0405 Randomized Controlled Clinical Polysomnography Trial of Suvorexant for Treating Insomnia in Patients with Alzheimer's Disease. Sleep 42:A164-A164.

Herring WJ, Snyder E, Budd K, Hutzelmann J, Snavely D, Liu K, Lines C, Roth T, Michelson D (2012a) Orexin receptor antagonism for treatment of insomnia: a randomized clinical trial of suvorexant. Neurology 79:2265-2274.

Herring WJ, Snyder E, Paradis E, Hutzelmann J, Liu MC, Snavely D, Walsh J, Krystal A, Roth T, Michelson D (2012b) Suvorexant, an orexin receptor antagonist, in preventing symptom return in patients with insomnia after 1 year of treatment: a randomised, double-blind, placebo-controlled study. J Sleep Res 21:351-351.

Heywood WE, Hallqvist J, Heslegrave AJ, Zetterberg H, Fenoglio C, Scarpini E, Rohrer JD, Galimberti D, Mills K (2018) CSF pro-orexin and amyloid-beta 38 expression in Alzheimer's disease and frontotemporal dementia. Neurobiol Aging 72:171-176.

Hobson JA, Pace-Schott EF (2002) The cognitive neuroscience of sleep: neuronal systems, consciousness and learning. Nat Rev Neurosci 3:679-693.

Hoever P, de Haas SL, Dorffner G, Chiossi E, van Gerven JM, Dingemanse J (2012a) Orexin receptor antagonism: an ascending multiple-dose study with almorexant. J Psychopharmacol 26:1071-1080.

Hoever P, de Haas S, Winkler J, Schoemaker RC, Chiossi E, van Gerven J, Dingemanse J (2010) Orexin receptor antagonism, a new sleep-promoting paradigm: an ascending single-dose study with almorexant. Clin Pharmacol Ther 87:593-600.

Hoever P et al. (2012b) Orexin receptor antagonism, a new sleep-enabling paradigm: a proof-of-concept clinical trial. Clin Pharmacol Ther 91:975-985.

Holth J, Patel T, Holtzman DM (2017a) Sleep in Alzheimer's Disease - Beyond Amyloid. Neurobiol Sleep Circadian Rhythms 2:4-14.

Holth JK, Mahan TE, Robinson GO, Rocha A, Holtzman DM (2017b) Altered sleep and EEG power in the P301S Tau transgenic mouse model. Ann Clin Transl Neurol 4:180-190.

Holth JK, Fritschi SK, Wang C, Pedersen NP, Cirrito JR, Mahan TE, Finn MB, Manis M, Geerling JC, Fuller PM, Lucey BP, Holtzman DM (2019) The sleep-wake cycle regulates brain interstitial fluid tau in mice and CSF tau in humans. Science 363:880-884.

Holtzman DM, Morris JC, Goate AM (2011) Alzheimer's disease: the challenge of the second century. Sci Transl Med 3:77sr71.

Hong M, Chen DC, Klein PS, Lee VM (1997) Lithium reduces tau phosphorylation by inhibition of glycogen synthase kinase-3. The Journal of biological chemistry 272:25326-25332.

Hong S, Beja-Glasser VF, Nfonoyim BM, Frouin A, Li S, Ramakrishnan S, Merry KM, Shi Q, Rosenthal A, Barres BA, Lemere CA, Selkoe DJ, Stevens B (2016) Complement and microglia mediate early synapse loss in Alzheimer mouse models. Science 352:712-716.

Hoover BR, Reed MN, Su J, Penrod RD, Kotilinek LA, Grant MK, Pitstick R, Carlson GA, Lanier LM, Yuan LL, Ashe KH, Liao D (2010) Tau mislocalization to dendritic spines mediates synaptic dysfunction independently of neurodegeneration. Neuron 68:1067-1081.

Hornung JP (2003) The human raphe nuclei and the serotonergic system. J Chem Neuroanat 26:331-343.

Horovitz SG, Braun AR, Carr WS, Picchioni D, Balkin TJ, Fukunaga M, Duyn JH (2009) Decoupling of the brain's default mode network during deep sleep. Proceedings of the National Academy of Sciences of the United States of America 106:11376-11381.

Horvath TL, Peyron C, Diano S, Ivanov A, Aston-Jones G, Kilduff TS, van Den Pol AN (1999) Hypocretin (orexin) activation and synaptic innervation of the locus coeruleus noradrenergic system. J Comp Neurol 415:145-159.

Hoyer D, Jacobson LH (2013) Orexin in sleep, addiction and more: is the perfect insomnia drug at hand? Neuropeptides 47:477-488.

Hoyer D, Allen A, Jacobson LH (2019) Hypnotics with novel modes of action. Br J Clin Pharmacol.

Hoyer D, Thakker DR, Natt F, Maier R, Huesken D, Muller M, Flor P, H VDP, Schmutz M, Bilbe G, Cryan JF (2006) Global down-regulation of gene expression in the brain using RNA interference, with emphasis on monoamine transporters and GPCRs: implications for target characterization in psychiatric and neurological disorders. J Recept Signal Transduct Res 26:527-547.

Hoyer D, Durst T, Fendt M, Jacobson LH, Betschart C, Hintermann S, Behnke D, Cotesta S, Laue G, Ofner S, Legangneux E, Gee CE (2013) Distinct effects of IPSU and suvorexant on mouse sleep architecture. Front Neurosci 7:235.

Hsiao K, Chapman P, Nilsen S, Eckman C, Harigaya Y, Younkin S, Yang FS, Cole G (1996) Correlative memory deficits, A beta elevation, and amyloid plaques in transgenic mice. Science 274:99-102.

Hu B, Yang N, Qiao QC, Hu ZA, Zhang J (2015) Roles of the orexin system in central motor control. Neurosci Biobehav Rev 49:43-54.

Huang MP, Radadia K, Macone BW, Auerbach SH, Datta S (2010) Effects of eszopiclone and zolpidem on sleep-wake behavior, anxiety-like behavior and contextual memory in rats. Behav Brain Res 210:54-66.

Huang Y, Potter R, Sigurdson W, Santacruz A, Shih S, Ju YE, Kasten T, Morris JC, Mintun M, Duntley S, Bateman RJ (2012a) Effects of age and amyloid deposition on Abeta dynamics in the human central nervous system. Arch Neurol 69:51-58.

Huang Y, Potter R, Sigurdson W, Kasten T, Connors R, Morris JC, Benzinger T, Mintun M, Ashwood T, Ferm M, Budd SL, Bateman RJ (2012b) beta-amyloid dynamics in human plasma. Arch Neurol 69:1591-1597.

Huang ZL, Qu WM, Li WD, Mochizuki T, Eguchi N, Watanabe T, Urade Y, Hayaishi O (2001) Arousal effect of orexin A depends on activation of the histaminergic system. Proc Natl Acad Sci U S A 98:9965-9970.

Huitron-Resendiz S, Sanchez-Alavez M, Gallegos R, Berg G, Crawford E, Giacchino JL, Games D, Henriksen SJ, Criado JR (2002) Age-independent and age-related deficits in visuospatial learning, sleep-wake states, thermoregulation and motor activity in PDAPP mice. Brain Res 928:126-137.

Hutton M et al. (1998) Association of missense and 5'-splice-site mutations in tau with the inherited dementia FTDP-17. Nature 393:702-705.

Iba M, Guo JL, McBride JD, Zhang B, Trojanowski JQ, Lee VM (2013) Synthetic tau fibrils mediate transmission of neurofibrillary tangles in a transgenic mouse model of Alzheimer's-like tauopathy. J Neurosci 33:1024-1037.

Iliff JJ, Lee H, Yu M, Feng T, Logan J, Nedergaard M, Benveniste H (2013) Brain-wide pathway for waste clearance captured by contrast-enhanced MRI. J Clin Invest 123:1299-1309.

Iliff JJ, Chen MJ, Plog BA, Zeppenfeld DM, Soltero M, Yang L, Singh I, Deane R, Nedergaard M (2014) Impairment of glymphatic pathway function promotes tau pathology after traumatic brain injury. J Neurosci 34:16180-16193.

Iliff JJ, Wang M, Liao Y, Plogg BA, Peng W, Gundersen GA, Benveniste H, Vates GE, Deane R, Goldman SA, Nagelhus EA, Nedergaard M (2012) A paravascular pathway facilitates CSF flow through the brain parenchyma and the clearance of interstitial solutes, including amyloid beta. Sci Transl Med 4:147ra111.

Imbimbo BP, Watling M (2019) Investigational BACE inhibitors for the treatment of Alzheimer's disease. Expert Opin Investig Drugs 28:967-975.

Iqbal K, Alonso Adel C, Chen S, Chohan MO, El-Akkad E, Gong CX, Khatoon S, Li B, Liu F, Rahman A, Tanimukai H, Grundke-Iqbal I (2005) Tau pathology in Alzheimer disease and other tauopathies. Biochim Biophys Acta-Mol Basis Dis 1739:198-210.

Ittner A, Ittner LM (2018) Dendritic Tau in Alzheimer's Disease. Neuron 99:13-27.

Ittner LM, Gotz J (2011) Amyloid-beta and tau--a toxic pas de deux in Alzheimer's disease. Nat Rev Neurosci 12:65-72.

Ittner LM, Ke YD, Delerue F, Bi M, Gladbach A, van Eersel J, Wolfing H, Chieng BC, Christie MJ, Napier IA, Eckert A, Staufenbiel M, Hardeman E, Gotz J (2010) Dendritic function of tau mediates amyloid-beta toxicity in Alzheimer's disease mouse models. Cell 142:387-397.

Ivgy-May N, Leibensperger H, Froman S, Hutzelmann J, Snavely D, Snyder E, Liu K, Walsh J, Roth T, Michelson D, Herring WJ (2012) Efficacy and safety of suvorexant, an orexin receptor antagonist, in patients with primary insomnia: a 3-month phase 3 trial (trial #2). J Sleep Res 21:351-352.

Jack CR, Jr., Holtzman DM (2013) Biomarker modeling of Alzheimer's disease. Neuron 80:1347-1358.

Jacobson LH, Callander GE, Hoyer D (2014) Suvorexant for the treatment of insomnia. Expert Rev Clin Pharmacol 7:711-730.

Jacobson LH, Bettler B, Kaupmann K, Cryan JF (2007) Behavioral evaluation of mice deficient in GABA(B(1)) receptor isoforms in tests of unconditioned anxiety. Psychopharmacology (Berl) 190:541-553.

Jacobson LH, Chen S, Mir S, Hoyer D (2017) Orexin OX2 Receptor Antagonists as Sleep Aids. Curr Top Behav Neurosci 33:105-136.

Jardanhazi-Kurutz D, Kummer MP, Terwel D, Vogel K, Dyrks T, Thiele A, Heneka MT (2010) Induced LC degeneration in APP/PS1 transgenic mice accelerates early cerebral amyloidosis and cognitive deficits. Neurochem Int 57:375-382.

Jeong J (2004) EEG dynamics in patients with Alzheimer's disease. Clin Neurophysiol 115:1490-1505.

Johnson PL, Federici LM, Fitz SD, Renger JJ, Shireman B, Winrow CJ, Bonaventure P, Shekhar A (2015) Orexin 1 and 2 Receptor Involvement in Co2 -Induced Panic-Associated Behavior and Autonomic Responses. Depress Anxiety 32:671-683.

Johnstone VPA, Wright DK, Wong K, O'Brien TJ, Rajan R, Shultz SR (2015) Experimental Traumatic Brain Injury Results in Long-Term Recovery of Functional Responsiveness in Sensory Cortex but Persisting Structural Changes and Sensorimotor, Cognitive, and Emotional Deficits. Journal of Neurotrauma 32:1333-1346.

Johren O, Bruggemann N, Dendorfer A, Dominiak P (2003) Gonadal steroids differentially regulate the messenger ribonucleic acid expression of pituitary orexin type 1 receptors and adrenal orexin type 2 receptors. Endocrinology 144:1219-1225.

Ju YE, Lucey BP, Holtzman DM (2014) Sleep and Alzheimer disease pathology--a bidirectional relationship. Nat Rev Neurol 10:115-119.

Ju YE, McLeland JS, Toedebusch CD, Xiong C, Fagan AM, Duntley SP, Morris JC, Holtzman DM (2013) Sleep quality and preclinical Alzheimer disease. JAMA Neurol 70:587-593.

Ju YE, Ooms SJ, Sutphen C, Macauley SL, Zangrilli MA, Jerome G, Fagan AM, Mignot E, Zempel JM, Claassen JAHR, Holtzman DM (2017) Slow wave sleep disruption increases cerebrospinal fluid amyloid-beta levels. Brain 140:2104-2111.

Kales HC, Gitlin LN, Lyketsos CG (2015) Assessment and management of behavioral and psychological symptoms of dementia. BMJ 350:h369.

Kalogiannis M, Hsu E, Willie JT, Chemelli RM, Kisanuki YY, Yanagisawa M, Leonard CS (2011) Cholinergic modulation of narcoleptic attacks in double orexin receptor knockout mice. PLoS One 6:e18697.

Kamenetz F, Tomita T, Hsieh H, Seabrook G, Borchelt D, Iwatsubo T, Sisodia S, Malinow R (2003) APP processing and synaptic function. Neuron 37:925-937.

Kanbayashi T, Inoue Y, Chiba S, Aizawa R, Saito Y, Tsukamoto H, Fujii Y, Nishino S, Shimizu T (2002) CSF hypocretin-1 (orexin-A) concentrations in narcolepsy with and without cataplexy and idiopathic hypersomnia. J Sleep Res 11:91-93.

Kang J, Lemaire HG, Unterbeck A, Salbaum JM, Masters CL, Grzeschik KH, Multhaup G, Beyreuther K, Muller-Hill B (1987) The precursor of Alzheimer's disease amyloid A4 protein resembles a cell-surface receptor. Nature 325:733-736.

Kang JE, Lim MM, Bateman RJ, Lee JJ, Smyth LP, Cirrito JR, Fujiki N, Nishino S, Holtzman DM (2009) Amyloid-beta dynamics are regulated by orexin and the sleep-wake cycle. Science 326:1005-1007.

Karakas S, Barry RJ (2017) A brief historical perspective on the advent of brain oscillations in the biological and psychological disciplines. Neurosci Biobehav Rev 75:335-347.

Kerbler GM, Fripp J, Rowe CC, Villemagne VL, Salvado O, Rose S, Coulson EJ, Alzheimer's Disease Neuroimaging I (2015) Basal forebrain atrophy correlates with amyloid beta burden in Alzheimer's disease. Neuroimage Clin 7:105-113.

Kester MI, van der Vlies AE, Blankenstein MA, Pijnenburg YA, van Elk EJ, Scheltens P, van der Flier WM (2009) CSF biomarkers predict rate of cognitive decline in Alzheimer disease. Neurology 73:1353-1358.

Kilduff TS, Peyron C (2000) The hypocretin/orexin ligand-receptor system: implications for sleep and sleep disorders. Trends Neurosci 23:359-365.

Kincheski GC, Valentim IS, Clarke JR, Cozachenco D, Castelo-Branco MTL, Ramos-Lobo AM, Rumjanek V, Donato J, Jr., De Felice FG, Ferreira ST (2017) Chronic sleep restriction promotes brain inflammation and synapse loss, and potentiates memory impairment induced by amyloid-beta oligomers in mice. Brain Behav Immun 64:140-151.

Kiyashchenko LI, Mileykovskiy BY, Maidment N, Lam HA, Wu MF, John J, Peever J, Siegel JM (2002) Release of hypocretin (orexin) during waking and sleep states. J Neurosci 22:5282-5286.

Kornum BR, Knudsen S, Ollila HM, Pizza F, Jennum PJ, Dauvilliers Y, Overeem S (2017) Narcolepsy. Nat Rev Dis Primers 3:16100.

Koss DJ, Robinson L, Drever BD, Plucinska K, Stoppelkamp S, Veselcic P, Riedel G, Platt B (2016) Mutant Tau knock-in mice display frontotemporal dementia relevant behaviour and histopathology. Neurobiol Dis 91:105-123.

Krueger JM, Frank MG, Wisor JP, Roy S (2016) Sleep function: Toward elucidating an enigma. Sleep Med Rev 28:46-54.

Kuduk SD, Skudlarek JW, DiMarco CN, Bruno JG, Pausch MH, O'Brien JA, Cabalu TD, Stevens J, Brunner J, Tannenbaum PL, Garson SL, Savitz AT, Harrell CM, Gotter AL, Winrow CJ, Renger JJ, Coleman PJ (2015) Identification of MK-8133: An orexin-2 selective receptor antagonist with favorable development properties. Bioorg Med Chem Lett 25:2488-2492.

Kuru M, Ueta Y, Serino R, Nakazato M, Yamamoto Y, Shibuya I, Yamashita H (2000) Centrally administered orexin/hypocretin activates HPA axis in rats. Neuroreport 11:1977-1980.

Langmead CJ, Jerman JC, Brough SJ, Scott C, Porter RA, Herdon HJ (2004) Characterisation of the binding of [3H]-SB-674042, a novel nonpeptide antagonist, to the human orexin-1 receptor. Br J Pharmacol 141:340-346.

Laws KR, Irvine K, Gale TM (2018) Sex differences in Alzheimer's disease. Curr Opin Psychiatry 31:133-139.

Lazic SE (2009) Statistical evaluation of methods for quantifying gene expression by autoradiography in histological sections. BMC Neurosci 10:5.

Lee MG, Hassani OK, Jones BE (2005a) Discharge of identified orexin/hypocretin neurons across the sleep-waking cycle. J Neurosci 25:6716-6720.

Lee MG, Hassani OK, Alonso A, Jones BE (2005b) Cholinergic basal forebrain neurons burst with theta during waking and paradoxical sleep. J Neurosci 25:4365-4369.

Lei P, Ayton S, Moon S, Zhang QH, Volitakis I, Finkelstein DI, Bush AI (2014) Motor and cognitive deficits in aged tau knockout mice in two background strains. Mol Neurodegener 9:12.

Leibiger J, Fendt M (2014) Behavioral analysis of narcoleptic episodes in orexin-deficient mice. Behav Genet 44:136-143.

Leonard CS, Kukkonen JP (2014) Orexin/hypocretin receptor signalling: a functional perspective. Br J Pharmacol 171:294-313.

Leroy K, Yilmaz Z, Brion JP (2007) Increased level of active GSK-3beta in Alzheimer's disease and accumulation in argyrophilic grains and in neurones at different stages of neurofibrillary degeneration. Neuropathol Appl Neurobiol 33:43-55.

Letavic MA, Bonaventure P, Carruthers NI, Dugovic C, Koudriakova T, Lord B, Lovenberg TW, Ly KS, Mani NS, Nepomuceno D, Pippel DJ, Rizzolio M, Shelton JE, Shah CR, Shireman BT, Young LK, Yun S (2015) Novel Octahydropyrrolo[3,4-c]pyrroles Are Selective Orexin-2 Antagonists: SAR Leading to a Clinical Candidate. Journal of medicinal chemistry 58:5620-5636.

Li J, Hu Z, de Lecea L (2014) The hypocretins/orexins: integrators of multiple physiological functions. Br J Pharmacol 171:332-350.

Li SB, Jones JR, de Lecea L (2016) Hypocretins, Neural Systems, Physiology, and Psychiatric Disorders. Curr Psychiatry Rep 18:7.

Liddelow SA et al. (2017) Neurotoxic reactive astrocytes are induced by activated microglia. Nature 541:481-487.

Liguori C, Chiaravalloti A, Nuccetelli M, Izzi F, Sancesario G, Cimini A, Bernardini S, Schillaci O, Mercuri NB, Fabio P (2017) Hypothalamic dysfunction is related to sleep impairment and CSF biomarkers in Alzheimer's disease. J Neurol 264:2215-2223.

Liguori C, Nuccetelli M, Izzi F, Sancesario G, Romigi A, Martorana A, Amoroso C, Bernardini S, Marciani MG, Mercuri NB, Placidi F (2016) Rapid eye movement sleep disruption and sleep fragmentation are associated with increased orexin-A cerebrospinal-fluid levels in mild cognitive impairment due to Alzheimer's disease. Neurobiol Aging 40:120-126.

Liguori C, Romigi A, Mercuri NB, Nuccetelli M, Izzi F, Albanese M, Sancesario G, Martorana A, Sancesario GM, Bernardini S, Marciani MG, Placidi F (2014a) Cerebrospinal-fluid orexin levels and daytime somnolence in frontotemporal dementia. J Neurol 261:1832-1836.

Liguori C, Romigi A, Nuccetelli M, Zannino S, Sancesario G, Martorana A, Albanese M, Mercuri NB, Izzi F, Bernardini S, Nitti A, Sancesario GM, Sica F, Marciani MG, Placidi F (2014b) Orexinergic system dysregulation, sleep impairment, and cognitive decline in Alzheimer disease. JAMA Neurol 71:1498-1505.

Lim AS, Kowgier M, Yu L, Buchman AS, Bennett DA (2013) Sleep Fragmentation and the Risk of Incident Alzheimer's Disease and Cognitive Decline in Older Persons. Sleep 36:1027-1032.

Lim AS, Yu L, Costa MD, Leurgans SE, Buchman AS, Bennett DA, Saper CB (2012) Increased fragmentation of rest-activity patterns is associated with a characteristic pattern of cognitive impairment in older individuals. Sleep 35:633-640B.

Lim MM, Gerstner JR, Holtzman DM (2014) The sleep-wake cycle and Alzheimer's disease: what do we know? Neurodegener Dis Manag 4:351-362.

Lin L, Faraco J, Li R, Kadotani H, Rogers W, Lin XY, Qiu XH, de Jong PJ, Nishino S, Mignot E (1999) The sleep disorder canine narcolepsy is caused by a mutation in the hypocretin (orexin) receptor 2 gene. Cell 98:365-376.

Lindwall G, Cole RD (1984) Phosphorylation affects the ability of tau protein to promote microtubule assembly. The Journal of biological chemistry 259:5301-5305.

Liu F, Grundke-Iqbal I, Iqbal K, Gong CX (2005) Contributions of protein phosphatases PP1, PP2A, PP2B and PP5 to the regulation of tau phosphorylation. Eur J Neurosci 22:1942-1950.

Liu M, Blanco-Centurion C, Konadhode RR, Luan L, Shiromani PJ (2016) Orexin gene transfer into the amygdala suppresses both spontaneous and emotion-induced cataplexy in orexin-knockout mice. Eur J Neurosci 43:681-688.

Liu M, Thankachan S, Kaur S, Begum S, Blanco-Centurion C, Sakurai T, Yanagisawa M, Neve R, Shiromani PJ (2008a) Orexin (hypocretin) gene transfer diminishes narcoleptic sleep behavior in mice. Eur J Neurosci 28:1382-1393.

Liu W, Miller BL, Kramer JH, Rankin K, Wyss-Coray C, Gearhart R, Phengrasamy L, Weiner M, Rosen HJ (2004) Behavioral disorders in the frontal and temporal variants of frontotemporal dementia. Neurology 62:742-748.

Liu Y, Yoo MJ, Savonenko A, Stirling W, Price DL, Borchelt DR, Mamounas L, Lyons WE, Blue ME, Lee MK (2008b) Amyloid pathology is associated with progressive monoaminergic neurodegeneration in a transgenic mouse model of Alzheimer's disease. J Neurosci 28:13805-13814.

Longstreth WT, Jr., Koepsell TD, Ton TG, Hendrickson AF, van Belle G (2007) The epidemiology of narcolepsy. Sleep 30:13-26.

Lucey BP, Bateman RJ (2014) Amyloid-beta diurnal pattern: possible role of sleep in Alzheimer's disease pathogenesis. Neurobiol Aging 35 Suppl 2:S29-34.

Lucey BP, Holtzman DM (2015) How amyloid, sleep and memory connect. Nat Neurosci 18:933-934.

Lucey BP, Mawuenyega KG, Patterson BW, Elbert DL, Ovod V, Kasten T, Morris JC, Bateman RJ (2017) Associations Between beta-Amyloid Kinetics and the beta-Amyloid Diurnal Pattern in the Central Nervous System. JAMA Neurol 74:207-215.

Lucey BP, Hicks TJ, McLeland JS, Toedebusch CD, Boyd J, Elbert DL, Patterson BW, Baty J, Morris JC, Ovod V, Mawuenyega KG, Bateman RJ (2018) Effect of sleep on overnight cerebrospinal fluid amyloid beta kinetics. Ann Neurol 83:197-204.

Lucey BP, McCullough A, Landsness EC, Toedebusch CD, McLeland JS, Zaza AM, Fagan AM, McCue L, Xiong C, Morris JC, Benzinger TLS, Holtzman DM (2019) Reduced non-rapid eye movement sleep is associated with tau pathology in early Alzheimer's disease. Sci Transl Med 11.

Ludewig S, Korte M (2016) Novel Insights into the Physiological Function of the APP (Gene) Family and Its Proteolytic Fragments in Synaptic Plasticity. Front Mol Neurosci 9:161.

Lyketsos CG, Lindell Veiel L, Baker A, Steele C (1999) A randomized, controlled trial of bright light therapy for agitated behaviors in dementia patients residing in long-term care. Int J Geriatr Psychiatry 14:520-525.

Mahlberg R, Walther S (2007) Actigraphy in agitated patients with dementia. Monitoring treatment outcomes. Z Gerontol Geriatr 40:178-184.

Makaron L, Moran CA, Namjoshi O, Rallapalli S, Cook JM, Rowlett JK (2013) Cognition-impairing effects of benzodiazepine-type drugs: role of GABAA receptor subtypes in an executive function task in rhesus monkeys. Pharmacology, biochemistry, and behavior 104:62-68.

Malherbe P, Borroni E, Pinard E, Wettstein JG, Knoflach F (2009a) Biochemical and electrophysiological characterization of almorexant, a dual orexin 1 receptor (OX1)/orexin 2 receptor (OX2) antagonist: comparison with selective OX1 and OX2 antagonists. Molecular pharmacology 76:618-631.

Malherbe P, Borroni E, Gobbi L, Knust H, Nettekoven M, Pinard E, Roche O, Rogers-Evans M, Wettstein JG, Moreau JL (2009b) Biochemical and behavioural characterization of EMPA, a novel high-affinity, selective antagonist for the OX(2) receptor. Br J Pharmacol 156:1326-1341.

Manaye KF, McIntire DD, Mann DM, German DC (1995) Locus coeruleus cell loss in the aging human brain: a non-random process. J Comp Neurol 358:79-87.

Manaye KF, Mouton PR, Xu G, Drew A, Lei DL, Sharma Y, Rebeck GW, Turner S (2013) Age-related loss of noradrenergic neurons in the brains of triple transgenic mice. Age (Dordr) 35:139-147.

Mandelkow EM, Drewes G, Biernat J, Gustke N, Van Lint J, Vandenheede JR, Mandelkow E (1992) Glycogen synthase kinase-3 and the Alzheimer-like state of microtubule-associated protein tau. FEBS Lett 314:315-321.

Mander BA, Winer JR, Jagust WJ, Walker MP (2016) Sleep: A Novel Mechanistic Pathway, Biomarker, and Treatment Target in the Pathology of Alzheimer's Disease? Trends Neurosci 39:552-566.

Mander BA, Rao V, Lu B, Saletin JM, Lindquist JR, Ancoli-Israel S, Jagust W, Walker MP (2013) Prefrontal atrophy, disrupted NREM slow waves and impaired hippocampal-dependent memory in aging. Nat Neurosci 16:357-364.

Mander BA, Marks SM, Vogel JW, Rao V, Lu B, Saletin JM, Ancoli-Israel S, Jagust WJ, Walker MP (2015) beta-amyloid disrupts human NREM slow waves and related hippocampus-dependent memory consolidation. Nat Neurosci 18:1051-1057.

Mang GM, Franken P (2012) Sleep and EEG Phenotyping in Mice. Curr Protoc Mouse Biol 2:55-74.

Mang GM, Durst T, Burki H, Imobersteg S, Abramowski D, Schuepbach E, Hoyer D, Fendt M, Gee CE (2012) The dual orexin receptor antagonist almorexant induces sleep and decreases orexin-induced locomotion by blocking orexin 2 receptors. Sleep 35:1625-1635.

Marcus JN, Aschkenasi CJ, Lee CE, Chemelli RM, Saper CB, Yanagisawa M, Elmquist JK (2001) Differential expression of orexin receptors 1 and 2 in the rat brain. J Comp Neurol 435:6-25.

Marshall L, Born J (2007) The contribution of sleep to hippocampus-dependent memory consolidation. Trends Cogn Sci 11:442-450.

Marshall L, Helgadottir H, Molle M, Born J (2006) Boosting slow oscillations during sleep potentiates memory. Nature 444:610-613.

Martin L, Latypova X, Terro F (2011) Post-translational modifications of tau protein: implications for Alzheimer's disease. Neurochem Int 58:458-471.

Masters CL, Simms G, Weinman NA, Multhaup G, McDonald BL, Beyreuther K (1985) Amyloid plaque core protein in Alzheimer disease and Down syndrome. Proceedings of the National Academy of Sciences of the United States of America 82:4245-4249.

Mattila MJ, Vanakoski J, Kalska H, Seppala T (1998) Effects of alcohol, zolpidem, and some other sedatives and hypnotics on human performance and memory. Pharmacol Biochem Be 59:917-923.

McAtee LC, Sutton SW, Rudolph DA, Li X, Aluisio LE, Phuong VK, Dvorak CA, Lovenberg TW, Carruthers NI, Jones TK (2004) Novel substituted 4-phenyl-[1,3]dioxanes: potent and selective orexin receptor 2 (OX(2)R) antagonists. Bioorg Med Chem Lett 14:4225-4229.

McCarley RW (2007) Neurobiology of REM and NREM sleep. Sleep Med 8:302-330.

McCormick DA, Bal T (1997) Sleep and arousal: thalamocortical mechanisms. Annu Rev Neurosci 20:185-215.

McGinty DJ, Harper RM (1976) Dorsal raphe neurons: depression of firing during sleep in cats. Brain Res 101:569-575.

McKenzie-Nickson S, Chan J, Perez K, Hung LW, Cheng L, Sedjahtera A, Gunawan L, Adlard PA, Hayne DJ, McInnes LE, Donnelly PS, Finkelstein DI, Hill AF, Barnham KJ (2018) Modulating Protein Phosphatase 2A Rescues Disease Phenotype in Neurodegenerative Tauopathies. ACS Chem Neurosci 9:2731-2740.

Mednick SC, McDevitt EA, Walsh JK, Wamsley E, Paulus M, Kanady JC, Drummond SP (2013) The critical role of sleep spindles in hippocampal-dependent memory: a pharmacology study. J Neurosci 33:4494-4504.

Menkes-Caspi N, Yamin HG, Kellner V, Spires-Jones TL, Cohen D, Stern EA (2015) Pathological tau disrupts ongoing network activity. Neuron 85:959-966.

Mesulam M, Shaw P, Mash D, Weintraub S (2004) Cholinergic nucleus basalis tauopathy emerges early in the aging-MCI-AD continuum. Ann Neurol 55:815-828.

Mesulam NM (1999) Neuroplasticity failure in Alzheimer's disease: Bridging the gap between plaques and tangles. Neuron 24:521-529.

Michelson D, Snyder E, Paradis E, Chengan-Liu M, Snavely DB, Hutzelmann J, Walsh JK, Krystal AD, Benca RM, Cohn M, Lines C, Roth T, Herring WJ (2014) Safety and efficacy of suvorexant during 1-year treatment of insomnia with subsequent abrupt treatment discontinuation: a phase 3 randomised, double-blind, placebo-controlled trial. Lancet Neurol 13:461-471.

Mieda M, Willie JT, Hara J, Sinton CM, Sakurai T, Yanagisawa M (2004) Orexin peptides prevent cataplexy and improve wakefulness in an orexin neuron-ablated model of narcolepsy in mice. Proceedings of the National Academy of Sciences of the United States of America 101:4649-4654.

Mieda M, Hasegawa E, Kisanuki YY, Sinton CM, Yanagisawa M, Sakurai T (2011) Differential roles of orexin receptor-1 and -2 in the regulation of non-REM and REM sleep. J Neurosci 31:6518-6526.

Mignot E (1998) Genetic and familial aspects of narcolepsy. Neurology 50:S16-22.

Mignot E, Lammers GJ, Ripley B, Okun M, Nevsimalova S, Overeem S, Vankova J, Black J, Harsh J, Bassetti C, Schrader H, Nishino S (2002) The role of cerebrospinal fluid hypocretin measurement in the diagnosis of narcolepsy and other hypersomnias. Arch Neurol 59:1553-1562.

Mileykovskiy BY, Kiyashchenko LI, Siegel JM (2005) Behavioral correlates of activity in identified hypocretin/orexin neurons. Neuron 46:787-798.

Minakawa EN, Miyazaki K, Maruo K, Yagihara H, Fujita H, Wada K, Nagai Y (2017) Chronic sleep fragmentation exacerbates amyloid beta deposition in Alzheimer's disease model mice. Neurosci Lett 653:362-369.

Mintzer MZ, Griffiths RR (1999) Selective effects of zolpidem on human memory functions. J Psychopharmacol 13:18-31.

Mirbaha H, Chen D, Morazova OA, Ruff KM, Sharma AM, Liu X, Goodarzi M, Pappu RV, Colby DW, Mirzaei H, Joachimiak LA, Diamond MI (2018) Inert and seed-competent tau monomers suggest structural origins of aggregation. eLife 7:29.

Mochizuki T, Crocker A, McCormack S, Yanagisawa M, Sakurai T, Scammell TE (2004) Behavioral state instability in orexin knock-out mice. J Neurosci 24:6291-6300.

Modirrousta M, Mainville L, Jones BE (2005) Orexin and MCH neurons express c-Fos differently after sleep deprivation vs. recovery and bear different adrenergic receptors. Eur J Neurosci 21:2807-2816.

Moe KE, Vitiello MV, Larsen LH, Prinz PN (1995) Sleep-Wake Patterns in Alzheimers-Disease - Relationships with Cognition and Function. J Sleep Res 4:15-20.

Mong JA, Baker FC, Mahoney MM, Paul KN, Schwartz MD, Semba K, Silver R (2011) Sleep, rhythms, and the endocrine brain: influence of sex and gonadal hormones. J Neurosci 31:16107-16116.

Morairty SR, Wilk AJ, Lincoln WU, Neylan TC, Kilduff TS (2014) The hypocretin/orexin antagonist almorexant promotes sleep without impairment of performance in rats. Front Neurosci 8:3.

Morairty SR, Revel FG, Malherbe P, Moreau JL, Valladao D, Wettstein JG, Kilduff TS, Borroni E (2012) Dual hypocretin receptor antagonism is more effective for sleep promotion than antagonism of either receptor alone. PLoS One 7:e39131.

Moran M, Lynch CA, Walsh C, Coen R, Coakley D, Lawlor BA (2005) Sleep disturbance in mild to moderate Alzheimer's disease. Sleep Med 6:347-352.

Morawska M, Buchi M, Fendt M (2011) Narcoleptic episodes in orexin-deficient mice are increased by both attractive and aversive odors. Behav Brain Res 222:397-400.

Morris M, Hamto P, Adame A, Devidze N, Masliah E, Mucke L (2013) Age-appropriate cognition and subtle dopamine-independent motor deficits in aged tau knockout mice. Neurobiol Aging 34:1523-1529.

Mufson EJ, Mash DC, Hersh LB (1988) Neurofibrillary tangles in cholinergic pedunculopontine neurons in Alzheimer's disease. Ann Neurol 24:623-629.

Musiek ES, Xiong DD, Holtzman DM (2015) Sleep, circadian rhythms, and the pathogenesis of Alzheimer disease. Exp Mol Med 47:e148.

Nakamura S, Takemura M, Ohnishi K, Suenaga T, Nishimura M, Akiguchi I, Kimura J, Kimura T (1993) Loss of Large Neurons and Occurrence of Neurofibrillary Tangles in the Tuberomammillary Nucleus of Patients with Alzheimers-Disease. Neurosci Lett 151:196-199.

Nakamura T, Uramura K, Nambu T, Yada T, Goto K, Yanagisawa M, Sakurai T (2000) Orexin-induced hyperlocomotion and stereotypy are mediated by the dopaminergic system. Brain Res 873:181-187.

Nambu T, Sakurai T, Mizukami K, Hosoya Y, Yanagisawa M, Goto K (1999) Distribution of orexin neurons in the adult rat brain. Brain Res 827:243-260.

Nelson PT et al. (2012) Correlation of Alzheimer disease neuropathologic changes with cognitive status: a review of the literature. J Neuropathol Exp Neurol 71:362-381.

Ngo HV, Martinetz T, Born J, Molle M (2013) Auditory closed-loop stimulation of the sleep slow oscillation enhances memory. Neuron 78:545-553.

Nisbet RM, Polanco JC, Ittner LM, Gotz J (2015) Tau aggregation and its interplay with amyloid-beta. Acta Neuropathol 129:207-220.

Nishino S, Ripley B, Overeem S, Lammers GJ, Mignot E (2000) Hypocretin (orexin) deficiency in human narcolepsy. Lancet 355:39-40.

Nishino S, Ripley B, Overeem S, Nevsimalova S, Lammers GJ, Vankova J, Okun M, Rogers W, Brooks S, Mignot E (2001) Low cerebrospinal fluid hypocretin (Orexin) and altered energy homeostasis in human narcolepsy. Ann Neurol 50:381-388.

O'Connor RM, Thakker DR, Schmutz M, van der Putten H, Hoyer D, Flor PJ, Cryan JF (2013) Adult siRNA-induced knockdown of mGlu7 receptors reduces anxiety in the mouse. Neuropharmacology 72:66-73.

O'Neil JN, Mouton PR, Tizabi Y, Ottinger MA, Lei DL, Ingram DK, Manaye KF (2007) Catecholaminergic neuronal loss in locus coeruleus of aged female dtg APP/PS1 mice. J Chem Neuroanat 34:102-107.

Oakley H, Cole SL, Logan S, Maus E, Shao P, Craft J, Guillozet-Bongaarts A, Ohno M, Disterhoft J, Van Eldik L, Berry R, Vassar R (2006) Intraneuronal beta-amyloid aggregates, neurodegeneration, and neuron loss in transgenic mice with five familial Alzheimer's disease mutations: potential factors in amyloid plaque formation. J Neurosci 26:10129-10140.

Oddo S, Vasilevko V, Caccamo A, Kitazawa M, Cribbs DH, LaFerla FM (2006) Reduction of soluble Abeta and tau, but not soluble Abeta alone, ameliorates cognitive decline in transgenic mice with plaques and tangles. The Journal of biological chemistry 281:39413-39423.

Oddo S, Caccamo A, Shepherd JD, Murphy MP, Golde TE, Kayed R, Metherate R, Mattson MP, Akbari Y, LaFerla FM (2003) Triple-transgenic model of Alzheimer's disease with plaques and tangles: Intracellular A beta and synaptic dysfunction. Neuron 39:409-421.

Oh J, Eser RA, Ehrenberg AJ, Morales D, Petersen C, Kudlacek J, Dunlop SR, Theofilas P, Resende E, Cosme C, Alho EJL, Spina S, Walsh CM, Miller BL, Seeley WW, Bittencourt JC, Neylan TC, Heinsen H, Grinberg LT (2019) Profound degeneration of wake-promoting neurons in Alzheimer's disease. Alzheimers Dement 15:1253-1263.

Ohayon MM (2002) Epidemiology of insomnia: what we know and what we still need to learn. Sleep Med Rev 6:97-111.

Olcese JM, Cao C, Mori T, Mamcarz MB, Maxwell A, Runfeldt MJ, Wang L, Zhang C, Lin X, Zhang G, Arendash GW (2009) Protection against cognitive deficits and markers of neurodegeneration by long-term oral administration of melatonin in a transgenic model of Alzheimer disease. J Pineal Res 47:82-96.

Ooms S, Overeem S, Besse K, Rikkert MO, Verbeek M, Claassen JA (2014) Effect of 1 night of total sleep deprivation on cerebrospinal fluid beta-amyloid 42 in healthy middle-aged men: a randomized clinical trial. JAMA Neurol 71:971-977.

Osorio RS, Pirraglia E, Aguera-Ortiz LF, During EH, Sacks H, Ayappa I, Walsleben J, Mooney A, Hussain A, Glodzik L, Frangione B, Martinez-Martin P, de Leon MJ (2011) Greater risk of Alzheimer's disease in older adults with insomnia. J Am Geriatr Soc 59:559-562.

Osorio RS et al. (2016) Orexin-A is Associated with Increases in Cerebrospinal Fluid Phosphorylated-Tau in Cognitively Normal Elderly Subjects. Sleep 39:1253-1260.

Otmani S, Demazieres A, Staner C, Jacob N, Nir T, Zisapel N, Staner L (2008) Effects of prolonged-release melatonin, zolpidem, and their combination on psychomotor functions, memory recall, and driving skills in healthy middle aged and elderly volunteers. Hum Psychopharmacol 23:693-705.

Pal D, Lipinski WJ, Walker AJ, Turner AM, Mashour GA (2011) State-specific effects of sevoflurane anesthesia on sleep homeostasis: selective recovery of slow wave but not rapid eye movement sleep. Anesthesiology 114:302-310.

Palop JJ, Mucke L (2010) Amyloid-beta-induced neuronal dysfunction in Alzheimer's disease: from synapses toward neural networks. Nat Neurosci 13:812-818.

Panossian LA, Avidan AY (2009) Review of sleep disorders. Med Clin N Am 93:407-425, ix.

Panza F, Lozupone M, Solfrizzi V, Sardone R, Piccininni C, Dibello V, Stallone R, Giannelli G, Bellomo A, Greco A, Daniele A, Seripa D, Logroscino G, Imbimbo BP (2018) BACE inhibitors in clinical development for the treatment of Alzheimer's disease. Expert Rev Neurother 18:847-857.

Parvizi J, Van Hoesen GW, Damasio A (2001) The selective vulnerability of brainstem nuclei to Alzheimer's disease. Ann Neurol 49:53-66.

Paul KN, Dugovic C, Turek FW, Laposky AD (2006) Diurnal sex differences in the sleep-wake cycle of mice are dependent on gonadal function. Sleep 29:1211-1223.

Perez-Nievas BG, Stein TD, Tai HC, Dols-Icardo O, Scotton TC, Barroeta-Espar I, Fernandez-Carballo L, de Munain EL, Perez J, Marquie M, Serrano-Pozo A, Frosch MP, Lowe V, Parisi JE, Petersen RC, Ikonomovic MD, Lopez OL, Klunk W, Hyman BT, Gomez-Isla T (2013) Dissecting phenotypic traits linked to human resilience to Alzheimer's pathology. Brain 136:2510-2526.

Peter-Derex L, Yammine P, Bastuji H, Croisile B (2015) Sleep and Alzheimer's disease. Sleep Med Rev 19:29-38.

Petit D, Gagnon JF, Fantini ML, Ferini-Strambi L, Montplaisir J (2004) Sleep and quantitative EEG in neurodegenerative disorders. J Psychosom Res 56:487-496.

Peyron C, Tighe DK, van den Pol AN, de Lecea L, Heller HC, Sutcliffe JG, Kilduff TS (1998) Neurons containing hypocretin (orexin) project to multiple neuronal systems. J Neurosci 18:9996-10015.

Peyron C et al. (2000) A mutation in a case of early onset narcolepsy and a generalized absence of hypocretin peptides in human narcoleptic brains. Nat Med 6:991-997.

Pick J, Chen Y, Moore JT, Sun Y, Wyner AJ, Friedman EB, Kelz MB (2011) Rapid eye movement sleep debt accrues in mice exposed to volatile anesthetics. Anesthesiology 115:702-712.

Piper DC, Upton N, Smith MI, Hunter AJ (2000) The novel brain neuropeptide, orexin-A, modulates the sleep-wake cycle of rats. Eur J Neurosci 12:726-730.

Platt B, Drever B, Koss D, Stoppelkamp S, Jyoti A, Plano A, Utan A, Merrick G, Ryan D, Melis V, Wan H, Mingarelli M, Porcu E, Scrocchi L, Welch A, Riedel G (2011) Abnormal cognition, sleep, EEG and brain metabolism in a novel knock-in Alzheimer mouse, PLB1. PLoS One 6:e27068.

Plaza-Zabala A, Martin-Garcia E, de Lecea L, Maldonado R, Berrendero F (2010) Hypocretins regulate the anxiogenic-like effects of nicotine and induce reinstatement of nicotine-seeking behavior. J Neurosci 30:2300-2310.

Plihal W, Born J (1997) Effects of early and late nocturnal sleep on declarative and procedural memory. J Cogn Neurosci 9:534-547.

Podcasy JL, Epperson CN (2016) Considering sex and gender in Alzheimer disease and other dementias. Dialogues in clinical neuroscience 18:437-446.

Poe GR (2017) Sleep Is for Forgetting. J Neurosci 37:464-473.

Pooler AM, Phillips EC, Lau DH, Noble W, Hanger DP (2013) Physiological release of endogenous tau is stimulated by neuronal activity. EMBO Rep 14:389-394.

Potvin O, Lorrain D, Forget H, Dube M, Grenier S, Preville M, Hudon C (2012) Sleep quality and 1-year incident cognitive impairment in community-dwelling older adults. Sleep 35:491-499.

Prince M, Bryce R, Albanese E, Wimo A, Ribeiro W, Ferri CP (2013) The global prevalence of dementia: a systematic review and metaanalysis. Alzheimers Dement 9:63-75.

Prinz PN, Vitaliano PP, Vitiello MV, Bokan J, Raskind M, Peskind E, Gerber C (1982) Sleep, Eeg and Mental Function Changes in Senile Dementia of the Alzheimer Type. Neurobiol Aging 3:361-370.

Puzzo D, Privitera L, Fa M, Staniszewski A, Hashimoto G, Aziz F, Sakurai M, Ribe EM, Troy CM, Mercken M, Jung SS, Palmeri A, Arancio O (2011) Endogenous amyloid-beta is necessary for hippocampal synaptic plasticity and memory. Ann Neurol 69:819-830.

Qian W, Shi JH, Yin XM, Iqbal K, Grundke-Iqbal I, Gong CX, Liu F (2010) PP2A Regulates Tau Phosphorylation Directly and also Indirectly via Activating GSK-3 beta. J Alzheimers Dis 19:1221-1229.

Querfurth HW, LaFerla FM (2010) Alzheimer's disease. N Engl J Med 362:329-344.

Quinn J, Kulhanek D, Nowlin J, Jones R, Pratico D, Rokach J, Stackman R (2005) Chronic melatonin therapy fails to alter amyloid burden or oxidative damage in old Tg2576 mice: implications for clinical trials. Brain Res 1037:209-213.

Rademakers R, Neumann M, Mackenzie IR (2012) Advances in understanding the molecular basis of frontotemporal dementia. Nat Rev Neurol 8:423-434.

Radl S (2013) Suvorexant Dual Orexin OX1/OX2 Receptor Antagonist Treatment of Sleep Disorders. Drugs of the Future 38:27-36.

Raichle ME, MacLeod AM, Snyder AZ, Powers WJ, Gusnard DA, Shulman GL (2001) A default mode of brain function. Proceedings of the National Academy of Sciences of the United States of America 98:676-682.

Rajendran L, Paolicelli RC (2018) Microglia-Mediated Synapse Loss in Alzheimer's Disease. J Neurosci 38:2911-2919.

Ramsden M, Kotilinek L, Forster C, Paulson J, McGowan E, SantaCruz K, Guimaraes A, Yue M, Lewis J, Carlson G, Hutton M, Ashe KH (2005) Age-dependent neurofibrillary tangle formation, neuron loss, and memory impairment in a mouse model of human tauopathy (P301L). J Neurosci 25:10637-10647.

Rapoport M, Dawson HN, Binder LI, Vitek MP, Ferreira A (2002) Tau is essential to beta -amyloid-induced neurotoxicity. Proceedings of the National Academy of Sciences of the United States of America 99:6364-6369.

Rhein V, Song X, Wiesner A, Ittner LM, Baysang G, Meier F, Ozmen L, Bluethmann H, Drose S, Brandt U, Savaskan E, Czech C, Gotz J, Eckert A (2009) Amyloid-beta and tau synergistically impair the oxidative phosphorylation system in triple transgenic Alzheimer's disease mice. Proceedings of the National Academy of Sciences of the United States of America 106:20057-20062.

Ricciarelli R, Fedele E (2017) The Amyloid Cascade Hypothesis in Alzheimer's Disease: It's Time to Change Our Mind. Curr Neuropharmacol 15:926-935.

Ripley B, Overeem S, Fujiki N, Nevsimalova S, Uchino M, Yesavage J, Di Monte D, Dohi K, Melberg A, Lammers GJ, Nishida Y, Roelandse FW, Hungs M, Mignot E, Nishino S (2001) CSF hypocretin/orexin levels in narcolepsy and other neurological conditions. Neurology 57:2253-2258.

Roberson ED, Scearce-Levie K, Palop JJ, Yan F, Cheng IH, Wu T, Gerstein H, Yu GQ, Mucke L (2007) Reducing endogenous tau ameliorates amyloid beta-induced deficits in an Alzheimer's disease mouse model. Science 316:750-754.

Rocher AB, Crimins JL, Amatrudo JM, Kinson MS, Todd-Brown MA, Lewis J, Luebke JI (2010) Structural and functional changes in tau mutant mice neurons are not linked to the presence of NFTs. Exp Neurol 223:385-393.

Rodriguez JJ, Noristani HN, Verkhratsky A (2012) The serotonergic system in ageing and Alzheimer's disease. Prog Neurobiol 99:15-41.

Roecker AJ et al. (2014a) Discovery of 5"-chloro-N-[(5,6-dimethoxypyridin-2-yl)methyl]-2,2':5',3"-terpyridine-3'-carbo xamide (MK-1064): a selective orexin 2 receptor antagonist (2-SORA) for the treatment of insomnia. ChemMedChem 9:311-322.

Roecker AJ et al. (2014b) Discovery of MK-3697: a selective orexin 2 receptor antagonist (2-SORA) for the treatment of insomnia. Bioorg Med Chem Lett 24:4884-4890.

Roh JH, Huang Y, Bero AW, Kasten T, Stewart FR, Bateman RJ, Holtzman DM (2012) Disruption of the sleep-wake cycle and diurnal fluctuation of beta-amyloid in mice with Alzheimer's disease pathology. Sci Transl Med 4:150ra122.

Roh JH, Jiang H, Finn MB, Stewart FR, Mahan TE, Cirrito JR, Heda A, Snider BJ, Li M, Yanagisawa M, de Lecea L, Holtzman DM (2014) Potential role of orexin and sleep modulation in the pathogenesis of Alzheimer's disease. The Journal of experimental medicine 211:2487-2496.

Rossi G, Tagliavini F (2015) Frontotemporal lobar degeneration: old knowledge and new insight into the pathogenetic mechanisms of tau mutations. Front Aging Neurosci 7:192.

Rothman SM, Herdener N, Frankola KA, Mughal MR, Mattson MP (2013) Chronic mild sleep restriction accentuates contextual memory impairments, and accumulations of cortical Abeta and pTau in a mouse model of Alzheimer's disease. Brain Res 1529:200-208.

Rub U, Del Tredici K, Schultz C, Thal DR, Braak E, Braak H (2000) The evolution of Alzheimer's disease-related cytoskeletal pathology in the human raphe nuclei. Neuropathol Appl Neurobiol 26:553-567.

Sahara N, Perez PD, Lin WL, Dickson DW, Ren Y, Zeng H, Lewis J, Febo M (2014) Age-related decline in white matter integrity in a mouse model of tauopathy: an in vivo diffusion tensor magnetic resonance imaging study. Neurobiol Aging 35:1364-1374.

Sakurai T (2007) The neural circuit of orexin (hypocretin): maintaining sleep and wakefulness. Nat Rev Neurosci 8:171-181.

Sakurai T (2014) The role of orexin in motivated behaviours. Nat Rev Neurosci 15:719-731.

Sakurai T et al. (1998) Orexins and orexin receptors: a family of hypothalamic neuropeptides and G protein-coupled receptors that regulate feeding behavior. Cell 92:573-585.

Salvadore G, Bonaventure P, Shekhar A, Johnson PL, Lord B, Shireman BT, Lebold TP, Nepomuceno D, Dugovic C, Brooks S, Zuiker R, Bleys C, Tatikola K, Remmerie B, Jacobs GE, Schruers K, Moyer J, Nash A, Van Nueten LGM, Drevets WC (2020) Translational evaluation of novel selective orexin-1 receptor antagonist JNJ-61393215 in an experimental model for panic in rodents and humans. Transl Psychiatry 10:308.

Samson WK, Taylor MM, Ferguson AV (2005) Non-sleep effects of hypocretin/orexin. Sleep Med Rev 9:243-252.

Sanchez PE, Zhu L, Verret L, Vossel KA, Orr AG, Cirrito JR, Devidze N, Ho K, Yu GQ, Palop JJ, Mucke L (2012) Levetiracetam suppresses neuronal network dysfunction and reverses synaptic and cognitive deficits in an Alzheimer's disease model. Proceedings of the National Academy of Sciences of the United States of America 109:E2895-2903.

Santacruz K, Lewis J, Spires T, Paulson J, Kotilinek L, Ingelsson M, Guimaraes A, DeTure M, Ramsden M, McGowan E, Forster C, Yue M, Orne J, Janus C, Mariash A, Kuskowski M, Hyman B, Hutton M, Ashe KH (2005) Tau suppression in a neurodegenerative mouse model improves memory function. Science 309:476-481.

Saper CB, Scammell TE, Lu J (2005) Hypothalamic regulation of sleep and circadian rhythms. Nature 437:1257-1263.

Saper CB, Fuller PM, Pedersen NP, Lu J, Scammell TE (2010) Sleep state switching. Neuron 68:1023-1042.

Sara SJ (2009) The locus coeruleus and noradrenergic modulation of cognition. Nat Rev Neurosci 10:211-223.

Sara SJ (2017) Sleep to Remember. J Neurosci 37:457-463.

Satoh A, Iijima KM (2019) Roles of tau pathology in the locus coeruleus (LC) in age-associated pathophysiology and Alzheimer's disease pathogenesis: Potential strategies to protect the LC against aging. Brain Res 1702:17-28.

Savonenko A, Xu GM, Melnikova T, Morton JL, Gonzales V, Wong MP, Price DL, Tang F, Markowska AL, Borchelt DR (2005) Episodic-like memory deficits in the APPswe/PS1dE9 mouse model of Alzheimer's disease: relationships to beta-amyloid deposition and neurotransmitter abnormalities. Neurobiol Dis 18:602-617.

Scammell TE (2015) Narcolepsy. N Engl J Med 373:2654-2662.

Scammell TE, Arrigoni E, Lipton JO (2017) Neural Circuitry of Wakefulness and Sleep. Neuron 93:747-765.

Scharf MT, Kelz MB (2013) Sleep and Anesthesia Interactions: A Pharmacological Appraisal. Curr Anesthesiol Rep 3:1-9.

Schenck CH, Mahowald MW (2002) REM sleep behavior disorder: clinical, developmental, and neuroscience perspectives 16 years after its formal identification in SLEEP. Sleep 25:120-138.

Schindelin J, Arganda-Carreras I, Frise E, Kaynig V, Longair M, Pietzsch T, Preibisch S, Rueden C, Saalfeld S, Schmid B, Tinevez JY, White DJ, Hartenstein V, Eliceiri K, Tomancak P, Cardona A (2012) Fiji: an open-source platform for biological-image analysis. Nat Methods 9:676-682.

Schneider F, Baldauf K, Wetzel W, Reymann KG (2014) Behavioral and EEG changes in male 5xFAD mice. Physiol Behav 135:25-33.

Schwartz MD, Nguyen AT, Warrier DR, Palmerston JB, Thomas AM, Morairty SR, Neylan TC, Kilduff TS (2016) Locus Coeruleus and Tuberomammillary Nuclei Ablations Attenuate Hypocretin/Orexin Antagonist-Mediated REM Sleep. eNeuro 3.

Selkoe DJ (1991) The Molecular Pathology of Alzheimers-Disease. Neuron 6:487-498.

Selkoe DJ (1997) Neuroscience - Alzheimer's disease: Genotypes, phenotype, and treatments. Science 275:630-631.

Selkoe DJ (2001) Alzheimer's disease: genes, proteins, and therapy. Physiological reviews 81:741-766.

Selkoe DJ (2002) Alzheimer's disease is a synaptic failure. Science 298:789-791.

Serfaty M, Kennell-Webb S, Warner J, Blizard R, Raven P (2002) Double blind randomised placebo controlled trial of low dose melatonin for sleep disorders in dementia. Int J Geriatr Psychiatry 17:1120-1127.

Seshadri S, Wolf PA, Beiser A, Au R, McNulty K, White R, D'Agostino RB (1997) Lifetime risk of dementia and Alzheimer's disease. The impact of mortality on risk estimates in the Framingham Study. Neurology 49:1498-1504.

Sethi M, Joshi SS, Webb RL, Beckett TL, Donohue KD, Murphy MP, O'Hara BF, Duncan MJ (2015) Increased fragmentation of sleep-wake cycles in the 5XFAD mouse model of Alzheimer's disease. Neuroscience 290:80-89.

Shan L, Bossers K, Unmehopa U, Bao AM, Swaab DF (2012) Alterations in the histaminergic system in Alzheimer's disease: a postmortem study. Neurobiol Aging 33:2585-2598.

Shi L, Chen SJ, Ma MY, Bao YP, Han Y, Wang YM, Shi J, Vitiello MV, Lu L (2018) Sleep disturbances increase the risk of dementia: A systematic review and meta-analysis. Sleep Med Rev 40:4-16.

Shi Y et al. (2017) ApoE4 markedly exacerbates tau-mediated neurodegeneration in a mouse model of tauopathy. Nature 549:523-527.

Siegel JM (2005) Clues to the functions of mammalian sleep. Nature 437:1264-1271.

Siegel JM, Boehmer LN (2006) Narcolepsy and the hypocretin system--where motion meets emotion. Nat Clin Pract Neurol 2:548-556.

Silveyra P, Lux-Lantos V, Libertun C (2007a) Both orexin receptors are expressed in rat ovaries and fluctuate with the estrous cycle: effects of orexin receptor antagonists on gonadotropins and ovulation. Am J Physiol Endocrinol Metab 293:E977-985.

Silveyra P, Catalano PN, Lux-Lantos V, Libertun C (2007b) Impact of proestrous milieu on expression of orexin receptors and prepro-orexin in rat hypothalamus and hypophysis: actions of Cetrorelix and Nembutal. Am J Physiol Endocrinol Metab 292:E820-828.

Silveyra P, Cataldi NI, Lux-Lantos V, Libertun C (2009) Gonadal steroids modulated hypocretin/orexin type-1 receptor expression in a brain region, sex and daytime specific manner. Regul Pept 158:121-126.

Simic G, Stanic G, Mladinov M, Jovanov-Milosevic N, Kostovic I, Hof PR (2009) Does Alzheimer's disease begin in the brainstem? Neuropathol Appl Neurobiol 35:532-554.

Singer C, Tractenberg RE, Kaye J, Schafer K, Gamst A, Grundman M, Thomas R, Thal LJ, Alzheimer's Disease Cooperative S (2003) A multicenter, placebo-controlled trial of melatonin for sleep disturbance in Alzheimer's disease. Sleep 26:893-901.

Slats D, Claassen JA, Verbeek MM, Overeem S (2013) Reciprocal interactions between sleep, circadian rhythms and Alzheimer's disease: focus on the role of hypocretin and melatonin. Ageing Res Rev 12:188-200.

Small SA, Duff K (2008) Linking Abeta and tau in late-onset Alzheimer's disease: a dual pathway hypothesis. Neuron 60:534-542.

Smart D, Sabido-David C, Brough SJ, Jewitt F, Johns A, Porter RA, Jerman JC (2001) SB-334867-A: the first selective orexin-1 receptor antagonist. Br J Pharmacol 132:1179-1182.

Smith MI, Piper DC, Duxon MS, Upton N (2003) Evidence implicating a role for orexin-1 receptor modulation of paradoxical sleep in the rat. Neurosci Lett 341:256-258.

Soininen H, Partanen J, Laulumaa V, Helkala EL, Laakso M, Riekkinen PJ (1989) Longitudinal Eeg Spectral-Analysis in Early Stage of Alzheimers-Disease. Electroen Clin Neuro 72:290-297.

Song L, Lu SX, Ouyang X, Melchor J, Lee J, Terracina G, Wang X, Hyde L, Hess JF, Parker EM, Zhang L (2015) Analysis of tau post-translational modifications in rTg4510 mice, a model of tau pathology. Mol Neurodegener 10:14.

Soto PL, Ator NA, Rallapalli SK, Biawat P, Clayton T, Cook JM, Weed MR (2013) Allosteric modulation of GABA(A) receptor subtypes:effects on visual recognition and visuospatial working memory in rhesus monkeys [corrected]. Neuropsychopharmacology 38:2315-2325.

Sperling RA, Laviolette PS, O'Keefe K, O'Brien J, Rentz DM, Pihlajamaki M, Marshall G, Hyman BT, Selkoe DJ, Hedden T, Buckner RL, Becker JA, Johnson KA (2009) Amyloid deposition is associated with impaired default network function in older persons without dementia. Neuron 63:178-188.

Spillantini MG, Goedert M (2013) Tau pathology and neurodegeneration. Lancet Neurol 12:609-622.

Spillantini MG, Murrell JR, Goedert M, Farlow MR, Klug A, Ghetti B (1998) Mutation in the tau gene in familial multiple system tauopathy with presenile dementia. Proceedings of the National Academy of Sciences of the United States of America 95:7737-7741.

Spira AP, Gamaldo AA, An Y, Wu MN, Simonsick EM, Bilgel M, Zhou Y, Wong DF, Ferrucci L, Resnick SM (2013) Self-reported sleep and beta-amyloid deposition in community-dwelling older adults. JAMA Neurol 70:1537-1543.

Spires-Jones TL, Hyman BT (2014) The intersection of amyloid beta and tau at synapses in Alzheimer's disease. Neuron 82:756-771.

Spires TL, Orne JD, SantaCruz K, Pitstick R, Carlson GA, Ashe KH, Hyman BT (2006) Region-specific dissociation of neuronal loss and neurofibrillary pathology in a mouse model of tauopathy. Am J Pathol 168:1598-1607.

Sprecher KE, Bendlin BB, Racine AM, Okonkwo OC, Christian BT, Koscik RL, Sager MA, Asthana S, Johnson SC, Benca RM (2015) Amyloid burden is associated with self-reported sleep in nondemented late middle-aged adults. Neurobiol Aging 36:2568-2576.

Sprecher KE, Koscik RL, Carlsson CM, Zetterberg H, Blennow K, Okonkwo OC, Sager MA, Asthana S, Johnson SC, Benca RM, Bendlin BB (2017) Poor sleep is associated with CSF biomarkers of amyloid pathology in cognitively normal adults. Neurology 89:445-453.

Staresina BP, Bergmann TO, Bonnefond M, van der Meij R, Jensen O, Deuker L, Elger CE, Axmacher N, Fell J (2015) Hierarchical nesting of slow oscillations, spindles and ripples in the human hippocampus during sleep. Nat Neurosci 18:1679-1686.

Steiner MA, Gatfield J, Brisbare-Roch C, Dietrich H, Treiber A, Jenck F, Boss C (2013) Discovery and characterization of ACT-335827, an orally available, brain penetrant orexin receptor type 1 selective antagonist. ChemMedChem 8:898-903.

Steriade M, McCormick DA, Sejnowski TJ (1993) Thalamocortical oscillations in the sleeping and aroused brain. Science 262:679-685.

Stern AL, Naidoo N (2015) Wake-active neurons across aging and neurodegeneration: a potential role for sleep disturbances in promoting disease. SpringerPlus 4:25.

Stickgold R (2005) Sleep-dependent memory consolidation. Nature 437:1272-1278.

Stokin GB, Lillo C, Falzone TL, Brusch RG, Rockenstein E, Mount SL, Raman R, Davies P, Masliah E, Williams DS, Goldstein LS (2005) Axonopathy and transport deficits early in the pathogenesis of Alzheimer's disease. Science 307:1282-1288.

Stratmann K, Heinsen H, Korf HW, Del Turco D, Ghebremedhin E, Seidel K, Bouzrou M, Grinberg LT, Bohl J, Wharton SB, den Dunnen W, Rub U (2016) Precortical Phase of Alzheimer's Disease (AD)-Related Tau Cytoskeletal Pathology. Brain Pathol 26:371-386.

Sun H, Kennedy WP, Wilbraham D, Lewis N, Calder N, Li X, Ma J, Yee KL, Ermlich S, Mangin E, Lines C, Rosen L, Chodakewitz J, Murphy GM (2013) Effects of suvorexant, an orexin receptor antagonist, on sleep parameters as measured by polysomnography in healthy men. Sleep 36:259-267.

Sutcliffe JG, de Lecea L (2002) The hypocretins: setting the arousal threshold. Nat Rev Neurosci 3:339-349.

Tabuchi M, Lone SR, Liu S, Liu Q, Zhang J, Spira AP, Wu MN (2015) Sleep interacts with abeta to modulate intrinsic neuronal excitability. Curr Biol 25:702-712.

Tabuchi S, Tsunematsu T, Black SW, Tominaga M, Maruyama M, Takagi K, Minokoshi Y, Sakurai T, Kilduff TS, Yamanaka A (2014) Conditional ablation of orexin/hypocretin neurons: a new mouse model for the study of narcolepsy and orexin system function. J Neurosci 34:6495-6509.

Takahashi K, Lin JS, Sakai K (2008) Neuronal activity of orexin and non-orexin waking-active neurons during wake-sleep states in the mouse. Neuroscience 153:860-870.

Tannenbaum PL, Tye SJ, Stevens J, Gotter AL, Fox SV, Savitz AT, Coleman PJ, Uslaner JM, Kuduk SD, Hargreaves R, Winrow CJ, Renger JJ (2016) Inhibition of Orexin Signaling Promotes Sleep Yet Preserves Salient Arousability in Monkeys. Sleep 39:603-612.

Tanzi RE, Gusella JF, Watkins PC, Bruns GA, St George-Hyslop P, Van Keuren ML, Patterson D, Pagan S, Kurnit DM, Neve RL (1987) Amyloid beta protein gene: cDNA, mRNA distribution, and genetic linkage near the Alzheimer locus. Science 235:880-884.

Tapiola T, Alafuzoff I, Herukka SK, Parkkinen L, Hartikainen P, Soininen H, Pirttila T (2009) Cerebrospinal Fluid beta-Amyloid 42 and Tau Proteins as Biomarkers of Alzheimer-Type Pathologic Changes in the Brain. Arch Neurol 66:382-389.

Tarasoff-Conway JM, Carare RO, Osorio RS, Glodzik L, Butler T, Fieremans E, Axel L, Rusinek H, Nicholson C, Zlokovic BV, Frangione B, Blennow K, Menard J, Zetterberg H, Wisniewski T, de Leon MJ (2015) Clearance systems in the brain-implications for Alzheimer disease. Nat Rev Neurol 11:457-470.

Tarawneh R, Holtzman DM (2010) Biomarkers in translational research of Alzheimer's disease. Neuropharmacology 59:310-322.

Terry RD (1996) The pathogenesis of Alzheimer disease: an alternative to the amyloid hypothesis. J Neuropathol Exp Neurol 55:1023-1025.

Thakker DR, Natt F, Husken D, van der Putten H, Maier R, Hoyer D, Cryan JF (2005) siRNA-mediated knockdown of the serotonin transporter in the adult mouse brain. Mol Psychiatry 10:782-789, 714.

Thakker DR, Natt F, Husken D, Maier R, Muller M, van der Putten H, Hoyer D, Cryan JF (2004) Neurochemical and behavioral consequences of widespread gene knockdown in the adult mouse brain by using nonviral RNA interference. Proceedings of the National Academy of Sciences of the United States of America 101:17270-17275.

Thannickal TC, Moore RY, Nienhuis R, Ramanathan L, Gulyani S, Aldrich M, Cornford M, Siegel JM (2000) Reduced number of hypocretin neurons in human narcolepsy. Neuron 27:469-474.

Thein SG, Bsharat M, Kemethofer M, Filippov G, Kubota N, Moline M (2019) Response to Treatment with Lemborexant: Subjects with Irregular Sleep-Wake Rhythm Disorder and Alzheimer's Disease Dementia. Alzheimer's & Dementia 15:P187.

Theofilas P, Dunlop S, Heinsen H, Grinberg LT (2015) Turning on the Light Within: Subcortical Nuclei of the Isodentritic Core and their Role in Alzheimer's Disease Pathogenesis. J Alzheimers Dis 46:17-34.

Tononi G, Cirelli C (2003) Sleep and synaptic homeostasis: a hypothesis. Brain Res Bull 62:143-150.

Tononi G, Cirelli C (2006) Sleep function and synaptic homeostasis. Sleep Med Rev 10:49-62.

Tononi G, Cirelli C (2014) Sleep and the Price of Plasticity: From Synaptic and Cellular Homeostasis to Memory Consolidation and Integration. Neuron 81:12-34.

Tournier JD, Smith R, Raffelt D, Tabbara R, Dhollander T, Pietsch M, Christiaens D, Jeurissen B, Yeh CH, Connelly A (2019) MRtrix3: A fast, flexible and open software framework for medical image processing and visualisation. Neuroimage 202:116137.

Tranah GJ, Blackwell T, Stone KL, Ancoli-Israel S, Paudel ML, Ensrud KE, Cauley JA, Redline S, Hillier TA, Cummings SR, Yaffe K, Group SOFR (2011) Circadian activity rhythms and risk of incident dementia and mild cognitive impairment in older women. Ann Neurol 70:722-732.

Trinczek B, Biernat J, Baumann K, Mandelkow EM, Mandelkow E (1995) Domains of tau protein, differential phosphorylation, and dynamic instability of microtubules. Mol Biol Cell 6:1887-1902.

Trojanowski JQ, Lee VM (2005) Pathological tau: a loss of normal function or a gain in toxicity? Nat Neurosci 8:1136-1137.

Tsujino N, Tsunematsu T, Uchigashima M, Konno K, Yamanaka A, Kobayashi K, Watanabe M, Koyama Y, Sakurai T (2013) Chronic alterations in monoaminergic cells in the locus coeruleus in orexin neuron-ablated narcoleptic mice. PLoS One 8:e70012.

Urrestarazu E, Iriarte J (2016) Clinical management of sleep disturbances in Alzheimer's disease: current and emerging strategies. Nat Sci Sleep 8:21-33.

Uslaner JM et al. (2013) Orexin receptor antagonists differ from standard sleep drugs by promoting sleep at doses that do not disrupt cognition. Sci Transl Med 5:179ra144.

Valentino RJ, Van Bockstaele E (2008) Convergent regulation of locus coeruleus activity as an adaptive response to stress. European journal of pharmacology 583:194-203.

van den Pol AN, Gao XB, Obrietan K, Kilduff TS, Belousov AB (1998) Presynaptic and postsynaptic actions and modulation of neuroendocrine neurons by a new hypothalamic peptide, hypocretin/orexin. J Neurosci 18:7962-7971.

Vanderheyden WM, Lim MM, Musiek ES, Gerstner JR (2018) Alzheimer's Disease and Sleep-Wake Disturbances: Amyloid, Astrocytes, and Animal Models. J Neurosci 38:2901-2910.

Vassalli A, Franken P (2017) Hypocretin (orexin) is critical in sustaining theta/gamma-rich waking behaviors that drive sleep need. Proceedings of the National Academy of Sciences of the United States of America.

Vassar R et al. (1999) Beta-secretase cleavage of Alzheimer's amyloid precursor protein by the transmembrane aspartic protease BACE. Science 286:735-741.

Verster JC, Volkerts ER, Schreuder AH, Eijken EJ, van Heuckelum JH, Veldhuijzen DS, Verbaten MN, Paty I, Darwish M, Danjou P, Patat A (2002) Residual effects of middle-of-the-night administration of zaleplon and zolpidem on driving ability, memory functions, and psychomotor performance. J Clin Psychopharmacol 22:576-583.

Vienne J, Lecciso G, Constantinescu I, Schwartz S, Franken P, Heinzer R, Tafti M (2012) Differential effects of sodium oxybate and baclofen on EEG, sleep, neurobehavioral performance, and memory. Sleep 35:1071-1083.

Vitiello MV, Prinz PN, Williams DE, Frommlet MS, Ries RK (1990) Sleep Disturbances in Patients with Mild-Stage Alzheimers-Disease. J Gerontol 45:M131-M138.

Vogelsberg-Ragaglia V, Schuck T, Trojanowski JQ, Lee VM (2001) PP2A mRNA expression is quantitatively decreased in Alzheimer's disease hippocampus. Exp Neurol 168:402-412.

Walker MP, Stickgold R (2006) Sleep, memory, and plasticity. Annu Rev Psychol 57:139-166.

Wang C, Holtzman DM (2020) Bidirectional relationship between sleep and Alzheimer's disease: role of amyloid, tau, and other factors. Neuropsychopharmacology 45:104-120.

Wang CM, Wang QQ, Ji BY, Pan YY, Xu C, Cheng BH, Bai B, Chen J (2018) The Orexin/Receptor System: Molecular Mechanism and Therapeutic Potential for Neurological Diseases. Front Mol Neurosci 11.

Wang Y, Balaji V, Kaniyappan S, Kruger L, Irsen S, Tepper K, Chandupatla R, Maetzler W, Schneider A, Mandelkow E, Mandelkow EM (2017a) The release and trans-synaptic transmission of Tau via exosomes. Mol Neurodegener 12:5.

Wang YY, Zheng W, Ng CH, Ungvari GS, Wei W, Xiang YT (2017b) Meta-analysis of randomized, double-blind, placebo-controlled trials of melatonin in Alzheimer's disease. Int J Geriatr Psychiatry 32:50-57.

Waters F, Chiu V, Atkinson A, Blom JD (2018) Severe Sleep Deprivation Causes Hallucinations and a Gradual Progression Toward Psychosis With Increasing Time Awake. Front Psychiatry 9:303.

Wei W, Nguyen LN, Kessels HW, Hagiwara H, Sisodia S, Malinow R (2010) Amyloid beta from axons and dendrites reduces local spine number and plasticity. Nat Neurosci 13:190-196.

Wells JA et al. (2015) In vivo imaging of tau pathology using multi-parametric quantitative MRI. Neuroimage 111:369-378.

Wesensten NJ, Balkin TJ, Reichardt RM, Kautz MA, Saviolakis GA, Belenky G (2005) Daytime sleep and performance following a zolpidem and melatonin cocktail. Sleep 28:93-103.

Westerberg CE, Mander BA, Florczak SM, Weintraub S, Mesulam MM, Zee PC, Paller KA (2012) Concurrent impairments in sleep and memory in amnestic mild cognitive impairment. J Int Neuropsychol Soc 18:490-500.

Whitehouse PJ, Price DL, Struble RG, Clark AW, Coyle JT, Delong MR (1982) Alzheimers-Disease and Senile Dementia - Loss of Neurons in the Basal Forebrain. Science 215:1237-1239.

Willie JT, Chemelli RM, Sinton CM, Yanagisawa M (2001) To eat or to sleep? Orexin in the regulation of feeding and wakefulness. Annu Rev Neurosci 24:429-458.

Willie JT, Chemelli RM, Sinton CM, Tokita S, Williams SC, Kisanuki YY, Marcus JN, Lee C, Elmquist JK, Kohlmeier KA, Leonard CS, Richardson JA, Hammer RE, Yanagisawa M (2003) Distinct narcolepsy syndromes in Orexin receptor-2 and Orexin null mice: molecular genetic dissection of Non-REM and REM sleep regulatory processes. Neuron 38:715-730.

Winrow CJ, Renger JJ (2014) Discovery and development of orexin receptor antagonists as therapeutics for insomnia. Br J Pharmacol 171:283-293.

Winrow CJ, Gotter AL, Cox CD, Doran SM, Tannenbaum PL, Breslin MJ, Garson SL, Fox SV, Harrell CM, Stevens J, Reiss DR, Cui D, Coleman PJ, Renger JJ (2011) Promotion of sleep by suvorexant-a novel dual orexin receptor antagonist. J Neurogenet 25:52-61.

Winrow CJ, Gotter AL, Cox CD, Tannenbaum PL, Garson SL, Doran SM, Breslin MJ, Schreier JD, Fox SV, Harrell CM, Stevens J, Reiss DR, Cui D, Coleman PJ, Renger JJ (2012) Pharmacological characterization of MK-6096 - a dual orexin receptor antagonist for insomnia. Neuropharmacology 62:978-987.

Winsky-Sommerer R, Yamanaka A, Diano S, Borok E, Roberts AJ, Sakurai T, Kilduff TS, Horvath TL, de Lecea L (2004) Interaction between the corticotropin-releasing factor system and hypocretins (orexins): a novel circuit mediating stress response. J Neurosci 24:11439-11448.

Wisor JP, Edgar DM, Yesavage J, Ryan HS, McCormick CM, Lapustea N, Murphy GM, Jr. (2005) Sleep and circadian abnormalities in a transgenic mouse model of Alzheimer's disease: a role for cholinergic transmission. Neuroscience 131:375-385.

Wright DK, Johnston LA, Kershaw J, Ordidge R, O'Brien TJ, Shultz SR (2017a) Changes in Apparent Fiber Density and Track-Weighted Imaging Metrics in White Matter following Experimental Traumatic Brain Injury. Journal of Neurotrauma 34:2109-2118.

Wright DK, Liu SJ, van der Poel C, McDonald SJ, Brady RD, Taylor L, Yang L, Gardner AJ, Ordidge R, O'Brien TJ, Johnston LA, Shultz SR (2017b) Traumatic Brain Injury Results in Cellular, Structural and Functional Changes Resembling Motor Neuron Disease. Cerebral Cortex 27:4503-4515.

Wright DK, Brady RD, Kamnaksh A, Trezise J, Sun M, McDonald SJ, Mychasiuk R, Kolbe SC, Law M, Johnston LA, O'Brien TJ, Agoston DV, Shultz SR (2019) Repeated mild traumatic brain injuries induce persistent changes in plasma protein and magnetic resonance imaging biomarkers in the rat. Sci Rep 9:14626.

Wu JW, Hussaini SA, Bastille IM, Rodriguez GA, Mrejeru A, Rilett K, Sanders DW, Cook C, Fu H, Boonen RA, Herman M, Nahmani E, Emrani S, Figueroa YH, Diamond MI, Clelland CL, Wray S, Duff KE (2016) Neuronal activity enhances tau propagation and tau pathology in vivo. Nat Neurosci 19:1085-1092.

Wulff K, Gatti S, Wettstein JG, Foster RG (2010) Sleep and circadian rhythm disruption in psychiatric and neurodegenerative disease. Nat Rev Neurosci 11:589-599.

Xi MC, Morales FR, Chase MH (2001) Effects on sleep and wakefulness of the injection of hypocretin-1 (orexin-A) into the laterodorsal tegmental nucleus of the cat. Brain Res 901:259-264.

Xie L, Kang H, Xu Q, Chen MJ, Liao Y, Thiyagarajan M, O'Donnell J, Christensen DJ, Nicholson C, Iliff JJ, Takano T, Deane R, Nedergaard M (2013) Sleep drives metabolite clearance from the adult brain. Science 342:373-377.

Yaffe K, Falvey CM, Hoang T (2014) Connections between sleep and cognition in older adults. Lancet Neurol 13:1017-1028.

Yamada K, Cirrito JR, Stewart FR, Jiang H, Finn MB, Holmes BB, Binder LI, Mandelkow EM, Diamond MI, Lee VM, Holtzman DM (2011) In vivo microdialysis reveals age-dependent decrease of brain interstitial fluid tau levels in P301S human tau transgenic mice. J Neurosci 31:13110-13117.

Yamada K, Holth JK, Liao F, Stewart FR, Mahan TE, Jiang H, Cirrito JR, Patel TK, Hochgrafe K, Mandelkow EM, Holtzman DM (2014) Neuronal activity regulates extracellular tau in vivo. The Journal of experimental medicine 211:387-393.

Yamaguchi H, Hopf FW, Li SB, de Lecea L (2018) In vivo cell type-specific CRISPR knockdown of dopamine beta hydroxylase reduces locus coeruleus evoked wakefulness. Nature Communications 9:8.

Yamanaka A, Tsujino N, Funahashi H, Honda K, Guan JL, Wang QP, Tominaga M, Goto K, Shioda S, Sakurai T (2002) Orexins activate histaminergic neurons via the orexin 2 receptor. Biochem Biophys Res Commun 290:1237-1245.

Yoshida H, Ihara Y (1993) Tau in paired helical filaments is functionally distinct from fetal tau: assembly incompetence of paired helical filament-tau. J Neurochem 61:1183-1186.

Yoshida Y, Fujiki N, Nakajima T, Ripley B, Matsumura H, Yoneda H, Mignot E, Nishino S (2001) Fluctuation of extracellular hypocretin-1 (orexin A) levels in the rat in relation to the light-dark cycle and sleep-wake activities. Eur J Neurosci 14:1075-1081.

Yoshiyama Y, Higuchi M, Zhang B, Huang SM, Iwata N, Saido TC, Maeda J, Suhara T, Trojanowski JQ, Lee VM (2007) Synapse loss and microglial activation precede tangles in a P301S tauopathy mouse model. Neuron 53:337-351.

Yue M, Hanna A, Wilson J, Roder H, Janus C (2011) Sex difference in pathology and memory decline in rTg4510 mouse model of tauopathy. Neurobiol Aging 32:590-603.

Yushkevich PA, Piven J, Hazlett HC, Smith RG, Ho S, Gee JC, Gerig G (2006) User-guided 3D active contour segmentation of anatomical structures: significantly improved efficiency and reliability. Neuroimage 31:1116-1128.

Zanin KA, Patti CL, Sanday L, Fernandes-Santos L, Oliveira LC, Poyares D, Tufik S, Frussa-Filho R (2013) Effects of zolpidem on sedation, anxiety, and memory in the plus-maze discriminative avoidance task. Psychopharmacology (Berl) 226:459-474.

Zhang B, Veasey SC, Wood MA, Leng LZ, Kaminski C, Leight S, Abel T, Lee VM, Trojanowski JQ (2005) Impaired rapid eye movement sleep in the Tg2576 APP murine model of Alzheimer's disease with injury to pedunculopontine cholinergic neurons. Am J Pathol 167:1361-1369.

Zhang J, Zhu Y, Zhan G, Fenik P, Panossian L, Wang MM, Reid S, Lai D, Davis JG, Baur JA, Veasey S (2014) Extended wakefulness: compromised metabolics in and degeneration of locus ceruleus neurons. J Neurosci 34:4418-4431.

Zhu B, Dong Y, Xu Z, Gompf HS, Ward SA, Xue Z, Miao C, Zhang Y, Chamberlin NL, Xie Z (2012) Sleep disturbance induces neuroinflammation and impairment of learning and memory. Neurobiol Dis 48:348-355.

Zhu Y, Fenik P, Zhan G, Somach R, Xin R, Veasey S (2016) Intermittent Short Sleep Results in Lasting Sleep Wake Disturbances and Degeneration of Locus Coeruleus and Orexinergic Neurons. Sleep 39:1601-1611.

Zhu Y, Zhan G, Fenik P, Brandes M, Bell P, Francois N, Shulman K, Veasey S (2018) Chronic Sleep Disruption Advances the Temporal Progression of Tauopathy in P301S Mutant Mice. J Neurosci 38:10255-10270.

Zielinski MR, McKenna JT, McCarley RW (2016) Functions and Mechanisms of Sleep. AIMS Neurosci 3:67-104.

Appendix I

Conference Presentations

Poster presentations

Ryan J. Keenan, Heather Daykin, David K. Wright, Kevin J. Barnham, Giancarlo Allocca, Daniel Hoyer, Laura H. Jacobson. *The effect of human mutant tau on cognition and sleep in the rTg4510 mouse model of tauopathy*. **Society for Neuroscience, San Diego, U.S.A., 3-7 Nov 2018.**

Oral presentations

Ryan J. Keenan, Linda Cornthwaite-Duncan, Heather Daykin, Sara Oberrauch, Maddison Brian, Jeremy Metha, Kevin J. Barnham, Giancarlo Allocca, Daniel Hoyer, Laura H. Jacobson. *Orexin receptor antagonist-induced effects on sleep, cognition and tau pathology in the rTg4510 mouse model of tauopathy*. **Society for Neuroscience, Chicago, U.S.A., 19-23 Oct 2019.**

Appendix II

In situ Hybridisation Data

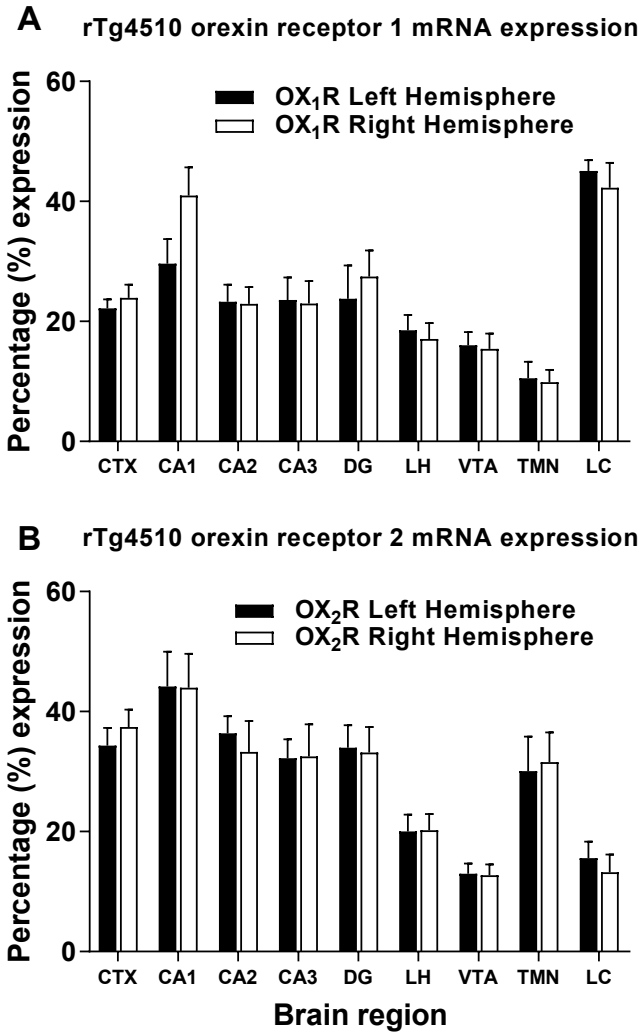

Figure A2.1. No effect of brain hemisphere on orexin receptor mRNA expression in rTg4510 mice.
A-B, Percentage expression of OX_1R mRNA (***A***) and OX_2R mRNA (***B***) per brain region across hemisphere. Data are means ± SEM. n = 10-11 per hemisphere. *CA1* CA1 subfield of hippocampus; *CA2* CA2 subfield of hippocampus; *CA3* CA3 subfield of hippocampus; *CTX* cerebral cortex; *DG* dentate gyrus; *LC* locus coeruleus; *LH* lateral hypothalamus; *TMN* tuberomammillary nucleus; *VTA* ventral tegmental area. Note that the PVT and DRN are not bilaterally distributed and therefore not included in hemisphere analysis.

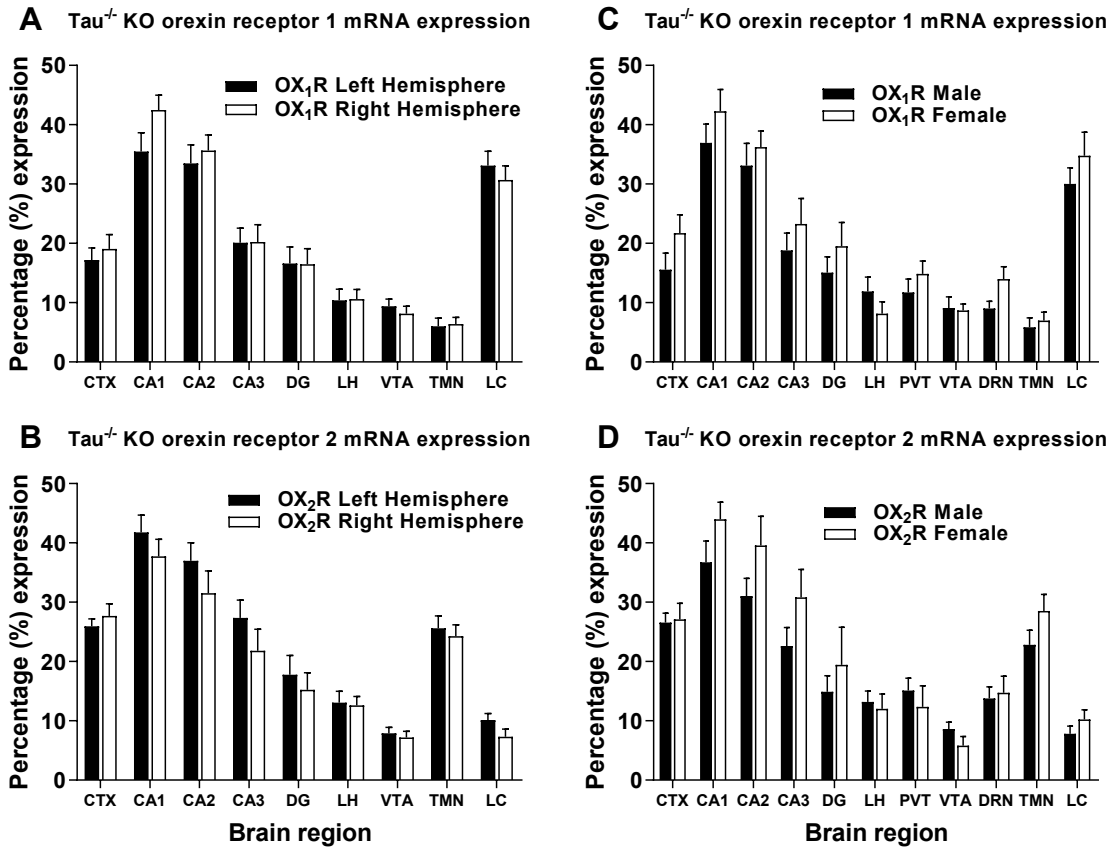

Figure A2.2. No effect of brain hemisphere or sex on orexin receptor mRNA expression in tau$^{-/-}$ KO mice. ***A-B***, Percentage expression of OX_1R mRNA (***A***) and OX_2R mRNA (***B***) per brain region across hemisphere. ***C-D***, Percentage expression of OX_1R mRNA (***C***) and OX_2R mRNA (***D***) per brain region between sexes. Data are means ± SEM. n = 15-17 per hemisphere; n = 6-10 per sex. *CA1* CA1 subfield of hippocampus; *CA2* CA2 subfield of hippocampus; *CA3* CA3 subfield of hippocampus; *CTX* cerebral cortex; *DG* dentate gyrus; *DRN* dorsal raphe nucleus; *LC* locus coeruleus; *LH* lateral hypothalamus; *PVT* paraventricular nucleus of the thalamus; *TMN* tuberomammillary nucleus; *VTA* ventral tegmental area. Note that the PVT and DRN are not bilaterally distributed and therefore not included in hemisphere analysis.

Appendix III

Barnes Maze Acquisition Data

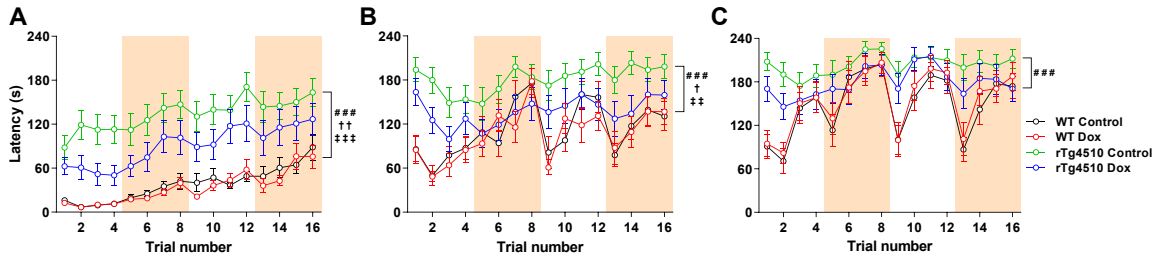

Figure A3.1. Barnes maze acquisition latency data in rTg4510 mice following doxycycline treatment.
A-C, Latency to investigate any hole on the maze (***A***), primary latency (***B***) and latency to enter the escape box (***C***) per acquisition trial in rTg4510 and WT mice administered doxycycline (Dox) or control diets. Alternate background shading distinguishes acquisition trial days (1-4). Data are means ± SEM. n = 16-19 per group. #, † and ‡ denote main effects of genotype, treatment and trial, respectively. ###P < 0.001 vs. WT; †P < 0.05, ††P < 0.01 vs. Control, by repeated measures linear mixed effects model with Tukey's multiple comparisons test.

Table A3.1. Barnes maze acquisition latency data statistical analyses summary (doxycycline).
Barnes maze acquisition trials latencies were analysed by a repeated measures linear mixed effects model in R, using the lmer function, incorporating the factors of genotype, treatment and trial (repeated factor). Indented Pr(>|t|) values indicate statistical significance.

Barnes maze acquisition latencies															
	Latency to investigate any hole					**Primary latency**					**Latency to enter escape hole**				
Fixed effect	Estimate	Std. error	df	t-value	Pr(>|t|)	Estimate	Std. error	df	t-value	Pr(>|t|)	Estimate	Std. error	df	t-value	Pr(>|t|)
Genotype	-101.536	18.773	86.051	-5.409	< 0.001	-82.036	20.070	117.326	-4.087	< 0.001	-72.431	18.318	141.532	-3.954	< 0.001
Treatment	-54.005	18.773	86.051	-2.877	< 0.01	-40.809	20.070	117.326	-2.033	< 0.05	-28.700	18.318	141.532	-1.567	> 0.05
Trial	3.847	0.529	1061.000	7.267	< 0.001	2.250	0.818	1061.000	2.750	< 0.01	1.196	0.846	1061.000	1.414	> 0.05
Genotype:Treatment	52.072	27.147	86.051	1.918	> 0.05	35.460	29.024	117.326	1.222	> 0.05	30.352	26.490	141.532	1.146	> 0.05
Genotype:Trial	0.616	0.759	1061.000	0.812	> 0.05	1.542	1.173	1061.000	1.314	> 0.05	2.094	1.213	1061.000	1.727	> 0.05
Treatment:Trial	1.279	0.759	1061.000	1.685	> 0.05	-0.379	1.173	1061.000	-0.323	> 0.05	0.536	1.213	1061.000	0.442	> 0.05
Genotype:Treatment:Trial	-1.546	1.098	1061.000	-1.409	> 0.05	0.371	1.697	1061.000	0.219	> 0.05	0.036	1.754	1061.000	0.020	> 0.05

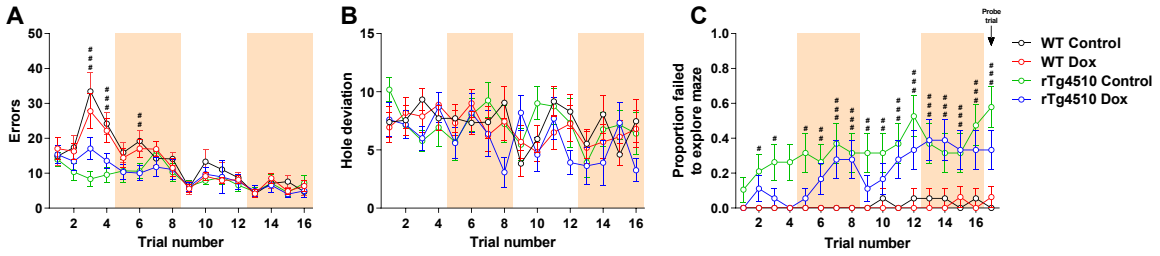

Figure A3.2. Barnes maze acquisition data in rTg4510 mice following doxycycline treatment.

A-C, Total errors made (***A***), hole deviation (***B***) and proportion of mice failing to explore the maze during the 4 min trial limit (***C***) per acquisition trial in rTg4510 and WT mice administered doxycycline (Dox) or control diets. Alternate background shading distinguishes acquisition trial days (1-4). Data are means ± SEM. n = 16-19 per group. $^{\#}P < 0.05$, $^{\#\#}P < 0.01$, $^{\#\#\#}P < 0.001$ vs. WT (genotype x trial) within acquisition trial, by repeated measures linear mixed effects model with Tukey's multiple comparisons test.

Table A3.2. Barnes maze acquisition data statistical analyses summary (doxycycline).

Barnes maze acquisition trials data were analysed by a repeated measures linear mixed effects model in R, using the lmer function, incorporating the factors of genotype, treatment and trial (repeated factor). Indented Pr(>|t|) values indicate statistical significance.

Barnes maze acquisition data															
	Errors					**Hole deviation**					**Failed to explore maze**				
Fixed effect	Estimate	Std. error	df	t-value	Pr(>|t|)	Estimate	Std. error	df	t-value	Pr(>|t|)	Estimate	Std. error	df	t-value	Pr(>|t|)
Genotype	11.210	1.899	592.907	5.904	< 0.001	-0.020	1.123	287.282	-0.018	> 0.05	-0.184	0.082	102.000	-2.251	< 0.05
Treatment	3.162	1.946	615.518	1.625	> 0.05	-0.451	1.142	302.571	-0.395	> 0.05	-0.174	0.082	102.000	-2.131	< 0.05
Trial	-0.465	0.152	955.907	-3.069	< 0.01	-0.116	0.078	952.953	-1.478	> 0.05	0.177	0.003	1132.000	6.402	< 0.001
Genotype:Treatment	-4.885	2.672	599.396	-1.828	> 0.05	0.538	1.587	279.598	0.339	> 0.05	0.170	0.118	102.000	1.442	> 0.05
Genotype:Trial	-0.786	0.199	939.909	-3.945	< 0.001	0.012	0.103	935.758	0.120	> 0.05	-0.015	0.004	1132.000	-3.777	< 0.001
Treatment:Trial	-0.291	0.210	959.306	-1.387	> 0.05	-0.059	0.109	953.862	-0.537	> 0.05	0.006	0.004	1132.000	1.452	> 0.05
Genotype:Treatment:Trial	0.360	0.282	941.996	1.273	> 0.05	0.001	0.146	935.111	0.005	> 0.05	-0.006	0.006	1132.000	-1.105	> 0.05

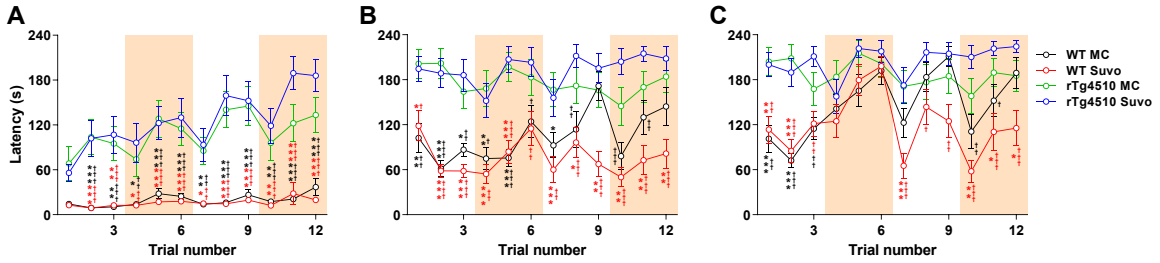

Figure A3.3. Barnes maze acquisition latency data in rTg4510 mice following suvorexant treatment.
A-C, Latency to investigate any hole on the maze (***A***), primary latency (***B***) and latency to enter the escape box (***C***) per acquisition trial in rTg4510 and WT mice administered 50 mg/kg/day suvorexant (Suvo) or methylcellulose (MC) vehicle. Alternate background shading distinguishes acquisition trial days (1-4). Data are means ± SEM. n = 13-16 per group. $^{*}P < 0.05$, $^{**}P < 0.01$, $^{***}P < 0.001$ vs. rTg4510 MC; $^{\dagger}P < 0.05$, $^{\dagger\dagger}P < 0.01$, $^{\dagger\dagger\dagger}P < 0.001$ vs. rTg4510 Suvo, by repeated measures linear mixed effects model with Tukey's multiple comparisons test. For clarity, not all statistically significant differences are graphically presented.

Table A3.3. Barnes maze acquisition latency data statistical analyses summary (suvorexant).
Barnes maze acquisition trials latencies were analysed by a repeated measures linear mixed effects model in R, using the lmer function, incorporating the factors of genotype, treatment and trial (repeated factor). Indented Pr(>|t|) values indicate statistical significance.

Barnes maze acquisition latencies															
	Latency to investigate any hole					**Primary latency**					**Latency to enter escape hole**				
Fixed effect	Estimate	Std. error	df	t-value	Pr(>|t|)	Estimate	Std. error	df	t-value	Pr(>|t|)	Estimate	Std. error	df	t-value	Pr(>|t|)
Genotype	-70.780	19.252	81.844	-3.677	< 0.001	-124.155	20.303	148.817	-6.115	< 0.001	-99.449	19.575	228.509	-5.081	< 0.001
Treatment	-14.687	19.859	81.844	-0.740	> 0.05	-15.265	20.303	148.817	-0.729	> 0.05	-13.241	20.192	228.509	-0.656	> 0.05
Trial	4.373	0.938	645.000	4.660	< 0.001	-2.488	1.474	645.000	-1.688	> 0.05	-2.051	1.636	645.000	-1.253	> 0.05
Genotype:Treatment	14.614	26.957	81.844	0.542	> 0.05	29.508	28.429	148.817	1.038	> 0.05	42.072	27.409	228.509	1.535	> 0.05
Genotype:Trial	-2.897	1.263	645.000	-2.293	< 0.05	8.025	1.984	645.000	4.044	< 0.001	9.014	2.203	645.000	4.093	< 0.001
Treatment:Trial	4.896	1.303	645.000	3.757	< 0.001	4.932	2.047	645.000	2.410	< 0.05	4.750	2.272	645.000	2.091	< 0.05
Genotype:Treatment:Trial	-5.413	1.769	645.000	-3.060	< 0.01	-11.473	2.779	645.000	-4.129	< 0.001	-13.244	3.084	645.000	-4.294	< 0.001

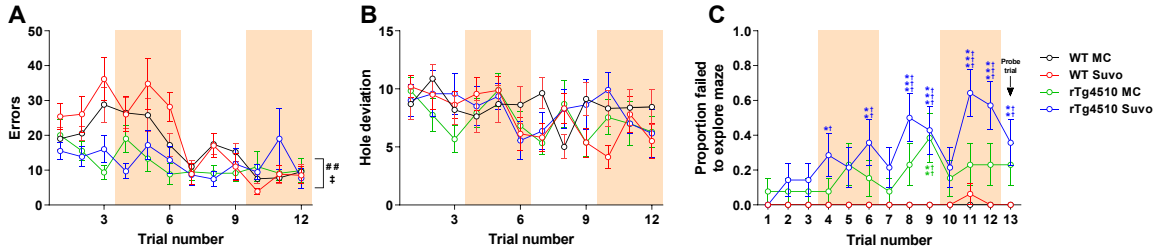

Figure A3.4. Barnes maze acquisition data in rTg4510 mice following suvorexant treatment.

A-C, Total errors made (***A***), hole deviation (***B***) and proportion of mice failing to explore the maze during the 4 min trial limit (***C***) per acquisition trial in rTg4510 and WT mice administered 50 mg/kg/day suvorexant (Suvo) or methylcellulose (MC) vehicle. Alternate background shading distinguishes acquisition trial days (1-4). Data are means ± SEM. n = 13-16 per group. # and ‡ denote main effects of genotype and trial, respectively. $^{\#\#}P < 0.01$ vs. WT; $^{*}P < 0.05$, $^{**}P < 0.01$, $^{***}P < 0.001$ vs. WT MC; $^{\dagger}P < 0.05$, $^{\dagger\dagger}P < 0.01$, $^{\dagger\dagger\dagger}P < 0.001$ vs. WT Suvo, by repeated measures linear mixed effects model with Tukey's multiple comparisons test. For clarity, not all statistically significant differences are graphically presented.

Table A3.4. Barnes maze acquisition data statistical analyses summary (suvorexant).

Barnes maze acquisition trials data were analysed by a repeated measures linear mixed effects model in R, using the lmer function, incorporating the factors of genotype, treatment and trial (repeated factor). Indented Pr(>|t|) values indicate statistical significance.

Barnes maze acquisition data															
	Errors					**Hole deviation**					**Failed to explore maze**				
Fixed effect	Estimate	Std. error	df	t-value	Pr(>|t|)	Estimate	Std. error	df	t-value	Pr(>|t|)	Estimate	Std. error	df	t-value	Pr(>|t|)
Genotype	10.626	3.429	404.243	3.099	< 0.01	0.628	1.286	377.536	0.488	> 0.05	-0.059	0.082	105.061	-0.722	> 0.05
Treatment	-1.591	3.695	424.201	-0.431	> 0.05	0.893	1.390	401.291	0.642	> 0.05	-0.001	0.085	105.061	-0.017	> 0.05
Trial	-0.801	0.350	584.047	-2.291	< 0.05	-0.174	0.130	582.936	-1.335	> 0.05	0.016	0.005	704.000	3.485	< 0.001
Genotype:Treatment	9.672	4.856	410.532	1.992	< 0.05	0.438	1.825	385.514	0.240	> 0.05	-0.003	0.115	105.061	-0.029	> 0.05
Genotype:Trial	-0.810	0.454	578.680	-1.782	> 0.05	0.080	0.169	577.221	0.473	> 0.05	-0.016	0.006	704.000	-2.589	< 0.01
Treatment:Trial	0.280	0.518	597.552	0.541	> 0.05	0.012	0.193	596.784	0.062	> 0.05	0.020	0.006	704.000	3.194	< 0.01
Genotype:Treatment:Trial	-1.164	0.660	588.087	-1.764	> 0.05	-0.356	0.246	587.014	-1.449	> 0.05	-0.019	0.009	704.000	-2.195	< 0.05

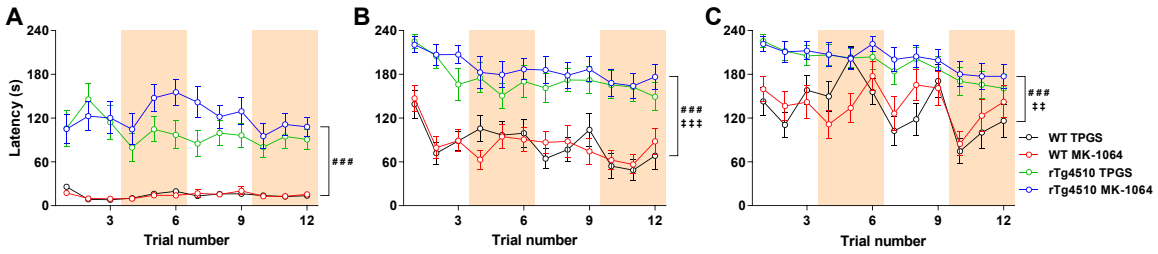

Figure A3.5. Barnes maze acquisition latency data in rTg4510 mice following MK-1064 treatment.

A-C, Latency to investigate any hole on the maze (***A***), primary latency (***B***) and latency to enter the escape box (***C***) per acquisition trial in rTg4510 and WT mice administered 40 mg/kg/day MK-1064 or TPGS vehicle. Alternate background shading distinguishes acquisition trial days (1-4). Data are means ± SEM. n = 16-18 per group. # and ‡ denote main effects of genotype and trial, respectively. $^{###}P < 0.001$ vs. WT, by repeated measures linear mixed effects model with Tukey's multiple comparisons test.

Table A3.5. Barnes maze acquisition latency data statistical analyses summary (MK-1064).

Barnes maze acquisition trials latencies were analysed by a repeated measures linear mixed effects model in R, using the lmer function, incorporating the factors of genotype, treatment and trial (repeated factor). Indented Pr(>|t|) values indicate statistical significance.

Barnes maze acquisition latencies															
	Latency to investigate any hole					**Primary latency**					**Latency to enter escape hole**				
Fixed effect	Estimate	Std. error	df	t-value	Pr(>|t|)	Estimate	Std. error	df	t-value	Pr(>|t|)	Estimate	Std. error	df	t-value	Pr(>|t|)
Genotype	-114.723	14.828	123.102	-7.737	< 0.001	-104.602	18.376	156.884	-5.692	< 0.001	-77.091	18.891	182.502	-4.081	< 0.001
Treatment	-8.886	15.064	123.102	-0.590	> 0.05	-12.902	18.668	156.884	-0.691	> 0.05	2.385	19.193	182.502	0.124	> 0.05
Trial	-0.748	0.838	755.000	-0.893	> 0.05	-3.936	1.191	755.000	-3.305	< 0.001	-3.723	1.306	755.000	-2.851	< 0.01
Genotype:Treatment	12.226	21.137	123.102	0.578	> 0.05	20.056	26.195	156.884	0.766	> 0.05	9.690	26.930	182.502	0.360	> 0.05
Genotype:Trial	1.056	1.203	755.000	0.878	> 0.05	0.410	1.709	755.000	0.240	> 0.05	2.255	1.874	755.000	1.203	> 0.05
Treatment:Trial	-2.081	1.222	755.000	-1.703	> 0.05	-0.178	1.736	755.000	-0.103	> 0.05	-1.503	1.904	755.000	-0.789	> 0.05
Genotype:Treatment:Trial	1.645	1.714	755.000	0.959	> 0.05	-0.950	2.436	755.000	-0.390	> 0.05	-1.137	2.672	755.000	-0.426	> 0.05

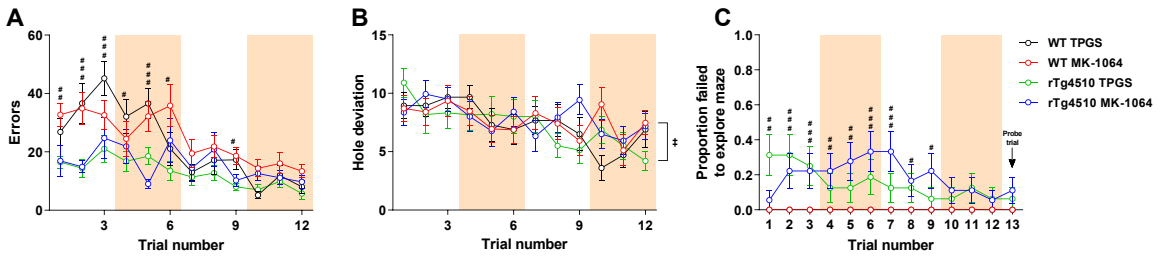

Figure A3.6. Barnes maze acquisition data in rTg4510 mice following MK-1064 treatment.

A-C, Total errors made (***A***), hole deviation (***B***) and proportion of mice failing to explore the maze during the 4 min trial limit (***C***) per acquisition trial in rTg4510 and WT mice administered 40 mg/kg/day MK-1064 or TPGS vehicle. Alternate background shading distinguishes acquisition trial days (1-4). Data are means ± SEM. n = 16-18 per group. ‡ denotes main effect of trial. $^{\#}P < 0.05$, $^{\#\#}P < 0.01$, $^{\#\#\#}P < 0.001$ vs. WT (genotype x trial) within acquisition trial, by repeated measures linear mixed effects model with Tukey's multiple comparisons test.

Table A3.6. Barnes maze acquisition data statistical analyses summary (MK-1064).

Barnes maze acquisition trials data were analysed by a repeated measures linear mixed effects model in R, using the lmer function, incorporating the factors of genotype, treatment and trial (repeated factor). Indented Pr(>|t|) values indicate statistical significance.

Barnes maze acquisition data															
	Errors					**Hole deviation**					**Failed to explore maze**				
Fixed effect	Estimate	Std. error	df	t-value	Pr(>|t|)	Estimate	Std. error	df	t-value	Pr(>|t|)	Estimate	Std. error	df	t-value	Pr(>|t|)
Genotype	17.627	4.001	402.646	4.406	< 0.001	-0.152	1.186	280.455	-0.128	> 0.05	-0.248	0.069	121.311	-3.579	< 0.001
Treatment	0.152	4.342	427.633	0.035	> 0.05	0.966	1.281	307.944	0.754	> 0.05	0.041	0.070	121.311	0.577	> 0.05
Trial	-0.769	0.357	709.260	-2.156	< 0.05	-0.196	0.097	704.009	-2.006	< 0.05	-0.009	0.004	824.000	-2.377	< 0.05
Genotype:Treatment	3.687	5.791	405.953	0.637	> 0.05	0.137	1.716	283.949	0.080	> 0.05	-0.041	0.099	121.311	-0.411	> 0.05
Genotype:Trial	-1.284	0.493	699.341	-2.603	< 0.01	0.003	0.135	695.180	0.021	> 0.05	0.009	0.005	824.000	1.656	> 0.05
Treatment:Trial	-0.394	0.530	709.746	-0.743	> 0.05	-0.241	0.145	704.053	-1.666	> 0.05	-0.011	0.005	824.000	-2.169	< 0.05
Genotype:Treatment:Trial	-0.524	0.712	700.322	-0.736	> 0.05	0.025	0.194	695.815	0.131	> 0.05	0.011	0.007	824.000	1.546	> 0.05